Online ISSN: 1920-3853

Vol. 10, No. 3, October 2016

Print ISSN : 1715-9997

Canadian Journal of pure & applied sciences

an International Journal

Published three times a year (Feb, June and Oct.)

SENRA Academic Publishers
British Columbia

Print ISSN 1715-9997
Online ISSN 1920-3853

Volume 10, Number 3
October 2016

CANADIAN JOURNAL OF PURE AND APPLIED SCIENCES

The Canadian Journal of Pure and Applied Sciences (CJPAS) is a peer reviewed multi-disciplinary international journal aimed at promoting research in all field of science and technology on the basis of its originality. The CJPAS is indexed in major indexing databases of different indexing services and universities.

Every effort is made by the editors, board of editorial advisors and publishers to see that no inaccurate or misleading data, opinions, or statements appear in this journal, they wish to make clear that data and opinions appearing in the articles are the sole responsibility of the contributor concerned. The CJPAS accept no responsibility for the misleading data, opinion or statements.

CJPAS is Abstracted/Indexed in:

Ulrich's Periodicals Directory, Scirus, CiteSeerX, Index Copernicus, Directory of Open Access Journals, Google Scholar, CABI, Chemical Abstracts, Global Impact Factor Australia, J-Gate, HINARI, WorldCat, British Library, European Library, Biblioteca Central, The Intute Consortium, Genamics JournalSeek, bibliotek.dk, OAJSE, Zurich Open Repository and Archive Journal Database, American Association for the Advancement of Science, OHSU Library.

Four Years Global Impact Factor
2012 2.657, 2013 2.756,
2014 2.845, 2015 2.988

Frequency:
3 times a year (Feb, June and Oct.)

Editorial Office
E-mail: editor@cjpas.ca, editor@cjpas.net

SENRA Academic Publishers
5919 129 B Street Surrey
British Columbia V3X 0C5 Canada
www.cjpas.net
E-mail: senra@cjpas.ca

Board of Editorial Advisors

Member
CANADIAN ASSOCIATION OF LEARNED JOURNALS

Canadian Journal of pure & applied sciences

Volume 10, Number 3
October 2016

CONTENTS

LIFE SCIENCES

PHYSICAL SCIENCES

Canadian Journal of Pure and Applied Sciences
Vol. 10, No. 3, pp. 3941-3949, Oct 2016
Online ISSN: 1920-3853; Print ISSN: 1715-9997
Available online at www.cjpas.net

SESSILE AEROBIC MICROBIOTA FROM THE WALL OF THE NATIONAL MUSEUM, BRAZIL: CHARACTERIZATION AND QUANTIFICATION

*Diogo Simas Bernardes Dias[1], Ulrich Vasconcelos[2], Márcia Teresa Soares Lutterbach[3], Cristiana Cravo-Laureau[4] and Eliana Flávia Camporese Sérvulo[1]
[1]Laboratório de Biossíntese, Biocorrosão e Biodegradação, Escola de Química
Universidade Federal do Rio de Janeiro, Rio de Janeiro-RJ, Brazil
[2]Laboratório de Microbiologia Ambiental, Centro de Biotecnologia, Universidade Federal da Paraíba
Campus I, João Pessoa-PB, Brazil
[3]Instituto Nacional de Tecnologia, Rio de Janeiro-RJ, Brazil
[4]Equipe Environnement et Microbiologie, MELODY Group
Université de Pau et des Pays de L'Adour, IPREM UMR CNRS 5254, BP 1155, 64013 Pau Cedex, France

ABSTRACT

The interest in preserving cultural heritage sites and artifacts has driven the development of additional measures to protect them from deterioration, which increases over time. The Garden of the Princess (Jardim da Princesa) located at the National Museum in Rio de Janeiro, Brazil, was the main site under evaluation in this work. Microbial colonization of the garden's walls was evaluated at two different areas by cultivation-based approach using specific media for fungi and bacteria, including total heterotrophic bacteria, acid and iron-producing bacteria. Results demonstrated that the higher cell density was detected in the sample from the higher humidity despite the limited humidity of the walls. Molecular identification of isolates revealed that Arthrobacter was the main bacterial genus in the biofilm, even though the others predominant genera have longer survival times during starvation and higher resistance to desiccation. Sessile fungi, despite fewer in number, were also quite diverse. In conclusion, even found in such hostile environment an interesting microbial diversity was observed in this study including four genera not yet reported as biodeterioration agents in heritage sites: bacteria *Ensifer*, *Enterobacter* and *Srenotrophomonas* and the fungus *Hypocreacea.*

Keywords: Jardim da Princesa, biodeterioration, biofilm, cultural heritage.

INTRODUCTION

The cultural heritage of a country is the legacy, including physical and intangible attributes, which make references to the identity, action and memory of different social groups. Therefore, cultural heritage includes natural environments such as landscapes, historic places and sites, buildings, and intangible items such as collections, past and continuing cultural experience, and knowledge (Tomaz, 2010; Ghirardello *et al.*, 2008; McKercher *et al.*, 2005).

One peculiarity of human civilization, since prehistory, is the ability to build temples and monuments motivated by religious principles or simply to show power (Mapelli *et al.*, 2012). Contemporary society finds in its cultural heritage their collective memory and is responsible to keep this living legacy for future generations. Therefore, the appreciation of historic monuments and the implementation of measures to maintain the cultural heritage of each nation is important (Tavin, 2004).

The preservation of assets exposed to outdoor environments is complex. Under this condition, the action of different physical and chemical factors such as rain, salinity, wind and air pollution, in association with microorganisms activity, particularly increases the wear of the materials, which contributes to the environmental disfigurement and restoration costs (Loh, 2011; Shirakawa *et al.*, 2008; Gaylarde and Gaylarde, 2005). The type of material and coatings used in buildings also has an influence on the colonization and biodeterioration. After metallic materials, concrete is the most susceptible material to deterioration process, which can be seen on its surface through crusting, loss of material, and color alterations (Resende, 2008; Sarró *et al.*, 2006). In addition, in outer walls, the composition of the structural material and the paint and dirt that accumulate in them can also be a nutritional source for microbial growth (Ciferri, 1999).

*Corresponding author e-mail: diogodias@eq.ufrj.br

The presence of microorganisms can increase the deterioration process by accelerating the kinetics of the reaction without altering the electrochemical phenomenon. However, the intensity of the biodeterioration depends on the amplitude of the microbial colonization, their composition, and their distribution on the surface (Beech and Gaylarde, 1999). In addition to the aesthetic problems, microbial colonization of solid surfaces can compromise the structure of the material and also be a health risk since bacterial and fungal spores can trigger respiratory problems and allergic reactions. Therefore, the biodeterioration process has been extensively studied since it involves constructions and human housing, such as bridges and buildings, and also cultural legacy represented by sculptures, statues and monuments (Sanchez-Moral *et al.*, 2005; Mapelli *et al.*, 2012).

The microbial colonization involves the adhesion of microorganisms to a given structure and the formation of biofilms. Biofilms are complex structures consisting of different microbial species embedded in a matrix made of extracellular polymeric substances (EPS), basically polysaccharides, and high content of water. In the biofilm, the coexistence of microorganisms of different metabolisms, and even the death of the cells enables a continuous supply of nutrients, which ensures the stability of the structure (Herrera and Videla, 2004; Costerton and Wilson, 2004).

In walls, different species from different microbial groups have been isolated, including bacteria, fungi and algae (Wei *et al.*, 2013; Murphy, 2002; Flores *et al.*, 1997). Among them, there are heterotrophic bacteria, particularly EPS-producing, considered primary colonizers, since the EPS favor the adhesion of cells to surfaces and its presence in biofilms allows the adherence of new microorganisms, and may serve as a substrate. The biogenesis of organic or inorganic acids may weaken the mineral structure of the wall or of the coating applied to them and also cause color changing. These acids may also encourage the development of other microbial species. The recurring problems of iron bacteria activity in outdoor walls are changes of color and the support for sulfur oxidizing bacteria activity. Fungi are mainly involved in the release of metabolites, which are often corrosive, whereas the mycelium contributes to the structure of the biofilm. However conventional microbiological techniques usually employed to characterize the microbial communities involved in biodeterioration processes allow only the identification of a small portion of the microorganisms involved (Lan *et al.*, 2010; Gu *et al.*, 1998).

The objective of this study was to investigate the microbial diversity on walls surrounding the Garden of the Princess, created by D. João VI in 1818, that was part of the residence of the Portuguese imperial family. Presently, the building is part of the National Museum of Rio de Janeiro, the largest museum of natural and anthropological history of Latin America. This is the first study characterizing biofilms on this site. The microbial characterization will allow better assessment of possible risks to property, as well as further insight into the conservation methods to be adopted (Lopez *et al.*, 2010).

MATERIALS AND METHODS

Site and Sampling Procedures

The Garden of the Princess is located in the Quinta da Boa Vista Park in the city of Rio de Janeiro, an urban area but with little vehicle traffic, wet and wooded. Samples were collected at two different areas in the concrete walls coated with paint. The wall is in a state of deterioration since the last recovery occurred more than 30 years ago (Fig. 1). The main constituents of the concrete, determined by X-ray diffraction were as follows: SiO_2 (60.6%), CaO (18.2%) and Al_2O_3 (4.0%).

The samples were collected by scraping the wall with a sterile spatula and a flexible plastic mold, disinfected by immersion in alcohol, to restrict the scraping zone to a known area. The mold had a square inner opening with $4cm^2$. Ten samples from each spot were collected for the microbiological analyzes. The samples were collected in penicillin bottles with 50 ml capacity containing 40 ml of reducing solution (0,85g/L sodium chloride, 0,134 g/L sodium thioglycolate, 0,1g/L ascorbic acid) previously weighed on an analytical balance to the tenth of a milligram. Samples were also collected in sterile Petri dishes to determine the moisture content of each material collected. Seasonal temperature in the area where the National Museum is located varied from 15.1 to 28.0°C, the relative humidity was between 31 to $81g/m^3$ and the average rainfall was 5.5 mL/day [data obtained during 15 days before sapling].

Microbiological Analyzes

The collected samples, previously homogenized and diluted, were poured on Petri dish using the spread plate technique. Different specific culture media were used including media for heterotrophic bacteria, acid producing bacteria and iron bacteria, as well as for fungi (Table 1), with addition of antimicrobials (nystatin or amoxilicin, $50mgL^{-1}$) to inhibit undesirable contaminants.

The specific media for growth of heterotrophic bacteria, acid producing bacteria, iron bacteria, and fungi were incubated in bacteriological incubator at 30°C for 2, 3, 4, and 5 days, respectively. After the incubation time the colonies were counted (colony forming units, CFU), or the growth was evaluated through the most probable number technique (MNP). All analyzes were performed in triplicate and the results shown in CFU/ cm^2 or NMP/cm^2.

Fig. 1. Wall from the garden of the princess. Numbers represented sampling sites.

Table 1. Cultivations conditions employed to determine the diversity of biofilms formed on the walls of the Garden of the Princess.

Microorganisms	Counting method	Media
Heterotrophic bacteria	SP	Nutrient agar added with Nys
Acid producing bacteria	MPN	Phenol red broth added with Nys
Iron bacteria	SP	Ammonium ferric citrate agar added with Nys
Total fungi	SP	Sabouraud agar added with Amx

SP – Spread Plate counting; MPN – Most Probable Number; Nys – nystatin (50mg.L^{-1}); Amx– amoxicilin (50mg.L^{-1}).

Identification of Predominant Groups of Bacteria and Fungi

The microorganisms were recovered from predominant colonies grown on agar plates. The DNA extraction was carried by thermal lysis. One isolated colony was picked and suspended in 50 µL ultrapure water (MilliQ^{TM}) in *eppendorf* tube (500 µL). The microbial suspension was treated by heat shock using dry bath, according to the program: 96°C for 10 minutes followed by 4°C for 30 minutes. Then, the material was centrifuged for 1 minute at 10,000g. The supernatant containing the DNA was transferred to a new tube and stored at -20°C until the amplification of DNA. The DNA amplification was conducted using the conventional PCR technique (PCR System 9700 thermocycler, Applied Biosystems) using the random primers, Sadir (5'-AGAGTTTGATCATGGCTCAGA-3') and S17 (5'-GTTACCTTGTTACGACTT-3') for bacteria. For fungi, the genomic DNA of each isolate was extracted employing the commercial *kit MOBio Ultra Clean^{TM}Microbial DNA Isolation*.

After the extraction, the concentration and degree of purity of the DNA were analyzed by spectrophotometer (NanoDrop Spectrophotometer - model ND-1000) at wavelengths of 230, 260 and 280 nm. The DNA amplification was conducted using the conventional PCR technique (PCR System 9700 thermocycler, Applied Biosystems) using the random primers, ITS4 (5'-TCCTCCGCTTATTGATATGC-3') and ITS5 (5'-GGAAGTAAAAGTCGTAACAAGG-3'). The conditions of amplification were 94°C/30 sec, 55°C/30 sec, 72°C/30 sec for bacteria and 94°C/30 sec, 50°C/30 sec, 72°C/30 sec for fungi with 30 cycles for both. All the

amplified products were analyzed in agarose gel (1%, m/v). After checking the efficiency of PCR procedures by electrophoresis, the amplified products were purified using the system Wizard® PCR Clean-Up System (Promega) according to the manufacturer's guidelines. The material was placed in a 96-well microplate containing from 30 to 60 ng of amplicon plus 2.5 pmol of primer suspended in ultrapure water (Milli-Q) qsp 6 uL. Each tube contained a single primer (Sadir and S17, for bacteria, and ITS4 and ITS5 for fungi) in duplicates per sample. The amplicons were labeled using primers in solution and 0.5 μL BigDye Terminator v3.1 reagent Standard Cycle Sequencing Kit (Applied Biosystems) in final volume of 10 μL. The labeling reactions were performed in a thermocycler LGC XP Cycler. The PCR conditions were 96°C/10 sec, 55°/5 sec, 60°C/4 sec, 25 cycles.

After the samples were purified by precipitation with isopropanol and washing with 75% to 60% ethanol, a dilution was performed with 10 μL Hi-Fi formamide (Applied Biosystems), denatured at 95°C for 5 min, cooled on ice for 5 min and electroinjecting Automatic Sequencer AB 3500 Genetic Analyzer with reinforced capillaries of 50 cm and polymer POP7 (Applied Biosystems). The sequences were edited and analyzed with an appropriate software (Chromas Lite® and Bioedit), GenBank (www.ncbi.nlm.nih.gov) and compared for similarity to other sequences already deposited by using BLAST software online.

RESULTS AND DISCUSSION

Even though the places where the two samples were collected were exposed to similar ranges of UV radiation and other climatic variations and were only 5-10 m apart from each other, both places had well-differentiated visual appearance of color and texture, revealing advanced process of biodeterioration (Fig. 1). At the time of sampling, the tropical climate characterized by mild temperatures and low precipitation, may have been the main factor for the low water content of the samples, 4.6 and 1.1%, in area 1 and 2, respectively.

The low humidity did not restrict the development of microbial biofilms on the walls. As shown in Table 2, both sampling areas had significant numbers of sessile microorganisms of different microbial groups. The highest microbial density was found in area 1, where the humidity was higher. The number of sessile microorganisms was different according to the place where the sample was taken from, particularly for iron bacteria. However, the number of fungi has remained in the same order of magnitude in both areas. The variation of microbial density may be due to variations in humidity, being lower in area 2.

Another study, Shirakawa *et al*. (2011) evaluated the characteristics of concrete walls coated with different formulations of acrylic paints for seven years of exposure to the elements, located in the urban area of São Paulo and in the coastal town of Ubatuba, State of São Paulo, Brazil. The discoloration and detachment of the coatings were more intense in Ubatuba. Phototrophic microorganisms and fungi were detected in all biofilms using standard microbiological methods. However, biofilms from Ubatuba had fewer numbers of fungi and higher number of phototrophic microorganisms. The authors attributed this fact to the higher humidity in the coastal region, due to increased precipitation.

Similarly, Guiamet *et al.* (2011), investigating the biofouling and biodeterioration of photos and maps stored at Historical Archive of the Museum of La Plata, Argentina, and two repositories of the National Archive of Cuba Republic, found an increased number of bacteria (2,148.7 CFU/m^3) and fungi (260.7 CFU/m^3) in areas where the relative humidity of the air and temperature were 75 g/m^3 and 28°C, respectively. In contrast, under 59 g/m^3 and 23.8°C, the microbial density decreased by 3 times for fungi and by 35 times for bacteria. Also, Papida *et. al.* (2000) observed that the microbial density was higher when the water content was also higher in constructions of dolomite (8.5%) and limestone (12.1%). According to these authors, the humidity increased the porosity of the material, resulting in the reduction of its strength and consequently increasing its vulnerability, leading to the erosion process.

Table 2. Biomass of cultivable microorganisms on the walls of the Garden of the Princess.

Microbial groups	**Cell counting**	
	Area 1	**Area 2**
Aerobic bacteria (CFU/cm^2)	$3.3x10^6$	$2.6x10^4$
Acid producing bacteria (MPN/cm^2)	$8.2x10^5$	$2.8x10^4$
Iron bacteria (CFU/cm^2)	$1.4x10^5$	ND
Fungi (CFU/cm^2)	$6.8x10^3$	$2.4x10^3$

ND – not detected (below the detection limit of the method).

The predominant cultivable sessile microbial cultures of each group, corresponding to 15 bacteria and 10 fungi. Table 3 shows the diversity of the microbial community in the biofilms formed on the walls of the Garden of the Princess in two different areas. According to López-Miras *et al.* (2014), bacteria and fungi that may survive as spores represent an important part of the microbial community which can accumulate on the surface for a long time.

The greater diversity of bacteria was found in the area with the lowest moisture content (area 2), which showed also the lower cell density. Likewise, in area 2 the diversity of fungi was slightly higher than that found in area 1, although the species constituents of each biofilm were quite different. Among the bacterial isolates obtained using culture-dependent methods, the *Artrobacter* genus stood out. And surprisingly, the other four genera of bacteria identified in this study have not yet been described in the literature as members of microbial communities in biofilms formed in buildings and historical heritage: *Ensifer*, *Stenotrophomonas rhizophila*, *Enterobacter* and *Rhodococcus*.

Artrobacter, belonging to the phylum Actinobacteria, is a common airborne and spore-forming microorganism inhabitant of the soil environment, in which it corresponds to more than one half of the total bacterial populations (Cross *et al.*, 2015; Scheublin and Leveau, 2013; Mongodin *et al.*, 2006). This genus, as well as *Pseudomonas* and *Bacillus*, are related to biofilm formation since they are typically heavily-encapsulated and fast-growing bacteria (López-Miras *et al.*, 2013). Interesting properties of these bacteria are the metabolic versatility, capable to growth at the expense of a minimum of nutrients and to degrade a wide variety of organic substances, including toxic ones, which contributes to recycle nutrients in the soil (Weiser *et al.*, 2014). In view of the above, the presence of these genera, in particular the genus *Arthrobacter*, in biofilms formed on the walls of the Garden of the Princess is mainly the result of the proximity of the sampling areas with soil and vegetation, as seen in figure 1. Heyrman *et al.* (2005) also isolated 21 bacterial strains from samples of biofilms from Servilia tomb (necropolis of Carmona, Spain) and the Saint-Catherine chapel (castle at Herberstein, Austria). All the isolates were allocated to the genus *Arthrobacter*, including six novel species, which proposed names were *A. castelli* spp. nov., *A. monumenti* spp. nov., *A. parietis* spp. nov., *A. pigmenti* spp. nov., *A. tecti* spp. nov. and A. *tumbae* spp. nov.

Similarly, to this present work, bacteria and fungi were isolated from microbial biofilms developing on the surfaces and within the painting layers of St Martin Church, Germany (Gorbushina *et al.*, 2004). The predominant bacteria belonged to the genera *Arthrobacter* and *Bacillus*. However, as reported by the authors, the microbial community was inactive. However, studies by Sarró *et al.* (2006) on the statues of lions, at the Alhambra Palace, Spain, attributed part of the responsibility on the monument deterioration process to *Arthrobacter*. While, Nuhoglu *et al.* (2006) stated that *Bacillus* sp. was the main responsible to the acceleration of the biodeterioration process of stone monuments in Turkey.

Among fungi, the predominance of *Fusarium* in area 1 was interesting as previous studies only identified it in isolated areas while *Cladosporium* and *Penicillium* stood out as the genera with higher prevalence (Elissawy *et al.*, 2015; Guiamet *et al.*, 2011; Nuhoglu *et al.*, 2006; Shirakawa *et al.*, 2002). Most *Fusarium* species is widely distributed in soil from temperate and subtropical regions. These fungi are able to grow in water and soil through the assimilation of organic matter in decomposition, and can also infect plants and animals. Some species are producers of mycotoxins, which can enter the food chain and affect the health of people and animals (Priest and Campbell, 1996).

In area 2, species of the *Pestalotiopsis* genus were predominant. In fact, *Pestalotiopsis* species are largely distributed worldwide (Jeewon *et al.*, 2003; Wang *et al.*, 2005). Similarly, to most fungi, they can grow from a wide range of substrata, as saprobes in soil, and plant pathogens, even though endophytic *Pestalotiopsis*are considered being the most important community in nature, inhabiting leaves, branches, stalks and seeds. Some endophytic *Pestalotiopsis* have been shown to produce important bioactive products such as antimicrobial and antitumor compounds of potential application in medicinal area (Wei *et al.*, 2007; Li *et al.*, 2001). Endophytic *Pestalotiopsis* have been isolated mainly in the subtropical and tropical regions (Liu *et al.*, 2007). In Brazil, *Pestalotiopsis* species have been reported in almost all the territory, although its identification is difficult due to the known morphological variation between different species (Jeewon *et al.*, 2003). Ramos-Mariano *et al.* (1998) found *P. palmarum* to be the main fungus in coconut in Brazil. More recently, two fungal species, *P. neglecta* and *P. maculiformans*, were isolated from the air inside the imperial coach, first used in the consecration and coronation ceremony of King Pedro II in 1841, and then on solemn occasions (Lutterbach *et al.*, 2013). Currently, the coach is part of the Imperial Museum collection, located in Petropolis, Rio de Janeiro.

Gorboushina *et al.* (2004) isolated thirty-two fungal species by cultivation methods. Most of the fungi were identified as *Acremonium*, *Aspergillus*, *Cladosporium*, and *Fusarium*. A *Cladosporium* specie was also detected in one of the biofilms of this present work, but unlike no *Aspergillus* species and only one *Pestalotiopsis* specie

Table 3. Microbial diversity of the biofilms on the walls of the Garden of the Princess.

Area 1		**Area 2**	
Bacteria	S	Bacteria	S
Artrobacter spp.[1]	85%	*Artrobacter* sp[1]	99%
Artrobacter sp.[1]	100%	*Bacillus megaterium*[3]	100%
Artrobacter spp.[1]	100%	*Bacillus megaterium*[3]	100%
Artrobacter spp.[1]	100%	*Enterobacter* sp.[4]	84%
Artrobacter spp.[1]	100%	*Enterobacter* sp.[4]	91%
Ensifer spp.[2]	97%	*Rhodococcus* sp.	90%
Ensifer spp.[2]	92%	*Stenotrophomonas rhizophila*	100%
Pseudomonas mexicana	100%		
Fungi	S	Fungi	S
Hypocreaceae sp.	100%	*Cladosporium* spp.	100%
Fusarium oxysporum	99%	*Hypocreales* spp.	100%
Fusarium domesticum	96%	*Pestalotiopsis* spp.[5]	99%
Penicillium spp.	99%	*Pestalotiopsis disseminata* [5]	99%
		Pleosporales spp.[5]	99%

S – similarity. [1] Six different isolates *Artrobacter*. [2] Two different isolates *Ensifer*. [3] Two different isolates *Bacillus megaterium.* [4] Two different isolates *Enterobacter*. [5] Three different isolates *Pestalotiopsis.*

could be detected by the conventional cultivation technique. This is unusual since spores of those fungi are frequently present in the air and soil. However, the investigation of microbial communities adhered to the obverse and the reverse sides of an oil painting on canvas, exhibiting signs of biodeterioration, employing culture-dependent technique also revealed the presence of solely *Penicillium* spp. (López-Miras *et al.*, 2013). According to the authors, the results may be related to the indoor quality of the air of the room where the painting was exposed. Air samples showed bacteria and fungi numbers ranging between 200 and 500 CFU/m^3, including fungal isolates from the genera *Alternaria*, *Ulocladium*, *Stachybotrys*, *Cladosporium*, and mainly *Penicillium* (46.2 % phylogenetically identified). *Mucor*, *Aspergillus* and *Eurotium* were solely detected through genetic techniques. Besides, differences in the community structure could be observed when using different techniques, wherein in some cases the counts were below the detection limit of the technique used.

In this study, the *Hypocreales* fungus was one of the most predominant in the biofilms. This is the first report on their presence associated to communities adhering to solid surfaces. These microorganisms form haustoria and occur naturally as parasites of plants and have a vibrant color in the fruiting body, usually yellow, orange or red. Species of this genus are also found in the lichen form (Silanes *et al.*, 2009). There are reports of the isolation of *Hypocreales* spp. from the anaerobic fermentation of organic waste (Kazda *et al.*, 2014) and marine-derived *Hypocreales* capable of producing bioactive terpenes (Elissawy *et al.*, 2015).

The present study demonstrates that structures of the same area are subject to different microbial colonization, which is a critical problem when setting the restoration strategy of cultural heritage. Moreover, it was possible to identify the presence of fungi and, mostly bacteria, whose metabolism can aggravate the deterioration by releasing substances that promote the change in color of the walls, or whose corrosive action damages the structure and coatings usually used for the protection of these buildings. Most of the identified species have low nutritional requirements and are high enzymatic producers of extracellular enzymes, such as proteases, esterases and lipases, which activities contribute to the loss of material (Ciferri, 1999). As pointed out by some researchers, the correct conservation and restoration of biodeteriorated buildings and monuments needs a detailed knowledge of the microbial communities associated with these substrates and changes of the natural environment and climate conditions (Capodicasa *et al.*, 2010; Suihko *et al.*, 2007; Schabereiter-Gurtner *et al.*, 2001). This type of research is still little explored in Brazil which has allowed many of the artifacts and monuments of the Brazilian heritage suffer from progressive deterioration. Therefore, ways to control biofilm formation must be studied in order not to miss the cultural heritage left by our ancestors.

CONCLUSION

The analysis of the microbial community adhered to the outdoor walls of the Garden of the Princess, part of the National Museum of Rio de Janeiro, Brazil was performed using culture-dependent techniques. Our

results demonstrated that fungi and particularly bacteria were the main members of the microbial communities adhered to the surfaces, despite the limited humidity of the walls. Molecular identification of isolates revealed that *Arthrobacter* was the main bacterial genus in the biofilm, even though the others predominant genera have longer survival times during starvation and higher resistance to desiccation. Sessile fungi, despite fewer in number, were also quite diverse in the communities' structures. Our results confirm that bacteria of the genera *Arthrobacter*, *Bacillus*, *Pseudomonas* and fungi of the genera *Pestalotiopsis*, *Pleosporales*, *Fusarium*, *Penicillium* and *Cladosporium* are widespread in microbial communities adhered to outdoor walls in tropical areas. In addition, three bacterial species that were identified as *Ensifer* spp., *Stenotrophomonas rhizophila*, *Enterobacter* spp. and one fungi species, *Hypocreaceae* spp., have not yet been described in wall as biodeterioring agent.

ACKNOWLEDGEMENT

The authors would like to thanks CNPq and CAPES (Fellowship Program number 99999.008278/2014-08) for the financial support and to CETEM for the mineralogical characterization analysis of the walls.

REFERENCES

Beech, IB. and Gaylarde, CC. 1999. Recent advances in the study of biocorrosion – an overview. Revista de Microbiologia. 30:177-190.

Capodicasa S., Fedia S., Porcellia AM. and Zannoni, D. 2010. The microbial community dwelling on a biodeteriorated 16th century painting. International Biodeterioration and Biodegradation. 64:727-733.

Ciferri, O. 1999. Microbial Degradation of Paintings. Applied and Environmental Microbiology. 65: 879-885.

Costerton, WJ. and Wilson, M. Introducing biofilms. 2004. Biofilms. 1:1-4.

Cross, T., Schoff, C., Chudoff, D., Graves, L., Broomell, H., Terry, K., Farina, J., Correa, A., Shade, D. and Dunbar, D. 2015. An optimized enrichment technique for the isolation of *Arthrobacter* bacteriophage species from soil sample isolates. Journal of Visualized Experiments. 98: doi:10.3791/52781.

Elissawy, AM., El-Shazly, M., Ebada, SS., Singab, ANB. and Proksch, P. 2015. Bioactive terpenes from marine-derived fungi. Marine Drugs. 13:1966-1992.

Flores, M., Lorenzo, J. and Gómez-Alarcón, G. 1997. Algae and bacteria on historic monuments at Alcala de Henares, Spain. International Biodeteriorioration Biodegradation. 40:241-246.

Gaylarde, CC. and Gaylarde, PM. 2005. A comparative study of the major microbial biomass of biofilms on exteriors of buildings in Europe and Latin America. International Biodegradation and Bioterioration. 55:131-139.

Ghirardello, N., Spisso, B., Faria, GGM., Conselho Regional de Engenharia, Arquitetura e Agronomia do Estado de São Paulo. 2008. O que é patrimônio cultural? In: Patrimônio Histórico: Como e por que preservar. Ed. Canal 6. Bauru, Brazil. pp13.

Gorbushina, AA. 2004. Fungi and Biochemical cycles. Cambridge University Press, Cambridge, UK.

Guiamet, P., Borrego, S., Lavin, P., Perdomo, P. and Saraiva, SG. 2011. Biofouling and biodeterioration in materials stored at the Historical Archive of the Museum of La Plata, Argentine and at the National Archive of the Republic of Cuba. Colloids and Surfaces B: Biointerfaces. 85:229-234.

Gu, JD., Ford, TE., Berke, NS. and Mitchell, R. 1998. Biodeterioration of concrete by the fungus *Fusarium*. International Biodegradation and Biodeterioration. 41:101-109.

Herrera, LK. and Videla, H. 2004. The importance of atmospheric effects on biodeterioration of cultural heritage constructional materials. International Biodeterioration and Biodegradation. 54: 125-134.

Heyrman, J., Verbeeren, J., Schumann, P., Swings, J. and de Vos, P. 2005. Six novel *Arthrobacter* species isolated from deteriorated mural paintings. International Journal of Systematics and Evolutionary Microbiology. 55:1457-1464.

Jeewon, R., Liew, ECY., Simpson, JA., Hodgkiss, IJ. and Hyde, KD. 2003. Phylogenetic significance of morphological characters in the taxonomy of *Pestalotiopsis* species. Molecular Phylogenetics and Evolution. 27:372-383.

Kazda, M., Langer S. and Bergelsdorf, FR. 2014. Fungi open new possibilities for anaerobic fermentation of organic residues. Energy, Sustentability and Society. 4:1-9.

Lan, W., Li, H., Wang, WD., Katayama, Y. and Gu, JD. 2010. Microbial community analysis of fresh and old microbial biofilms on Bayon Temple sandstone of Angkor thom, Cambodia. Environmental Ecology. 60:105-115.

Li, JY., Harper, J.K., Grant, DM., Tombe, BO., Bashyal, B., Hess, WM. and Strobel, GA. 2001. Ambuic acid, a highly functionalized cyclohexenine with antifungal activity from *Pestalotiopsis* spp. and *Monochaetia* sp. Phytochemistry. 6:463-168.

Liu, AR., Xu, T. and Guo, LD. 2007. Molecular and morphological description of *Pestalotiopsis hainanensis* sp. nov., a new endophyte from a tropical region of China. Fungal Diversity. 24:23-36.

Loh, KS. 2011. No more road to walk: cultures of heritage and leprosariums in Singapore and Malaysia. International Journal of Heritage Studies. 17:230-244.

Lopes, D., Vlamakis, H. and Kolter, R. 2010. Biofilms. Cold Spring Harbor Perspectives in Biology. 2:1-11.

López-Miras, MM., Martín-Sanchéz, I., Yebra-Rodriguéz, A., Romero-Noguera, J., Bolívar-Galiano, F., Ettenauer, J., Sterflinger, K. and Piñar, G. 2013. Contribution of the microbial communities detected on an oil painting on Canvas to its biodeterioration. PLoS one. 8:1-13.

Lutterbach, MTS., Oliveira, ALC., Zanatta, EM. and Costa, ACA. 2013. A berlinda de aparato do imperador D. Pedro II: identificação de fungos em partes selecionadas e sua relação com biodeterioração e aerobiologia. Conservation Património. 17:59-72.

Mapelli, F., Morasco, R., Balloi, A., Rolli, E., Cappitelli, F., Daffinchio, D. and Borin, S. 2012. Mineral-microbe, interactions: biotechnological potential of bioweathering. Journal of Biotechnology. 157:473-481.

McKercher, B., Ho, PSY. and Du Cros, H. 2005. Relationship between tourism and cultural heritage management: evidence from Hong Kong. Tourism Management. 26:539-548.

Mongodin, EF., Shapir, N., Daugherty, SC., Deboy, RT., Emerson, JB., Shvartzbeyn, A., Radunem D., Vamathevan, J., Riggs, F., Grinberg, V., Khouri, H., Wackett, LP., Nelson, KE. and Sadowsky, MJ. 2006. Secrets of soil survival revealed by the genome sequence of *Arthrobacter aurescens* TC1. PLoS Genetics. 2:2094-2106.

Murphy, C. 2002. Blue-green algae and its effect on fiber-cement roofing within a microclimate. Interface. 1:4-12.

Nuhoglu, Y., Oguz, E., Uslu, H., Ozbek, A., Ipekoglu, B., Ocak, I. and Hasenekoglu, I. 2006. The accelerating effects of the microorganisms on biodeterioration of stone monuments under air pollution and continental-cold climatic conditions in Erzurum, Turkey. Science of the Total Environment. 364:272-283.

Papida, S., Murphy, W. and May, E. 2000. Enhancement of physical weathering of building stones by microbial populations. International Biodeterioration and Biodegradation. 46:305-317.

Priest, FG. and Campbell, I. 1996. Brewing Microbiology. Chapman and Hall, London, UK.

Ramos-Mariano, RL., Fernandes-de-Lira, RV., Silveira, EB., Menezes, M., Ramos-Marino, R., Fenandes, LRV and Silveira, EB. 1998. Survey of endophytic and epiphytic fungi from coconut leaves in the Northeast of Brasil: Effect of the locality on the fungal population. Agrotropica. 10:1-8.

Resende, MA. 2008. Biodeterioração de monumentos históricos. EMBRAPA, Jaguariúna, Brazil.

Sanchés-Moral, S., Luque, L., Cuezva, S., Soler, V., Benavente, D., Laiz, L., Gonzáles, JM. and Saiz-Jimenez, C. 2005. Deterioration of building materials in Roman catacombs: the influence of visitors. Science of the Total Environment. 349:260-276.

Sarró, MI., García, AM., Rivalta, VM., Moreno, DA. and Arroyo, I. 2006. Biodeterioration of the lions fountain at the Alhambra palace, Granada (Spain). Building Environment. 41:1811-1820.

Silanes, MEL., Etayo, J. and Paz-Bermúdez, G. 2009. *Pronectria pilosa* (Hypocreaceae) spp. nov. and other lichenliconous fungi found on Collemataceae in the Iberian peninsula. The Bryologist. 1:101-108.

Schabereiter-Gutner, C., Pinar, G., Lubitz, W. and Rölleke, S. 2001. Analysis o fungal communities on historical church window glass by denaturing gradient gel electrophoresis and phylogenetic 18S rDNA sequence analysis. Journal of Microbiological Methods. 47:345-354.

Shirakawa, MA., Gaylarde, CC., Gaylarde, PM., John, V. and Gambale, W. 2002. Fungal colonization and succession on newly painted buildings and the effect of biocide. FEMS Microbiology Ecology. 39:165-173.

Shirakawa, MA., John, VM. and Cincotto, MA. 2008. Microbiologia Ambiental. EMBRAPA, Jaguariúna, Brazil.

Shirakawa, MA., John, VM., Silva, MES. and Gaylarde, CC. 2011. Biodeterioration of painted mortar surfaces in tropical urban and coastal situation: comparison of four paint formulations. International Biodeterioration and Biodegradation. 65:669-674.

Scheublin, TR. and Leveau, JH. 2013. Isolation of *Arthobacter* species from the phyllosphere and demonstration of their epiphytic fitness. Microbiology Open. 2:205-213.

Suihko, LM., Alakomi, LH., Gorbushina, AA., Fortune, I., Marquardt, J. and Saarela, M. 2007. Characterization of Aerobic Bacterial and Fungal Microbiota on Surfaces of Historic Scottish Monuments. Systematic and Applied Microbiology. 30:494-508.

Tavin, KM. 2004. If you see something, say something: visual events at the visual culture gathering. Visual Arts Research. 32:2-6.

Tomaz, PC. 2010. A preservação do patrimônio cultural e sua trajetória no Brasil. Revista de História e Estudos Culturais. 7:1-12.

Wang, Y., Guo, LD. and Hyde, KD. 2005. Taxonomic placement of sterile morphotypes of endophytic fungi from *Pinus tabulaeformis* (*Pinaceae*) in northeast China based on rDNA sequences. Fungal Diversity. 20:235-260.

Wei, S., Jiang, Z., Liu, H., Zhou, D. and Sanchez-Silva, M. 2013. Microbiologically induced deterioration of concrete-a review. Brazilian Journal of Microbiology. 44:1001-1007.

Wei, JG., Xu, T., Guo, LD., Liu, AR., Zhang, Y. and Pan, XH. 2007. Endophytic *Pestalotiopsis* species associated with plants of Podocarpaceae, Theaceae and Taxaceae in southern China. Fungal Diversity. 24:55-74.

Weiser, R., Donoghue, D., Weightman, A. and Mahenthiralingam, E. 2014. Evaluation of five selective media for the detection of *Pseudomonas aeruginosa* using a strain panel from clinical, environmental and industrial sources. Journal of Microbiological Methods. 99:8-14.

Received: May 27, 2016; Revised: June 23, 2016;
Accepted: June 29, 2016

Canadian Journal of Pure and Applied Sciences
Vol. 10, No. 3, pp. 3951-3960, October 2016
Online ISSN: 1920-3853; Print ISSN: 1715-9997
Available online at www.cjpas.net

FATTY ACID PROFILING AND CLASSICAL TAXONOMY FOR CHARACTERIZATION AND IDENTIFICATION OF ENDOPHYTIC COELOMYCETES

*Kamalraj Subban[1], Ramesh Subramani[2] and Muthumary Johnpaul[1]
[1]Centre for Advanced Studies in Botany, University of Madras, Guindy Campus, Chennai - 600 025, India
[2]Department of Biology, School of Sciences, College of Engineering, Science and Technology
Fiji National University, Natabua Campus, Lautoka, Fiji Islands

ABSTRACT

This study aimed to analyze the endophytic coelomycetes under direct and indirect methods from stems of *Mangifera indica*, *Rhododendron arboreum*, *Taxodium distichum* and *T. mucronatum*. Both direct and indirect methods were effective for isolation, and identifying endophytic coelomycetous fungi such as *Botryodiplodia* sp., *Colletotrichum* sp., *Pestalotiopsis* spp., *Bartalinia* sp., *Monochaetia* spp., *Seimatosporium* sp. and *Truncatella* sp. All the fungi are reported from this study has been identified up to species level based on classical taxonomy using microscopic techniques and chemotaxonomy. This study demonstrates first time that fatty acid profile can be used for chemotaxonomical identification of coelomycetous fungi, *Pestalotiopsis* spp. and other genera. In addition, the fatty acid profile has not only facilitated to determine chemotaxonomy distribution, also provided an evidence for further research in fungal secondary metabolites and mycodiesel technology.

Keywords: Endophytic fungi, Coelomycetes, *Pestalotiopsis* spp., Ascomycotina, Deuteromycotina.

INTRODUCTION

The term endophyte (Gr. Endon - within; phyton - plant) was first introduced by De Bary (1866) who defined it as 'organisms that colonize internal plant tissue'. The biological association between the fungus and its host is considered to be pathogenic (Sieber, 2002), mutualistic (Redman *et al*., 2002), commensalistic (Deckert *et al*., 2001) and latent pathogenic (Schulz *et al*., 1998). It was estimated that there are 1.5 million species of fungi on Earth; of which, only 75,000 species have been described so far (Hawksworth, 2001). Nevertheless, several novel or new fungal genera and species are hidden; it is possible to locate them by identifying their habitats (Hyde, 2001). The internal tissues of plants harbouring endophytes may well account for a substantial number of such new reports. Approximately 300,000 plant species growing in unexplored area on the Earth are host for number of endophytes (Strobel and Daisy, 2003). Earlier reports indicated that endophytic coelomycetous fungi were studied for over three decades (Webber and Gibbs, 1984; Stone *et al*., 1996; Suriyanarayanan and Vijaykrishna, 2001). The term coelomycete was mainly used to indicate that conidia are formed within a cavity lined by fungus or fungal host tissue. Hence, it may be considered as coelo-holo, mycetes-fungi. The growth of coelomycetous fungi mainly depends upon the host specificity and it may emerge as saprophytic or endophytic organisms for ecological commensalisms (Kirk *et al*., 2001). The diversity of endophytic coelomycetes from various tree species was subjected to biotechnological approach because of the colony frequencies accumulated over the time; the age of leaves and needles are strongly correlated with the fungal colonization (Helander *et al*., 1993; Carroll, 1995; Magan *et al*., 1996). Considering that, only few studies were carried out on endophytic coelomycetes (Lehtijarvi and Barklund, 2000; Poteri *et al*., 2001; Arnold and Herre, 2003). A recent report has motivated to evaluate and elucidate the potentials of these microorganisms applied on biotechnological processes focusing on the production of bioactive compounds (Pimentel *et al*., 2011). The production of bioactive substances by endophytic fungi is directly related to the independent evolution of these microorganisms, which may have incorporated genetic information from higher plants, allowing them for better adaptation to plant host and carry out some functions such as protection from pathogens, insects, and grazing animals (Strobel *et al*., 1996a). Endophytes are chemical synthesizer inside plants in other words; they play a role as a selection system for microbes to produce bioactive substances with low toxicity towards higher organisms (Strobel *et al*., 1996b). However, attempt has not been made so far to find out the

*Corresponding author e-mail: kamalsubban@gmail.com

endophytic coelomyceteous fungi from Chennai and Ootcamund in the Indian state of Tamil Nadu by direct method. Therefore, the present investigation has attempted on isolation of endophytic coelomyceteous fungi from inner stems of *Mangifera indica*, *Rhododendron arboreum*, *Taxodium distichum* and *T. mucronatum* using direct method and indirect method as well. In addition, this investigation reporting first time fatty acid profile can be used in chemotaxonomical identification of the endophytic fungi.

MATERIALS AND METHODS

Plants collection and sampling methods

The plant samples were collected from forest at Tamil Nadu Botanical Garden (2623 m above sea level) in Ootcamund, Nilgiri district is located between 10-38 and 11-49 North Latitude and between 76-0 and 77-15 East Longitude in South India.

Stems from the healthy plants, *Mangifera indica*, *Rhododendron arboreum*, *Taxodium distichum* and *T. mucronatum* were collected during four different season such as South West monsoon (July-September), North East monsoon (October-Navember), monsoon season (December-February) and summer season (April-June) between 2008 and 2009. In addition, leaflets and petioles were collected and brought to laboratory in separate plastic bags. All the samples were processed within 24 h. The bark and stem samples were subjected for surface sterilization as described by Kamalraj *et al*. (2008). One hundred and fifty small pieces of stems are approximately 0.5 cm diameter were cut from the upper, middle and lower portions of stems with the aid of a flame-sterilized scalpel blade.

The leaf were surface sterilized by immersion in 70% ethanol for 5 sec followed by 4% sodium hypochlorite for 90 sec and then rinsed in sterile distilled water for 10 sec. After surface sterilization, the tissues were dried on sterilize tissue paper.

Examination of endophytic fungi in stem by light microscopy using direct method

The stem samples fixed using 4% paraformaldehyde in 0.1 M phosphate buffer (pH 7.2) at 4°C for overnight. The fixed specimens were rinsed with the 0.1 M phosphate buffer for 3 times and then dehydrated by ethanol dilution series about 30%, 70%, 83%, 95% and 100% for 2 sec (Gao *et al*., 2005). The thin sections of healthy stems about 5-10 µm were taken manually by using sterile razor blade and placed in the sterile water. Then, the stem sections were taken with the help of a single eye lash brush and placed on a glass slide with a drop of sterile distilled water. The slides were then placed on the slide warmer at 50°C for 1 min for adhesion of the sample on to the slide. The sections were further stained with 2, 3, 5-triphenyltetrazolium chloride and 1% aniline blue and mounted using DPX mount. The sections were photomicrographed using phase contrast microscope (Carl Zeiss Axiostar plus-photomicroscope) with camera by using Konica films and Nikon HFX Labophot bright field microscope.

Isolation and identification of endophytic fungi from leaves by indirect method

The surface sterilized leaf segments were evenly placed in Petri dishes containing potato dextrose agar (PDA) media amended with chloramphenicol 150 mg l^{-1} and incubated at 26 ± 1°C in a light chamber (Bills and Polishook, 1992). The growth of endophytic fungal colonies from the leaf segments were monitored every day. The hyphal tips, which grew out from the leaves segments were isolated and subsequent sub-culture was made to bring as a pure culture. The purified endophytic fungi were identified to species level by using standard keys by microscopy characteristic features (Guba, 1961; Sutton, 1980; Nag Raj, 1993). All the purified fungal cultures are preserved using 15% glycerol and stored at -80 °C.

Illustration and photomicrographs of endophytic fungi using light microscope

Photomicrographs of conidiomata, conidiogenous cells and conidia were taken using phase contrast microscope with camera by using Konica films and Nikon HFX Labophot light microscope. The vertical sections of the conidiomata were taken and the conidia were observed under oil immersion microscope (100X, 320X and 700X) and photographed.

Identification of endophytic fungi

The microscopic characteristics of the isolated endophytic fungi were observed by microslide preparation of the fruiting bodies and conidia. The endophytic fungi were identified on the basis of the structure of fruiting body (conidiomata), conidiogenous cells and conidia (Sutton, 1980). As, the presence of appendage on the conidia is now being recognized as an important taxonomic criterion (Guba, 1961; Sutton, 1973a; 1973b), the present study is also critically examined the appendage on the conidia of the isolated endophytic fungi.

Identification of coelomycetes up to different morphospecies levels were carried out by using standard mycology manuals (Guba, 1961; Sutton, 1980; Nag Raj, 1993). Descriptions of the coelomycetous fungi are included in the present study along with the photomicrographs.

Scanning electron microscopy studies on endophytic fungi

The surface morphology of the fungal spore samples has been analyzed by using Scanning Electron Microscope (SEM) (Hitachi S-3400N, USA) employing

cathedoluminescence detector (CLD) to distinguish conidia, spores, septa and appendages were measured for the selective fungal samples (*Bartlinia robillardoides, Seimatosporium mariae, Monochaetia circularis, M. kansensis, Truncatella angustata* and *Pestalotiopsis mangiferae*). The sample preparation of endophytic fungal spores for SEM studies has followed described by Abdel-Kareem and Szostak-Kotowa (1999).

Fatty acids isolation from endophytic fungi

All the fungal pure cultures were grown in 250 ml Erlenmeyer flask containing 50 ml of potato dextrose broth (PDB) at 27 ± 2°C for 15 days under static condition. After incubation, the mycelial mat of each culture was filtered using filter paper and washed with sterile distilled water. The excess water was drained out by pressing the mycelial mat using blotting paper. The mycelial mat of each fungus was lyophilized (FlexiDry™) for desiccation.

Chemotaxonomy of *Pestalotiopsis* spp. and other genera

Two grams of each fungal mycelial mat were ground separately with sterile mortar and pestle by adding ether (100 ml). The mixture was shaken on a flatbed orbital shaker for 12-16 h, which was allowed to settle out until clear. Then, an aliquot of 10 ml was removed and diluted with 10 ml of 5% saline solution and extracted with hexane. The hexane fraction was allowed to dry under vacuum at 40°C. The each sample was added to a glass column (10×250 mm) packed with 1 g of dry silica gel (60-120 A°) and then it was eluted with a mixture of 100 ml chloroform and methanol (2:1). The collected sample was allowed to dry in rotary evaporator under vacuum at 45°C. The dried sample was re-dissolved in hexane and then it was subjected to GC-MS analysis.

RESULTS AND DISCUSSION

The endophytic flora differs on the type and number in their host depends upon the host geographical position (Arnold and Herre, 2003; Gange *et al*., 2007). In the present investigation, a total of 74 different morphospecies of coelomycetes have been isolated and identified from 14,400 segments of healthy tissues collected from four plants such as *M. indica, R. arboreum, T. distichum* and *T. mucronatum*. During the isolation of endophytes, some hyphomycetous fungal colonies were also obtained. The phylloplane fungi such as *Alternaria* sp., *Aureobasidium* sp. and *Cladosporium* sp. were routinely isolated as endophytes from the wide range of plant species (Bills, 1996). Moreover, the phylloplane fungi are capable of penetrating the superficial layers of the leaf or may be localized in the substomatal chambers (Cabral *et al*., 1993). Earlier reports on leaf and stem endophytes were largely based on cytological and visual examination (Stone, 1985), however in the present study, spores of coelomyctes were observed using light microscopy; *Botryodiplodia* sp., and *Colletotrichum* sp., mycelia were observed below epidermis and cortex regions in the young stems (Fig. 1). Very few mycelia with spores were also observed inside the xylem parenchymatous ray cells in *T. mucronatum* by direct section method. The mycelium infects single cells and establishes small intracellular thalli (Baayen *et al*., 2002). However, many fungi reported as endophytes on a broad range of hosts, but only few are achieved sporulation (Baayen *et al*., 2002). Among the host plants, the *T. mucronatum* exhibited three interesting appendage bearing coelomycetous fungi *P. microspora, M. circularis* and *T. angustata* followed by *T. distichum* (*M. karstenii* and *S. mariae*), *M. indica* (*P. microspora*) and *R. arboretum* (*B. robillardoides*). The results are clearly revealed that *T. mucronatum* bearing rich diversity of endophytic coelomycetous fungi (Kamalraj and Muthumary, 2013).

Fungal systematic is an essential part of biological research especially in the context of the ecological, economical and biotechnological approaches. Such important fungi is studied in this investigation such as *Pestalotiopsis* sp. MUBL1002, *Bartalinia* sp. MUBL1096, *Monochaetia* sp. MUBL 1100, *Seimatosporium* sp. MUBL1107 and *Truncatella* sp. MUBL1109 for species level identification and their antimicrobial properties. *Monochaetia* sp. MUBL 1101 and *Pestalotiopsis* sp. MUBL1013 are producing anticancer drug Taxol (Unpublished data). The *Pestalotiopsis* spp. were noted in the wanted list of fungal culture in American Mycological Society since 2006 (http://MSAfungi.org). *Pestalotiopsis* spp. is heterogeneous group of coelomycetous fungi and their inter-specific delineation of the genus has been based on the conidial morphology (Guba, 1961; Nag Raj, 1993), conidiogenesis (Sutton, 1980) and the telomorph associations (Zhu *et al*., 1991; Metz *et al*., 2000). There has been considerable ambiguity and confusions in inter-generic classification, which has been dealt in different aspects by various researchers (Guba, 1961; Sutton, 1980; Nag Raj, 1993; Jeewon *et al*., 2002). In addition, taxonomy of the coelomycetous fungi, *Pestalotiopsis* spp. and other closely related genera based on the morphological characters has also been equivocal. Therefore analysis of molecular data combined with morphological data resolves many disputes in the identification of coelomycetous fungi (Jeewon *et al*., 2002). However, this study used both classical- and chemo- taxonomy for the identification of *Pestalotiopsis* spp. and other allied genera. Similarly, Jeewon *et al*. (2002) and Li *et al*. (2013) applied chemotaxonomy along with classical taxonomy for identification of *Pestalotiopsis* and allied genera. In the classical taxonomy of this study, the size of conidia, length of appendages, pigmentation of the septa and cells, and appendages

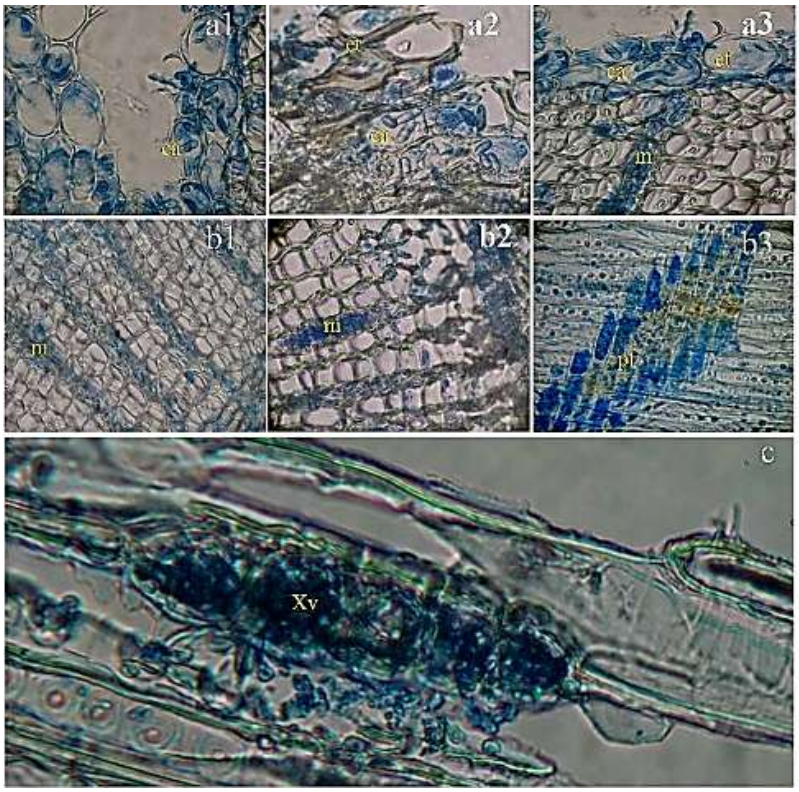

Fig. 1. Microscopic examination of fungal spores and mycelia from the plant samples.
a1-a3: Cross section of bark; b1-b3: Cross section of stem; c: Xylem vessels; ca: Conidia; et: Epidermis tissue; m: Mycelium; pt: Phloem tissue; Xv; Xylem vessels.

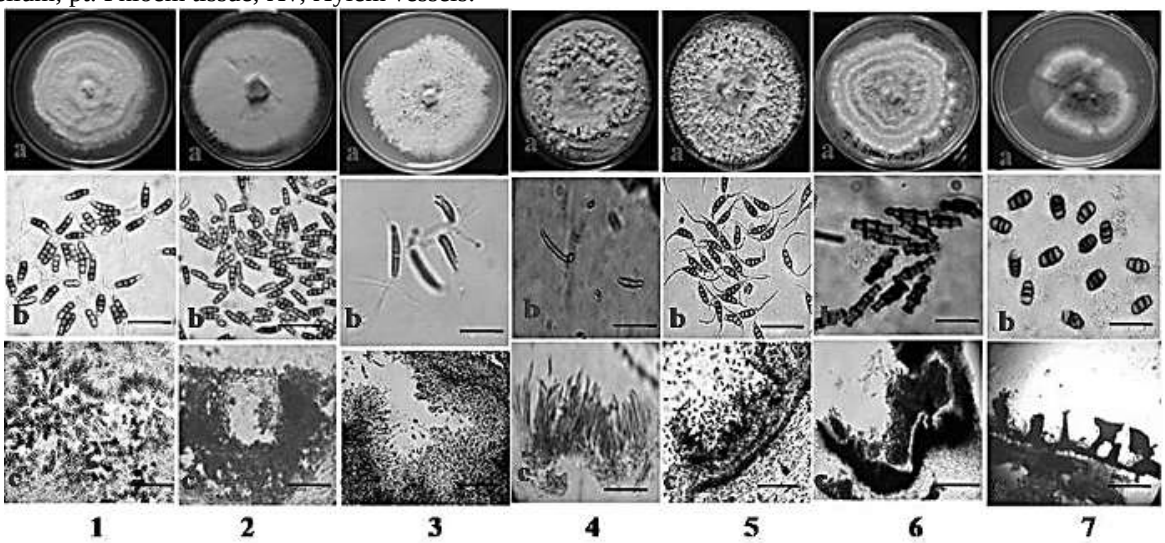

Fig. 2. Culture plate, size of conidia, length of appendages, pigmentation of the septa and cells, and appendages origination of *Pestalotiopsis* spp. and allied genera.
a. culture, b. conidia, c, conidiomata
1: *P. mangifera* ; 2: *P. microspora*; 3: *B. robillardoides*; 4: *M. circularis*; 5: *M. karstenii*; 6: *S. mariae*; 7: *T. angustata*

origination with mycelial morphology (Fig. 2) were analyzed for the identification. The characteristics such as number of median cells, which may or may not be pigmented, presence of apical and basal appendages and hyaline apical or basal cells have carefully been observed in the present study for coelomycetous fungi identification of *Pestalotiopsis* spp. and other genera as described by Jeewon *et al*. (2002). The characteristic feature of each fungus is given below:

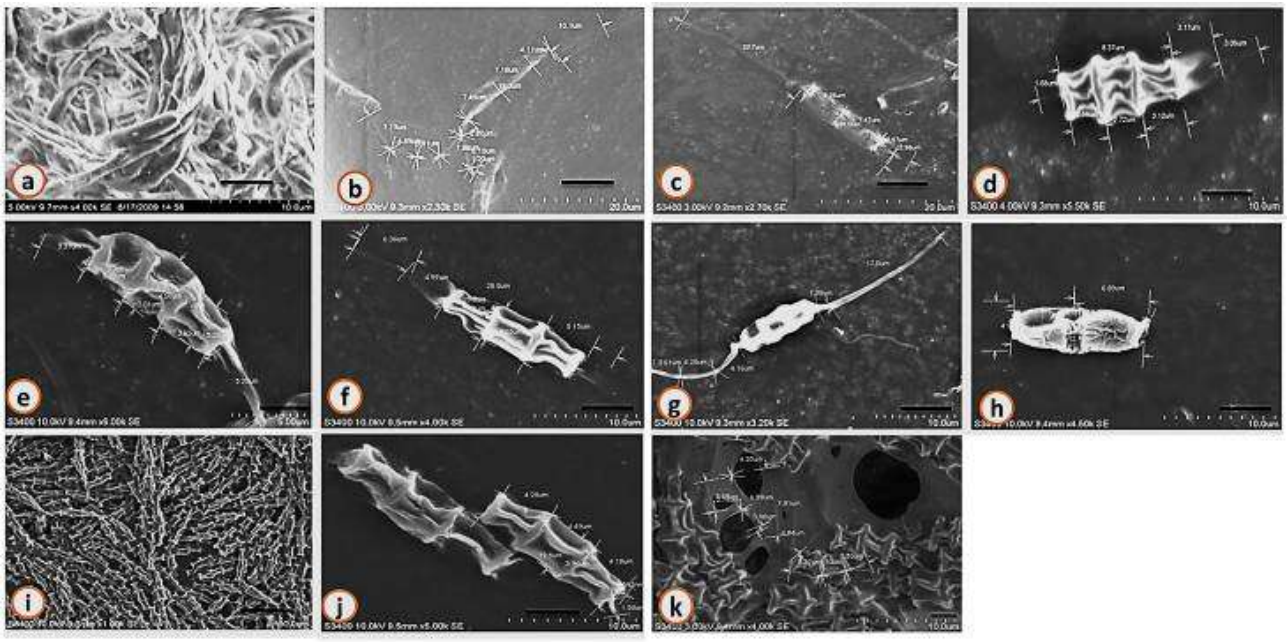

Fig. 3. Scanning electron microscopy of conidial surface morphology of *Pestalotiopsis* spp. and allied genera.
a-k: Conidial surface morphology of *Pestalotiopsis* spp. and allied genera; a-c: *B. robillardoides*; d: *S. mariae*; e-f: *M. circularis*; g: *M. karstenii*; h: *T. angustata*; i-k: *P. mangiferae*

Pestalotiopsis sp. MUBL1002/ *P. mangiferae* (Henn.): Conidia 5-celled, oblong-clavate 22-26 × 6-8 µm; colored cells 15-18 µm long, upper two of them amber to fuliginous or slightly darker than the lowest olivaceous colored cell, subglobose, the septa and walls sometimes black, indistinct; appendages 3, widely divergent, 19-26 µm long; pedicels short 6-7 µm long. Based on the microscopic results *Pestalotiopsis* MUBL1002 may be *Pestalotiopsis mangiferae* (Ell and Ev.) Steyaert (Fig. 3). *Isolated as endophyte from:* Leaves, stems and barks of *M. indica* from Botany Field Lab, University of Madras, Maduravoyal, Chennai, Tamil Nadu, India.

Pestalotiopsis sp. MUBL1013/ *P. microspora* (Speg.): Conidia clavate-fusoid, broad, tapering towards the base, 5-celled, straight, 15.69- 29 × 6.73-9.5 µm; intermediate colored cells guttulate, amber or olivaceous, equally colored, lowest colored cell sometimes slightly paler, 15-20 µm long, slightly constricted at septa. Apical appendages 1-2; 5-6 µm, and basal appendage 1, 2.92-4.5 µm long (Fig. 3). *Isolated as endophyte from*: Leaves, stems and barks of *T. mucronatum* from Government Botanical Garden, Ootacamund, Tamil Nadu, India.

Bartalinia sp. MUBL1096/ *B. robillardoides* (Tassi.): Conidia clavate to cylindrical, 4-septate, wall smooth, slightly constricted at septa, 15-20 × 2.5-3.5 µm with appendages, apical cell conic, colourless, 2.0-3.0 µm long, three apical appendages unbranched, attenuated towards the tip, flexuous, divergent, 8-18 µm long; median cells 3, cylindrical or subcylindrical, hyaline to pale brown, wall thicker than the apical and basal cells, together 11-15×2.5 – 30 µm; lower median cells longer than the upper cell, basal cell obconic with truncate base, hyaline, 2.5-3.0 µm long, with an excentric, filiform, unbranched, flexuous appendage, 3-5 µm long (Fig. 3). *Isolated as endophyte from*: Leaves, stem and bark of *R. arboreum* from Bryant Park, Kodaikanal, Tamil Nadu, India.

Monochaetia sp. MUBL1100/ *M. circularis*: Conidiomata acervular, irregular to subglobose, 250-300 µm diameter, wall composed of brown, pseudoparenchymatous cells. Conidiogenous cells lining the conidiomatal cavity, subcylindrical to irregular, hyaline, smooth. Conidia fusiform, 4-septate, 20-25×5-6 µm with three median cells, an apical and basal cell, apical and basal appendage, 10-15 µm long (Fig. 3). *Isolated as endophyte from*: Leaves, stem and bark of *T. mucronatum* from Government Botanical Garden, Ootacamund, Tamil Nadu, India.

Monochaetia sp. MUBL1101/ *M. karstenii* (Sacc. and P. Syd.): Conidia 4-celled, occasionally 2-celled, due to degeneration of end cells, slightly constricted at the median septum, 14 (12-16) × 6.5 (5.5-7) µm, two middle cells with thick walls, brown, (9-12) µm long, apical cell thin-walled, hyaline, with a short apical appendage, basal cell thin-walled, hyaline, sometimes with a minute central appendage, both hyaline cells sometimes collapsing (Fig. 3). *Isolated as endophyte from*: Leaves, stem and bark of *T. distichum* from Government Botanical Garden, Ootacamund, Tamil Nadu, India.

Seimatosporium sp. MUBL1107/ *S. mariae* (Clinton): Conidia are variable and cylindrical fusiform. 2-5 septate, 4 celled, lacking of appendage (Fig. 3). *Isolated as endophyte from*: Leaves, stem and bark of *T. distichum* from Government Botanical Garden, Ootacamund, Tamil Nadu, India.

Truncatella sp. MUBL1109/ *T. angustata* (Persoon: Fries): Conidia ellipsoid to fusiform, 4-celled, 18-25 × 5.5-7.5 µm, two median cells brown, 8-20 µm long, apical and basal cells hyaline, hemispherical, smaller than the median coloured cells, apical cell with 1-4 simple or 2-4 irregularly or dichotomously branched appendages, 10-30 µm long, basal cell with a simple, unbranched appendage, 2-3 µm long, which disappears at maturity of conidium (Fig. 3). *Isolated as endophyte from*: Leaves, stem and bark of *T. mucronatum* from Government Botanical Garden, Ootacamund, Tamil Nadu, India.

In taxonomy, the validity and delimitation of these genera are problematic (Steyeart, 1949). Concurrently, Fuckel's Fungi imperfecti concept and Saccardoan system of classification (Deuteromycetes) based on conidial and conidiophores morphology resulted in a comprehensive yet practical solution for classifying "asexual" fungi. The system was designed for convenience rather than for phylogenetic inference (Shenoy *et al*., 2007). In the present study, *Pestalotiopsis* spp. and other genera were identified up to species level. The conidia with non-pigmented median cells, axial single basal appendages arising from the particular locus and branches tubular outgrowth of the wall were found in *B. robillardoides* and *M. karstenii* (Muthumary, 1986). The *Bartalinia* spp. was characterized by spores having almost hyaline median cells with apical appendages arising from a particular locus and not separated by a septum; *Truncatella* spp. has two pigmented median cells and *Seimatosporium* spp. has two or three pigmented median cells with a single apical appendage and basal appendages that are excentric. *Monochaetia karstenii* was characterized by simple or complex eustromatic conidiomata and holoblastic conidia of variable morphology, mostly 3-euseptate, 2 unequal median cells olivaceous or very pale brown, the end cells hyaline, the apical one extended into a cellular appendage, sometimes the basal one with a central endogenously formed appendage (Muthumary, 1986). *Monochaetia circularis* differs slightly in morphology from *Pestalotiopsis* spp., in which, the spores possess median cells that have slightly thickened walls and are doliform shape, mostly verrucose in ornamentation and guttulate. They also have a slower growth rate on synthetic media compared to *P. mangiferae* and *P. microspora*. Most probably, the median cells have thicker walls and somehow distoseptate results in perplex during identification. The obtained result coincides with previous morphological hypothesis (Sutton, 1980; Nag Raj, 1993), in which, the median cells of *Pestalotiopsis* species such as *P. mangiferae* and *P. microspora* are not distoseptate as in *M. circularis*.

In contrast, Guba (1961) adopted a wide generic concept of the genus Pestalotia synonymizing *Pestalotiopsis*, Truncatella synonymized with Pestalotia and *Seiridium* synonymized with *Monochaetia*. Von Arx (1981) treated the genus, *Bartalinia* as a synonym of *Seimatosporium*, but, based on the morphology, however, Nag Raj (1993) disagreed as these two anamorphic genera are quite distinct whether the proposed synonym of von Arx (1981) was highly controversial. However, the findings are partially similar with Steyeart's view, which is an agreement with the commonly accepted taxonomic classification (Sutton, 1980; Nag Raj, 1993). The core of this study was to test the morphology-based hypothesis of Steyeart (1949) and Guba (1961) using molecular data. The present study opposes the concept proposed by Guba (1961) on wide generic treatment of *Bartalinia* and *Truncatella* as synonyms of *Seimatosporium* (1981). Traditionally, *Seimatosporium* has been regarded as having 3-5 euseptate conidia (the median cells of which are pigmented), usually a single apical cellular appendage and a single basal cellular appendage that is formed just above the truncate, unthickened basal scar.

According to Steyeart's concept, it is necessary to re-assign all four-septate conidia (three median cells) to *Pestalotiopsis*, a view supported by Sutton (1980; 1969) but Nag Raj (1993) preferred to adopt a wider generic concept of *Pestalotiopsis* by including three-septate (two median cells) form was originally assigned to *Truncatella* (Sutton, 1969). The classical taxonomy hypothesis of conidia with non-pigmented median cells and axial single basal appendages arising from the particular locus and branches tubular outgrowth from the wall was found in *B. robillardoides* and *M. karstenii* reported by Muthumary *et al*. (1986).

Chemotaxonomy is traditionally restricted to comprise fatty acids, proteins, carbohydrates and secondary metabolites. The researchers have suggested that volatile fungal metabolites, detected by chemical methods, might be used in the classification of fungi (Larsen and Frisvad, 1995a,b). Further, chemotaxonomic investigations were performed to confirm morphology-based identification (Fisher *et al*., 1996). The present study also applied chemotaxonomy for identification of *Pestalotiopsis* spp. and other genera. Intracellular fatty acids were analyzed and interpreted with the chemical library construction by using GC-MS analysis. Interestingly, total number of fatty acid peaks in *P. mangiferae, P. microspora, M. circularis, B. robillardoides, M. karstenii, S. mariae* and *T. angustata* were found to be 22, 21, 09, 07, 21, 13 and 27, respectively (Table 1). Each peak was represented to be a particular type of fatty acid derivatives in all the respective isolates. However, the fatty acid 2, 4-Di-

Table 1. Fatty acid profile of *Pestalotiopsis* spp. and other genera using GC-MS analysis.

S. No.	Mycelial fatty acid	Strain (Absorption area %)						
		Pm	*Pmi*	*Mc*	*Br*	*Mk*	*Ta*	*Sm*
1	n-[2-(3-Bromo-phenyl)-1-(morpholine-4-carbonyl)-vinyl]-4-methyl-benzamide	-	-	-	9.94	-	-	-
2	Purin-2,6-dione, 1,3-dimethyl-8-[2-[3,4-dimethoxyphenyl]ethenyl]-	-	-	-	16.84	-	-	-
3	1-Methylbutyl docosanoate	-	-	-	8.64	-	-	-
4	2,6-Dimethylheptan-4-one	-	-	-	11.22	-	-	-
5	2,4-Ditert-butylphenol	-	-	-	36.06	-	-	-
6	4-Ethoxy-N-(1-methylacetonyl)amphetamine	-	-	-	17.31	-	-	-
7	Hexanoic acid	4.99	2.12	-	-	-	2.53	1.36
8	Nonanal	1.53	0.64	-	-	0.21	0.58	0.26
9	Octanoic Acid	3.19	1.85	0.29	-	0.96	0.83	1.30
10	Dodecane	1.62	0.06	0.21	-	0.13	0.07	-
11	Decanal	0.58	0.20	-	-	-	0.07	-
12	1,3-Di-tert-butylbenzene	-	-	-	-	0.18	-	-
13	(2e)-2-Decenal	-	-	-	-	-	-	2.29
14	4-Hydroxy-3-nonenoic acid lactone	0.18	-	-	-	-	-	-
15	Nonanoic acid	7.13	2.87	-	-	1.35	1.28	1.28
16	8-Methyl-1-undecene	0.86	0.55	-	-	-	-	0.33
17	2-Undecen-1-al	-	0.05	-	-	-	-	-
18	Tetradecane	0.46	0.26	0.30	-	2.37	0.26	0.34
19	Eicosane	0.30	-	-	-	0.07	-	-
20	2,4-Di-tert-butylphenol	0.72	0.27	0.46	0.26	0.41	0.48	1.30
21	Heptadecane	0.36	-	-	-	0.23	-	-
22	8-Pentadecanone	0.24	-	-	-	-	-	-
23	2-Pentadecanone	0.67	-	-	-	0.14	0.19	-
24	Tetradecanoic acid	0.14	0.21	1.38	-	2.38	1.10	1.10
25	Fumaric acid, di(trans-4-tert-butylcyclohexyl) ester	0.28	-	-	-	-	-	-
26	Methyl tridecyl ketone	0.36	0.21	-	-	-	-	-
27	Hexadecanoic acid, methyl ester	1.77	0.54	-	-	-	0.38	0.52
28	1,2-Benzenedicarboxylic acid, bis(2-methoxyethyl) ester	1.77	-	-	-	-	-	-
29	n-Hexadecanoic acid	51.03	78.74	96.75	-	91.14	87.18	71.94
30	Octanal	-	1.20	-	-	-	-	-
31	7-Bromobicyclo[4.2.0]octa-1,3,5-triene	-	1.61	-	-	-	-	-
32	(2e)-2-Decinal	-	0.49	-	-	-	-	-
33	1,13-Tetradecadien-3-one	-	0.20	-	-	-	-	-
34	(E)-2-Dodecen-1-al	-	-	-	-	-	0.20	-
35	3-Nonen-2-one	-	-	-	-	-	0.27	-
36	(2z)-3-methyl-2-undecene	-	-	-	-	-	0.19	-
37	9-Oxononanoic acid	-	-	-	-	-	0.20	-
38	2-Butyloctan-1-ol	-	-	-	-	-	0.81	-
39	n,n-Bis(2-hydroxyethyl)dodecanamide	-	-	-	-	-	0.11	-
40	3-Methylpentadecane	-	-	-	-	-	0.12	-
41	(1-Ethyloctadecyl)benzene	-	-	-	-	-	0.43	-
42	1,5-Dodecadiene	-	-	-	-	-	0.13	-
43	Octadecanal	-	-	-	-	0.14	-	-

Continued..

Table 1 continue…

S. No.	Mycelial fatty acid	Strain (Absorption area %)						
		Pm	*Pmi*	*Mc*	*Br*	*Mk*	*Ta*	*Sm*
44	Trans-2-Decenal	-	-	-	-	0.19	-	-
45	2,6,11-Trimethyldodecane	-	-	-	-	0.04	-	-
46	Decanoyl chloride	-	-	-	-	0.27	-	-
47	(2e)-3,7-Dimethyl-2,6-octadien-1-ol, [13c] isotopic labeled	-	-	-	-	0.12	-	-
48	2,6,11,15-Tetramethylhexadecane	-	-	-	-	0.34	-	-
49	Octadec-9-enoic acid	-	-	-	-	0.65	-	-
50	5-Ethyl-2-methyloctane	-	-	0.05	-	-	-	-
51	Docosane	-	-	0.05	-	-	-	-
52	Hexadecane	-	-	0.24	-	-	-	-
53	Cyclohexylmethylamine	-	-	-	-	-	-	1.08
54	(2z)-2-Decenal	0.23	-	-	-	-	-	-
55	2- Undecenal	-	-	-	-	-	0.35	-
56	n- Decanoic acid	-	-	-	-	0.35	0.21	-
57	Octaiucanoic acid	-	0.37	-	-	0.95	0.96	1.30
58	1,2-Bezenedicarboxylic acid, bis(2-methoxyethyl) ester	0.84	0.41	-	-	-	0.48	-
59	Pentadecacoic acid	-	0.84	-	-	-	0.91	-
60	2-Bromo dodecane	-	-	-	-	-	0.28	-

Pm: *P. mangiferae* ; Pmi: *P. microspora*; Mc: *M. circularis*; Br: *B. robillardoides*; Mk: *M. karstenii*; Ta: *T. angustata*; Sm: *S. mariae*

tertbutylphenol was observed in all the isolates. The tetradecanoic acid, n-hexadecanoic acid and octanoic acid were observed in *T. angustata, P. mangiferae, P. microspora, M. karstenii, S. mariae* and *M. circularis* except in *B. robillardoides*. The nonanal and nonanoic fatty acids were found in *T. angustata, P. mangiferae, P. microspora, M. karstenii* and *S. mariae* excluding in *M. circularis* and *B. robillardoides* (Table 1). The absorption of area percentage was calculated in GC-MS analysis. Significantly, 2, 4-Ditert-butylphenol was observed at 36.06 area percentage in *B. robillardoides* (Table 1). Interestingly n-hexadecanoic acid was exhibited in all strains except *B. robillardoides* and the absorption area percentage was calculated as 51.03, 78.74, 96.75, 91.14, 71.94 and 87.18 respectively, in *P. mangiferae, P. microspora, M. circularis, M. karstenii, S. mariae* and *T. angustata* (Table 1). Based on literature survey, the cell wall fatty acid analysis in *Pestalotiopsis* spp. and other genera are not reported so far. However the present study applies fatty acid profile for the first time in identification of coelomycetous fungi, *Pestalotiopsis* spp. and other genera. Nevertheless, the secondary metabolites were already reported in *Pestalotiopsis* spp. and *Bartalinia* spp. (Gangadevi and Muthumary, 2009a,b), *Monochaetia* spp., *Seiridium* spp. and *Truncatella* spp. (Lee *et al*., 1996).

CONCLUSION

The present study reveals that both direct and indirect methods were efficient for isolating the endophytic coelomycetous fungi. Both classical- and chemo-taxonomy are used in this study for the species-level identification of *Pestalotiopsis* spp. and other allied genera. Further the fatty acid profiling used first time by this study for identification of coelomycetous fungi. Our findings indicates that the obtained fatty acids in the present study are the evidence of chemotaxonomy, which is strongly indicate that the distinguished relationship between *Pestalotiopsis* and other genera. Isolation of potential secondary metabolites and lipids from the isolated fungi obtained from this study would be taken for further research.

ACKNOWLEDGEMENT

The authors K.S and M.J are thankful to Prof. R. Rengasamy, former Director of CAS in Botany for providing necessary lab facilities. K.S sincerely acknowledge the University Grants Commission (UGC), under the scheme of Rajiv Gandhi National Fellowship (RGNF) (Award letter No. F. 14-2(SC)/2007(SA-III), Government of India for financial support. K.S is thankful to the DST-SERB-GOI, New Delhi, India for the Start-up Research Grant financial support.

REFERENCES

Abdel-Kareem, O. and Szostak-kotowa, J. 1999. Electron microscopical (SEM) studies on biodeteriorated archaeological Egyptian textiles. In Archaeological Science Conference, United Knigdom.3-13.

Arnold, AE. and Herre, EA. 2003. Canopy cover and leaf age affect colonization by tropical fungal endophytes: Ecological pattern and process in *Theobroma cacao* (Malvaceae). Mycologia. 95:388-398.

Baayen, RP., Bonants, PJ., Verkley, G., Carroll, GC., van der Aa, HA., de Weerdt, M., van Brouwershaven, IR., Schutte, GC., Maccheroni, W., de Blanco, CG. and Azevedo, JL. 2002. Nonpathogenic isolates of the Citrus black spot fungus, *Guignardia citricarpa*, identified as a cosmopolition endophyte of woody plants, *G. mangiferae* (*Phyllosticta capitalensis*). Phytopath. 92:464-477.

Bills, GF. 1996. Isolation and analysis of endophytic fungal communities from woody plants. In: Endophytic fungi in grasses and woody plants. Eds. Redlin, SC. and Carris, LM. APS Press, St. Paul, Minnesota, USA. 31-65.
Bills, GF. and Polishook, JD. 1992. Recovery of endophytic fungi from *Chamaecyparis thyoides*. Sydowia. 44:1-12.

Cabral, D., Stone, JK. and Carroll, GC. 1993. The internal mycobiota of *Juncus* spp.: microscopic and cultural observations of infection patterns. Mycol. Res. 97:367-376.
Carroll, GC. 1995. Forest endophytes: pattern and process. Can. J. Bot. 73:S1316-S1324.

De Bary, A. 1866. Morphologie und Physiologie der Pilze, Flechten, und Myxomyceten. Hofmeister's Handbook of Physiological Botany. Leipzig, Germany, Engelmann.
Deckert, RJ., Melville, L. and Peterson, RL. 2001. Structural features of a *Lophodermium* endophyte during the cryptic life cycle in the foliage of *Pinus strobus*. Mycol. Res. 105:991-997.

Fisher, PJ., Stradling, DJ., Sutton, BC. and Petrini, LE. 1996. Microfungi in the fungus gardens of the leaf-cutting ant *Atta cephalotes*: a preliminary study. Mycol. Res. 100:541-546.
Gangadevi, V. and Muthumary, J. 2009[a]. Taxol production by *Pestalotiopsis terminaliae*, an endophytic fungus of *Terminalia arjuna*. Biotechnol. Appl. Biochem. 52:9-15.

Gangadevi, V. and Muthumary, J. 2009[b]. A novel endophytic taxol-producing fungus *Chaetomella raphigera* isolated from a medicinal plant, *Terminalia arjuna*. Appl. Biochem. Biotechnol. 158:675-684.

Gange, AC., Dey, S., Currie, AF. and Sutton, BC. 2007. Site- and species-species differences in endophyte occurrence in two herbaceous plants. J. Ecol. 95:614-622.

Gao, XX., Zhou, H., Xu, DY., Yu, CH., Chen, YQ. and Qu, LH. 2005. High diversity of endophytic fungi from the pharmaceutical plant, *Heterosmilax japonica* Kunth revealed by cultivation-independent approach. FEMS Microbiol. Lett. 249:255-266.

Guba, EF. 1961. Monograph of Pestalotia and Monochaetia. Harvard University Press. Cambridge, Massachusetts.

Hawksworth, DL. 2001. The magnitude fungal biodiversity: the 1.5 million species estimate revisited. Mycol. Res. 105:1422-1432.

Helander, ML., Neuvonen, S., Sieber, T. and Petrini, O. 1993. Simulated acid rain affects birch leaf endophyte populations. Microbial Ecol. 26:227-234.

Hyde, KD. 2001. Increasing the likelihood of novel compound discovery from filamentous fungi. In: Bio-exploitation of filamentous fungi, fungal diversity research. Eds. Pointing, SB. and Hyde, KD. Fungal Diversity Press, Hong Kong.77-91.

Jeewon, R., Liew, ECY. and Hyde, KD. 2002. Phylogenetic relationships of *Pestalotiopsis* and allied genera inferred from ribosomal DNA sequences and morphological characters. Mol. Phylogenet. Evol. 25:378-392.
Kamalraj, S. and Muthumary, J. 2013. Prevalence and seasonal periodicity of endophytic coelomycetous fungi in Tamil Nadu, India. Int. J. Biodivers. Conserv. 5:469-477.

Kamalraj, S., Sridevi, S., Gangadevi, V., Venkatesan, A. and Muthumary, J. 2008. Effect of NaCl on biochemical changes and endophytic fungal assemblages in the leaves of a mangrove, *Ceriops roxburghiana* Arn. Indian J. Sci. Technol.1:1-7.
Kirk, PM., Cannon, PF., David, JC. and Stalpers, JA. 2001. Ainsworth and Bisby's dictionary of the fungi. (9th edi.). CABI Publishing, Wallingford.

Larsen, TO. and Frisvad, JC. 1995[a]. Chemosystematics of *Penicillium* based on profiles of volatile metabolites. Mycol. Res. 99:1167-1174.

Larsen, TO. and Frisvad. JC. 1995[b]. Characterization of volatile metabolites from 47 *Penicillium* taxa. Mycol. Res.99:1153-1166.
Lee, JC., Strobel, GA., Lobkovsky, E. and Clardy, JC. 1996. Torreyanic acid: a selectively cytotoxic quinine dimer from the endophytic fungus *Pestalotiopsis microspora*. J. Org. Chem. 61:3232-3233.

Lehtijarvi, A. and Barklund, P. 2000. Seasonal patterns of colonization of Norway spruce needles by *Lophodermium piceae*. Forest Pathology. 30:185-193.

Li, D., Yan, S., Proksch, P., Liang, Z., Li, Q. and Xu, J. 2013. Volatile metabolites profiling of a Chinese mangrove endophytic *Pestalotiopsis* sp. strain. African Journal of Biotechnology. 12:3802-3806.

Magan, N., Smith, MK. and Kirkwood, IA. 1996. Effects of atmospheric pollutants on phyllosphere and endophytic fungi. In: Fungi and environmental change. Eds.

Frankland, JC., Magan, M. and Gadd, GM. Cambridge University Press, New York, USA. 90-101.

Metz, AM., Haddad, A., Worapong, J., Long, DM., Ford, EJ., Hess, WM. and Strobel, GA. 2000. Induction of the sexual stage of *Pestalotiopsis microspora*, a taxol producing fungus. Microbiol. 146:2079-2089.

Muthumary, J., Qaiser Abbas, S. and Sutton, BC. 1986. A reassessment of *Monochaetia terminaliae*. Trans. Br. Mycol. Soc. 87:103-108.

Nag Raj, TR. 1993. Coelomycetous anamorphs with appendage bearing conidia. Mycologue Publications, Waterloo, Ontario, Canada.

Pimentel, MR., Molina, G., Dionísio, AP., Maróstica Junior, MR. and Pastore, GM. 2011. The use of endophytes to obtain bioactive compounds and their application in biotransformation process. Biotechnol. Res. Int. 2011:1-11.

Poteri, M., Helander, ML., Saikkonen, K. and Elamo, P. 2001. Effect of *Betula pendula* clone and leaf age on *Melampsoridium betulinum* rust infection in a field trial. Forest Pathology. 31:177-185.

Redman, RS., Sheehan, KB., Stout, RG., Rodriguez, RJ. and Henson, JM. 2002. Thermotolerance generated by plant/fungal symbiosis. Science. 298:1581.

Schulz, B., Guske, S., Dammann, U. and Boyle, C. 1998. Endophyte-host interaction. II. Defining symbiosis of the endophyte-host interaction. Symbiosis. 25:213- 227.

Shenoy, BD., Jeewon, R. and Hyde, KD. 2007. Impact of DNA sequence-data on the taxonomy of anamorphic fungi. Fungal Div. 26:1-54.

Sieber, TN. 2002. Fungal root endophytes. In: Plant roots-the hidden half. Eds. Waisel, Y., Eshel, A. and Kafkafi, U. Marcel Dekker, New York, Basel. 887-917.

Steyeart, RL. 1949. Contributions a retude *monographique* de *Pestalotia* de Not. Et *Monochaetia* Sacc. (*Truncatella* gen. nov. et *Pestalotiopsis* gen. nov.). Bull. Jard. Bot. Etat. Bruxelles. 19:285-354.

Stone, IK. 1985. Foliar endophytes of *Pseudotsuga amensiesii* (Mirb.) Franco. Cytology and physiology of the host-endophytes relationship. Ph.D. Thesis. University of Oregon, Eugene.

Stone, JK., Sherwood, MA. and Carroll, GC. 1996. Canopy microfungi: function and diversity. Northwest Science. 70:37-45.

Strobel, G. and Daisy, B. 2003. Bioprospecting for microbial endophytes and their natural products. Microbiol. Mol. Biol. Rev. 67:491-502.

Strobel, GA., Yang, X., Sears, J., Kramer, R., Sidhu, RS. and Hess, WM. 1996[a]. Taxol from *Pestalotiopsis microspora*, an endophytic fungus of *Taxus wallachiana*. Microbiol. 142:435-440.

Strobel, GA., Hess, M., Yang, X., Ford, EJ. and Sidhu, RS. 1996[b]. Taxol from fungal endophytes and the issue of biodiversity. J. Ind. Microbiol. Biotechnol. 17:417-423.

Suriyanarayanan, TS. and Vijaykrishna D. 2001. Fungal endophytes of aerial roots of *Ficus benghalensis*. Fungal Div. 8:155-161.

Sutton, BC. 1973[a]. Coelomycetes. In: The fungi an advanced treatise. (vol. IV). A taxonomic review with keys; Ascomycetes and Fungi imperfecti. Eds. Ainsworth, GC., Sparrow, FK. and Sussman, AS. Academic Press, New York, USA. 513-582.

Sutton, BC. 1980. The Coelomycetes. Fungi Imperfecti with pycnidia, acervuli and stromata. Commonwealth Mycologica

Sutton, BC. 1969. Forest Microfungi. III. The heterogeneity of *Pestalotia* de Not. Section Sexloculatae Klebahn sensu Guba. Can. J. Bot. 47:2083-2094.

Sutton, BC. 1973[b]. Hyphomycetes from Manitoba and Saskatchewan, Canada. Mycological Papers. 132:1-143.

Von Arx, JA. 1981. The genera of fungi sporulating in pure culture. (3rd edi.). Cramer, Vaduz. 1-424.

Webber, J. and Gibbs, JN. 1984. Colonization of elm bark by *Phomopsis oblonga*. Transactions of the British Mycological Society. 82:348-352.

Zhu, P., Ge, Q. and Xu, T. 1991. The perfect stage of *Pestalosphaeria* from China. Mycotaxon. 50:129-140.

Received: August 5, 2016; Accepted: September 15, 2016

Canadian Journal of Pure and Applied Sciences
Vol. 10, No. 3, pp. 3961-3969, Oct 2016
Online ISSN: 1920-3853; Print ISSN: 1715-9997
Available online at www.cjpas.net

ASSESSING INDUCED EFFECT OF CURCUMIN ON METHIMAZOLE HEPATIC DAMAGE IN ALBINO RATS: A HISTOLOGICAL AND HISTOCHEMICAL STUDY

Wael M. Al-Amoudi[1], *Faiza A. Mahboub[1], Hawazen A. Lamfon[1] and Nahid A. Lamfon[2]
[1]Department of Biology, Faculty of Applied Sciences, Umm Al-Qura University, Saudi Arabia
[2]King Saud bin Abdulaziz University for Health Science, College of Medicine, Family and Community Medicine
King Abullaziz Medical City / National Guard, Health Affair, Riyadh, Saudi Arabia

ABSTRACT

The present study investigates the possible protective effect of curcumin on Methimazole (MMZ). It is an anti-thyroid drug induced hepatotoxicity in albino rats. In this study the rats were randomly divided into four experimental groups; first group was used as control treated with a standard diet. The second group was treated with curcumin at dose of 150 mg/kg body weight. The third group was treated with the MMZ dissolved in drinking water at dose of 60mg/kg body weight. The fourth group was treated with a liquid mixture of MMZ and curcumin. The rats were dissected after 6 weeks of treatment and livers of these animal were collected separately and used for histological and histochemical methods. It was clear form the results obtained that the MMZ caused histological alterations in the liver tissue of the MMZ treated rats. These changes appeared as congestion of blood vessels, leucocytic infiltrations and cytoplasmic vaculation of the hepatocytes. The histochemical analysis has revealed a reduction in carbohydrates content, total proteins and DNA. The histochemical results of the same rats treated with MMZ showed an increase in serum level of ALT, AST and ALP. However, the group treated with curcumin showed a remarkable improvement in the histological structure of the liver tissue. The results revealed an increase in carbohydrates level, total proteins and DNA. In addition the Biochemical results of this group showed a noticeable decrease in the hepatic enzymes (ALT, AST and ALP). These finding have confirmed that curcumin is an effective agent with special antioxidant properties that prevent and protect the liver from histological and histochemical damages induced by MMZ.

Keywords. Methimazole, curcumin, hepatotoxicity, histochemistry, rats.

INTRODUCTION

Methimazole (MMZ) (1-methyl-2-mercaptoimidazole) is known as an antithyroid medication used to prevent thyroid hormone synthesis and described medically to treat hyperthyroidism. It has been documented in by Nakamura *et al*. (2007) that MMZ acts by interacting with thyroid peroxidase enzyme (TPO) function. This enzyme is expressed mainly in the thyroid and secreted into colloid. The MMZ function is to lower thyroid hormone levels and minimize the effects of thyroid manipulation by interrupting the iodination of tyrosine residues in thyroglobulin which cause a reduction in hormone secretion (Cooper, 2005). Another study, Aboul-Enein and Al-Badr (1979) have reported a similar observation confirming that when MMZ is absorbed by the thyroid gland it prevents the thyroid hormone production and stops the synthesis of hormone by oxidizing the anion iodide. However, it has been administrated that in 5-7% of patients taking MMZ different symptoms and side effects were reported including fever, skin rashes, gastrointestinal, loss of taste and neuropathy (Chevalley *et al*., 1954) and (Schmidt *et al*., 1986). In addition, agranulocytosis is another uncommon side effect of MMZ. This was occurred in three cases causing a death of one patient (Specht and Boehme, 1952).

Rivkees *et al*., (2010) has revealed that when one hundred consecutive pediatric patients were given MMZ other symptoms such as pruritus and hives were recognized in a few patients. Some other patients were suffered from diffuse arthralgia and joint agony and unusual symptoms known as neutropenia and Stevens-Johnson syndrome were noticed. One kid was suffered from a decrease in bile flow due to impaired secretion by hepatocytes, which is known as Cholestasis (Rivkees *et al*., 2010). It has been substantiated by Mikhail (2004) that MMZ could lead to a liver damage and injury causing intrahepatic cholestasis. While, Epeirier *et al*. (1996) has also reported that one patient had suffered from hyperthyroidism severe inflammation and hepatic necrosis as a result of 6 weeks treatment with MMZ carbimazole and propranolol.

*Corresponding author e-mail: famahboub@uqu.edu.sa

In some cases, it has been noticed that in a 43-year-old man suffering from hyperthyroidism and hepatitis B surface antigenemia acute hepatic failure was accrued during the treatment with MMZ (Epeirier *et al*., 1996) and (Kang *et al*., 1990). It was also reported that the needle biopsy post mortem examination showed micronodular cirrhosis characterized with mild septal/portal inflammation, cholestasis and scattered acidophilic bodies in liver tissue of some patient (Epeirier *et al*., 1996). Recently, Gallelli *et al*. (2015) has also stated that the MMZ has caused hepatotoxicity in a 54-year-old patient suffered from hyperthyroidism during treatment and biopsy examination of the liver tissue revealed diagnosis of cholestatic hepatitis in this patient. Morover, Tashkandi *et al*. (2014) has showed that hepatorenal toxicity was noticed in the rat's liver as a result of MMZ treatment.

Curcumin is the principle yellow pigments herbal plant from a species of Curcuma longa. It is a major component of turmeric and widely used in most tropical and subtropical region as a spice and food-coloring agent. It has been commercially used as a cosmetic component and also added into some medical preparations for some of its positive side effects (Menon and Sudheer, 2007). It has been commonly used in treatment of a wide variety of diseases and chronic illness to exhibit any anti-inflammatory, immunomodulatory, and anti-atherogenic effects (Srinivasan, 1952; Joe *et al*., 2004) and also described as a potent inhibitor of many reactive oxygen-generating enzymes (Chainani-Wu, 2003; Borra *et al*., 2013). It has been reported by Manikandan *et al*. (2004) and Venkatesan, (2000) that curcumin has a positive influence against free radical formation in animal rats suffered from myocardial ischemia and in lung toxicity.

Kadasa *et al*. (2015) has revealed in his study that curcumin showed a strong hepatoprotective effects against hepatocarcinogenesis caused by diethylnitrosamine (DENA) in rodents. He has also reported that curcumin improved the liver functions by modulating the hepatic enzymes serum levels and increasing the antioxidant hepatic system which cause a reduction in the pro-inflammatory cytokines (Kadasa *et al*., 2015). Palipoch *et al*. (2014) has demonstrated that a mixed of curcumin and α-tocopherol suppressed the induction of cisplatin and reduce the hepatotoxicity of liver. The present study aimed to investigate the effects of curcumin against the histological, histopathological and histochemical changes of hepatotoxicity induced by MMZ in albino rats.

MATERIALS AND METHODS

Animals

Mature healthy male albino rats were chosen for this experiment, they were weighted between 140-160g. The animals were housed in the animal care center and were treated and kept under normal conditions with minimal diurnal or seasonal variation in temperature, light cycle, or other environmental conditions. They were wire-floored cages under standard laboratory conditions of 12 h/12 h light/dark, 25 ± 2C ^{o} with free access to food and water in accordance with the Ethical Principles for the Care and Use of Laboratory Animals (NRC, 1995).

Experimental design

Animals were divided into four experimental groups:

Group 1. Rats were fed the standard diet and were served as control group.

Group 2. Rats were orally administrated curcumin at a dose of 150 mg/kg body weight daily for 6 weeks. Dry turmeric rhizomes of the plant *Curcuma longa* were purchased from a local market and were crashed into powder. The powder was then dissolved in distilled water and were orally given to the rats.

Group 3. Rats were orally given MMZ at a dose level of 60mg/kg body weight in distilled water. The solution was daily given to these animal for 6 weeks.

Group 4. Rats were given MMZ (60mg/kg body weight) followed by oral administration of curcumin extract dissolved in distilled water a dose level of 150mg/kg daily for 6 weeks.

Histological and Histochemical Examination

The treated animals and their controls were sacrificed by decapitation after 6 weeks of treatment and their liver were carefully separated and collected separately. The liver tissues were then washed in normal saline. Specimens were fixed in 10% phosphate buffered formalin (pH 7.4). Fixed materials were embedded in paraffin wax and then sections were cut at thickness of 5 micrometer. Slides were after stained with haematoxylin and eosin for histological observation. For the analysis of histochemical demonstration the total carbohydrates periodic acid Schiff's technique (PAS) (Kiernan, 1981) was applied. Total proteins were detected using the mercury bromophenol blue method (Pearse, 1972) and DNA was detected using Feulgen reaction (Kiernan, 1981).

Biochemical Assays

For biochemical measures, blood samples were taken and harvested from rats after 6 weeks of treatment. Sera were acquired by centrifugation of the blood samples and kept at -20°C. Aspartate aminotransferase (AST) and alanine aminotransferase (ALT) levels were detected colourimetrically as indicated by Reitman and Frankel (1957). Alkalin phosphatase (ALP) activity was measured by the method of Belfield and Goldberg (1971) using reagent kits acquired from Bio-Merieux Chemical Company (France).

STATISTICAL ANALYSIS

The results were expressed as mean ± SD of various groups. The differences between the mean values were assessed by ANOVA followed by Student's "t" test using Minitab 12 PC program (Minitab Inc., State Collage, P. A).

RESULTS AND DISCUSSION

Histological Observations

Histological examination of control sample of the liver tissue showed normal architecture. The hepatocytes were found arranged at normal shape and strands around the central vein, the sinusoids appeared natural and containing normal Kupffer cells as shown in Figure 1A.

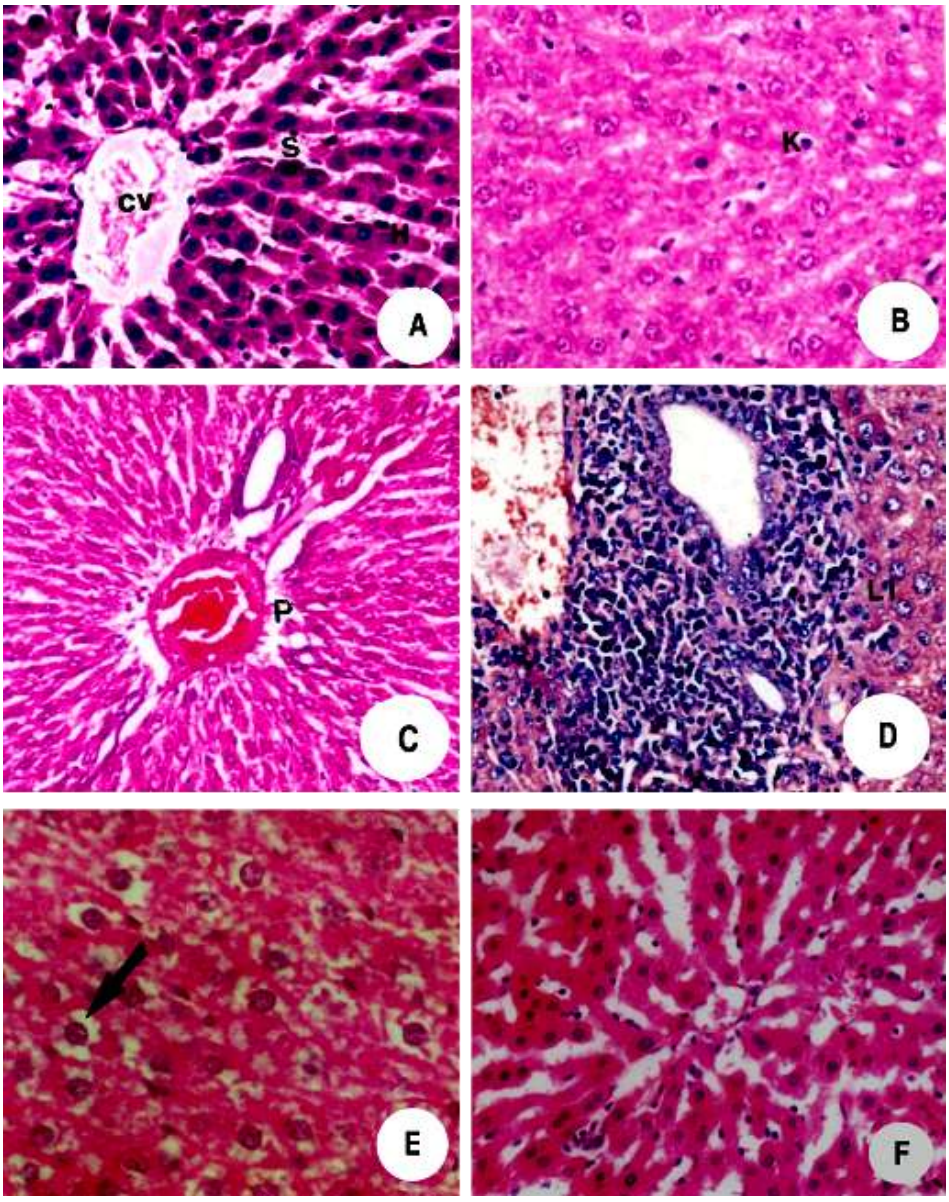

Fig. 1 A. Section in liver of a control rat showing hepatocytes (H), central vein (CV) and sinusoidal spaces(S), X 400.
B. Section in liver of a rat treated with curcumin showing activated kupffer cells (K),X400.
C. Section in liver of a rat treated with MMZ showing congested portal vein (P), X200.
D. Leucocytic infiltrations (LI) in liver of a rat treated with MMZ, X200.
E. Section in liver of a rat treated with MMZ showing cytoplasmic vacuolation of the hepatocytes (arrow), X400.
F. Section in liver of a rat treated with MMZ and curcumin showing an improvement in the liver structure,X200.

Animals treated with the curcumin solution appeared normal and no histopathological alterations were observed (Fig. 1B). On the other hand, animals treated with MMZ appeared to be congested with enlarged central and portal veins as shown in Figure 1C. Leucocytic infiltrations were observed in large areas of the liver tissue (Fig. 1D). The liver tissue treated with MMZ also showed cytoplasmic vacuolization of the hepatocytes with pyknotic nuclei (Fig. 1E). In the liver tissue of rats group treated with curcumin and MMZ different observations were obtained. In these sections there was a histological improvement in the structure of the liver tissue and the hepatocytes appeared to be normal with healthy nucleus and cytoplasm as shown in Figure 1F.

Histochemical Observations

Total carbohydrates of hepatocytes in the liver of control rats appeared as red or magenta color when stained with Schiff's reagent. The carbohydrates in the cells found to be concentrated at one pole, this is termed glycogen flight (Fig. 2A). The nuclei appeared entirely PAS-negative. In the liver cells of curcumin-treated animals the carbohydrates arrangement was natural and appeared normal. However, in the section of rats treated with MMZ the carbohydrates content was reduced as a consequence of MMZ treatment (Fig. 2B). In the section of rats treated with curcumin and MMZ, the observation was different, in this section as shown in Figure 2C, the carbohydrates content of the hepatocyte was increased significantly and appeared to be normal.

Total proteins contents in the control rats section appeared as blue color after staining with bromophenol blue. The proteins appeared as fine granules in the cytoplasm of the hepatocytes (Fig. 3A). Kupffer cells, endothelial lining cells of sinusoids and the walls of blood vessels exhibited strong stainability. In the rats treated with MMZ there was a noticeable dimension in the total protein contents in the liver cells (Fig. 3B). on the other hand, Hepatocytes of rats treated with curcumin and MMZ appeared with an increase in protein contents (Fig. 3C).

The DNA-containing particles (chromatin) appeared in the form of densely stained red particles distributed in the nucleoplasm and the peripheral rim of the nuclei of hepatocytes of control rats (Fig. 4A). Examination of hepatocytes of animals treated with MMZ revealed that most nuclei exhibited a weak Feulgen reaction of their chromatin granules (Fig. 4B). Animals treated with curcumin and MMZ showed that most of the nuclei appeared with normal amount of DNA-containing particles (Fig. 4C).

Biochemical Results

Treatment with MMZ for 6 weeks showed a highly significant increase ($P<0.05$) in the level of ALT and AST compared to the control animals. In contrast, these parameters were restored close to normal values in rats treated with curcumin and MMZ. Both control and curcumin treated rats showed no significant differences in serum content of ALT and AST (Figs. 5 and 6). Similarly, ALP was elevated in MMZ treated rats compared to the control group, and decreased in MMZ and curcumin treated group (Fig.7).

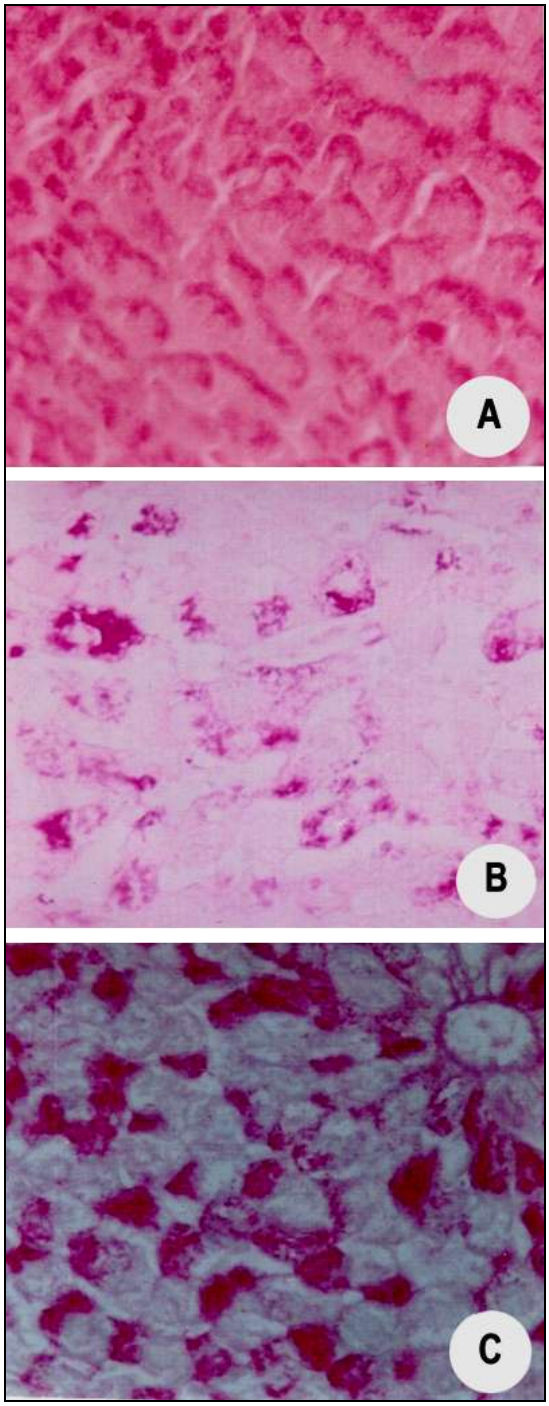

Fig. 2A. Section in liver of a control rat showing distribution of carbohydrates in the cytoplasm, X400. B. Section in liver of a rat treated with MMZ showing decrease of carbohydrates, X 400.

C. Restoration of carbohydrates in liver of a rat treated with MMZ and curcumin, X 400.

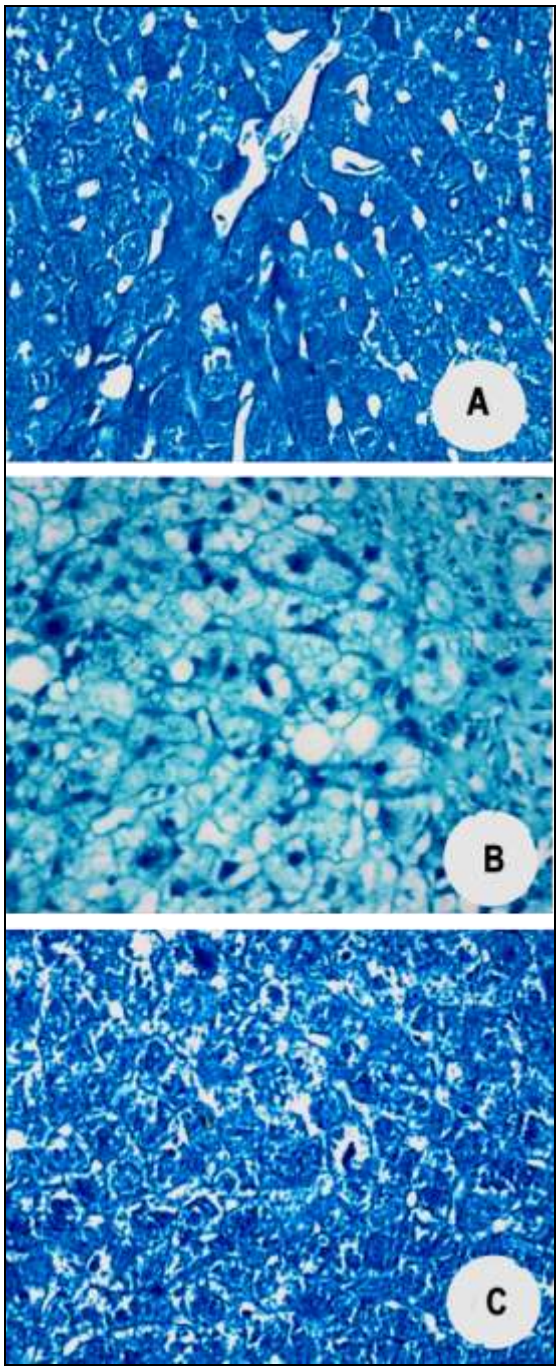

Fig. 3A. Section in liver of a control rat showing normal protein contents, X400
B. Reduction of proteins in liver of a rat treated with MMZ, X 400
C. An increase in protein contents in liver of a rat treated with MMZ and curcumin, X400.

Results our study showed that Methimazole caused histological, histochemical and biochemical changes in the liver of treated rats and induced hepatotoxicity and damage to the cells structure. Findings of our study is similar to the results reported by Tashkandi *et al*. (2014) and Zhao *et al*. (2014), when it has reported that MMZ leads to degenerative changes such as congestion of blood vessels, appearance of inflammatory infiltrative cells, cytoplasmic vacuolization of the hepatocytes and cell death. Moreover, ALT and AST levels were elevated in sera of the treated animals. It is well known that the normal level of AST and ALT serum play an essential role to maintain a normal liver function and any changes in these enzymes level cause a sever liver damage and could lead to dysfunction if the organ. Also in some studies done by (Cano-Europa *et al*., 2011; Gallelli *et al*., 2015), it has been documented that MMZ treatment has induced liver damage and showed abnormality in the enzymes liver, in accordance with this statement the obtained results have confirmed that MMZ is a hazard material that cause damage and abnormality to the liver function and structure.

Histochemical results showed that carbohydrates, total proteins and DNA are drained in liver rats treated with MMZ. This finding is similar to those reported by, Ram and Waxman (1992), it has stated that treatment with MMZ had caused a remarkable reduction of proteins at percentage of 75-85% in hepatic microsomal P450 reductase activity in both male and female rats. Also, Meisami *et al*. (1994) has reported that testicular weight and DNA content were significantly decreased in rat pups treated with propylthiouracil from birth. Snedecor *et al*. (1972) has administrated that some histochemical and histological changes were found in the animal exposed to MMZ such as reduction in liver weight and glycogen content. Moreover, Sakr *et al*. (2012) has reported that treating rats with carbimazole caused alterations in prostate gland tissue including decrease in the polysaccharide, total protein and nucleic acids contents.

There are some evidences that antithyroid drugs had used as a medication that lead to cause cellular damage and produced oxidative stress to cells and organs (Bruck *et al*., 2007). Another study, Valko *et al*. (2007) reported that MMZ can cause oxidant species that lead to lipid peroxidation, nitration, carbonylation or glutathionylation of proteins, and interrupt the hepatocytes DNA. This statement is consistent with the results obtained from this investigation. It also has been mentioned that MMZ is responsible for the cell damage (Ortiz-Butron *et al*., 2011), it has been made clear that the cell damage was associated with an increase of reactive oxygen species (ROS), lipid peroxidation and reduction of catalase activity. It has been reported that MMZ promoted oxidative stress causing an increase in liver malondialdehyde levels, and led to a reduction in glutathione, nonprotein thiols and vitamin C level (Sefi *et al*., 2014). The results revealed from this study is

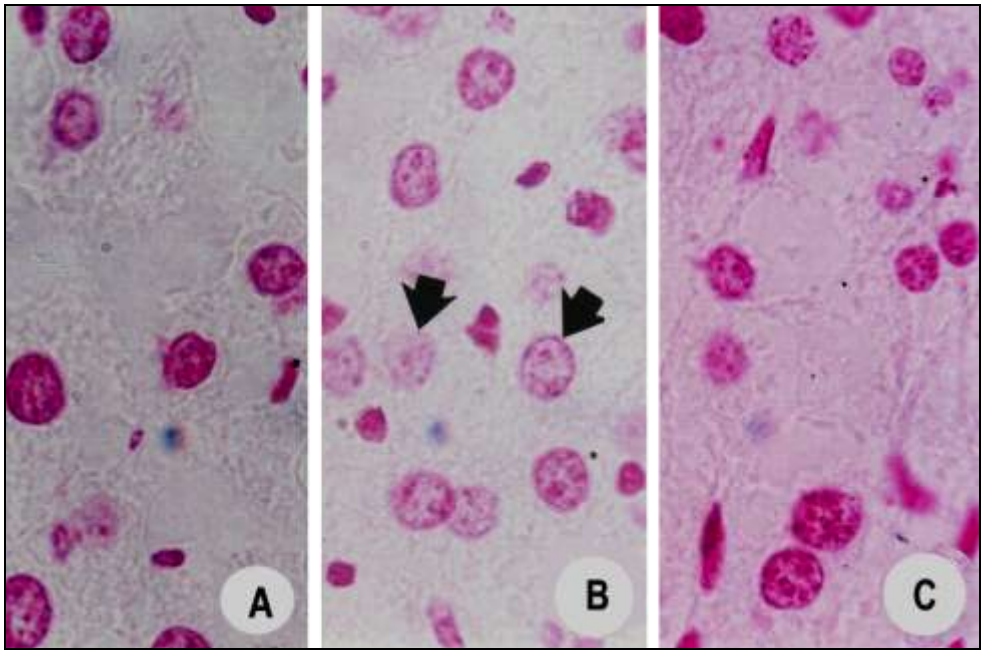

Fig. 4A. Nuclei of hepatocytes of a control rat showing normal content of DNA, X 1000
B. Decrease of DNA in hepatocytes of a rat treated with MMZ, X1000.
C. An increase in DNA hepatocytes of a rat treated with MMZ and curcumin, X1000

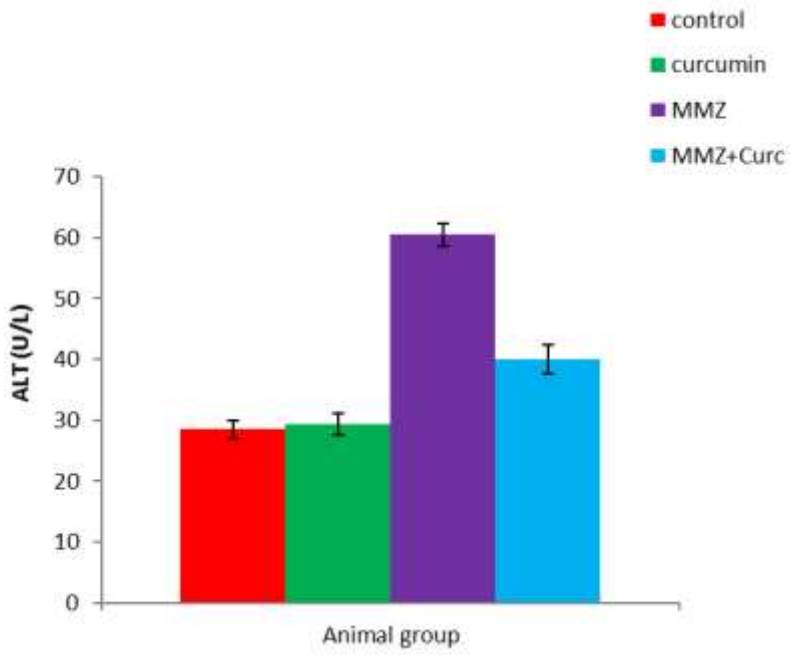

Fig. 5. Change in ALT in different groups.

contestant whit those reported by other researchers. The histochemical analysis showed in this study confirm that MMZ is a harm chemical that interact and create damage to the liver tissue.

Curcumin is a traditional herb used widely world wised. The results showed in this study have indicated that curcumin ameliorates and control the damage caused by MMZ and prevents the damaged appeared in the hepatotoxicity of rat liver. This result is consistent with

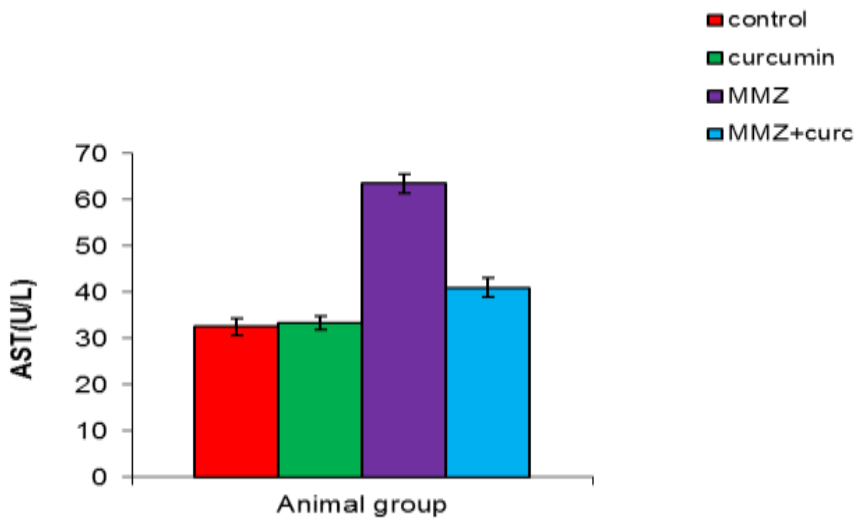

Fig. 6. Change in AST in different groups.

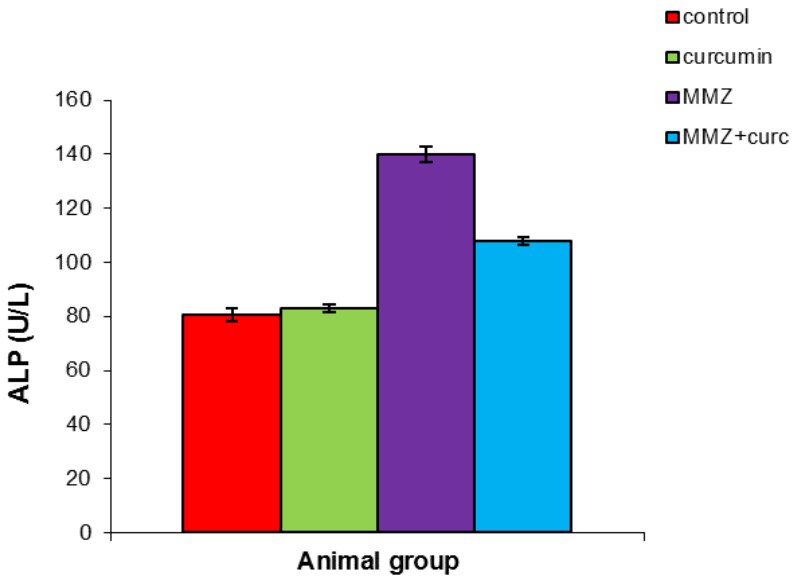

Fig. 7. Change in ALP in different groups.

the other results mentioned in previous study (Singh *et al*., 2013). It has been demonstrated that curcumin could prevent several hepatotoxin. Zhang *et al*. (2014) reported that pretreatment with curcumin has a protective effect against D-galactosamine (D-GalN), lipopolysaccharide (LPS)-induced acute liver damage in mice and rats feed with acetaminophen. Singh *et al*. (2013) and Kalpana *et al*. (2005) have noticed that Curcumin was found to modulate the elevated activities of the biochemical marker enzymes AST, ALP, ALT and of plasma lipid profiles in nicotine treated rats. Curcumin has been found to have some hepatoprotective properties against CCl_4 (Sengupta *et al*., 2011), ethanol (Singh *et al*., 2012), thioacetamide (Salama *et al*., 2013) and lead acetate (Baxla *et al*., 2013).

Curcumin considered as a class of antioxidants agents. It was documented to induce a noticeable increase in the activity of detoxifying enzymes such as glutathione peroxidase, glutathione reductase, glucose-6-phosphate dehydrogenase and catalase in liver (Iqbal *et al*., 2003), and hemeoxygenase-1 (Motterlini *et al*., 2000). It also was found to reduce lipid peroxidation in different organs (Okada *et al*., 2001; Kempaiah and Srinivasan, 2004). In conclusion, the results of this study indicate that the hepatotoxicity and oxidative stress caused by MMZ can be controlled and prevented by the curcumin antioxidant activity. In future more investigation may reveled more antioxidant properties for curcumin against other hyperthyroidism and antithyroid drugs.

REFERENCES

Aboul-Enein, HY. and Al-Badr, AA. 1979. Methimazole in: Analytical profiles of drug substances. Academic Press, New York, USA. 18:351.

Baxla, SL., Gora, RH., Kerketta, P., Kumar, N., Roy, BK. and Patra, PH. 2013. Hepatoprotective effect of Curcuma longa against lead induced toxicity in Wistar rats. Vet World 6(9):664-667.

Belfield, A. and Goldberg, DM. 1971. Revised assay for serum phenyl phosphatase activity using 4-amino-antipyrine. Enzyme. 12(5):561-573.

Borra, SK., Gurumurthy, P., Mahendra, M., Jayamathi, KM., Cherian, CN. and Ram, C. 2013. Antioxidant and free radical scavenging activity of curcumin determined by using different in vitro and ex vivo models. Journal of Medicinal Plants Research. 7(36):2680-2690.

Bruck, R., Weiss, S., Traister, A., Zvibel, I., Aeed, H., Halpern, Z. and Oren, R. 2007. Induced hypothyroidism accelerates the regression of liver fibrosis in rats. Journal of Gastroenterology and Hepatology. 22(12):2189-2194.

Cano-Europa, E., Blas-Valdivia, V., Franco-Colin, M., Gallardo-Casas, CA. and Ortiz-Butron, R. 2011. Methimazole-induced hypothyroidism causes cellular damage in the spleen, heart, liver, lung and kidney. Acta Histochem. 113(1):1-5.

Chainani-Wu. 2003. Safety and anti-inflammatory activity of curcumin: a component of tumeric (*Curcuma longa*). Journal of Alternative and Complementary Medicine. 9(1):161-168.

Chevalley, J., McGavack, TH., Kenigsberg, S. and Pearson, S. 1954. A four study of the treatment of hyperthyroidism with methimazole. J Clin Endocrinol Metab. 14 (8):948-60.

Cooper, SD. 2005. Antithyroid drugs. N Engl J Med. 352(9):905-917. DOI: 10.1056/NEJMra042972.

Epeirier, JM., Pageaux, GP., Coste, V., Perrigault, PF., Banc, P., Larrey, D. and Michel, H. 1996. Fulminant hepatitis after carbimazole and propranolol administration. Eur J Gastroenterol Hepatol. 8:287-288.

Gallelli, L., Staltari, O., Palleria, C., De Sarro, G. and Ferraro, M. 2015. Hepatotoxicity Induced by Methimazole in a Previously Health Patient. Current Drug Safety. 4(3):204-206.

Iqbal, M., Sharma, SD., Okazaki, Y., Fujisawa, M. and Okada, S. 2003. Dietary supplement of Curcuma enhances antioxidant and phase II metabolizing enzymes in ddY male mice: Possible role in protection against chemical carcinogenesis and toxicity. Pharmacol. Toxicol. 92(1):33-38.

Joe, B., Vijaykumar, M. and Lokesh, BR. 2004. Biological properties of curcumin-cellular and molecular mechanisms of action. Crit Rev Food Sci Nutr. 44 (2):97-111.

Kadasa, NM., Abdallah, H., Afifi, M. and Gowayed, S. 2015. Hepatoprotective effects of curcumin against diethyl nitrosamine induced hepatotoxicity in albino rats. Asian Pac J Cancer Prev. 16(1):103-8.

Kalpana, C., Rajasekharan, KN. and Menon, VP. 2005. Modulatory effects of curcumin and curcumin analog on circulatory lipid profiles during nicotine-induced toxicity in Wister rats. Journal of Medicinal Food. 8(2):246-250.

Kang, H., Do Choi, J., Jung, I., Kim, D., Kim, T. Shin, H., Kim, B., Park, C. and Yoo, J. 1990. A Case of methimazole-induced acute hepatic failure in a patient with chronic hepatitis B carrier. Korean J Intern Med. 5(1):69-73.

Kempaiah, RK. and Srinivasan, K. 2004. Influence of dietary curcumin, capsaicin and garlic on the antioxidant status of red blood cells and the liver in high-fat-fed rats, Ann Nutr Metab. 48 (5):314-320.

Kiernan, JA. 1981. Histological and Histochemical Methods, Theory and Practice. Pergamon Press. New York, USA.

Manikandan, P., Sumitra, M., Aishwarya, S., Manohar, M., Lokanadam, B. and Puvanakrishnan, R. 2004. Curcumin modulates free radical quenching in myocardial ischaemia in rats. The International Journal of Biochemistry and Cell Biology. 36(10):1967-1980.

Meisami, E., Najafi, A. and Timiras, PS. 1994. Enhancement of seminiferous tubular growth and spermatogenesis in testes of rats recovering from early hypothyroidism: a quantitative study. Cell Tissue Res. 275(3):503-511.

Menon, VP. and Sudheer, AR. 2007. Antioxidant and anti-inflammatory properties of curcumin. Adv Exp Med Biol. 595:105-25.

Mikhail, N. 2004. Methimazole-Induced Cholestatic Jaundice. South Med J. Feb;97(2):178-82.

Motterlini, R., Foresti, R., Bassi, R. and Green, CJ. 2000. Curcumin, an antioxidant and anti-inflammatory agent, induces hemeoxygenase-1 and protects endothelial cells against oxidative stress. Free Radic. Biol. Med. 28(8):1303-1312.

National Research Council (NRC). 1995. Guide for the Care and use of Laboratory Animals: Committee on care and use of laboratory animals. Institute of Laboratory Animal Resources. 20-246.

Nakamura, H., Noh, JY., Itoh, K., Fukata, S., Miyauchi, A.and Hamada, N. 2007. Comparison of methimazole and

propylthiouracil in patients with hyperthyroidism caused by Graves' disease. J Clin Endocrinol Metab. Jun. 92(6):2157-2162.

Okada, K., Wangpoengtrakul, C., Tanaka, T., Toyokuni, S., Uchida, K. and Osawa T. 2001. Curcumin and especially tetrahydrocurcumin ameliorate oxidative stress induced renal injury in mice. J Nutr. 131(8):2090-2095.

Ortiz-Butron, R., Blas-Valdivia, V., Franco-Colin, M., Pineda-Reynoso, M. and Cano-Europa, E. 2011. An increase of oxidative stress markers and the alteration of the antioxidant enzymatic system are associated with spleen damage caused by methimazole-induced hypothyroidism. Drug and Chemical Toxicology. 34(2): 180-188.

Palipoch, S., Punsawad, C., Koomhin, P. and Suwannalert, P. 2014. Hepatoprotective effect of curcumin and alpha-tocopherol against cisplatin-induced oxidative stress. BMC Complement Altern Med. 14:111. doi: 10.1186/1472-6882-14-111.

Pearse, AGE. 1972. Histochemistry, Theoretical and Applied. (vol. 2, 3rd edi.). Churchill Livingstone. London.

Ram, PA. and Waxman, DJ. 1992. Thyroid hormone stimulation of NADPH P450 reductase expression in liver and extrahepatic tissue. Regulation by multiple mechanisms. J. Biol. Chem. 267(5):3294-3301.

Reitman, S. and Frankel, S. 1975. A colorimetric method for the determination of serum glutamic oxalacetic and glutamic pyruvic transaminases. American Journal of Clinical Pathology. 28:56-63.

Rivkees, S., Stephenson, K. and Dinauer, C. 2010. Adverse events associated with methimazole therapy of Graves' disease in children. International Journal of Pediatric Endocrinology. 176970, doi:10.1155/2010/17697.

Sakr, S., Mahran, H. and Nofal, A. 2012. Effect of Selenium on Carbimazole-Induced Histopathological and Histochemical Alterations in Prostate of Albino Rats. American Journal of Medicine and Medical Sciences. 2(1):5-11.

Salama, SM., Abdulla, MA., AlRashdi, AS., Ismail, S., Alkiyumi**,** S. and Golbabapour, S. 2013. Hepatoprotective effect of ethanolic extract of *Curcuma longa* on thioacetamide induced liver cirrhosis in rats. BMC complementary and Alternative medicine.13:56.

Schmidt, G., Boersch, G., Mueller, KM. and Wegener, M. 1986. Methimazole-associated cholestatic liver injury: Case report and brief literature review. Hepatogastroenterol. 33(6):244-246.

Sefi, M., Ben Amara, I., Troudi, A, Soudani, N., Hakim, A., Zeghal, K., Boudawara, T. and Zeghal, N. 2014. Effect of selenium on methimazole-induced liver damage and oxidative stress in adult rats and their offspring. Toxicology and Industrial Health. 30(7):653-669.

Sengupta, M., Sharma, GD. and Chakraborty, B. 2011. Hepatoprotective and immunomodulatory properties of Aqueous extract of Curcuma longa in carbon tetrachloride intoxicated Swiss albino mice. Asian Pac J Trop Biomed. 1(3):193-199.

Singh, S., Jamal, F., Agarwal, R. and Singh, RK. 2013. Hepatoprotective Role of Curcumin against Acetaminophen induced toxicity in rats. International Research Journal of Biological Sciences. 2(12):42-49.

Snedecor, JG., Raheja , KL. and Freedland, RA. 1972. Effect of a single injection of l-thyroxine on glycogen, and on glycolytic and other enzymes in propylthiouracil-fed cockerels. General and Comparative Endocrinology. 18(2):199-209.

Specht, NW. and Boehme, EJ. 1952. Death due to agranulocytosis induced by methimazole therapy. JAMA. 149 (11):1010-1011.

Srinivasan, KR. 1952. The colouring matter in turmeric. Current Science. 311-313.

Tashkandi, B., Saleh, H. and Abdul Salam, H. 2014. The protective effect of vitamin E and selenium on methimazole-induced hepato-renal toxicity in adult rats**.** Life Science Journal. 11(10):893-899.

Valko, M., Leibfritz, D., Moncol, J., Cronin, M.T., Mazur, M. and Telser, J. 2007. Free radicals and antioxidants in normal physiological functions and human disease. International Journal of Biochemestry and Cell Biology. 39(1):44-84.

Venkatesan, N. 2000. Pulmonary protective effects of curcumin against paraquat toxicity. Life Sciences. 66(2):21-28.

Zhang, J., Xu, L., Zhang, L., Ying, Z., Su, W. and Wang, T. 2014. Curcumin attenuates D-galactosamine/ lipopolysaccharide-induced liver injury and mitochondrial dysfunction in mice. J. Nutr. 144(8):1211-8.

Zhao, J., Peng, L. and Geng, C. 2014. Preventive effect of hydrazinocurcumin on carcinogenesis of diethylnitrosamine-induced hepatocarcinoma in male SD Rats. Asian Pac J Cancer Prev. 15 (5):2115-21.

Received: Jan 12, 2016; Revised: June 9, 2016; Accepted: June 17, 2016

Canadian Journal of Pure and Applied Sciences
Vol. 10, No. 3, pp. 3971-3979, October 2016
Online ISSN: 1920-3853; Print ISSN: 1715-9997
Available online at www.cjpas.net

DIVERSITY AND ABUNDANCE OF FISH FAUNA AT HEAD MARALA, CHENAB RIVER, PUNJAB, PAKISTAN

*Maria Latif[1], Sumaira Siddiqui[1], Imtiaz Begum Minhas[1] and Samavia Latif[2]
[1]Fisheries Research and Training Institute, Manawan, Lahore, Department of Fisheries, Punjab, Pakistan
[2]College of Statistical and Actuarial Sciences, University of the Punjab
Quaid-E-Azam Campus, Lahore 54590, Pakistan

ABSTRACT

Marala headwork situated on River Chenab in Punjab, Pakistan was surveyed to assess the diversity and abundance of the fish fauna during the period September 2015 to June 2016. A total of five sampling sites were studied on monthly basis by using different fishing nets for assessing fish diversity. Total 1391 fish specimens belonging to 38 species, 30 genus, 14 families and 6 orders were recorded in the present study. Family Cyprinidae was found dominant with 14 fish species followed by Channidae (4 species) and Bagridae (3 Species). Fish abundance and diversity was assessed by using different diversity indices. The Shannon-Wiener diversity, Pielou's evenness and Margalef's richness indices were 2.950, 0.81 and 11.8, respectively. Present findings showed that the population of *Tor putitora* and *Nandus nandus* has declined while exotic fish species, *Cyprinus carpio, Ctenopharyngodon idella*, *Hypophthalmicthyus molitrix, Oreochromis niloticus* and *Oreochromis mossambicus* has become established. The low evenness in the river was an indication of the effects of anthropogenic activities such as habitat degradation, aquatic pollution, overfishing, damming and introduction of alien fish species. Present findings highlight the importance of instant mitigation measures for conserving fish diversity in the river.

Keywords: Chenab, fish fauna, freshwater, diversity, abundance.

INTRODUCTION

The freshwater icthyo diversity of Pakistan is represented by 193 species, out of which 86 species have been identified as "species of special importance"(Rafique and Khan, 2012). River Chenab is one of the most important water body in Pakistan providing habitat for aquatic biodiversity including fishes. Number of studies has been carried out on the fish diversity of River Chenab (Mirza and Khan, 1988; Khan *et al*., 1991; Afzal *et al*., 1995; Javed *et al*., 1997; Qazi *et al*., 2000; Mirza and Javed, 2003; Altaf *et al*., 2008; Qadir *et al*., 2009; Altaf *et al*., 2011 a,b; Altaf *et al*., 2015). In a riverine ecosystem fishes plays a vital role for maintaining the ecosystem. Anthropogenic stresses are responsible for bringing the climatic changes leading to the devastating effect on the ecosystems and biodiversity (Qureshi and Ali, 2011). The present study was aimed to investigate diversity, abundance and richness of fish fauna of Head Marala situated on River Chenab, Punjab, and to suggest conservative measures for declining fish species.

MATERIALS AND METHODS

The data was collected from September 2015 to June 2016 from Marala Headwork on monthly basis. During the study period fish samples were collected by using fishing nets of varying mesh sizes such as Cast, Drag and Drift nets, to capture as many as fish species as possible (Bhat, 2003). At the site of collection smaller fish samples were preserved in 10% formalin, while larger specimens were injected formalin intraperitonally. Later on, these samples were brought to the Fish Museum where they were shifted into 70% alcohol. On the basis of morphometric and meristics characteristics specimens were identified up to the species level by using regional fish identification keys (Mirza and Sharif, 1996; Mirza and Sandhu, 2007). The preserved specimens have been displayed at Fish Museum, Fisheries Research and Training Institute Manawan, Lahore.

STUDY AREA

River Chenab originates from India and near Diawara village enters into district Sialkot, Punjab. In the Pakistan side total length of this river is about 960 km. There are four Headworks on this river namely; Marala Headwork, Qadirabad Headwork, Khanki Headwork and Trimmu Headwork for regulating the flow and storage of water (Siddiqi and Tahir-Kheli, 2004). Marala Headwork (32^0 38′59 N, $74^0$28′05 E) is about 38.6 km away from district

*Corresponding author e-mail: marialatif5847@gmail.com

Sialkot. Fish sampling was done mainly from five sites viz Upstream and lower stream of Head Marala, Jammu Tawi, Manawar Tawi and Bajwat area (Figs. 1a-d). Sampling sites were intensvely sampled during the study period to capture as many as fish species as possible in an order to estimate the proportion to their abundance.

STATISTICAL ANALYSIS

Fish species diversity, richness and evenness from the study area were estimated by using the following formulas. Diversity Index, H' (Shannon-Wiener, 1963). $H' = -[\Sigma P_I \text{ In } P_I]$Margalef's richness index, D (Margalef's, 1958). R = S-1/logN, Evenness index, E= (Hill, 1973) E = H'/ln(S) Where: H'= diversity Index,

P_I=proportion of the species relative to the total number of species, In P_I natural logarithm of this proportion, D= dominance index, S= total no of species, N= total number of individuals, E= evenness index.

Fig. 1a. Location of Upstream of Marala Headwoks, River Chenab, Pakistan.

Fig. 1b. Location of Lower stream of Marala Headwoks, River Chenab.

Fig. 1c. Location of Jammu Tawi, River Chenab.

Fig. 1d. Location of Manawar Tawi, River Chenab.

Fig. 1e. Location of Bajwat area, River Chenab.

Table 1. Status of Fish fauna at Head Marala, River Chenab, Punjab, Pakistan.

S. No.	Family	Scientific Name	Common Name	R.A	$P_I InP_I$
I- 1.	Cyprinidae	*Labeo rohita*	Rohu	0.0381	-0.1244
2		*Cirrhinus mrigala*	Mori	0.0690	-0.1884
3		*Cirrhinus reba*	Reba Machali	0.0237	-0.0886
4		*Gibelion catla*	Thaila	0.0186	-0.0741
5		*Puntius sophore*	Sophore Popra	0.1603	-0.2934
6		*Puntius chola*	Chola popra	0.0625	-0.1732
7		*Tor putitora*	Masheer	0.0050	-0.0264
8		*Salmophasia punjabensis*	Punjabi Chal	0.0496	-0.1489
9		*Securicula gora*	Bari Chal	0.0416	-0.1322
10		*Esomus danricus*	Somara Machali	0.0150	-0.0629
11		*Osteobrama cotio*	Pali-ro Machali	0.0136	-0.0584
12		*Cyprinus carpio*	Gulfam	0.0265	-0.0962
13		*Ctenopharyngodon idella*	Grass Carp	0.0136	-0.0584
14		*Hypophthalmicthyus molitrix*	Silver Carp	0.0115	-0.0513
II-15	Bagridae	*Sperata sarwari*	Singhari	0.0194	-0.0764
16		*Mystus cavasius*	Kanghar	0.0438	-0.1370
17		*Mystus bleekeri*	Kanghar	0.0158	-0.0655
III-18	Sisoridae	*Bagarius bagarius*	Fauji Khaga	0.0079	-0.0382
19		*Gagata cenia*	Gagata cenia	0.0064	-0.0323
IV-20	Heteropneustidae	*Heteropneustes fossilis*	Sanghi Machali	0.0115	-0.0513
V-21	Siluridae	*Wallago attu*	Malli	0.0093	-0.0435
VI-22	Channidae	*Channa marulius*	Saul	0.0136	-0.0584
23		*Channa striata*	Sauli	0.0036	-0.0197
24		*Channa punctate*	Daula	0.0244	-0.0906
25		*Channa gachua*	Dauli	0.0050	-0.0264
VII-26	Chandidae	*Chanda nama*	Sheesha Machali	0.0740	-0.1926
27		*Parambassis ranga*	Ranga Sheesha	0.0258	-0.0943
VIII-28	Nandidae	*Nandus nandus*	Patta Machali	0.0014	-0.0091
IX-29	Gobiidae	*Glossogobius giuris*	Golu Machali	0.0079	-0.0382
X-30	Belontidae	*Colisa fasciata*	Bari Kanghi	0.0033	-0.0188
31		*Colisa laila*	Choti Kanghi	0.0208	-0.0805
XI-32	Cichlidae	*Oreochromis niloticus*	Chirra Machali	0.0474	-0.1445
33		*Oreochromis mossambicus*	Chirra Machali	0.0244	-0.0906
XII-34	Mastacembelidae	*Mastacembelus armatus*	Baam	0.0093	-0.0435
35		*Macrognathus pancalus*	Garoj	0.0050	-0.0264
XIII-36	Schilbeidae	*Eutropiichtys vacha*	Jhalli Machali	0.0222	-0.0845
37		*Clupiosoma garua*	Bachwa	0.0079	-0.0382
XIV-38	Notopteridae	*Notopterus notopterus*	But Pari	0.0093	-0.0435

Table 2. Morphometric measurements (cm) of the recorded fish species from Marala Headwork.

S. No.	T.L	S.L	F.L	B.W	B.H	Pr.L	Ps.L	H.L	L.C.P
1	25.3	20.2	22.1	7.1	7.4	9.8	7.2	5.3	3.9
2	15.3	12.4	13.4	3.5	3.8	6.1	4.7	2.9	2.2
3	14.5	12.1	12.9	3.4	3.9	5.6	5.1	2.8	2.1
4	42.1	35.4	38.2	11.2	12.3	18.2	11.9	9.6	3.8
5	8.7	7.1	7.9	3.1	3.2	3.7	2.5	2.1	1
6	7.1	6.1	6.4	2.2	2.4	3.1	2.1	1.6	0.8
7	16.2	14.8	15.9	4.3	4.6	7.3	8.1	3.9	2.6
8	7.2	5.3	5.7	1.5	1.7	3.3	2.3	1.6	0.8
9	15.3	13.4	14.3	2.8	3.2	8.9	3.9	2.9	2.4
10	5.4	4.9	5.1	1.1	1.3	2.9	1	1.1	0.6
11	9.5	7.5	7.7	3.5	3.8	4	3.7	1.7	0.9
12	18.7	15.1	15.9	5.9	6.3	7.2	2.5	4.5	2.9
13	31.3	26.3	27.9	6.2	6.5	13.9	11.5	6.2	3.7
14	36.5	30.2	32.2	9.3	10.4	16.8	11.7	8.7	5.5
15	32.1	25.2	25.6	4.4	4.6	11	11.3	6.4	4.2
16	13.3	10.4	10.9	2.5	3.1	4.2	5.7	2.2	2.5
17	5.2	4.1	4.4	1.2	1.4	1.9	0.8	1.4	0.5
18	39.3	35.1	37.2	7.3	7.6	21.4	14.1	6.3	4.2
19	4.9	3.9	4.5	2.1	2.3	2.1	3.2	1.9	1.3
20	10.9	9.9	-	2.1	2.3	3.9	6.7	1.6	-
21	47.5	43.5	44.3	9.5	9.9	12.6	30.1	9.7	1.1
22	48	41	-	9.5	10.7	11.9	1.5	11.8	2.5
23	47	37	-	7.1	7.5	11.3	2.5	10.3	2.9
24	16.3	13.7	-	4.1	4.4	6.9	1.1	5.3	0.9
25	8.2	6.9	-	2.1	2.2	2.6	0.6	2.9	0.4
26	4.2	3.2	3.7	1.3	1.4	1.5	0.3	1.2	0.2
27	8.3	6.2	7.9	3.2	3.3	3.2	1.1	2.2	0.9
28	15.5	13	-	5.5	5.8	6.1	1.7	5.3	1.6
29	4.9	3.7	-	1.2	1.4	2.1	0.9	1.4	1.1
30	8.1	6.6	-	3.1	3.3	2.4	0.6	1.9	0.2
31	5.3	4.8	-	2.6	2.9	1.8	0.3	1.2	0.1
32	19.5	16.3	-	7.3	7.5	6.3	2.9	4.5	2.3
33	9.5	7.6	-	3.5	3.8	3.3	1.1	2.1	1
34	36.2	34	-	3.6	3.7	23.2	-	5.4	-
35	29.3	28.2	-	3.1	3.3	18.3	-	4.3	-
36	13.6	11.7	13.2	2.7	3.6	8.2	3.7	2.9	1.4
37	35.3	30.2	31.3	6.8	7.9	8.9	19.1	6.2	6.5
38	16.8	16.1	-	3.8	4.9	8.5	7.6	3.5	-

Legend: T.L= Total length, S.L= Standard length, F.L= Forked length, B.W= Body width, B.H= Body height, Pr.L= Pre-dorsal length, Ps.L= Post-dorsal length, H.L= Head length, L.C.P= Length of caudal peduncle.

Table 3. Number and percentage composition of families, genera and species of fishes under various orders.

S. No.	Orders	Families	Genus	Species	% of families in an order	% of genera in an order	% of species in an order
1	Cypriniformes	01	12	14	7.14	40	37
2	Siluriformes	05	08	09	35.7	27	24
3	Channiformes	01	01	04	7.14	3.3	10
4	Perciformes	05	06	08	35.7	20	21
5	Synbranchioformes	01	02	02	7.14	6.6	5.3
6	Osteoglossiformes	01	01	01	7.14	3.3	2.6
Total		14	30	38			

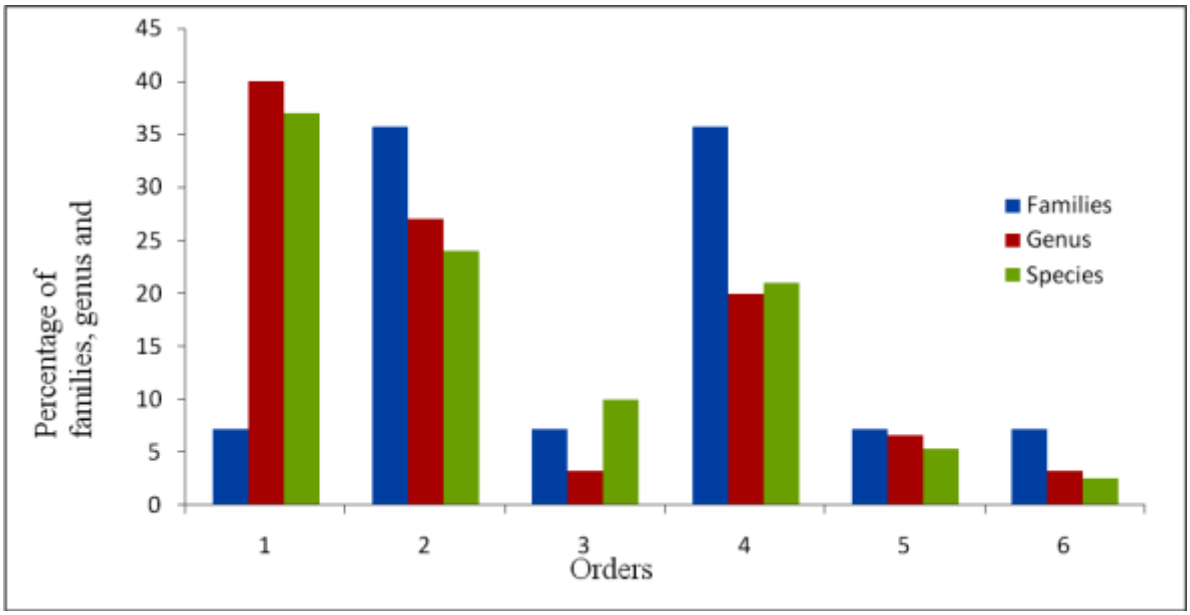

Fig. 2. Number and percentage contribution of families, genera and species.

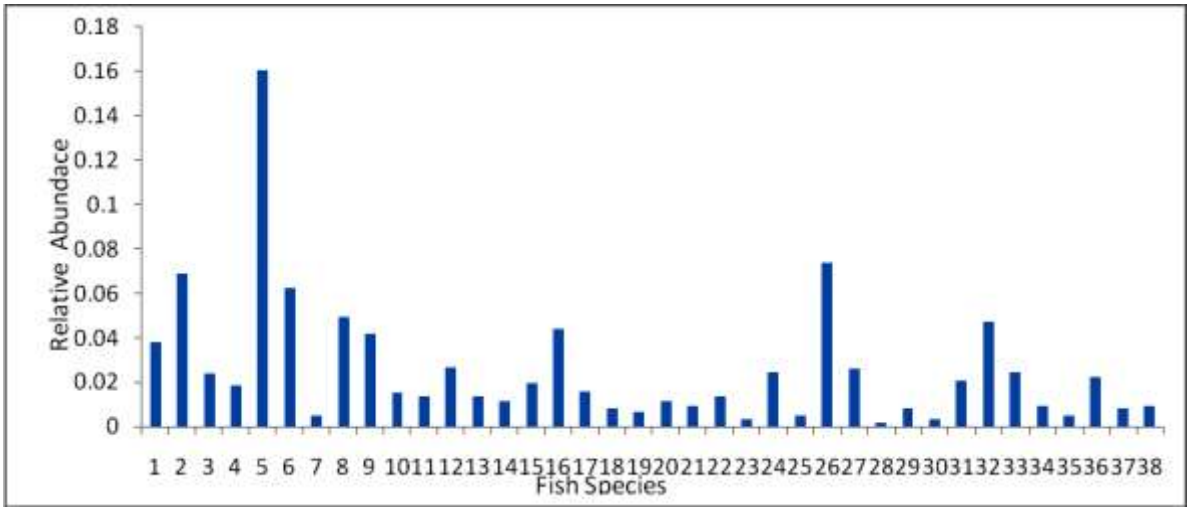

Fig. 3. Fish species diversity and their relative abundance from Head Marala, Chenab.

RESULTS AND DISCUSSION

A total of 1391 fish specimens were collected from all the sampling sites at Head Marala. These fishes belong to 6 orders, 14 families, 30 genera and 38 species. The list of recorded fish species is given in Table 1. Morphometric measurements of the largest specimen of all recorded fish species are given in Table 2. Order Cypriniformes was found dominant represented with 14 species included in a single family Cyprinidae. Order Siluriformes was represented with 9 species included into five families namely Bagridae, Sisoridae, Hetropneustidae, Siluridae and Schilbeidae. *Sperata sarwari*, *Mystus cavasius* and *Mystus bleekri* were represented under a single family Bagridae. Both Sisoridae and Schilbeidae families were represented with two species each. Hetropneustidae and Siluridae each represented with single species. Order Channiformes was represented with a single family Channidae having four species. Order Perciformes included 5 families, Chandidae, Cichlidae, Belontidae, Nandidae and Gobiidae. Families Chandidae, Belontidae and Cichlidae included two species each. Nandidae and Gobiidae were each represented with a single species. Order Synbranchioformes was represented with single family Mastacembelidae and two species. Order Osteoglossiformes was represented with single species under family Notopteridae. The number and percentage composition of these families, genera and species of fishes under various orders is given in Table 3 and Figure 2.

The highest value for the relative abundance was calculated for *Puntius sophore* (0.1603) followed by *Chanda nama* (0.0740) and *Puntius chola* (0.0625). *Nandus nandus* and *Tor putitora* showed lowest values for their relative abundance. The species diversity and their relative abundance showed in Figure 3. The diversity index was 2.95 for the study area. The value for the richness of the study area was 11.7. The value for the species evenness from all the sampling sites was found low (0.81). The statistical analysis of different diversity indices has been shown in Table 4.

Table 4. Statistical analysis of the fish diversity of Marala Headwork, Chenab.

Number of Species	38
Shannon diversity (H')	2.95
Evenness (E)	0.81
Margalef's (R)	11.7

In the present study, 38 fish species belonging to six genera (Cypriniformes, Osteoglossiformes, Perciformes, Siluriformes, Channiformes and Synbranchiformes) were recorded. Among these *Labeo rohita*, *Cirrhinus mrigala*, *Gibelion catla*, *Tor putitora*, *Sperata sarwari*, *Bagarius bagarius*, *Wallago attu*, *Channa marulius*, *Channa punctate*, *Mastacembelus armatus*, and *Eutropiicthyus vacha* were commercially and economically important fishes in Pakistan. Five commercially important exotic fish species *Cyprinus carpio*, *Ctenopharyngodon idella*, *Hypophthalmicthyus molitrix. Oreochromis mossambicus* and *Oreochromis niloticus* were also found in the present collection.

Among the collected fish specimens *Puntius sophore* and *Chanda nama* were abundantly found. This was may be due to their wide distribution in the river and also their smaller size rendering them inedible to the humans. *Tor putitora* and *Nandus nandus* were found from the upstream of head Marala. These species have shown lower relative abundance in the present collection. Their population has seemed to decline in the river due to the various anthropogenic stresses such as overfishing, pollution, Damming, and introduction of alien fish species.

Qazi *et al*. (2000) studied the fish fauna of Bajwat area, District Sialkot during the period 1998-99. They reported this area as an important wetland representing 37 species of fishes belonging to 13 families and 28 genera. Their collection included some remarkable cold water fish species (*Schizothorax plagiostomus*, *Racoma labiate*, *Lepidocephalus gentea* and *Glyptothorax cavia*) which were not found in present collection. Altaf *et al*. (2008) reported various threats to Indian and Chinese carps of river Chenab. Their results supports our findings as commercially important fishes were being highly exploited showed low relative abundance in the Chenab river.

Another study, Altaf *et al*. (2011a) reported 33 fish species from Head Qadirabad, Chenab. Their study found that *Oreochromis niloticus*, an exotic fish species in the river showed highest relative abundance. This species was also found with high (0.0474) relative abundance in the present collection. Various threats to ecology and fish diversity were also indicated in their report. Qadir *et al*. (2009) conducted a survey on the two tributaries of River Chenab in Pakistan namely Nullah Aik and Nullah Palkhu to assess the distribution of freshwater fish fauna. They collected 1506 fish specimens belonging to 24 species and 12 families. They reported that fish assemblage was relatively stable throughout the year at upstream of Nullah's; however, downstream are severely affected due to various anthropogenic activities. In a recent study on fish diversity of river Chenab conducted by Altaf *et al*. (2015) at the three heads of river and reported 34 species. The highest diversity index was found at Head Qadirabad followed by Khanki and Marala headworks. Their findings did not include these fish species *Nandus nandus*, *Channa striata*, *Channa gachua* and *Colisa laila* from Head Marala which were found in the present collection. Our findings showed that the relative abundance of these fish species is very low in the river.

Fresh water icthyo-diversity has been studied by different researchers in the country. Khan *et al*. (2008) conducted a survey at Chashma (Jhelum) and Taunsa (Indus) to analyze the freshwater fish status. Twenty fish species from Chashma Reservoir and twenty two species from Taunsa Reservoir were collected. Their collection was dominated with native fish species however; exotic fish species such as *Carassius auratus, Ctenopharyngodon idella, Hypopthalmichthys molitrix, Hypopthalmichthys nobilis and Cyprinus carpio* were also reported from these two important freshwater reservoirs. Another study, Mirza *et al*. (2011) reported 51 freshwater fish species from River Jhelum.

Their results showed that the population of a commercially important fish species, *Tor macrolepis* has diminished, while *Oreochromis aureus* an exotic fish has become established. Khan *et al*. (2011) studied the impact of exotic fish species on the native fish fauna of the rivers in Punjab and reported that these alien species has become invasive and are competing with economically important native fish species. Earlier, Iqbal *et al*. (2013) studied population dynamics of *Tor macrolepis* and other commercially high valued species in Attock region. They reported that population of commercial fishes is declining due to various anthropogenic activities. Their finding has supported our results.

CONCLUSION

River Chenab is an important water body in Pakistan supporting diverse fish fauna and other aquatic biodiversity. Various anthropogenic activities such as pollution, habitat destruction, overfishing, damming and introduction of alien fish species into the river are responsible for declining the population of commercially and economically important fish species in the river. Authorities should take necessary steps to conserve fish fauna by minimizing adverse human activities.

ACKNOWLEDGEMENT

The authors are very thankful to the field officer and officials of Punjab Fisheries Department and to the contractors and private fishermen for their cooperation in the field work.

REFERENCES

Afzal, M., Javed, MN.and Mirza, MR. 1995. Fishes of River Chenab in district Jhang. Biologia Pakistan. 41:133-137.

Altaf, M., Khan, AM., Umair, M. and Chattha, SA. 2008. Diversity and threats to Indian and Chinese carps of River Chenab in Pakistan. Punjab University Journal of Zoology. 23(1-2):09-17.

Altaf, M., Khan, AM., Umair, M., Irfan, M., Munir, MA.and Ahmed Z. 2011[a]. Ecology and diversity of freshwater fishes of Head Qadirabad, Gujranwala. Punjab University Journal of Zoology. 26(1): 1-7.

Altaf, M., Khan, AM., Umair, M. and Chattha, SA.2011[b]. Diversity of Carps in River Chenab, Pakistan.Punjab University Journal of Zoology. 26(2):107-114.

Altaf, M., Javid, A., Khan, AM., Hussain, A., Umair, M. and Ali, Z. 2015. The status of fish diversity of River Chenab, Pakistan. Journal of Animal and Plant Sciences. 25(3-2):564-569.

Bhat, A. 2003. Diversity and composition of freshwater fishes in river systems of Central Western Ghats, India. Environmental Biology of Fishes. 68:25-38.

Hill, MO. 1973. Diversity and its evenness, a unifying notation and its consequences. Ecology. 54:427-432.

Iqbal, Z., Pervaiz, K. and Javed, MN. 2013. Population dynamics of *Tor macrolepis* (Teleostei: Cyprinidae) and other fishes of Attock region, Pakistan. Canadian Journal of Pure and Applied Sciences. 7(1):2195-2201.

Javed, MN., Zafar, A., Shahbaz, M. and Mirza, MR. 1997. Biodiversity of fishes of the river Chenab between Khanki and Qadirabad in Pakistan. Biologia Pakistan. 43(2):149-156.

Khan, MI., Irshad, R. and Saga, FH. 1991. Fishes of River Chenab in Multan district. Biologia. 37(1):23-25.

Khan, AM., Shakir, HA., Abid, M. and Mirza, MR. 2008. Ichthy of annual survey of some fresh water reservoirs in Punjab. Journal of Animals and Plants Sciences. 18(4):151-154

Khan, AM., Ali, Z., Shelly, SY., Ahmad, Z. and Mirza, MR. 2011. Aliens; A catastrophe for native freshwater fish diversity in Pakistan. Journal of Animals and Plants Sciences. 21:435-440.

Margelf, R. 1958. Temporal succession and spatial heterogeneity in phytoplankton. In: Perspective in Marine Biology. Ed. Buzzati-Traverso, AA. University of California Press. Berkeley, California, USA. 323-347.

Mirza, MR. and Khan, AJ. 1988. Fishes of Marala, Sialkot district, Pakistan. Biologia Pakistan. 34:151-153.

Mirza, MR. and Sharif, HM. 1996. A Key to the Fishes of Punjab. Ilmi Katab Ghar, Urdu Bazar, Lahore.

Mirza, MR. and Javed, MN. 2003. Fishes of the Rive Chenab in Pakistan. Biologia. 49(1&2):57-64.

Mirza, MR. and Sandhu, IA. 2007. Fishes of the Punjab, Pakistan. Polymer Publications, Pakistan.

Mirza, ZS., Mirza, MR., Mirza, MA. and Sulehria, AQK. 2011. Icthyo faunal diversity of the River Jhelum, Pakistan. Biologia Pakistan. 57(1&2):23-32.

Qadir, A., Malik, RN., Ahmad, T. and Sabir, AM. 2009. Patterns and Distribution of Fish Assemblage in Nullah Aik and Nullah Palkhu Sialkot, Pakistan. Biological Diversity and Conservation. 2(2):110-124.

Qazi, MB., Mirza, MR. and Javed, MN. 2000. Fishes of Bajwat area district Sialkot, Pakistan. Pakistan Journal of Fisheries. 1(1):41-48.

Qureshi, NA. and Ali, Z. 2011. Climate change, biodiversity Pakistan's scenario. Journal of Animals and Plants Sciences. 21:358-363.

Rafique, M. and Khan, NUH. 2012. Distribution and status of significant freshwater fishes of Pakistan. Record of Zoological Survey of Pakistan. 21:90-95.

Shannon, CE. and Weaver, W. 1963. The Mathematical Theory of Communication. University of Illinois Press, Urbana, USA. 31-35.

Siddiqi, TA. and Tahir-Kheli, S. 2004. Water and security in South Asia. WASSA. pp234.

Received: August 25, 2016; Revised: Sept 24, 2016;
Accepted: Sept 27, 2016

Canadian Journal of Pure and Applied Sciences
Vol. 10, No. 3, pp. 3981-3990, October 2016
Online ISSN: 1920-3853; Print ISSN: 1715-9997
Available online at www.cjpas.net

VERNONIA AMYGDALINA, A LOCAL ANTI MALARIAL LEAVES EXTRACT INHIBIT LIPID PEROXIDATION AND EXHIBIT HEPATOPROTECTIVE AND NEPHROPROTECTIVE EFFECTS RESULTING FROM ARTESUNATE ADMINISTRATION IN RATS

*Olaniyi T Adedosu[1], Akinola N Adedosu[2], Gbadebo E Adeleke[1]and Gbemisola B Balogun[1]
[1] Department of Biochemistry, Faculty of Basic Medical Sciences, College of Health Sciences
Ladoke Akintola University of Technology, Ogbomoso, Nigeria
[2]Department of Medical Microbiology and Parasitology Federal Medical Centre Owo, Nigeria

ABSTRACT

With the common practice in poor Africa endemic area to take local antimalaria herbs in combination with orthodox medicine and the increasing resistance to anti-malarial drugs, this study investigates the roles of methanol leaves extract of *Vernonia amygdalina*, in combination with artesunate. 24 male wistar rats weighing 190g were randomly grouped, administered therapeutic doses of artesunate and extract. Plasma total protein, urea, creatinine. Alanine. amino transferase (ALT), Alkaline phosphatase (ALP) and Gamma glutamyl transferase (GGT) were determined using international standardized methods. Percentage inhibition of lipid peroxidation, Malondialdehyde, (MDA), reduced glutathione (GSH) levels were determined spectrophotometrically. Results shows that extract conferred above 50% cell protection as it inhibited lipid peroxidation ,decreases MDA level significantly ($P \leq 0.05$) and increases GSH level significantly ($P \leq 0.05$) compared with controls, Artesunate alone and combined treatment of artesunate and extract. Plasma total protein concentrations were significantly ($P \leq 0.05$) increased in all treatment groups . Artesunate alone significantly increased ($P \leq 0.05$) plasma ALT, ALP and liver GGT activities while the combined treatments showed a modulatory effect as these activities were significantly decreased ($P \leq 0.05$) nearly to control levels .Also, artesunate elicit significant ($P \leq 0.05$) increases in plasma urea and creatinine concentrations which were attenuated to control levels in the combined treatment.Results are indicative of extract ability to inhibit lipid peroxidation, boost GSH formation, increases antioxidant status, shows hepatoprotective and nephroprotective effects.

Keywords: Anti- malarial, lipid peroxidation, hepatoprotective, nephroprotective, antioxidants.

INTRODUCTION

In the developing countries of tropical Africa, Asia and Latin America, Malaria constitutes one of the major public health problems. It was estimated that over (350-500) million people are infected by malaria parasite world-wide where among the four species of Plasmodium parasites; *P. falciparum, P.vivax, P.ovale, P. malariae*, the *P. falciparum* is the most virulent parasite and is highly present in all malaria endemic regions of the world especially in Africa. (Miller *et al*., 1996; Singh *et al*., 2004; WHO, 2005; Kumar and Srivastava, 2005; Hilou *et al*., 2006; Mbatchi *et al.,* 2006). The greater virulence of *P. falciparum* is associated with its tendency to infect a large proportion of the red blood cells, while patients infected with this species exhibit ten times the number of parasites per cubic millimeter of blood than patients infected with the other three malaria species (WHO, 2005).

Many strains of *P. falciparum* have developed resistant to some of the drugs used to treat or prevent malaria, however the alarming rate at which *Plasmodium falciparum* has developed resistance to chloroquine, artesunate and other synthetic antimalarial drugs makes it necessary to search for more effective anti malarial compounds (Mbatchi *et al*., 2006). In Africa and other countries where malaria is endemic, traditional medicinal plants are frequently used to treat or cure malaria, while it is well known that the convectional anti malarial such as quinine and artemisininis were obtained from plants. However, since malaria treatment evolved originally from traditional folkloric medicines obtained from plant preparations as herbs by various traditional healers, this treatment method still remain a promising source of new anti-malarial compounds (Ouattara *et al*., 2006; Chukwujekwe *et al*., 2009) as the use of indigenous plants have played important roles in the treatment of malaria by

*Corresponding author e-mail: otadedosu@lautech.edu.ng

serving as good sources of novel anti plasmodia compounds whose natural products have been a good source for drug development (Mbatchi *et al*., 2006; Hilou *et al*., 2006; Challand and Wilcox, 2009).

Also with the advent of combination therapy involving artemisinins-based combinations with other anti malaria drugs, as currently approved by WHO (Looarwsuwan, 1996; Ridley, 2002) to ward off resistance. Certain bioactive agents which may serve as anti malarial drugs of plants origin abounds and are still yet to be discover while the continuous screening of these plants especially in Africa for effective malaria drugs may still be the best means or lead to either right combinations or single dosage of anti malarial drugs for overcoming resistance.

Although international efforts have been under way for decades to produce a vaccine, so far without success in order to immunize against *P. falciparum* resistance while combination of anti malarial agents has been introduced as a response to widespread drug resistance the advantages of combination therapy should be balanced against the increased chance of drug interactions (Giao and Vries, 2001).

During the last decade most of the pharmacokinetic and metabolic pathways involving anti malarial drugs have been elucidated, including the roles of the cytochrome P 450 (CYP) enzyme complex. In this way it is pertinent to note that a number of drugs currently in clinical use exert their pharmacological activities at least in part by increasing oxidative stress in the parasitized erythrocytes while ROS are often produced by the host immune system adds to the overall oxidative burden of the parasitized cell (Becker *et al*., 2004) .

Interestingly, based on the principle of oxidative stress associated with most anti malarial drugs action (Taylor and White, 2004), the present study explore the possibilities of using extract of known anti malarial medicinal plants as an agent for a possible means of an attempt to overcome drug resistance in malaria chemotherapy and in view of the common practice in poor Africa endemic area to take local anti malarial herbs in combination with orthodox medicine when privileged to have such drugs and with the increasing resistance to anti-malarial drugs, this study investigates the roles of methanol leaves extract of *Vernonia amygdalina*, a local anti malarial in combination with artesunate, a combinative therapy using artemisinins based drugs since treatment failures have been recorded with artemisinins combination treatment (ACTs) in some endemic regions especially in Africa, hence the justification for this study.

Vernonia amygdalina is a perennial herb belonging to the *Asteraceae* family. It is popularly known as bitter leaf, an under shrub of variable height with petiolate green leaves of about 6mm diameter. The leaves are usually bitter and are very popular soup vegetable in Nigeria (Iwu, 1982; Igile *et al*., 1995). The plant is found in Savannah regions and through central and south tropical Africa. All parts of the plant (leaves, stem and roots) are said to have medicinal uses such as cure of tonsillitis, fever, malaria, diabetes, pneumonia, jaundice, anaemia, stomach problem and ascaris (Iwu, 1982). Extracts of the plant have been used in various folk medicines as remedies against helminthes, protozoan and bacterial infections with few scientific support for these claims. In this study the combinative effect of the methanol extract of *Vernonia amygdalina* on artesunate activities as a possible model to study the potential effects of non-synthetic bioactive agents of medicinal plants with known anti malarial drug was examined.

MATERIALS AND METHODS

Materials

Materials and laboratory equipment used in this study includes: Cages, micropipette, test tubes, hand gloves, cotton wool, distilled water, electric blender, refrigerator, Artesunate tablets, *Vernonia amygdalina* leaves, Chemical Weighing balance, water bath, centrifuge, spectrophotometer, beakers, homogenizer, conical flask, cuvette, measuring cylinders, separating funnels, pH meter, thermometer, bottles, syringes, test tube racks etc.

Reagents

Methanol, sodium carbonate, sodium hydroxide, ascorbic acid, phosphate buffer, Tris HCl, potassium chloride, ferrous sulphate, Tris buffer , distilled water, normal saline, laboratory kits for determination of total protein, Alkaline phosphatase, Alanine aminotransferase, gamma glutamyl transferase activity, Trichoroacetic acid (TCA), Thiobarbituric acid (TBA) etc. All other chemicals were of the highest quality grade available obtained from British Drug house (BDH) and Sigma Chemical Company, USA.

Plants material and preparation of extract

Fresh healthy leaves of *Vernonia amygdalina* were collected within the premises of the Botanical garden Ladoke Akintola University of Technology, Ogbomoso Oyo State .The leaves were identified and confirmed by Dr. A.T.J Ogunkunle of the Botany Unit of the Department of Pure and Applied Biology of the same Institution with herbarium voucher number LHO 283 deposited. The leaves were air dried at room temperature for two weeks on the ceramic slabs in the laboratory and powdered. The powdered leaves was weighed and kept in a well labeled transparent plastic container. Methanol extract was prepared using 300g of the powdered leaves soaked in 3liters of methanol (95%v/v) and kept for 3 days in the dark cupboard. The colored methanol filtrate solution obtained from the mixture was decanted into a

clean dry breaker. The filtrate was concentrated by placing it in a water – bath at 40^0C to obtained the dry methanol extract.

Experimental Animals

Twenty four healthy male Wistar Albino rats obtained from the animal house of the Department of Biochemistry, University of Ibadan were used for this study. All animals were fed on rat pellets and maintained under standard laboratory conditions for two weeks before the start of the experiment. They were allowed food and water ad libitum before and during the experiment and randomly selected into four groups A, B, C, and D with six animals in each group. Handling and treatment of the animals throughout the experiment were based on the regulations and guard lines for handling laboratory animals by our institution which conform with international standards.

Experimental design and administration of test substances

Artesunate was administered at 2mg/kg body weight orally as its standard therapeutic dose for three days and this was applied to the administration of the extract based on the average weight of the experimental animals (190g). Hence four treatment groups (A, B, C, and D). were identified based on the experimental design and treated as follows; The control (Group A), given 0.1ml normal saline intravenously two times in a day morning and evening for three consecutive days).

Group B; administered orally with methanol extract of *Vernonia amygdalina* (in 0.1ml corn oil containing 0.38mg of extract twice a day for three days) while, 0.1ml containing 0.38mg of standard drug (Artesunate) was administered orally to the rats in Group C twice a day for three days.

Group D (combinative therapy or treatment) was also administered with 0.1ml of each drug and extract separately and simultaneous through oral means of route of administration, twice in a day for three consecutive days. The groups and the agents administered are shown below:

Group A: Control rats received only normal saline solution

Group B: Received only methanol extract at therapeutic dose

Group C: Received only artesunate at therapeutic dose

Group D: Received both artesunate and extract at therapeutic dose.

Collection of Blood Sample and preparation of plasma and tissue homogenates

All the animals in each group were sacrificed at the end of the treatment period by cervical dislocation. Blood was collected directly from the heart into plain and well-labelled sample bottles containing heparin anticoagulant and were centrifuged at 4000rpm for 5 minutes to obtain plasma for analysis of biochemical indices. One gram of the liver sample was homogenized in KCl [10 mM] phosphate buffer (1.15%) with ethylene-diamine tetra acetic acid (EDTA, pH 7.4) and centrifuged at 12, 000 rpm for 60 min. The supernatants were used to assay for reduced glutathione and malondialdehyde concentrations.

Biochemical indices

Plasma proteins, urea and creatinine concentrations were estimated by the principles and procedures of Lowry *et al*. (1951), Naito (1984) and Murray (1984) using diagnostic kits. Enzyme assays, Alanine Aminotransferase (ALT), Alkaline Phosphatase (ALP) and Gamma glutamyl transferase (γGT) were determined using the method of Wroblwski *et al*. (1956), Burtis (1999) and Szasz (1969) based on the standardized methods by the International Federation of Clinical Chemistry.

Antioxidants indices

Percentage inhibition of lipid peroxidation was determined using the method of Ruberto *et al*. (2000). Ferrous sulphate induces lipid peroxidation and measured lipid peroxide formed with ascorbic acid as standard were determined Spectrophotometrically. Malondialdehyde levels and reduced glutathione (GSH) determinations were carried out by the methods of Varshney and Kale (1990) and Beutler *et al*. (1963).

Statistical Analysis

Statistical analysis were based on the Duncan`s experimental analysis with mean standard deviation of sample analyzed using the student T test and $p< 0.05$ i.e. 95% level of significance or confidence limit (Bliss, 1967).

RESULTS AND DISCUSSION

Reports of chloroquine resistant strains of *P. falciparum* are being documented in all regions of the world where malaria is endemic while resistance to anti-malaria drugs other than Chloroquine such as Pyrimethamine /sulfadoxine, Mefloquine, Quinine, Halofantrine and artemisinins based drugs such as artesunate are occurring at an alarming rate such that WHO now recommends protocols, and change their drug policy significantly with the introduction of Artemisinins based combinative therapy ACTs. While artemisinins are one of the few classes of drugs useful to treat severe malaria that is resistant to Chloroquine, its compounds include artemether, artesunate and dihydroartemisinin which are sesquiterpene lactone with a peroxide bridge and their anti malarial activity has been attributed to their peroxide moiety (Klayman *et al*., 1985) that generates free radicals which damages the parasite membrane (Muller *et al*., 2004), while their possible toxicity such as neurotoxicity

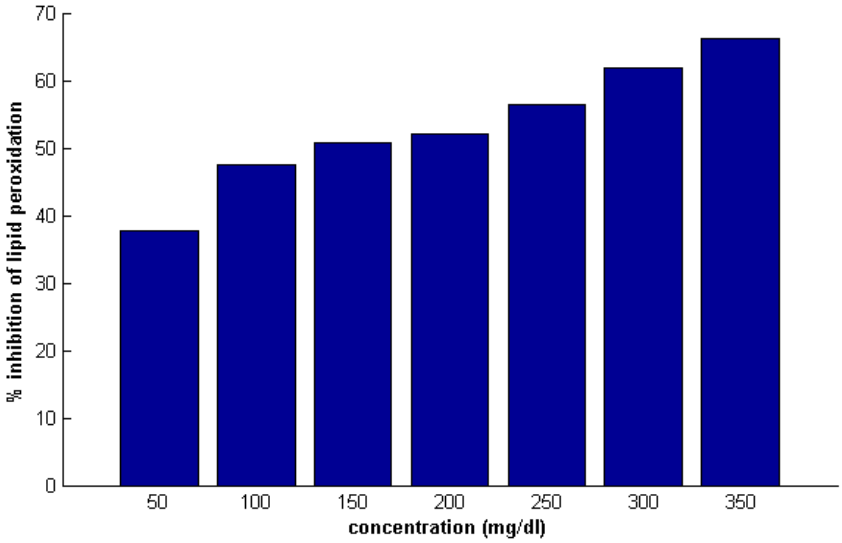

Fig. 1. Percentage Inhibition of lipid peroxidation by methanol extract of *Vernonia amygdalina* at various concentrations.
Values are given as mean and standard deviation of six determinations
P value (P≤ 0.05) as the level of significance.
of six determinations
P value (P≤ 0.05) as the level of significance.

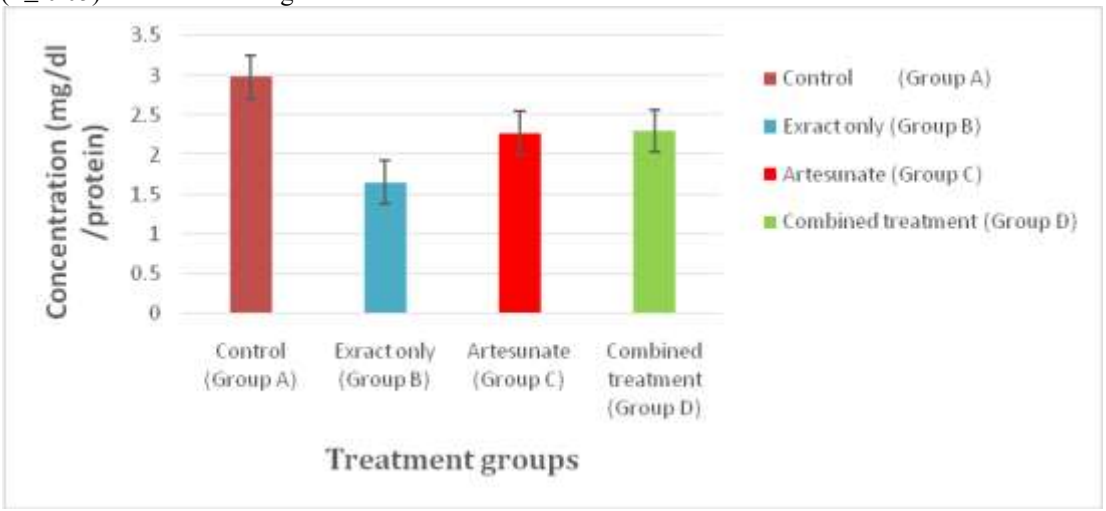

Fig. 2. Malondialdehyde (MDA) levels in the liver of various treatment groups.
Values are given as mean and standard deviation

and reproductive toxicity has been reported (Woedenbag *et al*., 1994; Li *et al*., 2005; Clark *et al*., 2008).

Medicinal plants have formed the basis of health care throughout the world right from the ancient times, the development of novel anti malarial drugs as a tool for combating malarial drug resistance is the reigning trend in malaria chemotherapy, hence search for new drugs with better and cheaper substitutes from plant origin is a natural choice especially in poor populations of malaria endemic regions in Africa. However studies have shown that the medicinal values of these plant lies in some bioactive substances present in them that produce a definite physiological action on human body (Ames and Forward, 1994), hence investigating them in a relation to most claims by the traditional healers and users is imperative in order to determine their potentials as sources of new anti malarial agents (Farombi, 2003).

In this study co-administration of artesunate and methanol extract of *Vernonia amigdalina* leaves used and known locally in Nigeria and across West Africa as a potent anti malarial plant was examined with the aims of validating or recognition of ACTs and as a means to source for

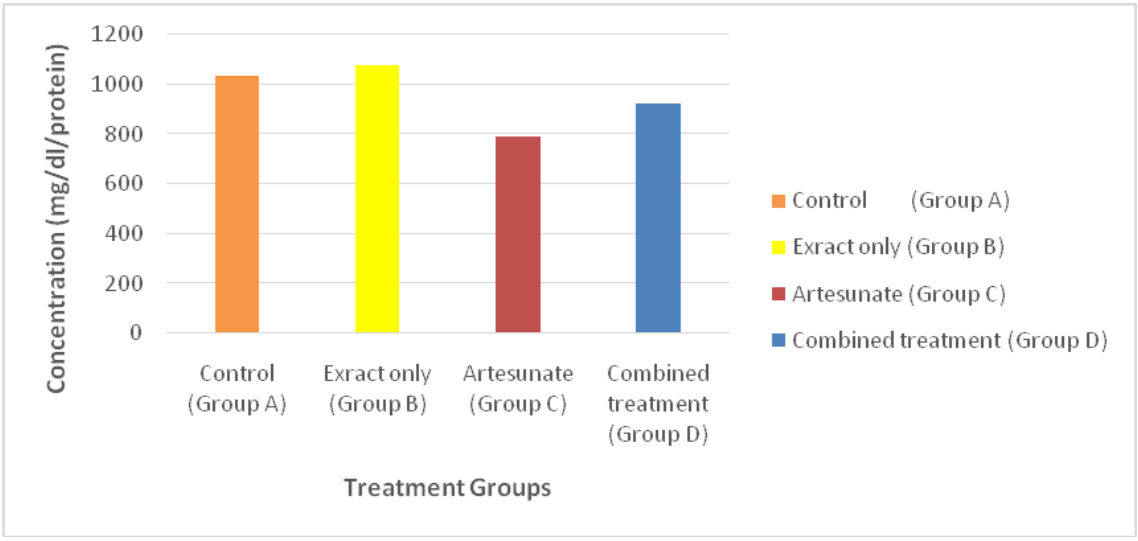

Fig. 3. Reduced Glutathione (GSH) Concentrations in the liver of various treatment groups.
Values are given as mean and standard deviation of six determinations
P value (P≤ 0.05) as the level of significance.

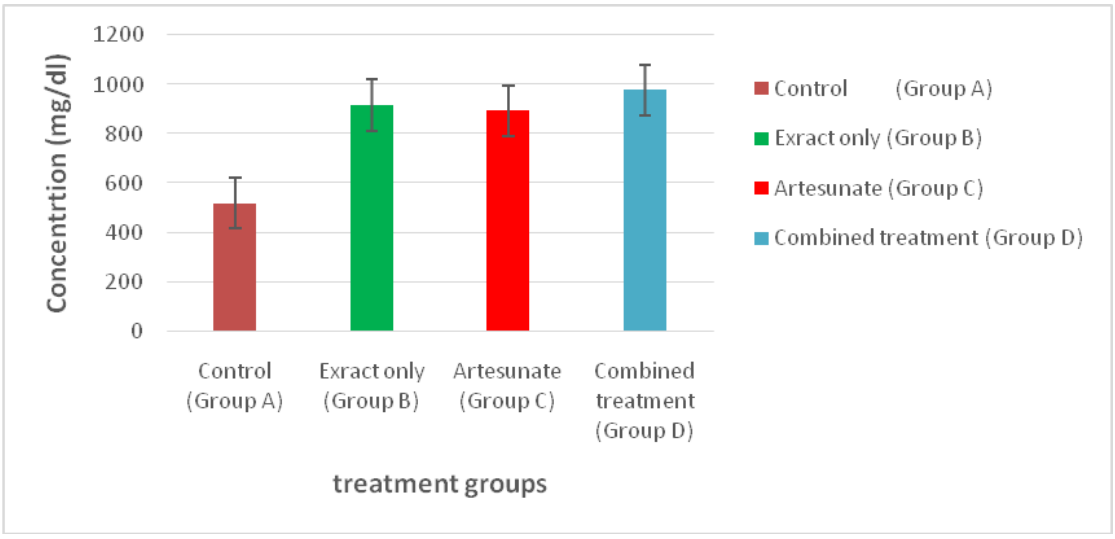

Fig. 4. Plasma protein concentrations of various treatment groups.
Values are given as mean and standard deviation of six determinations
P value (P≤ 0.05) as the level of significance.

indigenous plant based anti malarials whose bioactive agents may be useful and could be combined with artesunate probably as a common practice among poor African countries which depends solely on these herbs and often combined them with synthetic drugs when they are privileged to have them or whenever they are available or affordable.

Numerous studies have suggested that oxidative stress take part in the pathogenesis of thrombocytopenia associated with malaria as a result of the cumulative effects of free radicals and ultimately the chain process of lipid peroxidation whose continuous reactions leads to the formation of Malondialdehyde (MDA) and conjugated di -ene compounds which are cytotoxic and mutagenic damaging cell membranes (De Vries *et al*., 1997; Taylor and White, 2004; Ejiofor *et al*., 2006). However, one of the important marker for evaluation of natural herbal products that can be harnessed as an anti malarial is the ability of such agents or compounds to arrest the process of lipid peroxidation (Marnett, 1999). In Figure 1, Ferrous sulphate -induced lipid peroxidation in the liver homogenates was inhibited in a concentration –dependent manner by the extract and maximally at 350µg/ml by

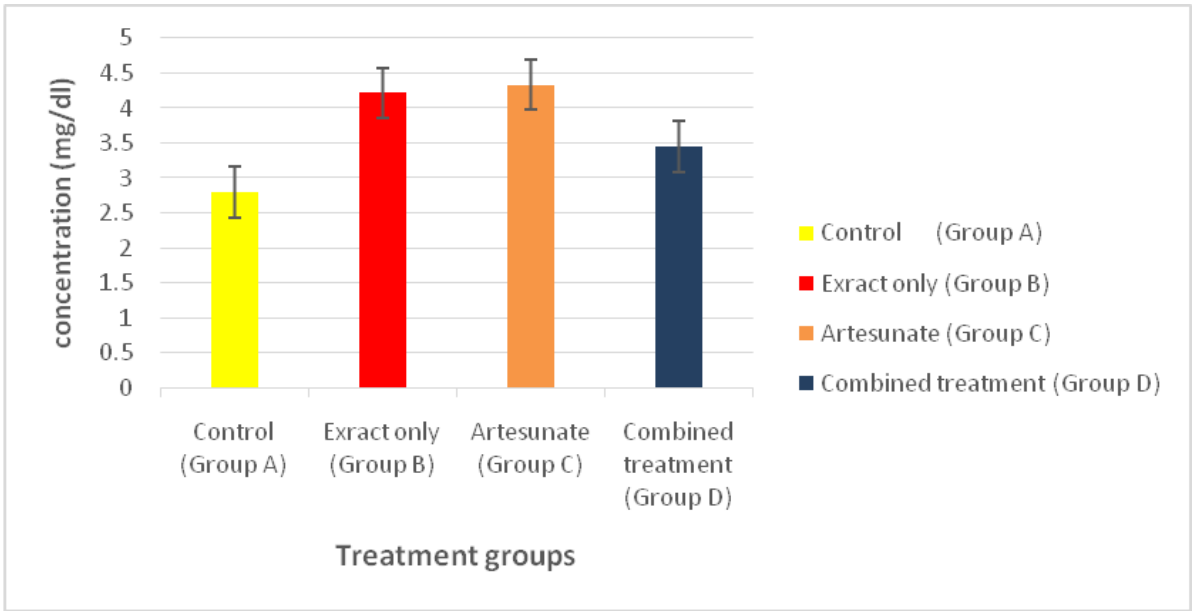

Fig. 5. Plasma urea concentrations of various treatment groups.
Values are given as mean and standard deviation of six determinations
P value (P≤ 0.05) as the level of significance.

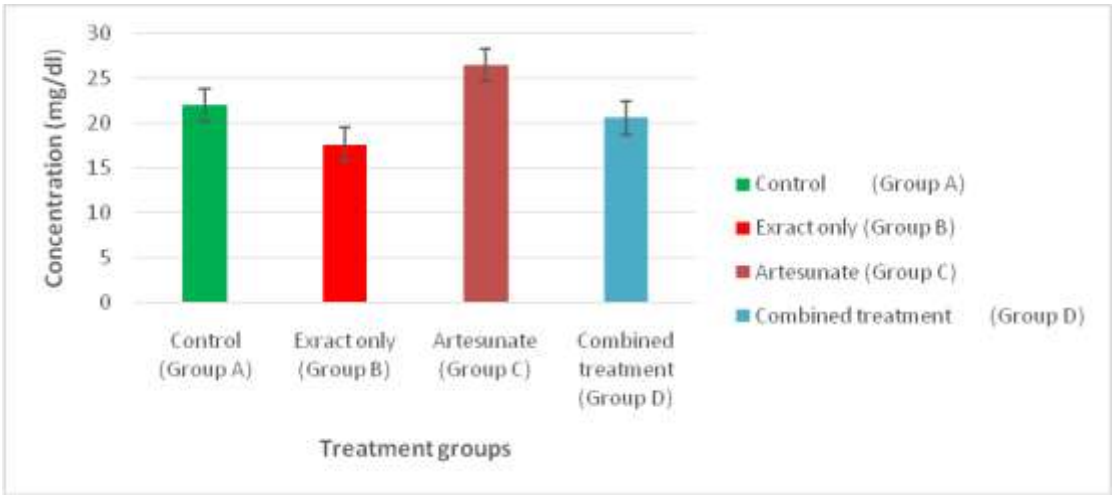

Fig. 6. Plasma Creatinine concentration of various treatment groups.
Values are given as mean and standard deviation of six determinations
P value (P≤ 0.05) as the level of significance.

66.19% an indication that the extract convered 50% cellular protection. Likewise in Figure 2, the extract alone elicit significant decreases ($p<0.05$) in the level of MDA (group B) compared with the controls and the artesunate group. The extract also modulates artesunate activity in bringing the MDA to control level when the combined treatment (group D) is compared with the standard drug artesunate (group C). The ability of the extract to inhibit MDA formation and lipid peroxidation is an indication of its potential to inhibit a variety of acute or chronic patho physiological processes associated with diseases (Ames *et al*., 1993; Adedosu *et al*., 2015).

Reduced glutathione (GSH) is a tri peptide of glycine, glutamic acid and cysteine, it is the most abundant intracellular small molecule thiol, an important antioxidant with roles in detoxification of variety of electrophilic compounds and peroxides via catalysis by glutathione S-transferases (GST) and glutathione peroxidases (Gpx) preventing damage to important cellular components caused by oxidants and free radicals (Pompella *et al*., 2003). A deficiency of GSH put the cell at risk of oxidative damage especially with oxidative stress associated with most anti malarial hence an imbalance of GSH level observed in a wide range of

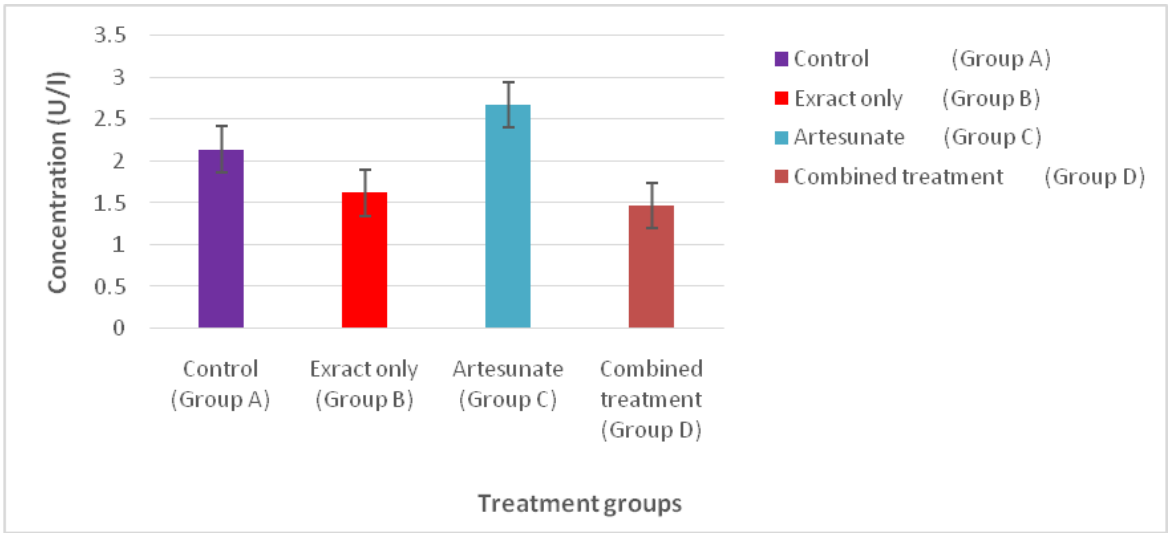

Fig. 7. Plasma ALT activities of various treatment groups.
Values are given as mean and standard deviation of six determinations
P value (P≤ 0.05) as the level of significance.

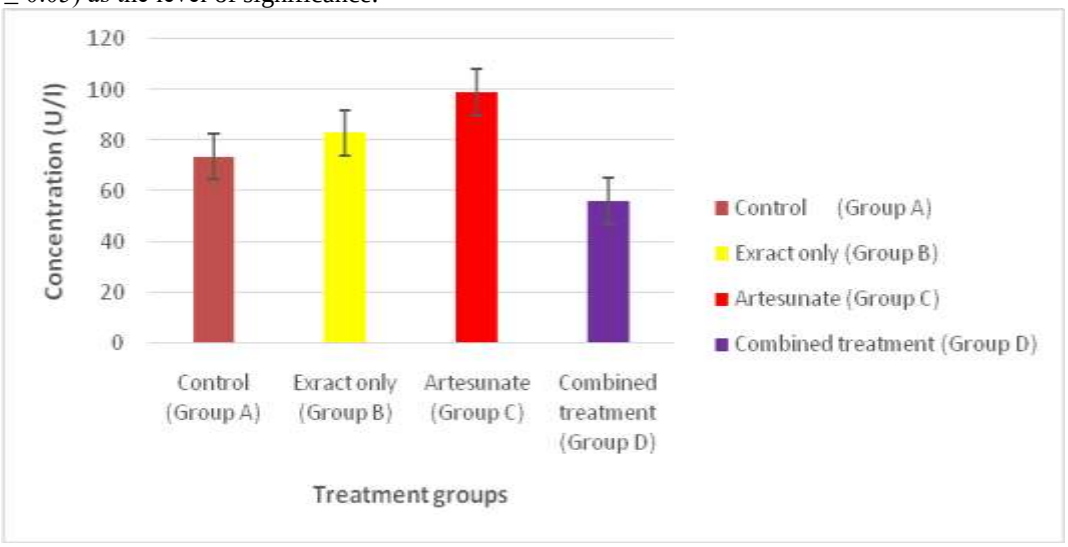

Fig. 8. Plasma ALP activities of various treatment groups.
Values are given as mean and standard deviation of six determinations
P value (P≤ 0.05) as the level of significance.

pathologies including malaria, diabetes, cancer, neurodegenerative disorders, cystic fibrosis, HIV and aging serves as a measure of cellular toxicities (Pastore *et al*., 2003). In this study *Vernonia amygdalina* methanol extract boost GSH levels as it significantly increase ($p<0.05$) GSH concentrations compared with other treatment groups (Fig. 3). The standard drug, artesunate however elicit a significant decrease ($p<0.05$) in GSH concentrations suggestive of overproduction of free radical associated with the mechanism of the drug action which may be implicated with diminished hepatic glutathione GSH concentrations ,as to combat the over production of the free radicals ,hepatic GSH stores might have been exhausted. However, with the combined treatment of the extract and artesunate, this shows significant increases in GSH level compared with the standard drug alone, suggestive of the extract ability to boost body's antioxidant status, protects ,detoxifies and modulates the activity of the drug (Mitchell *et al*., 1973).

In Figure 4, a significant increase ($P\leq0.05$) in plasma total protein concentrations in all the treatment groups compare to controls were observed. However, the combined treatment (artesunate + extract) has the highest increase in plasma protein concentration when compared with other treated groups. Behaviour exhibited by the combined treatment might not be unconnected with their ability to increase certain tissue protein concentrations which might

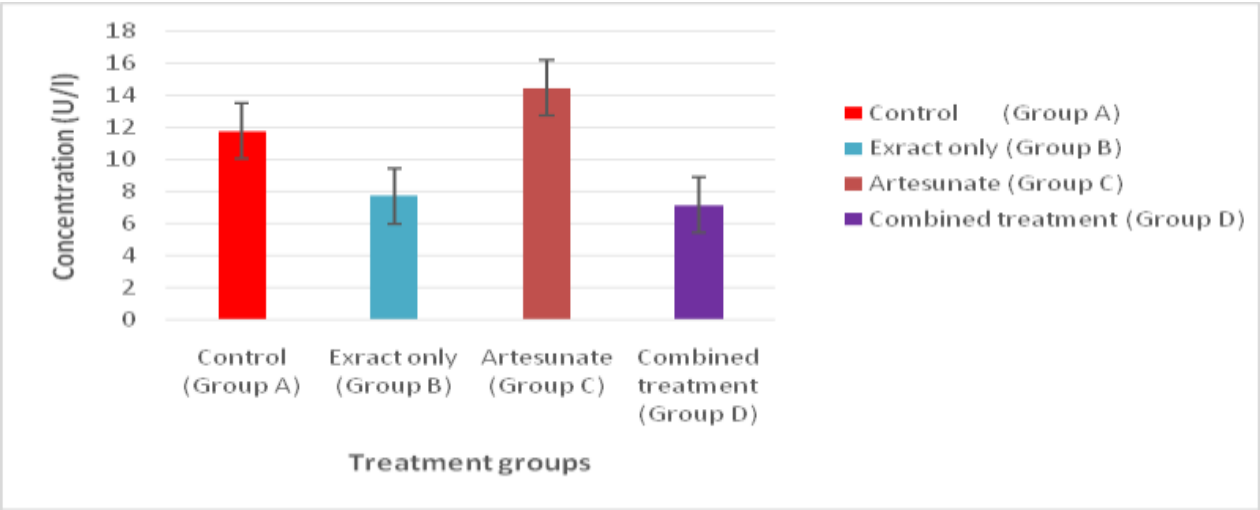

Fig. 9. GGT activities in the liver of various treatment groups.
Values are given as mean and standard deviation of six determinations
P value ($P \leq 0.05$) as the level of significance.

have been reduced due to their degradation by malaria parasites.

Also, in the current study, the concentrations of plasma urea and creatinine were examined as obtained in Figures 5 and 6 in various treatment groups. Significant elevation of plasma levels of urea and creatinine in Group C ,may explain the presence of strong correlation between nephrotoxicity and oxidative stress associated with the drug in the treatment of malaria (Li *et al*., 2006). The elevated H_2O_2 and O_2^- production alters the filtration surface area and modifies the filtration coefficient; both factors could decrease the glomerular filtration leading to accumulation of urea and creatinine in the blood. The combined treatment group reduces plasma urea at nearly control level while similar trends were obtained in creatinine clearance with the combined treatment showing the highest creatinine clearance thus showing a modulatory effect on the drugs action.

Administration of artesunate alone resulted in the significant increases ($P \leq 0.05$),in the plasma activities ofAlanine Aminotransferase and Alkaline phosphatase (Fig. 7 and 8) which are membrane bound enzymes found primarily in the liver with small amountsof ALP produced by cell lining intestines,the placenta and the kidney(in the proximal convulated tubules).This increases may be due to lipid peroxidation of biomembranes which causes leakage of cellular components into the blood (Matsuo *et al*., 1989). However rats treated with the drugs and the extract showed significant decreases in plasma levels of these enzymes , the results of this effects are suggestive of the extract capabilityto accelerate parenchymal regeneration,thus protecting against membrane fragility and subsequent decreasing leakage of marker enzymes into the circulation. That the extract has the potential to protect the liver and the kidney from artesunate - dependent damage as revealed in this report by modulating artesunate activities may be interpreted on the basis of the antioxidant properties of the extract and their constituent bioactive agents. If artesunate toxicity were dependent on radical-generating mechanisms, one would expect that an antioxidant might protect the organs from such oxidative damage which might be responsible for the anti malarial potency of the plant as shown from this study.

Similarly, the results of the activities of gamma- glutamyl transferase (Fig. 9) also indicated the modulatory potential of the extact on the drug action.

The results above suggested that the methanol extract of *Vernonia amygdalina* have anti-oxidant activities with potential protective role on the liver and the kidney in administration with artesunate and is able to modulate the effect of the drug as an anti malarial probably as a result of oxidative stress associated with its mode of action, an indication that the extract bioactive agents may be useful in drug design, template or as food supplements for prevention or combating resistance in malarial chemotherapy, hence the wide spectrum of phytochemicals ‘bottled up’ in this leaf extract, could help in preventing man from the present burden of malaria.

CONCLUSION

While clinical studies would definitely be needed to establish the safety of combining the extract with artesunate, the present study suggests that such combination may actually protect the tissues from the likely dangers associated with prolonged artesunate administration however, further research must be carried

out to identify or isolate the active compounds responsible for these effects which may be helpful in drug design and development towards eradication of resistance to malaria drugs while the local usage of the extract as anti malarial in poor endemic countries could be encouraged as more has to be done, to transform the large volume of research already done on the plant into practical, readymade nutraceuticals or phytherapeutics so that mankind may begin to effectively utilize the plant for maximal benefits especially towards malaria treatment.

ACKNOWLEDGMENT

The authors wishes to acknowledge the efforts of staff of the Botany unit of the Department of Pure and Applied Biology, Ladoke Akintola University of Technology Ogbomoso for the useful information on the plant.

REFERENCES

Adedosu, OT., Badmus, JA., Adeleke, GE., Afolabi, OK., Adekunle, AS., Fatoki, JO. and Fakunle, PB. 2015. Oxidative Damage and Dietary Antioxidants: The Roles of Extract and Fractions of *Solanium aethiopicum* Leaves. Canadian Journal of Pure and Applied Sciences. 9(1):3185-3192.

Ames, BN., Shigenaga, MK. and Hagen, TM. 1993. Oxidants, antioxidants and the degenerative diseases of aging. Proc. Natl . Acad. Sci. 90:7915-7922.

Ames, G. and Forward, P. 1994. Natural antioxidants in human health and diseases. Academy Press, San Diego.

Becker, K., Leann, T., Jonathan, LV., David, R., Stephen, R. and Hagai, G. 2004. Oxidative stress in malaria parasite-infected erythrocytes: host-parasite interactions. International Journal for Parasitology. 34:163-189.

Beutler, EO. and Duran-Kelly, BM. 1963. Improved method for the determination of blood glutathione. Lab. Clin. Med. 61:882-888.

Bliss, CI. 1967. Statistics in biology. Statistical methods for research in the Natural Sciences. Mc Graw Hill Book Company, N.Y, USA. 1:558.

Burtis, A. 1999. Tietz Text book of clinical chemistry. (3rd edi.). AACCC. 44:123-130.

Challand, S. and Willcox, M. 2009. A clinical trial of the traditional medicine *Vernonia amygdalina* in the treatment of uncomplicated malaria. J. Altern. ComMed. 15(11):1231-1237.

Chukwujekwu, JC., Lategan, CA., Smith, PJ., Van Heerden, FR. and Van Staden, J. 2009. Antiplasmodial and cytotoxic activity of isolated sesquiterpene lactones from the acetone leaf extract of *Vernonia colorata*. South Afr. J. Bot. 75:176-179.

Clark, RL., Lerman, SA., Cox, EM., Gristwood, WE. and White, TE. 2008. Developmental toxicity of artesunate in the rat: Comparison to other artemisinins, comparison of embryotoxicity and kinetics by oral and intravenous routes, and relationship to maternal reticulocyte cogunt. Birth Defects. Res. B. Dev. Reprod. Toxicol. 83:397-406.

De Vries, PJ., Nguyen, XK. and Tran, KD. 1997. The pharmacokinetics of a single dose of artemisinin in subjects with liver cirrhosis. Bach Mai-Amsterdam Research Group on Artemisinin. Trop. Med. Int. Health. 2:957-962.

Ejiofor, JI., Kwanashie, HO. and Anuka, JA. 2006. Some pregnancy-related effects of artemether in laboratory animals. Pharmacology. 77:166-170.

Farombi, EO. 2003. African indigenous plants with chemotherapeutic potentials and biotechnological approach to the production of bioactive prophylactic agents. Afr. J. Biotech. 2:662-667.

Giao, PT. and de Vries, PJ. 2001. Pharmacokinetic interactions of antimalarial agents. Clin. Pharmacokinet. 40:343-373.

Hilou, A., Nacoulma, OG. and Guiguemde, TR. 2006. *In vivo* anti malarial activities of extracts from *Amaranthus spinosus* L. and *Boerhaavia erecta* L. in mice. J. Ethnopharmacol. 103:236-240.

Iwu, MM.1982. Traditional Igbo Medicine. Institute of African studies, University of Nigeria. Nsukka, Nigeria. 104-110.

Igile, GO., Oleszek, W., Burda, S. and Jurzysta, M.1995. Nutritional assessment of *Vernonia amygdalina* leaves in growing mice. J. Agr. Food. Chem. 43:2162-2166.

Kumar, S. and Srivastava, S. 2005. Establishment of artemisinin combination therapy as first line treatment for combating malaria: *Artemisia annua* cultivation in India needed for providing sustainable supply chain of artemisinin. Curr. Sci. 89:1097-1102.

Klayman, DL. 1985. Qinghaosu (artemisinin): an antimalarial drug from China. Science 228:1049-1055.

Klayman, DL. 1993. *Artemisia annua*: from weed to respectable anti malarial plant. In: Human medicinal agents from plants. Eds. Kinghorn, AD. and Balandrin, MF. American Chemical Society, Washington, DC., USA. 242-255.

Lowry, OH., Rosebrough, NJ., Farr, AL. and Randall, RJ. 1951. Protein measurement with the folinphenol reagent. J. boil. Chem. 193:265-275.

Li, Q., Xie, LH., Si, Y. and Wong, E. 2005. Toxicokinetics and hydrolysis of artelinate and artesunate in malaria-infected rats. Int. J. Toxicol. 24:241-250.

Li, Q., Xie, LH., Haeberle, A., Zhang, J. and Weina, P. 2006. The evaluation of radiolabeled artesunate on tissue distribution in rats and protein binding in humans. Am. J. Trop. Med. Hyg. 75(5):817-826.

Looareesuwan, S. 1996. Clinical studies of atovaquone, alone or in combination with other Anti malarial drugs for the treatment of acute uncomplicated malaria in Thailand. American Journal of Tropical Medicine and Hygiene. 54:62-66.

Mbatchi, S.F., Mbatchi, B., Banzouzi., JT., Bansimba, T., Nsonde Ntandou, GF., Ouamba, JM., Berry, A. and Benoit-Vical, F. 200. *In vitro* antiplasmodial activity of 18 plants used in Congo Brazzaville traditional medicine. J. Ethnopharmacol. 104:168-174.

Marnett, LJ. 1999. Lipid peroxidation- DNA damage by malondialdehyde (MDA). Mut. Res. 424(1-2):83-95.

Mitchell, JR., Jollow, DJ., Potter, WZ., Davis, DC., Gillette, JR. and Brodi, BB. 1973. Acetaminophen-induced hepatic necrosis. I. Role of drug metabolism. J. Pharmacol. Exer. Therap. 187:185-194.

Miller, LH., Good, MF. and Milon, G. 1994. Malaria pathogenesis. Science. 264:1878-1882.

Miller, AL. 1996. Antioxidant flavonoids: Structure, function and Clinical Usage. Alternative Medicine Review. 1:103-111.

Muller, FL., Liu, Y. and Van Remmen, H. 2004. Complex III releases superoxide to both sides of the inner mitochondrial membrane. J. Biol. Chem. 279:49064-49073.

Murray, RL.1984. Creatinine. In: Clinical Chemistry; Theory analysis and correllation. Eds. Kaplan, LA and Pesce, AJ. CV Mosby Co., Louis. 1247-1253.

Matsuo, T., Kashiwaki, Y. and Itoo, S. 1989. Membrane damage caused by exposure to butylhydroperoxide. Cytochemistry. 28:1003-1006.

Naito, HK. 1984. Clin Chem. The C.V Mosby Co. St. Louis. Toronto. Princeton. 437:1194-11206.

Ouattara, Y., Sanon, S., Traore, Y., Mahiou, V., Azas, N. and Sawadogo, L. 2006. Antimalarial activity of *Swartzia madagascariensis* DESV. (Leguminosae), *Combretum glutinosum* GUILL. and PERR. (Combretaceae) and *Tinospora bakis* NMIERS. (Menispermaceae), Burkina Faso medicinal plants. Afr. J. CAM. 3(1):75-81.

Pastore, A., Piemonte, F., Locatelli, M., LoRusso, L., Gaeta, M., Tozzi, G. and Federici, G. 2003. Determination of blood total reduced and oxidized glutathione in pediatric subjects'. Clinical Chemistry. 47(8):1467-1469.

Pompella, A.,Visvikis, A., Paolicchi, A., Tata, V. and Casini, A. 2003. The changing faces of glutathione, a cellular protagonist. Biochemical Pharmacology. 66(8):1499-1503.

Ridley, RG. 2002. Medical need, scientific opportunity and the drive for anti-malaria drugs. Nature. 415:686-693.

Ruberto, G., Baratta, MT., Deans, SG. and Dorman, HJD. 2000. Analysis of chemical composition and bioactive property evaluation. Asian. Pac. J. 31:3-15.

Szasz, G. 1969. A kinetic photometric method for serum gamma glutamyl transterase. Clin. Chem. 15:124-136.

Singh, B., Kim, SL., Matusop, A., Radhakrishann, A., Shamsul, SS., CoxSingh, J., Thomas, A. and Conway, DJ. 2004. A large focus of naturally acquired *Plasmodium knowlesi* infections in human beings. Lancet. 363:1017-1024.

Taylor, WR. and White, NJ. 2004. Antimalarial drug toxicity: a review. Drug safety. 27:25-61

Varshney, R. and Kale, RK.1990. Effects of *calmodulin antagonist* on radiation induced lipid peroxidation in microsomes. Int. J. Radiation. Biol. 58(5):733-743.

Wroblewski., F. and La Due, JS. 1956. Serum and Plasma Alkaline phosphatase determination. Ann. Intern. Med. 45:801.

Woedenbag, HJ., Pras, N. and Uden, W. 1994. Progress in the research of Artemisinin related anti malarials: An update. Pharmaceutical World Science. Uploaded Nov. 10. 2014

World Health Organization. 2005. World Malaria Report by Roll Back Malaria Partnership. L.

Received: May 10, 2016; Accepted: July 4, 2016

Canadian Journal of Pure and Applied Sciences
Vol. 10, No. 3, pp. 3991-3995, October 2016
Online ISSN: 1920-3853; Print ISSN: 1715-9997
Available online at www.cjpas.net

STUDIES ON GROWTH AND IMMUNE RESPONSE OF *LABEO ROHITA* AFTER FEEDING *LACTOBACILLUS ACIDOPHILLUS* AND *SACCHAROMYCES CEREVISIAE*

*Sidra Nazeer, Ehsan Mahmood Bhatti and Imtiaz Begum
Fisheries Research and Training Institute Manawan, Lahore, Pakistan

ABSTRACT

In this study, the individual as well as combined effect of commercially available probiotics containing *Lactobacillus acidophillus* and *Sacchromyces cerevisiae* was studied on the growth performance. The study was also extended to protection against infectious bacteria *Aeromonas hydrophila* which is the cause of abdominal dropsy in fish. Three different concentrations of probiotics (2, 3 and 4%) were fed to fish fingerlings (*Labeo rohita*) in 30% commercial artificial feed for 60 days. In combination group, dietary probiotics at 4% dose showed significant average increase in growth i.e. 80% and survival rate was 99% when challenged with *Aeromonas hydrophila*, followed by 3% and then 2% doses. *Sacchromyces cerevisiae* and *Lactobacillus acidophillus* individually showed their significant effect on the growth of fish which was very close to each other, as the % age increase in weight for *Sacchromyces cerevisiae* was 67.7% and for *Lactobacillus acidophillus* it was 67% at 4% dose. Feeding of supplemented diets showed reduced mortality in combination group (1%) followed by *Sacchromyces cerevisiae* (3%) and then *Lactobacillus acidophillus* (6%) in comparison to control group where 93.33% mortality was observed.

Keywords: *Aeromonas hydrophila*, *Labeo rohita*, probiotic, immunity, growth.

INTRODUCTION

In Pakistan major carps, particularly *Labeo rohita* is the most preferred farmed fish because of the rapid growth and higher adequacy to consumers. The rapid development and intensification of carp farming to bridge up the gap of animal protein demand had led to the epidemic of contagious diseases caused by bacteria, viruses and parasites, inflicting rigorous loss on production of fish. The extensive utilization of wide-ranged chemotherapeutants to combat these diseases has led to the enhancement of antibiotic-resistant bacterial strains, in addition to this; could cause water contamination in the aquatic environment (Lunden *et al*., 2002). In order to resolve this condition, better emphasis is being placed on improved water quality, better nutrition and the application of immunostimulants and vaccines in the last decade. In recent times, the use of probiotics has been focused with the requirement for environmentally friendly aquaculture (Bandyopadhyay and Mohapatra, 2009).

Currently, probiotics are becoming an essential part of the aquaculture practices to achieve high production. Probiotics are live microorganisms contemplated to be useful to the host organism.

*Corresponding author e-mail: sidra666@gmail.com

The World Health Organization (WHO) has defined probiotic bacteria as "live microorganisms which when administrated in adequate amounts confer a health benefit on the host" (FAO/WHO, 2001). In fish, the contribution of probiotics as nutrition, in disease resistance and other advantageous activities has been studied. Among the various health benefits attributed to probiotics, inflection of the immune system is one of the major benefits of the probiotics and their effectiveness to stimulate the local and systemic immunity. Probiotics may possibly improve nutrition by the manufacture of vitamins; stimulate appetite and detoxification of compounds in the diet (Harikrishnan *et al*., 2010).

The use of probiotics as dietary live microbial supplements and biological control agents in commercial fish culture is possible to improve growth as well as immune function of the fish (Irianto and Austin, 2002; Kesarcodi-Watson *et al*., 2008).

Earlier studies reported that the positive effect of using viable microorganisms in probiotic mixtures into fish diets (Li and Gatlin, 2004; Brunt and Austin, 2005; Pangrahi *et al*., 2005; Barnes *et al*., 2006; AboState *et al*., 2009). The aim of this study was to analyze and check the

individual as well as combined effect of *Lactobacillus acidophillus* and *Sacchromyces cerevisiae* on the growth and immune response of *Labeo rohita*.

MATERIALS AND METHODS

Experimental design

The present study was conducted at Fisheries Research and Training Institute, Manawan Lahore. Six hundred Rohu fingerlings of size 5-8gm were procured from Fish Seed Hatchery, Chenawan, District Gujranwala. Before the start of experiment, the fish were fed to the control diet (commercially available feed with 30% protein) for 10 days in aquaria for acclimatization. Total 30 glass aquaria (50 L) filled with fresh water were used for the experiment, each aquarium was stocked with 20 *Labeo rohita* fingerlings. Aquaria were divided into four groups with each of three replicates, one group served as control and the other groups were used as experimental.

Preparation of Experimental Diet

A commercially available feed (with 30% protein) at the rate of 3% body weight was used as a basal diet for the experimental fish. Fish were fed twice daily in 60 days. The basal diet was used as the control diet. Nine experimental diets were prepared from basal diet adding 2.0, 3.0, and 4.0% of *Lactobacillus acidophillus* and *Sacchromyces cerevisiae* and a combination of above two probiotics by using the water spraying method. The feed was dried in oven at 50ºC overnight. The growth rate in fish for each experimental diet was noted every 15 days and the feeding was adjusted according to the body weight of fish in each aquarium.

Water Quality Analysis

Important water quality parameter such as pH, temperature and dissolved oxygen, were recorded daily and kept within the range throughout the experimental period (Table 1).

Preparation of Antigen for Challenge Study

Pathogenic strain of *Aeromonas hydrophila* was collected from commercial source (Microbiologist USA, Exon Scientific Corporation, 4 Leek Road Chuburji Chowk, Lahore). *Aeromonas hydrophila* was grown in lab on sheep blood agar for 24 h at 37°C. In order to prepare the bacterial suspension, the growth of bacteria was mixed in sterile phosphate buffer saline (PBS, pH 7.4). The turbidity of solution was checked by turbidity meter to get same concentration of bacterial culture. After feeding fish with experimental doses of probiotics for 60 days, 10 fish from each aquarium were injected intraperitoneally with 100µl of bacterial suspension and the mortality was observed for 15 days.

Growth Parameters

The percentage increase in weight in *Lactobacillus acidophillus, Sacchromyces cerevisiae* and in combination was checked by applying formula:

$$\%\text{weight gain} = \frac{\text{Final weight- Initial weight}}{\text{Initial weight}} \times 100$$

RESULTS

Water Quality

Water quality parameter such as pH, temperature and dissolved oxygen was monitored with their minimum and maximum range for the growth and survival of *Labeo rohita* (Table 1). All the faecal matter was removed daily by siphoning method.

Growth Performance

The growth of *Labeo rohita* was increase in all the treatments as compared to control. The highest %age weight gain of fish was observed in combination group (*Sacchromyces cerevisiae and Lactobacillus acidophillus*) at 4% dose, followed by 3% and then 2% (Table 4). *Sacchromyces cerevisiae* and *Lactobacillus acidophillus* individually showed their significant effect on the growth of fish which was very close to each other, as the %age increase in weight for *Sacchromyces cerevisiae* was

Table 1. Range of selected water quality parameters.

S. No.	pH	Temperature ºC	Dissolved oxygen (ppm)
Minimum	7.18	19.3	5.5
Maximum	8.09	28.8	6.2

Table 2. Average % age increases in weight of fish for probiotic *Lactobacillus acidophillus.*

Treatments	Probiotic *Lactobacillus* %	Initial body weight (g)	Final weight (g)	Percentage increase in weight %
Control	0.0	5.0	6.2	24
T1D1	2.0	5.4	8.3	53
T1D2	3.0	5.3	8.5	60
T1D3	4.0	5.2	8.7	67

67.7% and for *Lactobacillus acidophillus* it was 67% at

Table 3. Average % age weight gain of fish for probiotic *Sacchromyces cerevisiae*.

Treatments	Probiotic *Sacchromyces cerevisiae* %	Initial body weight (g)	Final weight (g)	Percentage increase in weight %
Control	0.0	6.1	7.6	24.5
T2D1	2.0	6.3	9.8	55
T2D2	3.0	6.1	10.0	63
T2D3	4.0	6.2	10.4	67.7

Table 4. Average %age weight gain of fish for probiotics *Lactobacillus* and *Sacchromyces cerevisiae* in combination.

Treatments	Combination of two Probiotics (L.B+Yeast) %	Initial body weight (g)	Final weight (g)	Percentage increase in weight %
Control	0.0	7.1	8.8	23.9
T3D1	2.0	7.2	12.5	73
T3D2	3.0	7.2	12.8	77.7
T3D3	4.0	7.3	13.2	80

4% dose (Table 2, 3).

Disease Resistance

Feeding of probiotic supplemented diets after 60 days led to a considerable decrease in fish mortality after challenge with *A. hydrophila*. Therefore, highest 93.33% mortality was observed for the control when compared with probiotic fed groups (Fig. 1). Significant decline in mortality was found in combination group (1%) followed by *Sacchromyces cerevisiae* (3%) and then *Lactobacillus acidophillus* (6%). Highest survival of fish was found to be in combination group.

DISCUSSION

In the present study, *Labeo rohita* fed diets supplemented with probiotic *Lactobacillus acidophillus* and *Sacchromyces cerevisiae* along with their combination in different doses 2, 3 and 4% for 60 days were challenged with *Aeromonas hydrophila*. The mortality of fish was decreased significantly by dietary probiotic as compared with fish fed the basal diet, and the result analysis indicated that the maximum disease resistance ability of *Labeo rohita* occurred at 4% diet supplementation of probiotic i.e combination of *Sacchromyces cerevisiae* and *Lactobacillus acidophillus* (Fig. 1). It showed that combination of yeast and bacterial strain was found to be

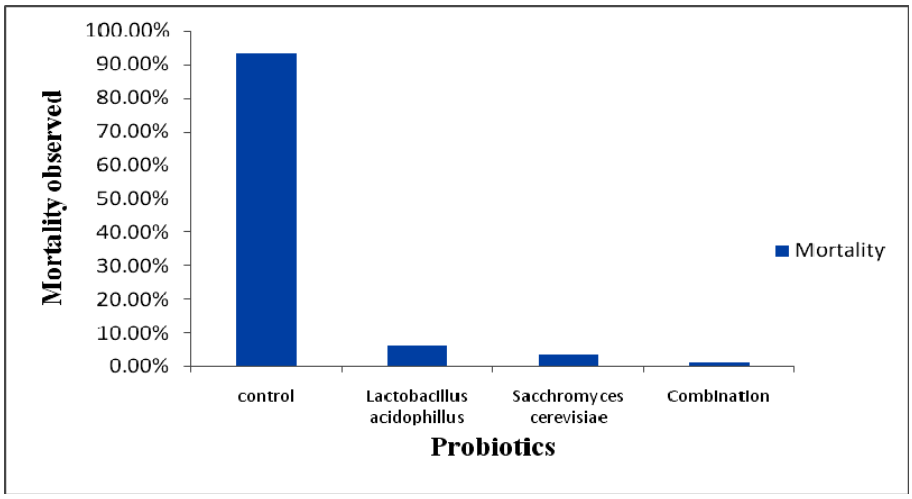

Fig. 1. Immunity in fish against *Aeromonas hydrophila* for different probiotics.

very effective and resulted in modulation of immune system of fish. In this study, the growth of *Labeo rohita* was notably increased by dietary probiotic. Enhancement in the growth of aquatic animals fed with probiotic diets resulted in increased enzymatic activity, improved digestive activity, synthesis of vitamins and weight gain (Nayak, 2010). Another study, Giri *et al*. (2013) reported that Probiotic supplementation improves growth parameters and immune responses in *Labeo rohita*.

In this study, combination group showed the highest growth rate at 4% dose followed by 3% and then 2% (Table 4). It is reported that by mixing experimental diets including *Bacillus subtilis* and *Lactobacillus acidophillus* showed significant improvement in growth of Iranian sturgeon fish (*Acipencer perscius*) for 30 days (Querroz and Boyd, 2008). Similar results were found in Tilapia by using yeast *Sacchromyces cerevisiae*, as yeast was found to be good promoter of growth and immune system (Lara-flores *et al*., 2003).

In Rainbow trout (*Oncorhynchus mykiss*), maximum growth and survival rate was observed when administrated with probiotics *Sacchromyces cerevisiae* and *Lactobacillus acidophillus* individually as compared to control when challenged with *Aeromonas hydrophila* (kesarcodi-watson *et al*., 2008). In *Cyprinus carpio*, the survival rate was 63% when supplemented with *Bacillus* NL110, whereas it was just 11% in control; not treated with probiotics when when challenged with *Aeromonas hydrophila* for two weeks (Ortuno *et al*., 2002). In the present study, average increase in growth of *Labeo rohita* was 67.7% at dose of 4% by using *Sacchromyces cerevisiae* (Table 3) and 67% in case of *Lactobacillus acidophillus* (Table 2) for 60 days. Immunity in fish was also modulated in case of yeast as compared to *Lactobacillus acidophillus*. In the control group the mortality of fish was found to be 93.33% which showed a significance of probiotics against *Aeromonas hydrophila* (Fig. 1).

CONCLUSION

Under the experimental conditions, it is concluded that probiotics are not only beneficial for the growth but it is an important immunostimulant for *Labeo rohita*. Dietary probiotics *Lactobacillus acidophillus, Sacchromyces cerevisiae* and its combination significantly increase growth as well as immunity against *Aeromonas hydrophila*, pathogenic bacteria that cause infection in fish. To elevate the immune resistance ability and growth in *Labeo rohita*, the dose at 4% of probiotic was found to be very effective as compared to control group which showed highest mortality. These results indicates that dietary probiotics are very advantageous for the fish and it should be taken into account by the farmers to treat their fish from different bacterial diseases as well as for the improvement of growth.

ACKNOWLEDGMENT

The authors are thankful to Dr. Imtiaz Begum, Director Research and Training Institute, who supported and guided us during the whole study.

REFERENCES

Abo-State, HA., El-Kholy, KHF. and Al-Azab, AA. 2009. Evaluation of probiotic (EMMH) as a growth promoter for Nile tilapia (*Oreochromis niloticus*) fingerlings. Egyptian Journal of Nutrition and Feeds. 12(2):347-358.

Brunt, J. and Austin, B. 2005. Use of probiotic to control Lactococcosis and Streptococcus in Rainbow trout, *Oncorhynchus mykiss* (Walbaum). Journal of Fish diseases. 28:693-701.

Barnes, ME., Durben, DJ., Reeves, SG. and Sanders, R. 2006. Dietary yeast culture supplementation improves initial rearing of Mc conaughy strain Rainbow trout. Aquaculture Nutrition. 12(5):388-394.

Bandyopadhyay, P. and Mohapatra, PKD. 2009. Effect of a probiotic bacterium *Bacillus circulans* PB7 in the formulated diets: on growth, nutritional quality and immunity of *Catla catla* (Ham.). Fish Physiology Biochemestry. 35:467-478.

FAO/WHO, 2001. Report on Joint FAO/WHO Expert Consultation on Evaluation of Health and Nutritional Properties of Probiotics in Food Including Powder Milk with Live Lactic Acid Bacteria. 1–4 October Cordoba, Argentina. Available at: ftp:// ftp.fao.org/ es/esn/food/probio_report_en.pdf (Accessed on September 10, 2016).

Giri, SK., Sukumaran, V. and Oviya, M. 2013. Potential probiotic *Lactobacillus plantarum* VSG3 improves the growth, immunity, and disease resistance of tropical freshwater fish, *Labeo rohita*. Fish & Shellfish Immunology. 34(2):660-666.

Harikrishnan, R., Balasundaram, C. and Heo, MS. 2010. *Lactobacillus sakei* BK19 enriched diet enhances the immunity status and disease resistance to streptococcosis infection in kelp grouper. Fish Shellfish Immunology. 29:1037-1043.

Irianto, A. and Austin, B. 2002. Use of probiotics to control furunculosis in Rainbow trout, *Oncorhynchus mykiss* (Walbaum). Journal of Fish Disease. 25:333- 342.

Kesarcodi-Watson, A., Kaspar, H., Lategan, MJ. and Gibson, L. 2008. Probiotics in aquaculture: the need, principles and mechanisms of action and screening processes. Aquaculture. 274:1-14.

Lara-Flores, M., Olvera-Novoa, M., Guzma´N-Me´Ndez, B. and Lo´Pez-Madrid, W. 2003. Use of the bacteria *Streptococcus faecium* and *Lactobacillus acidophilus*, and the yeast *Saccharomyces cerevisiae* as growth promoters in Nile tilapia (*Oreochromis niloticus*). Aquaculture. 216(1-4):193-201.

Li, P. and Gatlin, DM. 2004. Dietary brewer's yeast and the prebiotic grobiotic TM AE influence growth performance, immune responses and resistance of Striped bass (Morone chrysops x M. saxatilis) to Streptococcus iniae infection. Aquaculture. 231:445-456.

Lunden, T., Lilius, EM. and Bylund, G. 2002. Respiratory burst activity of Rainbow trout (*Oncorhynchus mykiss*) phagocytes is modulated by antimicrobial drugs. Aquaculture. 207:203-212.

Nayak, SK. 2010. Probiotics and immunity: A fish perspective. Fish and Shellfish Immunology. 29:2-14.

Ortuno, J., Cuesta, A., Rodríguez, A., Esteban, MA. and Meseguer, J. 2002. Oral administration of yeast, *Saccharomyces cerevisiae*, enhances the cellular innate immune response of gilthead seabream (*Sparus aurata* L.). Veterinary Immunology and Immunopathology. 85:41-50.

Pangrahi, A., Kiron, V., Puangkaew, J., Kobayashi, T., Satoh, S. and Sugita, H. 2005. The viability of probiotic bacteria as a factor influencing the immune response in Rainbow trout *Oncorhynchus mykiss*. Aquaculture. 243:241-254.

Querroz, JF. and Boyd, CE. 2008. Effects of bacterial inoculums in channel Cat fish ponds. Journal of World Aquaculture Society. 29:67-73.

Received: August 24, 2016; Accepted: September 15, 2016

Canadian Journal of Pure and Applied Sciences
Vol. 10, No. 3, pp. 3997-4009, October 2016
Online ISSN: 1920-3853; Print ISSN: 1715-9997
Available online at www.cjpas.net

A REVIEW OF DISTRIBUTION, THREATS, CONSERVATION AND STATUS OF FRESHWATER TURTLES IN SINDH

*M Zaheer Khan, Roohi Kanwal, Syed Ali Ghalib, Farina Fatima, Afsheen Zehra, Saima Siddiqui, Ghazala Yasmeen, Amtyaz Safi, Muhammad Usman A Hashmi, Babar Hussain, Muhammad Asif Iqbal, Uzma Manzoor and Ubaid Ullah
Faculty of Science, Department of Zoology (Wildlife Section), University of Karachi, Karachi-75270, Pakistan

ABSTRACT

There are two families, six genera and eight species of freshwater turtles found in Pakistan, and the same species have also been recorded in Sindh province, six of which are threatened, and all species are listed in CITES Appendices I / II. Family Geoemydidae consists of Hard shelled turtles viz Spotted Pond turtle (*Geoclemys hamiltonii*), Crowned river turtle (*Hardella thurjii*), Brown roofed turtle (*Pangshura smithii*), and Indian roofed turtle (*Pangshura tectum*) and the second Family Trionychidae comprises of Soft shell turtles viz. Indian narrow-headed soft-shell turtle (*Chitra indica*), Indian soft-shell turtle (*Nilssonia gangeticus*), Indian peacock soft –shell turtle (*Nilssonia hurum*) and Indian flapshell turtle (*Lissemys punctata*). In Sindh province, Thatta, Sujawal, Badin, Dadu, Khairpur, Sanghar and Sukkur Districts have been identified as hotspots for freshwater turtle populations. Legally, all freshwater turtles in Sindh have been protected under the Sindh Wildlife Protection Ordinance 1972. Many efforts have been made by the Government, Non-governmental organizations and Academia for the protection and conservation of turtle population in Pakistan. The World Conservation Union for Nature - IUCN, WWF Pakistan, Sindh Wildlife Department, Zoological Survey of Pakistan and Department of Zoology (Wildlife Section), University of Karachi are contributing in efforts for the conservation of freshwater turtles in Sindh. But still, freshwater turtles are facing serious threats due to habitat destruction, urbanization, developmental projects and illegal trading.

Keywords: Sindh, population, distribution, freshwater turtles, threats.

INTRODUCTION

Freshwater turtles play a major role in maintaining balance in ecosystem of any wetland. They act as scavengers by decaying dead organic matter. They act as indicators of a healthy aquatic ecosystem. Some are carrion eating species that feed on aquatic weeds and reduce eutrophication. There are 313 species of Tortoises and Fresh water Turtles present worldwide, while 128 Freshwater Turtle species have been included in IUCN Red List of Threatened species (Fritz and Havas, 2007). Economically, freshwater turtles are considered as more valuable as compared to the fisheries because of the presence of good quality flesh and fats which are highly demanded by international markets for different purposes. Flesh of turtles is mostly used in different Continental and American cuisines, which serve as a luxurious dish in many restaurants. The calipee is the fatty gelatinous yellowish material present over the lower shell of a turtle, which is the symbol of delicacy in dishes of many cuisines. Their fat is also used as a major component of cosmetic industry in USA and other countries.

Pharmaceutical industries are also utilizing plastron of Turtles for preparing specific medicines. In China and Taiwan, specialized medicinal compositions are prepared by using plastrons. China and Taiwan are considered as the major markets that are famous for plastron imports. According to a statistical review, annually hundreds of tons of plastron are imported by Taiwan.

Guilinggao jelly is the specialized medicinal composition that made up from boiling of plastron of turtles along with some herbs so it is also called as Turtle Herbal Jelly. It is also used for improvement of circulation in body, good muscle growth, resolving acne problems and for cure of many kidney diseases.

Pakistan has eight species of freshwater turtles. Based on absence or presence of horny scutes or scales on their carapace, freshwater turtles divide into two categories, Soft shell Turtles and Hard shell Turtles, respectively.

*Corresponding author e-mail: zaheer@scspkarachi.org

Soft shell turtle species includes Indian softshell turtle, Peacock softshell turtle, Indian narrow-headed softshell turtle, and Indian flapshell turtle, while Spotted pond turtle, Indian roofed turtle, Brown roofed turtle and Crowned river turtle are Hard shell Turtles.

Freshwater turtles are residing in the whole Indus River system. This system is comprises of many canals, irrigation ditches, ponds, agricultural ponds and water reservoirs. All these tributaries of Indus River system are providing rich habitat for turtles. Major threats to the species are illegal hunting, poaching, and trading for export.

Pakistan is continuously struggling for conservation and protection of these threatened species and became the signatory of the Convention of International Trade in Endangered Species of Wild Fauna and Flora (CITES) and CITES appendix I contains the four species and appendix II contains three freshwater turtles from Pakistan.

Conservation measures of all the species of wildlife are directly associated with legal decisions. In Pakistan, Provincial governments are responsible for adopting all conservational measures in their own provinces. Implementation of Wildlife Protection Ordinances is the major task for all provincial governments. In 1981, Federal Government passed a rule to ban the export of all wild mammals and reptiles. It also includes the restricted export to all parts and products of wildlife.

Formerly in legal ordinances of provinces of Pakistan, no protection was given to the species of freshwater turtles and they were not considered as Protected in different wildlife protection acts of the provinces. However, present situation is different from past. Along with several other conservational measures, there are amended acts, which have declared the freshwater turtles as protected species. Appendices I and II of the CITES restricted the international trade, export and import of wildlife species including the freshwater turtles, their parts and their products as well. Section 12 of Sindh Wildlife Protection Ordinance, 1972 also banned the export of protected wildlife species including freshwater turtles. Pakistan has also been facing threats to freshwater turtles which include scarcity of water in rivers, and canals, water diversion and extraction projects for irrigation purposes, water pollution, habitat deterioration and fragmentation due to unsustainable development. In this paper we reviews the distribution, threats, conservation efforts and status of freshwater turtles in Sindh.

DISCUSSION

Sindh is the third largest province of Pakistan located in West of South Asia, having the area of about 140,915 square kilometers (Fig. 1). Sindh is having very strong belongings to Indus River and having a great variety of ecosystems. In east, desert ecosystem lies in the form of

Fig. 1. Map of Sindh with Districts.

Table 1. Status of Freshwater Turtles in Sindh.

S. No.	Family	Scientific Name	Common Name	IUCN Status	CITES Appendix	
					I	II
1	Geoemydidae	*Geoclemys hamiltoni*	Spotted Pond Turtle	Vulnerable	+	
2		*Pangshura smithii*	Brown Roofed Turtle	Near Threatened		+
3		*Pangshura tectum*	Indian Roofed Turtle	Vulnerable	+	
4		*Hardella thurjii*	Crowned River Turtle	Vulnerable		
5	Trionychidae	*Nilssonia gangeticus*	Indian Soft shell Turtle	Vulnerable	+	
6		*Nilssonia hurum*	Peacock Soft shell Turtle	Vulnerable	+	
7		*Lissemys punctata*	Indian Flapshell Turtle	Least Concern		+
8		*Chitra indica*	Indian narrow headed soft shell Turtle	Endangered		+

Fig. 2. *Geoclemys hamiltoni* (Spotted Pond Turtle).

vast Thar Desert commonly known as Tharparkar. In the west, mountainous ranges are existing known as Khirthar mountain range. In north, Punjab province is present while from southern side, Sindh is bordered by the Arabian Sea.

The climatic conditions are moderate, hot in summer, and mild in winter. In summer season, temperature varies from 35 to 48 degree Celsius, while during winter temperature ranges from 2 to 20 degree Celsius. Sindh is directly affected by two different monsoonal systems, one from southwest system that comes from Indian Ocean while other from northeast system coming from Himalayan Mountains. Annual average rainfall is about six to seven inches.

Distribution and Status of Freshwater Turtles

There are six genera and eight species of Freshwater Turtles recorded in Sindh (Fig. 2 - 9) (Khan *et al.*, 2012a , Khan, 2015), six of which are globally threatened. All species are listed in CITES Appendices I / II (Table 1) and their import and export is prohibited.

Distribution

Following areas of Sindh which are considered as hotspots for Freshwater Turtles, these includes Thatta District, Sujawal District, Badin District, Dadu District, Khairpur District, Sanghar District and Sukkur District.

1. Thatta District

Thatta is the historical district of Sindh Province. This district is having very strong bonding with Indus River. Thatta district is situated in southern portion of Sindh province. According to climatic distribution, this is included in lower region of Sindh. Major livelihood for the people of Thatta is dependent on the fishing practices. Thatta is distributed into four tehsils, Thatta, Mirpur Sakro, Ghora bari and Keti Bander. The Keti Bander is

Fig. 3. *Pangshura smithi* (Brown Roofed Turtle).

Fig. 4. *Pangshura tectum* (Indian Roofed Turtle).

the coastal area, while Ghora bari is very famous because of the presence of various fish farms there. Mir Pur Sakro contains a major canal named as Ghulamullah Canal (Fig. 10) or Mirpur Sakro Canal (Fig. 11). This canal and fish farms at Ghora bari (Fig. 12) serves as a very rich habitat for freshwater turtle populations. Major wetlands in Thatta district are Keenjhar, Haleji and Hadero Lakes.

Keenjhar Lake

Keenjhar Lake (Fig. 13) is a Ramsar site located in Thatta District of Sindh. It covers approximately 14,000 ha of area and having latitude and longitude of 68^{o} 03' E and 24^{o} 56' N. It is considered as one of largest freshwater lakes of Sindh and it is the major source of water supply to Karachi city, Thatta city and Ketibunder. The main

Fig. 5. *Hardella thurjii* (Crowned River Turtle).

Fig. 6. *Nilssonia gangeticus* (Indian soft shell Turtle or Ganges Soft shell Turtle).

water supply to Keenjhar Lake comes from River Indus. The location of Keenjhar Lake is about 19km North and North East to Thatta District, while it is situated 113km away from Karachi city. Many seepage lagoons and marshes are surrounding the Keenjhar Lake, which are connected with semi desert areas bearing limestone rock beds. This man made freshwater lake was formed in 1930 when two small lakes named Keenjhar and Kalri Lake were merged together after development of a dam at Bangla (Khan and Abbas, 2011). This lake provides a rich habitat for Fresh water turtles survival.

Haleji Lake

Haleji Lake (Fig. 14) is an important wetland of Sindh located in Thatta district. Its total area is about 6.58km^2 along with the maximum depth of 5 to 6 m**.** This

Fig. 7. *Nilssonia hurum* (Indian Peacock soft shell Turtle).

Fig. 8. *Lissemys punctata* (Indian Flap shell Turtle).

important Ramsar site is situated at 67^{o} 46’38"E and 24^{o} 48’N having an altitude of 4 m. This lake is located 88km away from Karachi (Khan *et al*., 2012a,b; Khan *et al*., 2014). It is very rich in Biodiversity and a variety of species of fauna and flora are inhabitant of this lake. Haleji Lake is surrounded by lagoons which serves as a natural habitat for fresh water turtles.

Hadero Lake

Hadero Lake is a saline water lake which is located at longitude of 24 ^{o} 49'N and latitude of 67 ^{o} 52'E in Thatta district of Sindh province. Primarily it affirmed as Game Sanctuary in 1971 but later on it was declared as Wildlife Sanctuary in 1977. Hadero Lake is natural lake that is located at the periphery of the stony desert. Its covered area is 1321 hectares. Livelihood of the local population

Fig. 9. *Chitra indica* (Indian narrow headed soft shell Turtle).

Fig. 10. Ghulamullah Canal.

is dependent on fishing from the lake. In past a number of fresh water turtles had been observed in the vicinity of this lake.

2. Badin District

Badin District is located in the lower portion of Sindh called as Lar, It is having a critical geographical location that lies in between Tharparkar Desert and Arabian Sea.

Fig. 11. In Mirpur Sakro Canal, Brown Roofed Turtle (*Pangshura smithii*) is ready for jumping.

Fig. 12. Fish farms at Ghora Bari.

The geographical coordinates are 24º-5' to 25º-25' north and 68º21' to 69º 20' east. Badin District is distributed in five tehsils which includes Matli, Talhar, Tando Bago, Badin and Golarchi.

There are 24 important lakes and wetlands present in Badin District which serve as key potential areas for distribution of freshwater turtle populations. Major canal running through Thatta and Badin District is LBOD (Left

Fig. 13. A view of Keenjhar Lake.

Fig. 14. A view of Haleji Lake.

Bank Outfall Drain). Fish farming is the major profession of the local population of Badin district. There are about 370 Fish farms developed by local people that also have freshwater turtle population.

3. Sujawal District

Sujawal is a newly formed district of Sindh Province. Its Latitude is 24°36'23" of North and longitude is 68°4'19" of East. Indus River is the main demarcation line between

Fig. 15. Nara Canal.

Fig. 16. A view of Sukkur Barrage.

Thatta District and Sujawal District. Administratively, it is subdivided into five tehsils named as Jaati, MirPur Bathoro, Shah Bandar, Kharochan and Sujawal. The total area covered by this district is about 7335 km². The major livelihood for local people is cultivation of agricultural crops. Fish farming is also common. Important fish of this district is Palla that has been cultured in fish farms. Freshwater turtles have been mostly recorded from the near Sujawal.

4. Dadu District

Dadu District is an important district of Sindh Province. It comprises of Mehar, Khairpur Nathan Shah, Dadu, Johi and Sehwan tehsils. Its total area is about 190704 square km. Geography of Dadu district is unique. It contains three different types of ecosystems, Kohistan or Hilly areas, Barrage area, and Lower lands river area. In east Indus River is existing. There are many waterways which are flowing in this district locally called as Nais. The major wetland in Dadu District is Manchhar Lake. Other important lakes are Sanjri Dhand and Unheri Dhand.

Manchar Lake

Manchar Lake is a natural freshwater shallow lake that created by a vast depression formed in between hilly ranges. Khirthar Hills are present in the west, while Laki hills are present in the south and Indus River flows in the east. The deepness of this lake is 10km. This big water reservoir is sufficient to supply water for drinking purposes to whole district as well as it is also a major supplier of water to irrigation canals and agricultural croplands. This is also an important source of livelihood for local communities in the form of fishing practices. Local anglers called as Mohanas or Meerbahar used to live in boats inside the lake. In past it was considered as major roosting area for migratory birds but because of construction of MVND (Main Nara Valley Drain), most of saline water drains out into Manchar Lake that result in loss of natural fauna and flora from the lake. Drainage of Chemical effluents and other pollutants in lake also result in serious contaminations in water that leads to biodiversity loss including that of turtles.

5. Khairpur District

Its total covered area is 15910 km^2. There is complete network of canals present to irrigate the whole area, that is the reason Khairpur is a very fertile area for cultivation of all types of crops.

Nara Canal

It a major canal emerging from Nara Tehsil of Khairpur district. It considered as largest canal of Sindh that originates from Sukkur Barrage, extends from Nara Tehsil of Khairpur District to Sanghar, and finally drains off in Runn of Kutch Area. Nara wetland complex is very famous and ecologically important combination of approximately 200 wetlands of different sizes, which are present on both sides of Nara Canal (Fig. 15). These serve as important habitats for freshwater turtles.

6. Sanghar District

Sanghar District situated in the middle area of Sindh Province. It comprises of six tehsils named as Jam Nawaz Ali, Khipro, Sanghar, Shadad Pur, Sinjoro and Tando Adam. Total covered area of Sanghar District is 9874km^2. It is famous because of the presence of a wetland complex called as Chotiari wetland complex. Bakar Lake and Sanghriaro Lake are the important lakes of Sanghar District.

Chotiari Wetland Complex

Chotiari Wetland Complex is the combination of many freshwater and Saline wetlands that covers an area of about 18000 hectares. This complex has the major water reservoir named as Chotiari Dam. The geographical coordinates of Chotiari wetlands complex are 26°1' N latitude and 69°4' E longitude. It is bounded by Thar desert from East and North while in southern portion Nara canal is present. The major wetlands in Chotiari wetland complex are Naro, Khor, Meena, Sajaran, Phuleil, Gun, Wari, Jajur, Bholo and Jadpur (Rais *et al*., 2008).

7. Sukkur District

Sukkur District comprises of four tehsils includes Sukkur, Rohri, Saleh Pat and Pano Aqil. Climatic condition of Sukkur is very harsh and intense. Sukkur is famous for Sukkur Barrage. Thick and dense Riverine forest is also a unique ecological characteristic of Sukkur. It grows along with the bank of Indus River.

Sukkur Barrage

Sukkur Barrage (Fig. 16) was constructed in 1932 over River Indus to control the flow of water in River Indus. In past it was also called as Lloyd Barrage. It has 66 gates. It irrigates about 7.63 million acres of area. The land of Sukkur is very fertile and productive due to presence of this major irrigation canal system. Sukkur barrage is not only responsible to fertile lands of Sukkur district but it also supply water through its canal system to Khairpur district, Mirpurkhas district, Sanghar district, Tharparkar district and Hyderabad district. Sukkur Barrage is also responsible for drinking water supply, irrigation and flood control in Sukkur district. There is a very well developed canal system that form unique networking and irrigation system. There are seven canals that emerge out from Sukkur Barrage. Four canals originate from left bank while three canals originate from right bank. Nara Canal is the major canal which is largest canal in Sindh. After Nara Canal, Rohri Canal exist and the third canal is Mir Wah Canal, while forth is Abul Wah Canal. Three canals originate from Right bank named as Dadu Canal, Rice Canal and Khirthar Canal. All other canals are permanent, while Rice Canal is a seasonal canal for cultivation of Rice fields.

Threats

Sindh is the highly populated province of Pakistan. Most of the districts are under-developed and poverty is one of the main reasons for their interest in trade of turtles. River Indus, Indus basin and the tributaries of River Indus includes canals, lakes, waterways, streams, swamps, marshes and ponds, all provides feeding and breeding grounds for freshwater turtles.

Another threat for freshwater turtles in Sindh is the profession of the local communities residing near wetlands, and people depend on fishing for their survival. Most of those areas in interior Sindh are rural areas and local tribal communities like Mohana communities or Kail communities are involved in trade of turtles along with fishing.

Sand mining also has very disastrous effects on ecology and habitat of freshwater turtles. Commercial sand mining from the rivers not only cause erosion but also destruct the nesting areas of the turtles. It also modifies the direction of flow of water, configuration of riverbanks and makes water more turbid. All these factors directly influence on the growth of waterweeds, on under water activities of turtles and it also has hazardous effects on health of that aquatic ecosystem. Another important factor which is influenced by sand mining in rivers is reduction in dissolved oxygen in water which ultimately results in disturbance of aquatic life.

Trade of Calipee

Calipee is the soft cartilaginous part of plastron of Soft shell Turtles. It is considered as most valuable part of turtle`s body. It can use in soups and other dishes. It is very interesting fact that being a Muslim country, Pakistan is not utilizing these parts of turtle for edible purposes but most of these used to export to neighboring countries like China.

People from rural areas utilize this resource of nature to earn their riches. Mostly middlemen play an important role by connecting the link between local fishermen and foreign traders. It recorded that many consignments seized by custom in Pakistan, which supplied to China. The shipment contains tons of calipee, and tagged as dried fish.

Turtle habitats are being extensively degraded, destroyed and fragmented because of anthropogenic activities (Klemens, 2000). Some time natural habitat of freshwater turtles destructed because of developmental activities and urbanization. In Sindh, several developmental projects are under progress like Wind Mill projects Jhimpir (Thatta), Thar Coal project (Tharparkar), Double carriageway project (Thatta to Karachi), Solar power project (Khairpur) and Thermal power projects. All these sort of developmental activities although are beneficial for mankind but also hazardous to natural habitat of wild fauna.

All crop growing activities and major deforestation also responsible for water seepage problems, modification of waterways and canal blockage. Agricultural wastewater and pesticides usage is also disastrous to population of fresh water turtles, Khan and Law (2005) also reported pesticides threats to turtles.

Industrial waste material is an important cause of reduced population of freshwater turtles. It results in disturbed breeding biology, infertility, eggs shell thinning and physiological disorders in freshwater turtles.

Most of the soft shell turtles in Sindh are struggling for their existence and continuously fighting with high level of illegal killing for trade and export. The people kill them and cut their parts to sell them to local consumers. Alternate livelihood opportunities should be provided to them for enhancing their financial resources.

China is the major market for Freshwater turtles. Being a neighboring country, it is very easy for traders to export whole turtles or their parts to China.

Environmental and climate changes and natural disasters are also major threats for turtle survival. Pollution, contamination of water with industrial, agricultural, or domestic waste, pesticides sprays, fertilizers, global warming, and pathogens, all serve as threat for existence of Freshwater turtles. Habitat modification, habitat degradation, and destruction are also important factors for their loss.

Urbanization, developmental projects, construction of dams, barrages and roads are also important reason for their decreased populations. Globally, turtle habitats are being extensively degraded, destroyed and fragmented, and where they still exist in reasonable populations turtles are being subjected to subsistence hunting as well as for collection for regional and international consumption markets, in addition to the growing international pet trade (Klemens, 2000).

Conservation Efforts

In Pakistan, many efforts have been made by the different governmental and nongovernmental organizations for the conservation of turtles. IUCN Pakistan, WWF Pakistan, Sindh Wildlife Department, Zoological Survey of Pakistan and Department of Zoology, University of Karachi are actively working and contributing for making studies regarding the protection and conservation of freshwater turtles in Sindh. The Scientific and Cultural Society of Pakistan (SCSP) provided capacity development through training workshops to university students for conservation and management of freshwater turtles. The IUCN Commission on Ecosystem Management (CEM), West Asia also conducted several training programs for conservation and management of ecosystem at University of Karachi during 2013-2016.

Many researchers have worked on the distribution and conservation of freshwater turtles particularly in different locations in Sindh. Noureen (2009) reported eight species of freshwater turtles in Indus River system. Arshad and

Noureen (2010) conducted a survey to identify the causes of mass scale mortality of freshwater turtles downstream Sukkur Barrage. Regarding illegal trading, Noureen *et al*. (2012) investigated the consequences and status of freshwater turtles in Pakistan. Recently, Khan (2015) reported the distribution of freshwater turtles in Indus Valley with morphology, natural history, and threats. Habitat loss was found to be the major threat for all species. Another study, Khan *et al*. (2015) described the distribution and status of freshwater turtles in Sindh and Khyber Pakhtun Khuwa (KPK). In this study, eight species of freshwater turtles were recorded in Sindh and population of turtles was estimated to be higher in Sindh as compared to that in KPK.

Recommendations

The legislation for conservation of turtles should be properly implemented. Distribution areas and hotspots should highlighted. Community based awareness should be utilized. Alternate livelihood opportunities should be provided to local people to avoid fresh water turtle trade. Major threats should be detected and resolved. Habitat destruction should be discouraged. Export of parts of turtles should be checked, and local markets should be monitored to minimize the use of turtles in as pet trade.

REFERENCES

Arshad, M. and Noureen, U. 2010. Investigating mass scale mortality of freshwater turtles downstream Sukkur Barrage, Indus River, Sindh. A report submitted to the Ministry of Environment's Pakistan Wetlands Program. pp10.

Fritz, U. and Havas, P. 2007. Checklist of Chelonians of World. Vertebrate Zoology. 57(2)149-368.

Khan, MZ. and Law, FCP. 2005. Adverse Effects of Pesticides and related Chemicals on Enzyme and Hormone Systems of Fish, Amphibians and Reptiles. Proc. Pakistan Acad. Sci. 42(4):315-323.

Khan, MZ. and Abbas, D. 2011. Aquatic Vertebrates of Haleji and Keenjhar Lakes. Lap Lambert Academic Publishing, Germany. pp216.

Khan, MZ., Ghalib, SA., Siddiqui, S., Siddiqui, TF., Farooq, RY., Yasmeen, G, Abbas, D. and Zehra, A. 2012[a]. Current Status and Distribution of Reptiles of Sindh. Journal of Basic & Applied Sciences. 8(1):26-34. DOI: http://dx.doi.org/10.6000/1927-5129.2012.08.01.05.

Khan, MZ., Abbas, D., Ghalib, SA, Yasmeen, R., Siddiqui, S., Mehmood, N., Zehra, A., Begum, A., Jabeen, T., Yasmeen, G. and Latif, T. 2012[b]. Effects of Environmental Pollution on Aquatic Vertebrate and Inventories of Haleji and Keenjhar Lakes: Ramsar Sites. Canadian Journal of Pure and Applied Sciences. 6(1):1759-1783.

Khan, MZ., Jabeen, T., Ghalib, SA., Siddiqui, S., Alvi, MS., Khan, IS., Yasmeen, G., Zehra, A., Tabbassum, F., Hussain, B. and Sharmeen, R. 2014. Effect of Right Bank Outfall Drain (RBOD) on Biodiversity of the Wetlands of Haleji Wetland Complex, Sindh. Canadian Journal of Pure and Applied Sciences. 8(2):2871-2900.

Khan, MS. 2015. Status and Distribution of Freshwater Turtles in Pakistan. Bull. Chicago Herp. Soc. 50(4):51-53.

Khan, MZ., Safi, A., Fatima, F., Ghalib, SA., Hashmi, MUA., Khan, IS., Siddiqui, S., Zehra, A. and Hussain, B. 2015. An Evaluation of Distribution, Status and Abundance of Freshwater Turtles in Selected areas of Sindh and Khyber Pakhtunkhwa Provinces of Pakistan. Canadian Journal of Pure and Applied Sciences. 9(1):3201-3219.

Klemens, MW. 2000. A new paradigm of conservation. Turtle Conservation. 1-334.

Noureen, U. 2009. Freshwater Turtles of Pakistan: Illegal trade in Sindh: Preliminary findings of trade in Freshwater Turtle Parts. A survey report submitted to the Ministry of Environment's Pakistan Wetlands Programme. pp 36.

Noureen, U., Khan, A. and Arshad, M. 2012. Exploring illegal trade in freshwater turtles of Pakistan. Rec. Zool. Surv. Pakistan 21:19-24.

Rais, M., Khan, MZ., Ghalib, SA., Nawaz, R., Akbar, G., Islam, SL. and Begum, A. 2008. Global conservation significance of Chotiari wetlands complex, Sanghar, Sindh. The Journal of Animal and Plant Sciences. 23 (6):1609-1617.

Received: August 10, 2016; Revised: Sept 26, 2016;
Accepted: Sept 28, 2016

Canadian Journal of Pure and Applied Sciences
Vol. 10, No. 3, pp. 4011-4028, October 2016
Online ISSN: 1920-3853; Print ISSN: 1715-9997
Available online at www.cjpas.net

ON PIEZOGRAVITOCOGRAVITOELECTROMAGNETIC SHEAR-HORIZONTAL ACOUSTIC WAVES

Aleksey Anatolievich Zakharenko
International Institute of Zakharenko Waves (IIZWs)
660014, ul. Chaikovskogo, 20-304, Krasnoyarsk, Russia

ABSTRACT

This paper relates to the first centenary of the prediction of the existence of gravitational waves by Albert Einstein in 1916 and their prediction was experimentally confirmed in 2016 in one hundred years after the prediction. This work develops the theory of the wave propagation in the solids possessing the piezoelectric, piezomagnetic, and magnetoelectric effects as well as the piezogravitic, piezocogravitic, and gravitocogravitic effects, and the other exchange coeffects. Exploiting the quasi-static approximation in the theory of electromagnetism and gravitoelectromagnetism, the thermodynamics and the coupled equations of motion are developed in the common form. To simplify the problem of the wave propagation in these solids, the shear-horizontal (SH) wave propagation in the transversely isotropic materials was then treated. Considering all the aforementioned effects and coeffects, the explicit forms of the propagation velocities of the bulk and new surface acoustic waves (SH-BAW and new SH-SAW coupled with four potentials) were theoretically obtained. This theoretical work has the additional purpose to stimulate experimental measurements of all the necessary material parameters when a solid possesses all the effects and coeffects including the ones from the theory of gravitoelectromagnetism.

PACS: 51.40.+p, 62.65.+k, 68.35.Gy, 68.35.Iv, 68.60.Bs, 74.25.Ld, 74.25.Ha, 75.20.En, 75.80.+q, 81.70.Cv, 96.20.Jz, 04.30.-w, 04.90.+e, 95.30.Sf
Keywords: transversely isotropic solids, piezoelectric and piezomagnetic effects, magnetoelectric effect and other exchange effects, piezogravitic and piezocogravitic effects, new nondispersive SH-SAW.

INTRODUCTION

Before to start any description of very complicated problem of wave propagation in solids possessing many effects that can be taken into account, it is necessary to fist review the history and evolution of the discovery of different effects that can be revealed in the studied solids. It is necessary to state right away that the studied solids can simultaneously have the following known different effects: piezoelectric, piezomagnetic, magnetoelectric, piezogravitic, piezocogravitic, gravitocogravitic effects. These solids can also possess several coeffects that can be studied and discussed below. So, it is possible to review the problems of wave propagation from simple to more complicated.

The well-known piezoelectric effect can cause the propagation of the shear-horizontal surface acoustic waves (SH-SAWs) in the transversely isotropic (6 *mm*) piezoelectrics. This is the simplest case of SH-SAWs known as the surface Bleustein-Gulyaev (BG) wave independently discovered by Bleustein (1968) and Gulyaev (1969) in their developed theories to the end of the 1960s. There is also the second SH-SAW theoretically discovered by Bleustein (1968) for the other electrical boundary conditions. This SH-SAW is frequently called the surface Bleustein wave. However, the author of this theoretical report can use the words of the slower and faster surface BG-waves instead of the surface Bleustein-Gulyaev wave and surface Bleustein wave, respectively, to distinguish them from each other. The speeds of both the SH-SAWs must be slightly slower than the speed of the shear-horizontal bulk acoustic wave (SH-BAW) and the existence of the SH-SAWs demonstrates the fact of the instability of the SH-BAW for certain cuts and propagation directions in suitable solids. Studying the wave propagation in piezoelectrics, the well-known equations of electrostatics in the quasi-static approximation are used because the speed of light is approximately five orders faster than any acoustic wave speed. The slower and faster surface BG-waves can also propagate in piezomagnetics possessing the piezomagnetic effect when the piezoelectric and electric constants are substituted by the piezomagnetic and magnetic constants, respectively. Here the equations of magnetostatics in the quasi-static approximation are used for the same reason mentioned above.

Corresponding author e-mail: aazaaz@inbox.ru

There are also piezoelectromagnetics (magneto-electroelastics) as a class of magnetoelectric materials that can simultaneously possess both the piezoelectric and piezomagnetic effects resulting in the existence of the magnetoelectric effect. In these smart materials there is a possibility to control the magnetic subsystem by changes in the electric subsystem via the mechanical subsystem, or vice versa. Smart transversely isotropic (6 *mm*) piezoelectromagnetic (PEM) materials were only recently exhaustively treated regarding to the problems of different instabilities of the SH-BAW, i.e. the existence of various SH-SAWs when different electrical and magnetic boundary conditions are applied. Indeed, the equations of the electrostatics and magnetostatics must be also used for the problem of wave propagation in piezoelectromagnetics. There is the single review (Zakharenko, 2013a) concerning the problems of the wave propagation in piezoelectromagnetics. One decade ago Melkumyan (2007) has discovered several SH acoustic waves propagating in the transversely isotropic piezoelectromagnetics. However, only three of them can be called the Melkumyan SH-SAWs: the surface Bleustein-Gulyaev-Melkumyan (BGM) wave, the piezoelectric exchange surface Melkumyan (PEESM) wave, and the piezomagnetic exchange surface Melkumyan (PMESM) wave. The first Melkumyan PEM-SH-SAW is called the BGM wave to have an analogy with the surface BG-wave (Bleustein, 1968; Gulyaev, 1969). Following the theoretical work by Melkumyan (2007), several new PEM-SH-SAWs were also discovered in theoretical work (Zakharenko, 2010; Zakharenko, 2013b; Zakharenko, 2015a,b). It is now possible to state that more than ten new PEM-SH-SAWs can propagate in the transversely isotropic piezoelectromagnetics in contrast to two SH-SAWs existing in pure piezoelectrics or pure piezomagnetics. This is due to the fact of competition of three different effects mentioned above that can coexist in piezoelectromagnetics. The magnetoelectric effect is extremely weak effect compared with the piezoelectric or piezomagnetic effect. However, it can cause a dramatic influence on the existence of some new SH-SAWs (Zakharenko, 2015b).

It is obvious that any gravitational effect or relevant exchange coeffect can be extremely weak similar to the magnetoelectric effect. However, it is possible that consideration of some extremely weak effects can disclose the existence of some relevant new SH-SAWs that can propagate in the apt solids. Indeed, the gravitational effect can be readily recordable when very massive bodies (preferably solids) are treated. For instance, in the two-body system such as Moon-Earth, a slight but remarkable attraction of Earth surface towards Moon can be experimentally observed when Moon is orbiting Earth. Concerning the microworld when microwaves are propagating in a bulk solid or on the solid surface, it is thought that it is hard to record any changes caused by extremely small possible perturbations of local gravitational fields. Note that solids for the problem of acoustic wave propagation are naturally treated as continua but not discrete materials consisting of atoms. So, it is necessary to theoretically demonstrate that in solid continua some extremely weak gravitational effects or some relevant coeffects can cause the existence of some corresponding new SH-SAWs. This can be similar to the new SH-SAW existence caused by the extremely weak magnetoelectric effect in piezoelectromagnetics.

For the purpose of a deep study of the influence of some relevant gravitational effects on the existence of new SH-SAWs, it is natural to exploit the known equations of the gravitoelectromagnetism. These equations are similar to the well-known equations of electromagnetism (Heaviside, 1893; Maxwell, 1954; Jefimenko, 1992; Jefimenko, 2000; Jefimenko, 2006; Assis, 1994; Assis, 1999). One century ago, namely in 1916 Albert Einstein has predicted the existence of gravitational waves in the context of his theory of general relativity (Einstein, 1916). It is also known that gravitational waves propagate in a vacuum with the speed of light, namely the speed of the electromagnetic waves. So, the quasistatic approximation incorporating gravitational effects is fitting here as well. Using the equations of the gravitoelectromagnetism instead of the equations of the electromagnetism, one can find that the final explicit forms obtained for the propagating velocities in (Melkumyan, 2007; Zakharenko, 2010; Zakharenko, 2013a,b; Zakharenko, 2015a,b) can be readily rewritten down. Indeed, the utilization of the piezogravitic, piezocogravitic, and gravitocogravitic effects instead of the piezoelectric, piezomagnetic, and magnetoelectric effects, respectively, results in a substitution of piezoelectric, piezomagnetic, electric, magnetic, and magnetoelectric constants by the piezogravitic, piezocogravitic, gravitational, cogravitational, and gravitocogravitic constants, correspondingly. However, this substitution is questionable because anisotropic solids (monocrystals or composite materials) can be piezomagnetics or noncentrosymmetric piezoelectrics, or piezoelectromagnetics. This can mean that it is necessary to treat the gravitational exchange effects only in a coupe with the electromagnetic effects. Figure 1 schematically shows a solid continuum that can possess the mechanical, electrical, magnetic, gravitational (gravitoelectric), and cogravitational (gravitomagnetic) subsystems. Figure 1a shows that there is an interaction between any two subsystems somewhat directly (some exchange must occur) and via the mechanical subsystem. Figure 1b shows the simpler case when the gravitational or cogravitational subsystem can interact with the electrical or magnetic subsystem only via the mechanical subsystem.

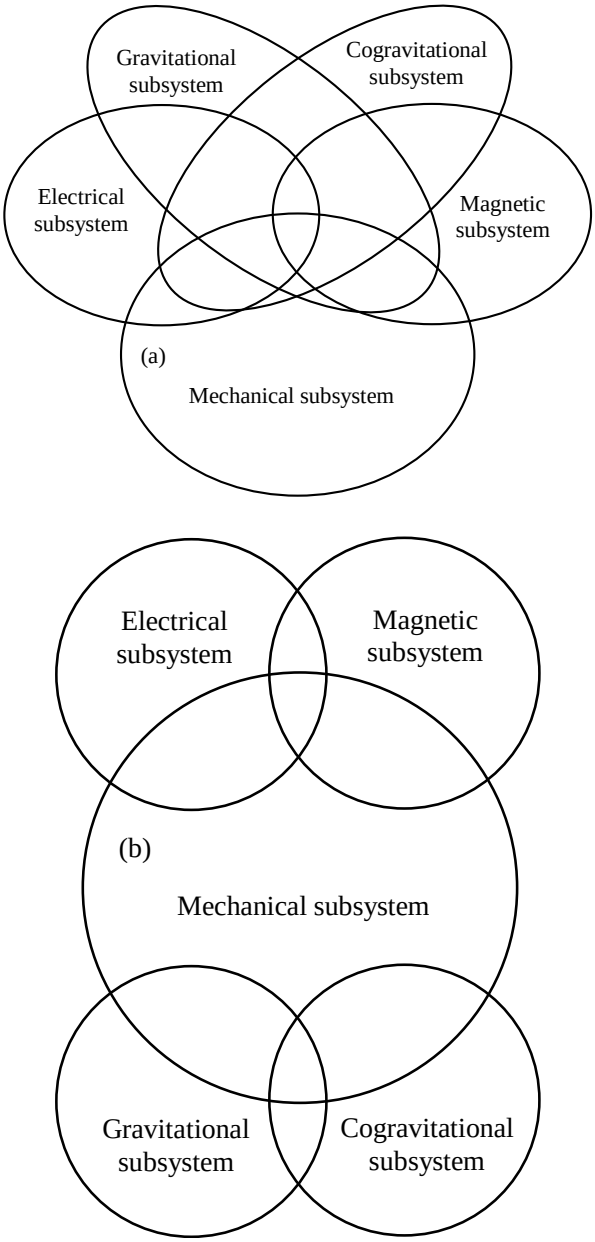

Fig. 1. The schematic demonstration of possible connections among the used subsystems such as the mechanical, electrical, magnetic, gravitational, and cogravitational ones: (a) there is an interaction between each pair of subsystem via the mechanical one and (b) the electrical subsystem can interact only with the magnetic subsystem (or vice versa) via the mechanical one and the gravitational subsystem can interact only with the cogravitational one (or vice versa) via the mechanical one.

Scientists have recently measured the gravitational equivalent of a magnetic field for the first time in a laboratory under certain special conditions. This effect is much larger than expected from general relativity. In general, scientists preferably study gravitational fields passively by observing for grasp of existing gravitational fields produced by large inertial masses such as stars or planets and there is no ability to change them, for instance, with magnetic fields. In his publication Füzfa (2016) has described one revolutionary approach for the creation of gravitational fields from well-controlled magnetic fields and observing how these magnetic fields could bend space-time. He has proposed a theoretical device based on superconducting electromagnets (modern technologies exhaustively used at CERN or the ITER reactor) for creation of detectable gravitational fields. It could disclose many new applications, for instance, in telecommunications with gravitational waves. The ability to produce, detect, and control gravitational fields would certainly be a major achievement in modern physics. So, scientific interest in the problem of interactions between the gravitational and electromagnetic waves continuously increases, for instance, see in (Hegarty, 1969; Kleidis *et al*., 2010; Forsberg *et al*., 2010). The great interest in the problem of the gravitational wave detection can be supported by the fact that the European Space Agency (ESA, the European Union) together with the National Aeronautics and Space Administration (NASA, the United States) have collaborated a series of expensive space experiments called the Laser Interferometer Space Antenna (LISA). The LISA is a proposed space-based piezoelectric device (Möhle, 2013) for gravitational waves' detection in the low frequency range from 0.1 mHz to 1.0 Hz that is not accessible by ground-based detectors. However, this expensive space journey has lost any financial support by the NASA. Also, in February, 2016, it was reported by Professor Dr. David Reitze, the executive director of the LIGO (Laser Interferometer Gravitational-Wave Observatory) that the gravitational waves were detected by the LIGO (Abbott *et al*., 2016). It is obvious that the theoretical work developed in this report does not require a multi-billion USD financial support and can be developed at an Earth laboratory, even in the International Space Station, Moon, or Mars.

The following section deals wth the thermodynamic description of a piezoelectromagnetic bulk material when the gravitational and cogravitational forces are also taken into account. The third section provides both the differential and tensor forms for the coupled equations of motion concerning the case of the shear-horizontal wave propagation. The fourth section discusses the boundary conditions that can lead to the existence of new surface SH-waves.

Thermodynamics

It is natural to consider a bulk solid continuum that simultaneously possesses the piezoelectric, piezomagnetic, and magnetoelectric effects. It is natural to assume that the gravitational (gravitoelectric) and

cogravitational (gravitomagnetic) forces must be also considered. This complex continuum can be thermodynamically described by means of suitable thermodynamic variables and functions. Indeed, it is necessary to choose a thermodynamic potential to properly describe thermo gravitocogravitoelectro-magnetoelastic interactions in the continuum. It is preferable for this case to cope with the thermodynamic potential called enthalpy H_e to obtain adiabatic rather than isothermal conditions. It is well known that an adiabatic process can be characterized by the constant entropy, $S = S_0$ = const, and this thermodynamic variable illuminates a level of disorder in the system. Treating a linear case, it is possible to consider only linear terms in a Taylor series for the enthalpy H_e relative to an equilibrium condition $H_e(S_0)$. It is apparent that $S = S_0$ = const actually gives zero change, namely dS = 0. So, this thermodynamic variable can be excluded from the further analysis, for instance, see in Zakharenko (2010).

For this case, these linear terms in a Taylor series for the suitable thermodynamic potential can contain the following thermodynamic variables frequently written in the tensor forms: strain τ_{ij}, electrical field E_i, magnetic field H_i, gravitational (gravitoelectric) field GE_i, and cogravitational (gravitomagnetic) field GH_i, where the indexes i and j run from 1 to 3. Energetic terms of such complex system described by a thermodynamic potential can be naturally coupled with the following subsystems shown in Figure 1: elastic subsystem (thermodynamic variable τ_{ij}), electric subsystem (variable E_i), magnetic subsystem (variable H_i), gravitational subsystem (variable GE_i), cogravitational subsystem (variable GH_i) and thermal subsystem (entropy S).

Therefore, for the fitting thermodynamic potential T, one can write the following: $T = f\left(\tau_{kl}, E_k, H_k, GE_k, GH_k, S\right)$ and $\mathrm{d}T = f_0\left(\mathrm{d}\tau_{kl}, \mathrm{d}E_k, \mathrm{d}H_k, \mathrm{d}GE_k, \mathrm{d}GH_k, \mathrm{d}S = 0\right)$. Next, it is natural that for the problem of acoustic wave propagation in such continua, it is preferable to use the following thermodynamic functions: stress σ_{ij}, electrical displacement (induction) D_i, magnetic displacement (induction or flux) B_i, gravitational displacement (gravitoelectric induction) GD_i, and cogravitational displacement (gravitomagnetic induction) GB_i. These five thermodynamic functions depend on five independent thermodynamic variables described above as follows:

$$\sigma_{ij} = f_1\left(\tau_{kl}, E_k, H_k, GE_k, GH_k\right),$$
$$D_i = f_2\left(\tau_{kl}, E_k, H_k, GE_k, GH_k\right),$$
$$B_i = f_3\left(\tau_{kl}, E_k, H_k, GE_k, GH_k\right),$$
$$GD_i = f_4\left(\tau_{kl}, E_k, H_k, GE_k, GH_k\right),$$
$$GB_i = f_5\left(\tau_{kl}, E_k, H_k, GE_k, GH_k\right).$$

In this linear case, the coupled constitutive relations can be therefore written as follows:

$$\sigma_{ij} = C_{ijkl}\tau_{kl} - e_{kij}E_k - h_{kij}H_k - g_{kij}GE_k - f_{kij}GH_k \quad (1)$$
$$D_i = e_{ikl}\tau_{kl} + \varepsilon_{ik}E_k + \alpha_{ik}H_k + \zeta_{ik}GE_k + \xi_{ik}GH_k \quad (2)$$
$$B_i = h_{ikl}\tau_{kl} + \alpha_{ik}E_k + \mu_{ik}H_k + \beta_{ik}GE_k + \lambda_{ik}GH_k \quad (3)$$
$$GD_i = g_{ikl}\tau_{kl} + \zeta_{ik}E_k + \beta_{ik}H_k + \gamma_{ik}GE_k + \vartheta_{ik}GH_k \quad (4)$$
$$GB_i = f_{ikl}\tau_{kl} + \xi_{ik}E_k + \lambda_{ik}H_k + \vartheta_{ik}GE_k + \eta_{ik}GH_k \quad (5)$$

In expressions from (1) to (5), the used indices i, j, k, and l run from 1 to 3. The first equation indicates that the mechanical thermodynamic function such as the stress σ_{ij} also depends on the corresponding factors at the independent thermodynamic mechanical (τ_{ij}), electrical (E_i), magnetic (H_i), gravitational (GE_i), and cogravitational (GH_i) variables. These factors represent the corresponding proportionality coefficients for the linear case and are thermodynamically defined below. They are called the elastic stiffness constants C_{ijkl}, piezoelectric constants e_{kij}, piezomagnetic coefficients h_{kij}, piezogravitic constants g_{kij}, and piezocogravitic coefficients f_{kij}.

In equations (2) and (3), the thermodynamic functions such as the electrical and magnetic displacements (D_i and B_i) also depend on the corresponding factors at the thermodynamic variables and they can be divided into two groups. The first group is for the dielectric permittivity coefficients (electrical constants) ε_{ik}, magnetic permeability coefficients (magnetic constants) μ_{ik}, and electromagnetic constants α_{ik}. The second group is for the following exchange tensors: material exchange constants ζ_{ik}, ξ_{ik}, β_{ik}, and λ_{ik} that symbolize possible exchanges between the electrical and magnetic subsystems on one side and the gravitational and cogravitational subsystems on the other side. It is necessary to keep in mind that these exchange tensors must be nonzero even in the case when their possible values are very small. However, these small material parameters must be taken into account in the common case shown in figure 1a and can be neglected for the case shown in figure 1b. It was found that consideration of very small but nonzero material parameters can be very important. This fact was demonstrated in work (Zakharenko, 2010; Zakharenko, 2013b; Zakharenko, 2015a,b) concerning the wave propagation in piezoelectromagnetics when the extremely small electromagnetic constant α can cause the existence of several new SH-SAWs. In the common case, the tensor of the electromagnetic constants α_{ik} is non symmetric in contrast to the symmetric tensors of the electrical ε_{ik} and magnetic μ_{ik} constants. However, for the cubic and transversely isotropic (6 *mm*) materials the tensor α_{ik} is symmetric (Schmid, 2008; Rivera, 2009). This symmetry

can be also applied to other exchange tensors such as ζ_{ik}, ξ_{ik}, β_{ik}, and λ_{ik} in the first approximation, assuming that the values of the material parameters of the tensors can be very small. Similar to the exchange between the electrical and magnetic subsystems characterized by the tensor of the electromagnetic constants α_{ik} there must also exist an exchange between the gravitational and cogravitational subsystems. This exchange is taken into account by the presence of the exchange tensor ϑ_{ik} in equations (4) and (5). The tensor ϑ_{ik} can be called the tensor of the gravitocogravitic constants and it is possible to assume that the tensors α_{ik} and ϑ_{ik} can be symmetric for the same materials. Equations (4) and (5) also contain the tensors of the gravitic and cogravitic constants, γ_{ik} and η_{ik}, respectively. It is possible to require that they are symmetric similar to the tensors of ε_{ik} and μ_{ik}.

In five equations written above, the first independent thermodynamic variable such as the strain tensor τ_{ij} can be defined by the following well known relation between the strain and the mechanical displacements for small perturbations: $\tau_{ij} = 0.5\left(\partial U_i / \partial x_j + \partial U_j / \partial x_i\right)$, where the indices i and j also run from 1 to 3. So, this relation represents the dependence of the strain tensor components τ_{ij} on the corresponding partial first derivatives of the mechanical displacement components U_1, U_2, and U_3 with respect to the real space components x_1, x_2, and x_3. Each mechanical displacement component is directed along the corresponding real space component for the rectangular coordinate system shown in Figure 2.

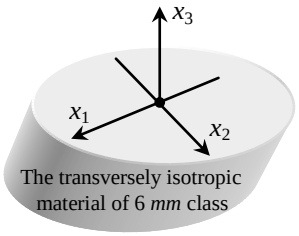

Fig. 2. The rectangular coordinate system. The coordinate beginning is situated at the vacuum-solid interface. The propagation direction is managed along the x_1-axis. The surface normal is directed along the x_3-axis. The 6-fold symmetry axis of the studied transversely isotropic (6 *mm*) material is parallel to the x_2-axis.

In equations from (1) to (5), the other independent thermodynamic variables such as the electrical field E_i, magnetic field H_i, gravitational field GE_i, and cogravitational field GH_i can be also defined by corresponding partial first derivatives. Using the corresponding potentials (electrical potential φ, magnetic potential ψ, gravitational potential Φ, and cogravitational potential Ψ) in the quasi-static (irrotational field) approximation, the components of all the fields are determined as the following partial first derivatives with respect to the real space components x_1, x_2, and x_3: $E_i = -\partial\varphi/\partial x_i$, $H_i = -\partial\psi/\partial x_i$, $GE_i = -\partial\Phi/\partial x_i$, $GH_i = -\partial\Psi/\partial x_i$. It is natural to exploit the quasi-static approximation when all the derivatives with respect to the time t in the corresponding Maxwell equations of electromagnetism (or the corresponding equations of the gravitoelectromagnetism) are omitted because the speed of the electromagnetic (or gravitational) wave is approximately five orders larger than the speed of any elastic wave (Dieulesaint and Royer, 1980; Auld, 1990; Zakharenko, 2010).

In the constitutive relations from (1) to (5), all the material tensors such as C_{ijkl}, e_{kij}, h_{kij}, g_{kij}, f_{kij}, ε_{ik}, μ_{ik}, α_{ik}, γ_{ik}, η_{ik}, ϑ_{ik}, ζ_{ik}, ξ_{ik}, β_{ik}, λ_{ik} can be thermodynamically expressed. For the thermodynamic definition of the elastic stiffness constants C_{ijkl}, these material parameters can be naturally defined from expression (1) as follows:

$$C_{ijkl} = \left(\frac{\partial\sigma_{ij}}{\partial\tau_{kl}}\right)_{E,H,GE,GH=\text{const}} \tag{6}$$

Thermodynamic definition (6) of the elastic stiffness constants C_{ijkl} states that they can be determined at constant electrical, magnetic, gravitational, and cogravitational fields. Symmetry arguments allow some simplifications of the quantity of the C_{ijkl} because the stress and strain tensors are symmetric: $\sigma_{ij} = \sigma_{ji}$ and $\tau_{ij} = \tau_{ji}$. Therefore, the stiffness tensor C_{ijkl} must also possess a corresponding degree of symmetry resulting in the following simplifications:

$$C_{ijkl} = C_{klij} = C_{jikl} = C_{klji} = C_{ijlk} = C_{lkij} = C_{jilk} = C_{lkji} \tag{7}$$

Using Voigt's notation, (3×3×3×3) tensor form (6) for the elastic stiffness constants C_{ijkl} can be rewritten in a form of (6×6) symmetric matrix (Dieulesaint and Royer, 1980; Auld, 1990; Zakharenko, 2010). The transformation procedure of a tensor form into a matrix is wellknown. For this purpose, the following rules are used for the indices: 11 → 1, 22 → 2, 33 → 3, 23 → 4, 13 → 5, 12 → 6 and therefore, $ijkl \rightarrow PQ$ and $C_{ijkl} \rightarrow C_{PQ}$, where the indices P and Q run from 1 to 6.

With equations from (1) to (5), the thermodynamic description of the piezoelectric constants e_{kij}, piezomagnetic coefficients h_{kij}, piezogravitic constants g_{kij}, and piezocogravitic coefficients f_{kij} can be correspondingly given by the following definitions:

$$e_{ijk} = -\left(\frac{\partial\sigma_{ij}}{\partial E_k}\right)_{\tau,H,GE,GH=\text{const}} = e_{ikl} = \left(\frac{\partial D_i}{\partial\tau_{kl}}\right)_{E,H,GE,GH=\text{const}} \tag{8}$$

$$h_{ijk} = -\left(\frac{\partial \sigma_{ij}}{\partial H_k}\right)_{\tau,E,GE,GH=\text{const}} = h_{ikl} = \left(\frac{\partial B_i}{\partial \tau_{kl}}\right)_{E,H,GE,GH=\text{const}} \quad (9)$$

$$g_{ijk} = -\left(\frac{\partial \sigma_{ij}}{\partial GE_k}\right)_{\tau,E,H,GH=\text{const}} = g_{ikl} = \left(\frac{\partial GD_i}{\partial \tau_{kl}}\right)_{E,H,GE,GH=\text{const}} \quad (10)$$

$$f_{ijk} = -\left(\frac{\partial \sigma_{ij}}{\partial GH_k}\right)_{\tau,E,H,GE=\text{const}} = f_{ikl} = \left(\frac{\partial GB_i}{\partial \tau_{kl}}\right)_{E,H,GE,GH=\text{const}} \quad (11)$$

It is necessary to state that the quantities of the tensors h_{kij}, e_{kij}, g_{kij}, and f_{kij} can be decreased. The symmetry arguments such as $\sigma_{ij} = \sigma_{ji}$ and $\tau_{ij} = \tau_{ji}$ can also demonstrate the corresponding degrees of symmetry for the h_{kij}, e_{kij}, g_{kij}, and f_{kij}. The symmetry influences allow the existence of the following equalities:

$$e_{kij} = e_{ijk} = e_{kji} = e_{jik} \quad (12)$$

$$h_{kij} = h_{ijk} = h_{kji} = h_{jik} \quad (13)$$

$$g_{kij} = g_{ijk} = g_{kji} = g_{jik} \quad (14)$$

$$f_{kij} = f_{ijk} = f_{kji} = f_{jik} \quad (15)$$

Exploiting Voigt's notation, all of the (3×3×3) tensor forms for the h_{kij}, e_{kij}, g_{kij}, and f_{kij} can be then rewritten as the asymmetric (6×3) or (3×6) matrices: $e_{kij} \rightarrow e_{kP}$ or $e_{ijk} \rightarrow e_{Pk}$, $h_{kij} \rightarrow h_{kP}$ or $h_{ijk} \rightarrow h_{Pk}$, $g_{kij} \rightarrow g_{kP}$ or $g_{ijk} \rightarrow g_{Pk}$, $f_{kij} \rightarrow f_{kP}$ or $f_{ijk} \rightarrow f_{Pk}$, where the index P runs from 1 to 6.

Next, the rest material tensors such as ε_{ik}, μ_{ik}, α_{ik}, γ_{ik}, η_{ik}, ϑ_{ik}, ζ_{ik}, ξ_{ik}, β_{ik}, λ_{ik} can be divided into three groups. The first group (ε_{ik}, μ_{ik}, α_{ik}) is for the electrical and magnetic subsystems and their interaction. The second (γ_{ik}, η_{ik}, ϑ_{ik}) is for the gravitational and cogravitational subsystems and their interaction. Thus, the third group contains the rest four exchange tensors. With the first group, the thermodynamic definitions for the dielectric permittivity coefficients ε_{ik}, magnetic permeability coefficients μ_{ik}, electromagnetic constants α_{ik} (see equations (2) and (3)) read:

$$\varepsilon_{ik} = \left(\frac{\partial D_i}{\partial E_k}\right)_{\tau,H,GE,GH=\text{const}} \quad (16)$$

$$\mu_{ik} = \left(\frac{\partial B_i}{\partial H_k}\right)_{\tau,E,GE,GH=\text{const}} \quad (17)$$

$$\alpha_{ik} = \left(\frac{\partial D_i}{\partial H_k}\right)_{\tau,E,GE,GH=\text{const}} = \left(\frac{\partial B_i}{\partial E_k}\right)_{\tau,H,GE,GH=\text{const}} \quad (18)$$

In the thermodynamic relations (16) and (17), the constants ε_{ik} and μ_{ik} represent symmetric tensors of the second rank (matrices): $\varepsilon_{ik} = \varepsilon_{ki}$ and $\mu_{ik} = \mu_{ki}$. It is also natural to treat $\alpha_{ik} = \alpha_{ki}$ because it is symmetric for the cubic and transversely isotropic (6 *mm*) materials (Schmid, 2008; Rivera, 2009). Indeed, the components of the tensors ε_{ik}, μ_{ik}, and α_{ik} are naturally written as (3×3) matrices (Schmid, 2008; Rivera, 2009; Zakharenko, 2010).

With expressions (4) and (5), the second group of the material tensors of the gravitic constants γ_{ik} and cogravitic constants η_{ik} can be also written as (3×3) symmetric matrices: $\gamma_{ik} = \gamma_{ki}$ and $\eta_{ik} = \eta_{ki}$. Also, it is possible also to treat the tensor of the gravitocogravitic constants ϑ_{ik} as symmetric for cubic and transversely isotropic (6 *mm*) materials. The thermodynamically defined as follows:

$$\gamma_{ik} = \left(\frac{\partial GD_i}{\partial GE_k}\right)_{\tau,E,H,GH=\text{const}} \quad (19)$$

$$\eta_{ik} = \left(\frac{\partial GB_i}{\partial GH_k}\right)_{\tau,E,H,GE=\text{const}} \quad (20)$$

$$\vartheta_{ik} = \left(\frac{\partial GD_i}{\partial GH_k}\right)_{\tau,E,H,GE=\text{const}} = \left(\frac{\partial GB_i}{\partial GE_k}\right)_{\tau,E,H,GH=\text{const}} \quad (21)$$

In the rest third group there are four exchange tensors such as ζ_{ik}, ξ_{ik}, β_{ik}, λ_{ik}. They are present in expressions from (2) to (5) of the constitutive relations and manifest possible exchange mechanisms between the electromagnetism and gravitoelectromagnetism. One has to be sure that some exchange occurs because there are recently performed experiments (Füzfa, 2016) in a laboratory on Earth concerning the evidence of creation of gravitational fields from well-controlled magnetic fields. So, it is even possible to require that the exchange tensors ζ_{ik}, ξ_{ik}, β_{ik}, and λ_{ik} must be also symmetric at least for the cubic and transversely isotropic (6 *mm*) materials. This requirement is enough for this study because it deals for simplicity with the 6 *mm* hexagonal materials. Consequently, the rest exchange tensors are thermodynamically defined as follows:

$$\zeta_{ik} = \left(\frac{\partial D_i}{\partial GE_k}\right)_{\tau,E,H,GH=\text{const}} = \left(\frac{\partial GD_i}{\partial E_k}\right)_{\tau,H,GE,GH=\text{const}} \quad (22)$$

$$\xi_{ik} = \left(\frac{\partial D_i}{\partial GH_k}\right)_{\tau,E,H,GE=\text{const}} = \left(\frac{\partial GB_i}{\partial E_k}\right)_{\tau,H,GE,GH=\text{const}} \quad (23)$$

$$\beta_{ik} = \left(\frac{\partial B_i}{\partial GE_k}\right)_{\tau,E,H,GH=\text{const}} = \left(\frac{\partial GD_i}{\partial H_k}\right)_{\tau,E,GE,GH=\text{const}} \quad (24)$$

$$\lambda_{ik} = \left(\frac{\partial B_i}{\partial GH_k}\right)_{\tau,E,H,GE=\text{const}} = \left(\frac{\partial GB_i}{\partial H_k}\right)_{\tau,E,GE,GH=\text{const}} \quad (25)$$

This study deals with wave propagation in anisotropic solid continua, i.e. crystals. This means that the propagation velocity must be different for different propagation directions in crystals. In general, all the material parameters are obtained in a crystallographic coordinate system that can naturally provide minimum set of independent material constants for simplicity. This study relates to surface acoustic SH-wave propagation coupled with all the potentials (electrical potential φ, magnetic potential ψ, gravitational potential Φ, and cogravitational potential Ψ) in such smart materials. However, surface SH-waves can be supported only in suitable propagation directions. It is necessary to rotate around the x_1-axis, x_2-axis, or x_3-axis in order to obtain a new propagation direction in the new suitable coordinate system called the work coordinate system. The new propagation direction must be directed along the x_1-axis in the work coordinate system. This situation requires a recalculation of all the values of the independent material constants. Therefore, the number of independent material constants and their values must be recalculated. It is obvious that the values of the new material constants are obtained using the values of the old ones. Exploiting the rules for tensor transformations (Dieulesaint and Royer, 1980; Auld, 1990; Zakharenko, 2010), some new values of the material constants with the indexes *i*, *j*, *k*, and *l* can be obtained by application of the transformation matrices such as a_{im}, a_{jn}, a_{kp}, and a_{lq} to the original values of the material constants with the indexes *m*, *n*, *p*, and *q*. Therefore, the transformation formulae for all the material tensors introduced above read:

$$C_{ijkl} = a_{im}a_{jn}a_{kp}a_{lq}C_{mnpq} \tag{26}$$

$$e_{ijk} = a_{im}a_{jn}a_{kp}e_{mnp} \tag{27}$$

$$h_{ijk} = a_{im}a_{jn}a_{kp}h_{mnp} \tag{28}$$

$$g_{ijk} = a_{im}a_{jn}a_{kp}g_{mnp} \tag{29}$$

$$f_{ijk} = a_{im}a_{jn}a_{kp}f_{mnp} \tag{30}$$

$$\varepsilon_{ij} = a_{im}a_{jn}\varepsilon_{mn} \tag{31}$$

$$\mu_{ij} = a_{im}a_{jn}\mu_{mn} \tag{32}$$

$$\alpha_{ij} = a_{im}a_{jn}\alpha_{mn} \tag{33}$$

$$\gamma_{ij} = a_{im}a_{jn}\gamma_{mn} \tag{34}$$

$$\eta_{ij} = a_{im}a_{jn}\eta_{mn} \tag{35}$$

$$\vartheta_{ij} = a_{im}a_{jn}\vartheta_{mn} \tag{36}$$

$$\zeta_{ij} = a_{im}a_{jn}\zeta_{mn} \tag{37}$$

$$\xi_{ij} = a_{im}a_{jn}\xi_{mn} \tag{38}$$

$$\beta_{ij} = a_{im}a_{jn}\beta_{mn} \tag{39}$$

$$\lambda_{ij} = a_{im}a_{jn}\lambda_{mn} \tag{40}$$

So, all the properly transformed material constants given by transformations from (26) to (40) will be used in the following section. The following section provides both the differential and tensor form of the coupled equations of motion. The equations of motion must be resolved for construction of apt boundary conditions' determinants for determination of propagation velocity. To obtain the propagation velocity based on the thermodynamic principles developed in this section is the main purpose of this theoretical investigation.

Coupled equations of motion

One of the common work tools in the physical acoustics is the application of the quasi-static approximation because the speed of the electromagnetic wave or gravitational wave is approximately five orders larger than the speed of any acoustic wave. Indeed, the acoustic waves propagating in solids are extremely slow in comparison with the electromagnetic (or gravitational) wave propagating in the same material. However, propagation of the acoustic waves in suitable solid continua can be naturally coupled with the electrical (φ), magnetic (ψ), gravitational (Φ), and cogravitational (Ψ) potentials in the quasi-static approximation. Using the four field equations of his electromagnetic theory, Maxwell has creatively formulated the laws of electrostatics, magnetostatics, and electromagnetism. The electrostatic and magnetostatic equilibrium equations can be written using the differential forms of the corresponding Maxwell equations which can be written as follows: $\mathrm{div}\mathbf{D} = 0$ and $\mathrm{div}\mathbf{B} = 0$. The first equality with the electrical displacement vector **D** represents Gauss's law without free charge and currents and the second equality represents a divergence of the magnetic displacement vector **B**. Using the analogy (Heaviside, 1893; Maxwell, 1954; Assis, 1994; Assis, 1999; Jefimenko, 1992; Jefimenko, 2000; Jefimenko, 2006) between the electromagnetism and gravitoelectromagnetism, it is possible to write down the gravitostatic (gravitoelectrostatic) and cogravitostatic (gravitomagnetostatic) equilibrium equations for the studied case as follows: $\mathrm{div}\mathbf{GD} = 0$ and $\mathrm{div}\mathbf{GB} = 0$, where **GD** and **GB** are the gravitational (gravitoelectrical) and cogravitational (gravitomagnetic) displacement vectors, respectively.

Further exploitation of the analogy between the electromagnetism and gravitoelectromagnetism, the governing electrostatic, magnetostatic, gravitostatic, and cogravitostatic equilibrium equations can be respectively exposed in the following differential forms: $\partial D_i/\partial x_i = 0$, $\partial B_i/\partial x_i = 0$, $\partial GD_i/\partial x_i = 0$ and $\partial GB_i/\partial x_i = 0$. These equations represent the partial first derivatives of the electrical, magnetic, gravitational, and cogravitational displacement components (i.e. D_i, B_i,

GD_i, and GB_i, respectively) with respect to the real space components x_i, where the index i runs from 1 to 3. Besides, the governing mechanical equilibrium equation is also written as the following partial first derivative of the stress tensor components σ_{ij} with respect to the components x_j (i and j run from 1 to 3): $\partial\sigma_{ij}/\partial x_j = 0$.

In the theory of the wave motions of a solid material in dependence on time t, equations of motion can be described by the following common form (Dieulesaint and Royer, 1980; Auld, 1990; Zakharenko, 2010):

$$\frac{\partial\sigma_{ij}}{\partial x_j} = \rho\frac{\partial^2 U_i}{\partial t^2} \tag{41}$$

where ρ is the mass density of the bulk solid continuum. On the right-hand side in equation (41), the partial second derivatives of the mechanical displacement components U_i with respect to time t represent corresponding accelerations with the dimension of m/s^2.

In addition to equation of motion (41), it is necessary to account the electrostatics, magnetostatics, gravitostatics, and cogravitostatics in the quasi-static approximation:

$$\frac{\partial D_i}{\partial x_j} = 0\,,\ \frac{\partial B_i}{\partial x_j} = 0\,,\ \frac{\partial GD_i}{\partial x_j} = 0\,,\ \frac{\partial GB_i}{\partial x_j} = 0 \tag{42}$$

It is obvious that equations (41) and (42) represent the coupled equations of motion in the differential form. The coupled equations of motion can be readily rewritten in the corresponding expended forms when the mechanical displacements U_i, electrical potential φ, magnetic potential ψ, gravitational potential Φ, and cogravitational potential Ψ are exploited. These four potentials are defined in the context above equation (6). Utilizing these four potentials for equations from (1) to (5), equations (41) and (42) take the following expanded forms:

$$\begin{aligned}\rho\frac{\partial^2 U_i}{\partial t^2} &= C_{ijkl}\frac{\partial^2 U_l}{\partial x_j\partial x_k} + e_{kij}\frac{\partial^2\varphi}{\partial x_j\partial x_k}\\ &+ h_{kij}\frac{\partial^2\psi}{\partial x_j\partial x_k} + g_{kij}\frac{\partial^2\Phi}{\partial x_j\partial x_k} + f_{kij}\frac{\partial^2\Psi}{\partial x_j\partial x_k}\end{aligned} \tag{43}$$

$$\begin{aligned}0 &= e_{ijk}\frac{\partial^2 U_k}{\partial x_i\partial x_j} - \varepsilon_{ij}\frac{\partial^2\varphi}{\partial x_i\partial x_j}\\ &- \alpha_{ij}\frac{\partial^2\psi}{\partial x_i\partial x_j} - \zeta_{ij}\frac{\partial^2\Phi}{\partial x_i\partial x_j} - \xi_{ij}\frac{\partial^2\Psi}{\partial x_i\partial x_j}\end{aligned} \tag{44}$$

$$\begin{aligned}0 &= h_{ijk}\frac{\partial^2 U_k}{\partial x_i\partial x_j} - \alpha_{ij}\frac{\partial^2\varphi}{\partial x_i\partial x_j}\\ &- \mu_{ij}\frac{\partial^2\psi}{\partial x_i\partial x_j} - \beta_{ij}\frac{\partial^2\Phi}{\partial x_i\partial x_j} - \lambda_{ij}\frac{\partial^2\Psi}{\partial x_i\partial x_j}\end{aligned} \tag{45}$$

$$\begin{aligned}0 &= g_{ijk}\frac{\partial^2 U_k}{\partial x_i\partial x_j} - \zeta_{ij}\frac{\partial^2\varphi}{\partial x_i\partial x_j}\\ &- \beta_{ij}\frac{\partial^2\psi}{\partial x_i\partial x_j} - \gamma_{ij}\frac{\partial^2\Phi}{\partial x_i\partial x_j} - \vartheta_{ij}\frac{\partial^2\Psi}{\partial x_i\partial x_j}\end{aligned} \tag{46}$$

$$\begin{aligned}0 &= f_{ijk}\frac{\partial^2 U_k}{\partial x_i\partial x_j} - \xi_{ij}\frac{\partial^2\varphi}{\partial x_i\partial x_j}\\ &- \lambda_{ij}\frac{\partial^2\psi}{\partial x_i\partial x_j} - \vartheta_{ij}\frac{\partial^2\varphi}{\partial x_i\partial x_j} - \eta_{ij}\frac{\partial^2\psi}{\partial x_i\partial x_j}\end{aligned} \tag{47}$$

In equations from (43) to (47), the indexes i, j, k, and l run from 1 to 3. These five homogeneous equations represent partial differential equations of the second order. They are actually seven equations because equation (43) can be also written in the form of three equations corresponding to the mechanical displacement components U_1, U_2, and U_3. These coupled equations of motion constitute the wave propagation in a suitable solid continuum possessing the piezoelectric, piezomagnetic, piezoelectromagnetic, piezogravitic, piezocogravitic, gravitocogravitic effects and the other coeffects.

Next, it is convenient to further deal with the well known tensor form of the coupled equations of motion that can be obtained from the differential form written above. First of all, it is required to state that these homogeneous partial differential equations of the second order written above must have natural solutions in the plane wave forms (Dieulesaint and Royer, 1980; Auld, 1990; Zakharenko, 2010). Therefore, these solutions read:

$$U_I = U_I^0\exp\left[\mathrm{j}\left(k_1x_1 + k_2x_2 + k_3x_3 - \omega t\right)\right] \tag{48}$$

where the index I runs from 1 to 7.

In solutions (48) there is the following: $U_I = U_i$ for $I = i = 1, 2, 3$; $U_4 = \varphi$, $U_5 = \psi$, $U_6 = \Phi$ and $U_7 = \Psi$. Also, U_I^0, $\mathrm{j} = (-1)^{1/2}$, and ω stand for the initial amplitudes, imaginary unity, and angular frequency, respectively. The angular frequency ω is defined by the linear frequency ν: $\omega = 2\pi\nu$. The values of U_1^0, U_2^0, U_3^0, $U_4^0 = \varphi^0$, $U_5^0 = \psi^0$, $U_6^0 = \Phi^0$, and $U_7^0 = \Psi^0$ called the eigenvector components should be determined further. In (48), the parameters k_1, k_2, and k_3 represent the components of the wavevector **k** directed towards the wave propagation:

$(k_1, k_2, k_3) = k(n_1, n_2, n_3)$, where n_1, n_2, and n_3 are the directional cosines, namely $n_1 = 1$, $n_2 = 0$, and $n_3 \equiv n_3$. It is worth noting that the wavenumber k in the direction of wave propagation is coupled with the wavelength λ as follows: $k\lambda = 2\pi$.

It is transparent that the utilization of solutions (48) and the directional cosines for the differential form of the coupled equations from (43) to (47) can actually lead to coupled equations written in a tensor form. These homogeneous equations can be naturally written in the following compact form of the well-known Green-Christoffel equation (Zakharenko, 2010):

$$\left(GL_{IJ} - \delta_{IJ}\rho V_{ph}\right)U_I^0 = 0 \qquad (49)$$

where the indices I and J run from 1 to 7 and the phase velocity is defined by $V_{ph} = \omega/k$.

In equation (49), GL_{IJ} stands for the components of the modified tensor in the well-known Green-Christoffel equation (Zakharenko, 2010). δ_{IJ} represents the Kronecker delta-function with the following conditions: $\delta_{IJ} = 1$ for $I = J < 4$, $\delta_{IJ} = 0$ for $I \neq J$, and $\delta_{44} = \delta_{55} = \delta_{66} = \delta_{77} = 0$. It is also fundamental to state that the symmetric modified Green-Christoffel tensor GL_{IJ}, i.e. $GL_{IJ} = GL_{JI}$, can have only 28 independent tensor components. Compact form (49) represents the common problem for determination of the eigenvalues and eigenvectors. In this case, the suitable values of n_3 for the corresponding phase velocity represent the eigenvalues and a corresponding eigenvector $\left(U_1^0, U_2^0, U_3^0, U_4^0 = \varphi^0, U_5^0 = \psi^0, U_6^0 = \Phi^0, U_7^0 = \Psi^0\right)$ should exist for each of the suitable eigenvalues.

However, this report relates to the study of the SH-wave propagation and therefore, only suitable several equations must be used from common compact form (49) corresponding to fitting propagation directions. According to excellent books (Dieulesaint and Royer, 1980; Auld, 1990), it is possible to find high symmetry propagation directions in crystals relating to all classes of symmetry, but the lowest triclinic symmetry. In such propagation directions, tensor form (49) can consist of two independent sets of homogeneous equations due to the fact that some GL-tensor components can become equal to zero when acoustic waves propagate in certain directions on certain cuts. In some certain directions (Dieulesaint and Royer, 1980; Auld, 1990) of wave propagation, the in-plane polarized waves can be coupled with the four potentials (electrical φ, magnetic ψ, gravitational Φ, and cogravitational Ψ potentials) and the anti-plane polarized (SH) waves represent purely mechanical waves. Therefore, the corresponding eigenvectors are respectively written as follows: $\left(U_1^0, U_3^0, U_4^0, U_5^0, U_6^0, U_7^0\right)$ and $\left(U_2^0\right)$. In the other certain directions (Dieulesaint and Royer, 1980; Auld, 1990), the in-plane polarized waves represent purely mechanical waves and the anti-plane polarized (SH) waves can be coupled with the four potentials. This case corresponds to the following eigenvectors: $\left(U_1^0, U_3^0\right)$ and $\left(U_2^0, U_4^0, U_5^0, U_6^0, U_7^0\right)$.

This study has an interest in investigation of the pure SH-waves in the suitable high symmetry propagation directions in the transversely isotropic materials of class 6 *mm*. There are certain cuts and certain propagation directions in such materials (Dieulesaint and Royer, 1980; Auld, 1990; Gulyaev, 1998; Zakharenko, 2010) in which the propagation of the pure SH-waves can be coupled with the four potentials. Figure 2 shows the suitable propagation direction managed along the x_1-axis in the work coordinate system (x_1, x_2, x_3) in which the six fold symmetry axis is directed along the x_2-axis. The work coordinate system was obtained from the original crystallographic coordinate system (x'_1, x'_2, x'_3) in which the six fold symmetry axis is directed along the surface normal. In this case, the SH-wave has the mechanical displacement component U_2 directed along the x_2-axis. In the studied propagation direction, it is unnecessary to expand compact tensor form (49) because it actually decomposes into two independent parts and there is only an interest in the part corresponding to the pure SH-wave propagation.

Dealing only with the suitable GL-tensor components of compact tensor form (49) representing the coupled equations of motion, the SH-wave propagation coupled with the four potentials can be then expressed by the following five homogeneous equations:

$$\begin{pmatrix} GL_{22} - \rho V_{ph}^2 & GL_{24} & GL_{25} & GL_{26} & GL_{27} \\ GL_{42} & GL_{44} & GL_{45} & GL_{46} & GL_{47} \\ GL_{52} & GL_{54} & GL_{55} & GL_{56} & GL_{57} \\ GL_{62} & GL_{64} & GL_{65} & GL_{66} & GL_{67} \\ GL_{72} & GL_{74} & GL_{75} & GL_{76} & GL_{77} \end{pmatrix} \begin{pmatrix} U_2^0 \\ U_4^0 \\ U_5^0 \\ U_6^0 \\ U_7^0 \end{pmatrix} =$$

$$\begin{pmatrix} C\left[m - \left(V_{ph}/V_{t4}\right)^2\right] & em & hm & gm & fm \\ em & -\varepsilon m & -\alpha m & -\zeta m & -\xi m \\ hm & -\alpha m & -\mu m & -\beta m & -\lambda m \\ gm & -\zeta m & -\beta m & -\gamma m & -\vartheta m \\ fm & -\xi m & -\lambda m & -\vartheta m & -\eta m \end{pmatrix} \begin{pmatrix} U^0 \\ \varphi^0 \\ \psi^0 \\ \Phi^0 \\ \Psi^0 \end{pmatrix} = \begin{pmatrix} 0 \\ 0 \\ 0 \\ 0 \\ 0 \end{pmatrix} \qquad (50)$$

where $m = 1 + n_3^2$ and $\left(U^0, \varphi^0, \psi^0, \Phi^0, \Psi^0\right) = \left(U_2^0, U_4^0, U_5^0, U_6^0, U_7^0\right)$.

In equation (50), the independent material constants for the case are $C = C_{44} = C_{66}$, $e = e_{16} = e_{34}$, $h = h_{16} = h_{34}$, $g = g_{16} = g_{34}$, $f = f_{16} = f_{34}$, $\varepsilon = \varepsilon_{11} = \varepsilon_{33}$, $\mu = \mu_{11} = \mu_{33}$, $\alpha = \alpha_{11} = \alpha_{33}$, $\gamma = \gamma_{11} = \gamma_{33}$, $\eta = \eta_{11} = \eta_{33}$, $\vartheta = \vartheta_{11} = \vartheta_{33}$, $\zeta = \zeta_{11} = \zeta_{33}$, $\xi = \xi_{11} = \xi_{33}$, $\beta = \beta_{11} = \beta_{33}$, $\lambda = \lambda_{11} = \lambda_{33}$. The suitable eigenvalues $n_3 = k_3/k$ can be found when the determinant of the coefficient matrix in equations (50) equals to zero. Therefore, it is possible to write down this determinant of the coefficient matrix already in the following convenient form consisting of five cofactors:

$$\begin{vmatrix} C\left[m-\left(V_{ph}/V_{t4}\right)^2\right] & e & h & g & f \\ em & -\varepsilon & -\alpha & -\zeta & -\xi \\ hm & -\alpha & -\mu & -\beta & -\lambda \\ gm & -\zeta & -\beta & -\gamma & -\vartheta \\ fm & -\xi & -\lambda & -\vartheta & -\eta \end{vmatrix} \times m \times m \times m \times m = 0 \tag{51}$$

The first factor representing the determinant in equation (51) is quite complicated and the rest ones give the following four pairs of identical eigenvalues:

$$n_3^{(1,2)} = n_3^{(3,4)} = n_3^{(5,6)} = n_3^{(7,8)} = \pm \mathrm{j} \tag{52}$$

Expanding the determinant in equation (51) leads to the following fifth pair of the eigenvalues:

$$n_3^{(9,10)} = \pm \mathrm{j}\sqrt{1-\left(V_{ph}/V_{temgc}\right)^2} \tag{53}$$

where

$$V_{temgc} = \sqrt{C/\rho}\left(1+K_{emgc}^2\right)^{1/2} \tag{54}$$

$$K_{emgc}^2 = \frac{A_1}{A_2} \tag{55}$$

$$\begin{aligned} A_1 &= e^2\left(\mu\gamma\eta + 2\beta\lambda\vartheta - \lambda^2\gamma - \beta^2\eta - \vartheta^2\mu\right) \\ &+ h^2\left(\varepsilon\gamma\eta + 2\zeta\xi\vartheta - \vartheta^2\varepsilon - \zeta^2\eta - \xi^2\gamma\right) \\ &+ g^2\left(\varepsilon\mu\eta + 2\alpha\xi\lambda - \lambda^2\varepsilon - \alpha^2\eta - \xi^2\mu\right) \\ &+ f^2\left(\varepsilon\mu\gamma + 2\alpha\beta\zeta - \beta^2\varepsilon - \alpha^2\gamma - \zeta^2\mu\right) \\ &+ 2eh\left(\vartheta^2\alpha + \zeta\beta\eta + \xi\gamma\lambda - \alpha\gamma\eta - \zeta\lambda\vartheta - \xi\beta\vartheta\right) \\ &+ 2eg\left(\alpha\beta\eta + \lambda^2\zeta + \xi\vartheta\mu - \alpha\lambda\vartheta - \zeta\mu\eta - \xi\beta\lambda\right) \\ &+ 2ef\left(\alpha\gamma\lambda + \zeta\vartheta\mu + \beta^2\xi - \alpha\beta\vartheta - \zeta\beta\lambda - \xi\mu\gamma\right) \\ &+ 2hg\left(\varepsilon\lambda\vartheta + \zeta\alpha\eta + \xi^2\beta - \varepsilon\eta\beta - \zeta\lambda\xi - \xi\vartheta\alpha\right) \\ &+ 2hf\left(\varepsilon\beta\vartheta + \zeta^2\lambda + \xi\alpha\gamma - \varepsilon\lambda\gamma - \zeta\vartheta\alpha - \xi\zeta\beta\right) \\ &+ 2gf\left(\varepsilon\beta\lambda + \alpha^2\vartheta + \xi\mu\zeta - \varepsilon\mu\vartheta - \alpha\zeta\lambda - \alpha\beta\xi\right) \end{aligned} \tag{56}$$

$$\begin{aligned} A_2 &= C\left(\varepsilon\mu-\alpha^2\right)\left(\gamma\eta-\vartheta^2\right) \\ &+ C\left(\beta^2\xi^2 - \xi^2\mu\gamma - \beta^2\varepsilon\eta\right) + C\left(\lambda^2\zeta^2 - \lambda^2\varepsilon\gamma - \zeta^2\mu\eta\right) \\ &+ 2C\left(\gamma\alpha\xi\lambda + \eta\alpha\beta\zeta + \varepsilon\beta\lambda\vartheta + \mu\zeta\xi\vartheta - \zeta\xi\beta\lambda - \alpha\zeta\lambda\vartheta - \alpha\beta\xi\vartheta\right) \end{aligned} \tag{57}$$

Expressions (54) and (55) represent the definitions for the four-potential shear-horizontal bulk acoustic wave (4P-SH-BAW) and the coefficient of the electromagnetogravitocogravitomechanical coupling (CEMGCMC), respectively. This coefficient can be dramatically reduced for the case of $\zeta = 0$, $\xi = 0$, $\beta = 0$, $\lambda = 0$ when there is no direct exchange between the electrical (magnetic) subsystem and gravitational (cogravitational) subsystem. The reduced coefficient reads:

$$\begin{aligned} K_{emgc}^{*2} &= K_{em}^2 + K_{gc}^2 \\ &= \frac{\mu e^2 + \varepsilon h^2 - 2\alpha eh}{C\left(\varepsilon\mu-\alpha^2\right)} + \frac{\eta g^2 + \gamma f^2 - 2\vartheta gf}{C\left(\gamma\eta-\vartheta^2\right)} \end{aligned} \tag{58}$$

where

$$\begin{aligned} K_{em}^2 &= \frac{\mu e^2 + \varepsilon h^2 - 2\alpha eh}{C\left(\varepsilon\mu-\alpha^2\right)} \\ &= \frac{e\left(e\mu - h\alpha\right) - h\left(e\alpha - h\varepsilon\right)}{C\left(\varepsilon\mu-\alpha^2\right)} = \frac{eM_2 - hM_1}{CM_3} \end{aligned} \tag{59}$$

$$\begin{aligned} K_{gc}^2 &= \frac{\eta g^2 + \gamma f^2 - 2\vartheta gf}{C\left(\gamma\eta-\vartheta^2\right)} \\ &= \frac{g\left(g\eta - f\vartheta\right) - f\left(g\vartheta - f\gamma\right)}{C\left(\gamma\eta-\vartheta^2\right)} = \frac{gM_5 - fM_4}{CM_6} \end{aligned} \tag{60}$$

Definitions (59) and (60) stand for the coefficient of the magnetoelectromechanical coupling (CMEMC) and the coefficient of the gravitocogravitomechanical coupling (CGCMC), respectively. They depend on the following corresponding coupling mechanisms:

$$M_1 = e\alpha - h\varepsilon \tag{61}$$

$$M_2 = e\mu - h\alpha \tag{62}$$

$$M_3 = \varepsilon\mu - \alpha^2 \tag{63}$$

$$M_4 = g\vartheta - f\gamma \tag{64}$$

$$M_5 = g\eta - f\vartheta \tag{65}$$

$$M_6 = \gamma\eta - \vartheta^2 \tag{66}$$

The coupling mechanisms M_1, M_2, and M_3 are discussed in (Zakharenko, 2013c) and the others are introduced in this study. Using reduced coefficient (58), the reduced 4P-SH-BAW speed can be inscribed as follows:

$$V_{temgc}^{*}=\sqrt{C/\rho}\left(1+K_{emgc}^{*2}\right)^{1/2} \tag{67}$$

With known eigenvalues (52) and (53), it is now possible to find all the suitable eigenvectors. This is a quite complicated problem. Therefore, the appendix below lists all the suitable eigenvectors. The reader can find in the appendix that there are several suitable cases. Using the eigenvalues and the corresponding eigenvectors, it is possible to write down the complete parameters based on expression (48) and to exploit them in the apt boundary conditions. This is the purpose of the following section.

Boundary conditions leading to new SH-SAW

First of all, based on definition (48), it is indispensable to write down the explicit forms for the following complete parameters in the plane wave forms: the complete mechanical displacement $U_2^{\Sigma}=U^{\Sigma}$, complete electrical potential $U_4^{\Sigma}=\varphi^{\Sigma}$, complete magnetic potential $U_5^{\Sigma}=\psi^{\Sigma}$, complete gravitational potential $U_6^{\Sigma}=\Phi^{\Sigma}$, and complete cogravitational potential $U_7^{\Sigma}=\Psi^{\Sigma}$. These complete parameters are very important and used further to construct the determinants of the boundary conditions. These complete parameters can be naturally introduced in the following forms:

$$U_2^{\Sigma}=U^{\Sigma}=\sum_{s=1,3,5,7,9}F^{(s)}U_2^{0(s)}\exp\left[\mathrm{j}\left(k_1x_1+k_2x_2+k_3^{(s)}x_3-\omega t\right)\right]$$
$$=FU^{0(1)}\exp\left[\mathrm{j}k\left(x_1+n_3^{(1)}x_3-V_{ph}t\right)\right]+F_9U^{0(9)}\exp\left[\mathrm{j}k\left(x_1+n_3^{(9)}x_3-V_{ph}t\right)\right] \tag{68}$$

$$U_4^{\Sigma}=\varphi^{\Sigma}=\sum_{s=1,3,5,7,9}F^{(s)}U_4^{0(s)}\exp\left[\mathrm{j}\left(k_1x_1+k_2x_2+k_3^{(s)}x_3-\omega t\right)\right]$$
$$=F\varphi^{0(1)}\exp\left[\mathrm{j}k\left(x_1+n_3^{(1)}x_3-V_{ph}t\right)\right]+F_9\varphi^{0(9)}\exp\left[\mathrm{j}k\left(x_1+n_3^{(9)}x_3-V_{ph}t\right)\right] \tag{69}$$

$$U_5^{\Sigma}=\psi^{\Sigma}=\sum_{s=1,3,5,7,9}F^{(s)}U_5^{0(s)}\exp\left[\mathrm{j}\left(k_1x_1+k_2x_2+k_3^{(s)}x_3-\omega t\right)\right]$$
$$=F\psi^{0(1)}\exp\left[\mathrm{j}k\left(x_1+n_3^{(1)}x_3-V_{ph}t\right)\right]+F_9\psi^{0(9)}\exp\left[\mathrm{j}k\left(x_1+n_3^{(9)}x_3-V_{ph}t\right)\right] \tag{70}$$

$$U_6^{\Sigma}=\Phi^{\Sigma}=\sum_{s=1,3,5,7,9}F^{(s)}U_6^{0(s)}\exp\left[\mathrm{j}\left(k_1x_1+k_2x_2+k_3^{(s)}x_3-\omega t\right)\right]$$
$$=F\Phi^{0(1)}\exp\left[\mathrm{j}k\left(x_1+n_3^{(1)}x_3-V_{ph}t\right)\right]+F_9\Phi^{0(9)}\exp\left[\mathrm{j}k\left(x_1+n_3^{(9)}x_3-V_{ph}t\right)\right] \tag{71}$$

$$U_7^{\Sigma}=\Psi^{\Sigma}=\sum_{s=1,3,5,7,9}F^{(s)}U_7^{0(s)}\exp\left[\mathrm{j}\left(k_1x_1+k_2x_2+k_3^{(s)}x_3-\omega t\right)\right]$$
$$=F\Psi^{0(1)}\exp\left[\mathrm{j}k\left(x_1+n_3^{(1)}x_3-V_{ph}t\right)\right]+F_9\Psi^{0(9)}\exp\left[\mathrm{j}k\left(x_1+n_3^{(9)}x_3-V_{ph}t\right)\right] \tag{72}$$

where $F = F^{(1)} + F^{(3)} + F^{(5)} + F^{(7)}$ and $F_9 = F^{(9)}$.

It is clearly seen in the complete parameters written above that one deals here with a five-partial wave because each complete parameter must be formed by five terms due to the summation over the index s = 1, 3, 5, 7, 9. This summation corresponds to five suitable eigenvalues of ten defined by expressions (52) and (53). The suitable eigenvalues n_3 are those with a negative sign ($x_3 < 0$ in the solid shown in Figure 2. In order to have the wave damping towards the depth of the solid because this report has an interest in a study of surface wave propagation localized at the interface between two different continua, namely a vacuum and the solid. This is usual thing for investigation of surface wave propagation in solids (Dieulesaint and Royer, 1980; Auld, 1990; Zakharenko, 2010). So, for these five-partial waves there are the following five weight factors $F^{(1)}$, $F^{(3)}$, $F^{(5)}$, $F^{(7)}$, and $F^{(9)}$. The complete parameters depend on them. However, it is clearly seen in expression (52) that there are four identical eigenvalues n_3 and they will give the same eigenvectors. As a result, all the complete parameters can be written down in convenient and simplified forms with only two weight factors such as F and F_9 defined right away after expression (72). With F and F_9, it is possible to conclude that these five-partial waves can be introduced as some hidden two-partial waves. This fact can be used further for determination of the propagation velocity of the acoustic waves coupled with the four potentials: four-potential shear-horizontal surface acoustic wave or 4P-SH-SAW.

The boundary conditions used in this theoretical report relates to the interface between a vacuum and the solid. The mechanical boundary condition for the mechanical subsystem is the mechanically free surface of the solid, i.e. the normal component of the stress tensor σ_{32} must vanish at the interface between the solid surface and a vacuum: $\sigma_{32}(x_3 = 0) = 0$. Using expression (1), this condition reads:

$$\sigma_{32}=\sum_{s=1,3,5,7,9}F^{(s)}\left[Ck_3^{(s)}U^{0(s)}+ek_3^{(s)}\varphi^{0(s)}+hk_3^{(s)}\psi^{0(s)}+gk_3^{(s)}\Phi^{0(s)}+fk_3^{(s)}\Psi^{0(s)}\right]$$
$$=0$$

The electrical boundary condition for the electrical subsystem is that the electrical potential must vanish at x_3 = 0, i.e. $\varphi=\sum_{s=1,3,5,7,9}F^{(s)}\varphi^{0(s)}=0$ representing the electrically closed case (Al'shits *et al*., 1992). The magnetic boundary condition at x_3 = 0 for the magnetic subsystem is as follows: $\psi=\sum_{s=1,3,5,7,9}F^{(s)}\psi^{0(s)}=0$ representing the magnetically open case (Al'shits *et al*., 1992). Analogically, for the gravitational subsystem and the cogravitational subsystem it is possible to require that both the gravitational and cogravitational potentials must vanish at the interface x_3 = 0: $\Phi=\sum_{s=1,3,5,7,9}F^{(s)}\Phi^{0(s)}=0$

and $\Psi = \sum_{s=1,3,5,7,9} F^{(s)} \Psi^{0(s)} = 0$. It is thought that these boundary conditions are the most simple and more complicated boundary conditions will be not treated in this report.

Therefore, these five boundary conditions lead to five homogeneous equations written the following matrix form:

$$\begin{pmatrix} e\varphi^{0(1)} + h\psi^{0(1)} + g\Phi^{0(1)} + f\Psi^{0(1)} & e\varphi^{0(3)} + h\psi^{0(3)} + g\Phi^{0(3)} + f\Psi^{0(3)} & e\varphi^{0(5)} + h\psi^{0(5)} + g\Phi^{0(5)} + f\Psi^{0(5)} & e\varphi^{0(7)} + h\psi^{0(7)} + g\Phi^{0(7)} + f\Psi^{0(7)} & b(CU^{0(9)} + e\varphi^{0(9)} + h\psi^{0(9)} + g\Phi^{0(9)} + f\Psi^{0(9)}) \\ \varphi^{0(1)} & \varphi^{0(3)} & \varphi^{0(5)} & \varphi^{0(7)} & \varphi^{0(9)} \\ \psi^{0(1)} & \psi^{0(3)} & \psi^{0(5)} & \psi^{0(7)} & \psi^{0(9)} \\ \Phi^{0(1)} & \Phi^{0(3)} & \Phi^{0(5)} & \Phi^{0(7)} & \Phi^{0(9)} \\ \Psi^{0(1)} & \Psi^{0(3)} & \Psi^{0(5)} & \Psi^{0(7)} & \Psi^{0(9)} \end{pmatrix} \times \begin{pmatrix} F^{(1)} \\ F^{(3)} \\ F^{(5)} \\ F^{(7)} \\ F^{(9)} \end{pmatrix} = \begin{pmatrix} 0 \\ 0 \\ 0 \\ 0 \\ 0 \end{pmatrix} \tag{73}$$

where $b = \sqrt{1 - \left(V_{ph} / V_{temgc}\right)^2}$.

It is well-known that a set of homogeneous equations has a solution when the determinant of the coefficient matrix is equal to zero. The experienced reader can find that the determinant of the coefficient matrix in expression (73) is always equal to zero because the first, second, third, and fourth columns of the determinant are identical due to four identical eigenvalues (52). It is obvious that the identical eigenvalues give identical eigenvector components that can be found in the appendix, for instance, see in definitions (A18) and (A19) or (A30) and (A31), or the others. Indeed, it is well-known fact that a matrix determinant is equal to zero when there are two (several) identical columns or two (several) identical rows. This is also true when a column represents a linear combination of two (several) columns and or a row represents a linear combination of two (several) rows. However, this fact that there are identical columns in expression (73) does not determine the propagation velocity because all the eigenvector components do not depend on the propagation velocity, i.e. the phase velocity V_{ph} that must be found. The main peculiarity of the studied case is that only the factor b defined right away after equation (73) depends on the V_{ph}. The factor b is only present in the first row and the last column of the matrix determinant. For the sound determination of the propagation velocity, one has to treat the rows instead of the columns of the matrix determinant in (73). It is blatant that the first row actually represents a linear combination of all the rest rows. Indeed, the reader can successively subtract the second, third, fourth, and fifth rows with the factors of *e*, *h*, *g*, and *f*, respectively, from the first row and the certain value for the propagation velocity can be soundly obtained.

For this purpose, it is convenient to deal with an equivalent set of two instead of five homogeneous equations. With the five homogeneous equations written in matrix form (73) and the weight factors F and F_9 defined after expression (72), it is possible to introduce the following equivalent set of two homogeneous equations for the determination of the propagation velocity:

$$\begin{pmatrix} e\varphi^{0(1)} + h\psi^{0(1)} + g\Phi^{0(1)} + f\Psi^{0(1)} & b\left(CU^{0(9)} + e\varphi^{0(9)} + h\psi^{0(9)} + g\Phi^{0(9)} + f\Psi^{0(9)}\right) \\ e\varphi^{0(1)} + h\psi^{0(1)} + g\Phi^{0(1)} + f\Psi^{0(1)} & e\varphi^{0(9)} + h\psi^{0(9)} + g\Phi^{0(9)} + f\Psi^{0(9)} \end{pmatrix} \times \begin{pmatrix} F \\ F_9 \end{pmatrix} = \begin{pmatrix} 0 \\ 0 \end{pmatrix} \tag{74}$$

It is clearly seen in reduced set (74) that the first row in reduced set (74) represents the first row on complete set (73) and the second row in set (74) represents a linear combination of the rest rows in set (73). It is obvious that in reduced set (74), it is unnecessary to use the second, third, and fourth columns from complete set (73) because they are identical to the first column. This is the usual procedure to reduce a complicated set of equations by replacing it with a more simplified but equivalent set of equations. This can be convenient when more complicated case can be treated in the future. Exploiting reduced set (74), the propagation velocity can be determined from the following common form:

$$b = \sqrt{1 - \left(V_{ph} / V_{temgc}\right)^2} = \frac{e\varphi^{0(9)} + h\psi^{0(9)} + g\Phi^{0(9)} + f\Psi^{0(9)}}{CU^{0(9)} + e\varphi^{0(9)} + h\psi^{0(9)} + g\Phi^{0(9)} + f\Psi^{0(9)}} \tag{75}$$

All the eigenvector components such as $U^{0(9)}$, $\varphi^{0(9)}$, $\psi^{0(9)}$, $\Phi^{0(9)}$, and $\Psi^{0(9)}$ can be found in the appendix that offers six different cases, each of which contains two pairs of different eigenvectors. Also, the weight factors F and F_9 can be determined from the first equation in set (74). They can be exposed as follows:

$$F = -b\left(CU^{0(9)} + e\varphi^{0(9)} + h\psi^{0(9)} + g\Phi^{0(9)} + f\Psi^{0(9)}\right) \tag{76}$$

$$F_9 = e\varphi^{0(1)} + h\psi^{0(1)} + g\Phi^{0(1)} + f\Psi^{0(1)} \tag{77}$$

Expression (75) can be also obtained from complete set (73) by a successive subtraction of the second, third, fourth, and fifth rows with the factors of *e*, *h*, *g*, and *f*, respectively, from the first row. This was already mentioned in the context above expression (74). The reader can check that the utilization of any of possible eigenvectors given in the appendix by formulae (A19) and (A31) soundly leads to the following propagation velocity of the new 4P-SH-SAW:

$$V_{newSAW} = V_{temgc}\left[1-\left(\frac{K^2_{emgc}}{1+K^2_{emgc}}\right)^2\right]^{1/2} \tag{78}$$

where the 4P-SH-BAW velocity V_{temgc} and the coefficient of the electromagnetogravitocogravito mechanical coupling (CEMGCMC) K^2_{emgc} are respectively defined by formulae (54) and (55).

Also, the CEMGCMC K^2_{emgc} can be dramatically reduced for the case of $\zeta = 0$, $\xi = 0$, $\beta = 0$, $\lambda = 0$. This is the case of no direct exchange between the electrical (magnetic) subsystem and gravitational (cogravitational) subsystem. For this case, the reduced CEMGCMC K^{*2}_{emgc} defined by (58) must be used along with the other 4P-SH-BAW velocity V^*_{temgc} defined by formula (67). Therefore, the value of the new 4P-SH-SAW velocity can be calculated with the following formula:

$$\begin{aligned} V^*_{newSAW} &= V^*_{temgc}\left[1-\left(\frac{K^{*2}_{emgc}}{1+K^{*2}_{emgc}}\right)^2\right]^{1/2} \\ &= V^*_{temgc}\left[1-\left(\frac{K^2_{em}+K^2_{gc}}{1+K^2_{em}+K^2_{gc}}\right)^2\right]^{1/2} \end{aligned} \tag{79}$$

where the coefficient of the magnetoelectromechanical coupling (CMEMC) K^2_{em} and the coefficient of the gravitocogravito mechanical coupling (CGCMC) K^2_{gc} are respectively defined by (59) and (60).

It is also necessary to discuss the case when the gravitational and cogravitational effects can be neglected, i.e. the material parameters $g = 0$ and $f = 0$ resulting in $K^2_{gc} = 0$. For this case, reduced velocity (84) further reduces to the velocity V_{BGM} of the surface Bleustein-Gulyaev-Melkumyan (BGM) wave (Melkumyan, 2007; Zakharenko, 2010, 2013a) discovered by Melkumyan (2007). This velocity reads:

$$V_{BGM} = V_{tem}\left[1-\left(\frac{K^2_{em}}{1+K^2_{em}}\right)^2\right]^{1/2} \tag{80}$$

where $V_{tem} = \sqrt{C/\rho}\left(1+K^2_{em}\right)^{1/2}$ stands for the SH-BAW velocity coupled with both the electrical and magnetic potentials.

The surface BGM wave can propagate in the piezoelectromagnetic smart materials, in which more than ten SH-SAWs were recently discovered pertaining to different boundary conditions. This report has no purpose to treat the other boundary conditions different from those used in this section. Indeed, the four-potential wave propagation is significantly more complicated case compared with the wave propagation in piezoelectromagnetic materials. Also, one can find in formula (80) that a substitution of K^2_{gc} instead of K^2_{em} can result in the existence of new piezogravitoco gravitational wave because neither Bleustein nor Gulyaev, nor Melkumyan has studied the gravitational effects. However, none has reported that such wave can be recorded at the current level of experimental development. Maybe this is a problem for this (next) century.

The connection between the surface BGM wave and the well-known surface Bleustein-Gulyaev (BG) wave can be also discussed. Indeed, $h = 0$ results in $K^2_{em} \to K^2_e = e^2/C\varepsilon$ and $V_{tem} \to V_{te} = \sqrt{C/\rho}\left(1+K^2_e\right)^{1/2}$ in formula (80). The coefficient of the electromechanical coupling K^2_e and the velocity V_{te} of the SH-BAW coupled with the electrical potential φ are the characteristics for a pure piezoelectrics. On the other hand, $e = 0$ results in $K^2_{em} \to K^2_m = h^2/C\mu$ and $V_{tem} \to V_{tm} = \sqrt{C/\rho}\left(1+K^2_m\right)^{1/2}$ in formula (80). This is the case of the wave propagation in a pure piezomagnetics characterized by the coefficient of the magneto mechanical coupling K^2_m and the velocity V_{tm} of the SH-BAW coupled with the magnetic potential ψ. Therefore, the velocity of the surface BG-wave propagating in a pure piezoelectrics or pure piezomagnetics can be calculated with the following well-known formulae (Bleustein, 1968; Gulyaev, 1969):

$$V_{BG} = V_{te}\left[1-\left(\frac{K^2_e}{1+K^2_e}\right)^2\right]^{1/2} \tag{81}$$

$$V_{BG} = V_{tm}\left[1-\left(\frac{K^2_m}{1+K^2_m}\right)^2\right]^{1/2} \tag{82}$$

For the case when some suitable materials can possess the mechanical, magnetic, and gravitational subsystems, formula (80) must be replaced by formula (83) written below. This can be the case analogical to the experimentally realized one by Professor André Füzfa (2016) when the magnetic and gravitational forces can interact, i.e. the gravitational field can be controlled by the magnetic field. If the magnetic subsystem can interact with the cogravitational subsystem, the final expression for the new propagation velocity is given by formula (84) written below.

$$V_{1new} = V_{tmg}\left[1-\left(\frac{K_{mg}^2}{1+K_{mg}^2}\right)^2\right]^{1/2} \tag{83}$$

$$V_{2new} = V_{tmc}\left[1-\left(\frac{K_{mc}^2}{1+K_{mc}^2}\right)^2\right]^{1/2} \tag{84}$$

where $V_{tmg} = \sqrt{C/\rho}\left(1+K_{mg}^2\right)^{1/2}$ stands for the velocity of the SH-BAW coupled with both the magnetic and gravitational potentials and $V_{tmc} = \sqrt{C/\rho}\left(1+K_{mc}^2\right)^{1/2}$ stands for the velocity of the SH-BAW coupled with both the magnetic and cogravitational potentials.

In formula (83), the introduced material parameter K_{mg}^2 can be called the coefficient of magnetogravito mechanical coupling (CMGMC). In expression (84), the introduced material parameter K_{mc}^2 can be analogically called the coefficient of magnetocogravito mechanical coupling (CMCMC). They are respectively defined by

$$\begin{aligned} K_{mg}^2 &= \frac{\mu g^2+\gamma h^2-2\beta hg}{C\left(\mu\gamma-\beta^2\right)} \\ &= \frac{g\left(g\mu-h\beta\right)-h\left(g\beta-h\gamma\right)}{C\left(\mu\gamma-\beta^2\right)} = \frac{gM_8-hM_7}{CM_9} \end{aligned} \tag{85}$$

$$\begin{aligned} K_{gc}^2 &= \frac{\mu f^2+\eta h^2-2\lambda hf}{C\left(\mu\eta-\lambda^2\right)} \\ &= \frac{f\left(f\mu-h\lambda\right)-h\left(f\lambda-h\eta\right)}{C\left(\mu\eta-\lambda^2\right)} = \frac{fM_{11}-hM_{10}}{CM_{12}} \end{aligned} \tag{86}$$

In definitions (85) and (86), the following corresponding mechanisms of coupling are introduced:

$$M_7 = g\beta - h\gamma \tag{87}$$

$$M_8 = g\mu - h\beta \tag{88}$$

$$M_9 = \mu\gamma - \beta^2 \tag{89}$$

$$M_{10} = f\lambda - h\eta \tag{90}$$

$$M_{11} = f\mu - h\lambda \tag{91}$$

$$M_{12} = \mu\eta - \lambda^2 \tag{92}$$

CONCLUSION

This theoretical report has predicted the existence of the new four-potential shear-horizontal surface acoustic wave (4P-SH-SAW) propagation in suitable solids when the wave motion is coupled with the following four potentials: the electrical potential φ, magnetic potential ψ, gravitational potential Φ, and cogravitational potential Ψ. The velocity of the new 4P-SH-SAW was obtained in an explicit form. The obtained theoretical results can be used for further development of some problems of gravitation, the problem of 4P-SH-wave propagation in plates, and constitution of smart technical devices. This can usher gravitation into a new experimental and industrial era.

ACKNOWLEDGEMENTS

The author is thankful to the referees for their valuable comments and suggestions to improve the quality of the paper for the Journal reader. The author is also thankful to the participants (Professor Dr. A.F. Sadreev, Professor Dr. V.I. Zinenko, Professor Dr. S.I. Burkov and Dr. P.P. Turchin) of the workshop on the 8th of April, 2015 at the SB RAS L.V. Kirensky Institute of Physics, Krasnoyarsk, Siberia, Russia, for some useful notes and fruitful discussion.

Appendix I.

To find all the suitable eigenvectors corresponding to found eigenvalues (52) and (53), it is necessary to treat equations' set (50) anew. It is natural to utilize the first equation in set (50) for determination of the first eigenvector component U^0 as a function of the rest components φ^0, ψ^0, Φ^0, and Ψ^0. So, this dependence reads:

$$U^0 = -m\left(e\varphi^0 + h\psi^0 + g\Phi^0 + f\Psi^0\right)/CA \tag{A1}$$

where $m = 1+n_3^2$ and

$$\begin{cases} A = m-\left(V_{ph}/V_{t4}\right)^2 = -\left(V_{ph}/V_{t4}\right)^2 \text{ for eigenvalue (52)} \\ A = m-\left(V_{ph}/V_{t4}\right)^2 = -mK_{emgc}^2 \text{ for eigenvalue (53)} \end{cases} \tag{A2}$$

Utilization of definition (A1) for equations' set (50) allows one to exclude the eigenvector component U^0 from the further consideration and to deal with a reduced set of equations. This is the usual mathematical procedure for

finding of the unknowns for the set of five equations in five unknowns. It is also useful to state that formulae (A2) are also applicable for the problem of finding of suitable eigenvectors when the wave propagation in piezoelectromagnetics (Zakharenko, 2010; Zakharenko, 2013a,b; Zakharenko, 2015a,b) (i.e. $K_{emgc}^2 \to K_{em}^2$) is investigated.

I.A1. The first order of equations

So, the new set of four homogeneous equations can be written as follows:

$$\begin{cases} \varepsilon\left(1+mK_e^2/A\right)\varphi^0+\alpha\left(1+mK_\alpha^2/A\right)\psi^0 \\ +\zeta\left(1+mK_\zeta^2/A\right)\Phi^0+\xi\left(1+mK_\xi^2/A\right)\Psi^0=0 \\ \alpha\left(1+mK_\alpha^2/A\right)\varphi^0+\mu\left(1+mK_m^2/A\right)\psi^0 \\ +\beta\left(1+mK_\beta^2/A\right)\Phi^0+\lambda\left(1+mK_\lambda^2/A\right)\Psi^0=0 \\ \zeta\left(1+mK_\zeta^2/A\right)\varphi^0+\beta\left(1+mK_\beta^2/A\right)\psi^0 \\ +\gamma\left(1+mK_g^2/A\right)\Phi^0+\vartheta\left(1+mK_\vartheta^2/A\right)\Psi^0=0 \\ \xi\left(1+mK_\xi^2/A\right)\varphi^0+\lambda\left(1+mK_\lambda^2/A\right)\psi^0 \\ +\vartheta\left(1+mK_\vartheta^2/A\right)\Phi^0+\eta\left(1+mK_f^2/A\right)\Psi^0=0 \end{cases} \quad \text{(A3)}$$

where

$$K_e^2=e^2/C\varepsilon \quad \text{(A4)}$$

$$K_\alpha^2=eh/C\alpha \quad \text{(A5)}$$

$$K_\zeta^2=eg/C\zeta \quad \text{(A6)}$$

$$K_\xi^2=ef/C\xi \quad \text{(A7)}$$

$$K_m^2=h^2/C\mu \quad \text{(A8)}$$

$$K_\beta^2=hg/C\beta \quad \text{(A9)}$$

$$K_\lambda^2=hf/C\lambda \quad \text{(A10)}$$

$$K_g^2=g^2/C\gamma \quad \text{(A11)}$$

$$K_\vartheta^2=gf/C\vartheta \quad \text{(A12)}$$

$$K_f^2=f^2/C\eta \quad \text{(A13)}$$

Next, from the first equation in set (A3) it is possible to determine the second eigenvector component φ^0 as a function of the components ψ^0, Φ^0, and Ψ^0. It can be composed as follows:

$$\varphi^0=-\frac{\alpha\left(A+mK_\alpha^2\right)}{\varepsilon\left(A+mK_e^2\right)}\psi^0-\frac{\zeta\left(A+mK_\zeta^2\right)}{\varepsilon\left(A+mK_e^2\right)}\Phi^0-\frac{\xi\left(A+mK_\xi^2\right)}{\varepsilon\left(A+mK_e^2\right)}\Psi^0 \quad \text{(A14)}$$

Definition (A14) for φ^0 can be then utilized in set (A3) to reduce the set of four homogeneous equations in four undetermined. Indeed, it is natural to use definition (A14) for the second, third, and fourth equations in set (A3). As a result, the new reduced set of three homogeneous equations with three unknown components ψ^0, Φ^0, and Ψ^0 read:

$$\begin{cases} \left(\frac{\mu\left(A+mK_m^2\right)}{A}-\frac{\alpha^2\left(A+mK_\alpha^2\right)^2}{A\varepsilon\left(A+mK_e^2\right)}\right)\psi^0 \\ +\left(\frac{\beta\left(A+mK_\beta^2\right)}{A}-\frac{\alpha\zeta\left(A+mK_\alpha^2\right)\left(A+mK_\zeta^2\right)}{A\varepsilon\left(A+mK_e^2\right)}\right)\Phi^0 \\ +\left(\frac{\lambda\left(A+mK_\lambda^2\right)}{A}-\frac{\alpha\xi\left(A+mK_\alpha^2\right)\left(A+mK_\xi^2\right)}{A\varepsilon\left(A+mK_e^2\right)}\right)\Psi^0=0 \\ \left(\frac{\beta\left(A+mK_\beta^2\right)}{A}-\frac{\alpha\zeta\left(A+mK_\alpha^2\right)\left(A+mK_\zeta^2\right)}{A\varepsilon\left(A+mK_e^2\right)}\right)\psi^0 \\ +\left(\frac{\gamma\left(A+mK_g^2\right)}{A}-\frac{\zeta^2\left(A+mK_\zeta^2\right)^2}{A\varepsilon\left(A+mK_e^2\right)}\right)\Phi^0 \\ +\left(\frac{\vartheta\left(A+mK_\vartheta^2\right)}{A}-\frac{\xi\zeta\left(A+mK_\xi^2\right)\left(A+mK_\zeta^2\right)}{A\varepsilon\left(A+mK_e^2\right)}\right)\Psi^0=0 \\ \left(\frac{\lambda\left(A+mK_\lambda^2\right)}{A}-\frac{\alpha\xi\left(A+mK_\alpha^2\right)\left(A+mK_\xi^2\right)}{A\varepsilon\left(A+mK_e^2\right)}\right)\psi^0 \\ +\left(\frac{\vartheta\left(A+mK_\vartheta^2\right)}{A}-\frac{\xi\zeta\left(A+mK_\xi^2\right)\left(A+mK_\zeta^2\right)}{A\varepsilon\left(A+mK_e^2\right)}\right)\Phi^0 \\ +\left(\frac{\eta\left(A+mK_f^2\right)}{A}-\frac{\xi^2\left(A+mK_\xi^2\right)^2}{A\varepsilon\left(A+mK_e^2\right)}\right)\Psi^0=0 \end{cases} \quad \text{(A15)}$$

Exploiting the first equation in set (A15), the third eigenvector component ψ^0 represents the following function of the eigenvector components Φ^0 and Ψ^0:

$$\psi^0=-\frac{\beta\left(A+mK_\beta^2\right)-\frac{\alpha\zeta\left(A+mK_\alpha^2\right)\left(A+mK_\zeta^2\right)}{\varepsilon\left(A+mK_e^2\right)}}{\mu\left(A+mK_m^2\right)-\frac{\alpha^2\left(A+mK_\alpha^2\right)^2}{\varepsilon\left(A+mK_e^2\right)}}\Phi^0 \quad \text{(A16)}$$
$$-\frac{\lambda\left(A+mK_\lambda^2\right)-\frac{\alpha\xi\left(A+mK_\alpha^2\right)\left(A+mK_\xi^2\right)}{\varepsilon\left(A+mK_e^2\right)}}{\mu\left(A+mK_m^2\right)-\frac{\alpha^2\left(A+mK_\alpha^2\right)^2}{\varepsilon\left(A+mK_e^2\right)}}\Psi^0$$

Finally, function $\psi^0(\Phi^0, \Psi^0)$ (A16) must be used for substitution in the second and third equations in set (A15). This substitution results in the final two homogeneous equations in two unknowns Φ^0 and Ψ^0 that already can be readily used for definition of both Φ^0 and Ψ^0. These two complicated equations can be composed in the following forms:

$$
\begin{cases}
0=\left(\dfrac{\gamma\left(A+mK_g^2\right)}{A}-\dfrac{\zeta^2\left(A+mK_\zeta^2\right)^2}{A\varepsilon\left(A+mK_e^2\right)}-\dfrac{\left(\dfrac{\beta\left(A+mK_\beta^2\right)}{A}-\dfrac{\alpha\zeta\left(A+mK_\alpha^2\right)\left(A+mK_\zeta^2\right)}{A\varepsilon\left(A+mK_e^2\right)}\right)^2}{\dfrac{\mu\left(A+mK_m^2\right)}{A}-\dfrac{\alpha^2\left(A+mK_\alpha^2\right)^2}{A\varepsilon\left(A+mK_e^2\right)}}\right)\Phi^0 \\
+\left(\dfrac{\vartheta\left(A+mK_\vartheta^2\right)}{A}-\dfrac{\xi\zeta\left(A+mK_\xi^2\right)\left(A+mK_\zeta^2\right)}{A\varepsilon\left(A+mK_e^2\right)}\right)\Psi^0 \\
-\dfrac{\left(\dfrac{\beta\left(A+mK_\beta^2\right)}{A}-\dfrac{\alpha\zeta\left(A+mK_\alpha^2\right)\left(A+mK_\zeta^2\right)}{A\varepsilon\left(A+mK_e^2\right)}\right)\left(\lambda\left(A+mK_\lambda^2\right)-\dfrac{\alpha\xi\left(A+mK_\alpha^2\right)\left(A+mK_\xi^2\right)}{\varepsilon\left(A+mK_e^2\right)}\right)}{\mu\left(A+mK_m^2\right)-\dfrac{\alpha^2\left(A+mK_\alpha^2\right)^2}{\varepsilon\left(A+mK_e^2\right)}}\Psi^0 \\
0=\left(\dfrac{\vartheta\left(A+mK_\vartheta^2\right)}{A}-\dfrac{\xi\zeta\left(A+mK_\xi^2\right)\left(A+mK_\zeta^2\right)}{A\varepsilon\left(A+mK_e^2\right)}\right)\Phi^0 \\
-\dfrac{\left(\dfrac{\beta\left(A+mK_\beta^2\right)}{A}-\dfrac{\alpha\zeta\left(A+mK_\alpha^2\right)\left(A+mK_\zeta^2\right)}{A\varepsilon\left(A+mK_e^2\right)}\right)\left(\lambda\left(A+mK_\lambda^2\right)-\dfrac{\alpha\xi\left(A+mK_\alpha^2\right)\left(A+mK_\xi^2\right)}{\varepsilon\left(A+mK_e^2\right)}\right)}{\mu\left(A+mK_m^2\right)-\dfrac{\alpha^2\left(A+mK_\alpha^2\right)^2}{\varepsilon\left(A+mK_e^2\right)}}\Phi^0 \\
+\left(\dfrac{\eta\left(A+mK_f^2\right)}{A}-\dfrac{\xi^2\left(A+mK_\xi^2\right)^2}{A\varepsilon\left(A+mK_e^2\right)}-\dfrac{\left(\dfrac{\lambda\left(A+mK_\lambda^2\right)}{A}-\dfrac{\alpha\xi\left(A+mK_\alpha^2\right)\left(A+mK_\xi^2\right)}{A\varepsilon\left(A+mK_e^2\right)}\right)^2}{\dfrac{\mu\left(A+mK_m^2\right)}{A}-\dfrac{\alpha^2\left(A+mK_\alpha^2\right)^2}{A\varepsilon\left(A+mK_e^2\right)}}\right)\Psi^0
\end{cases}
\tag{A17}
$$

Equations' set (A17) represents a set of two homogeneous equations in two unknowns Φ^0 and Ψ^0. This pair of equations can be schematically written as follows: $a_1x + by = 0$ and $bx + a_2y = 0$. Therefore, the unknowns x and y can be chosen in two different ways: (1) $x = -b$ and $y = a_1$; (2) $x = a_2$ and $y = -b$. Taking into account this fact it is natural to write down below two different sets (i1) and (ii1) of the eigenvector components for the case of equations (A3).

(i1) The first eigenvectors for case (A3)

The first eigenvectors can be composed with the first equation in set (A17) and definitions (A1), (A14), and (A16). For eigenvalues (52), $m = 0$ and therefore, the corresponding eigenvector components are relatively simple. So, these eigenvector components are

$$
\begin{pmatrix} U^{0(1)} \\ \varphi^{0(1)} \\ \psi^{0(1)} \\ \Phi^{0(1)} \\ \Psi^{0(1)} \end{pmatrix}
=\begin{pmatrix} U^{0(3)} \\ \varphi^{0(3)} \\ \psi^{0(3)} \\ \Phi^{0(3)} \\ \Psi^{0(3)} \end{pmatrix}
=\begin{pmatrix} U^{0(5)} \\ \varphi^{0(5)} \\ \psi^{0(5)} \\ \Phi^{0(5)} \\ \Psi^{0(5)} \end{pmatrix}
=\begin{pmatrix} U^{0(7)} \\ \varphi^{0(7)} \\ \psi^{0(7)} \\ \Phi^{0(7)} \\ \Psi^{0(7)} \end{pmatrix}
$$

$$
=\begin{pmatrix}
U^0=0 \\
\varphi^0=-\dfrac{\alpha}{\varepsilon}\psi^0-\dfrac{\zeta}{\varepsilon}\Phi^0-\dfrac{\xi}{\varepsilon}\Psi^0 \\
\psi^0=-\dfrac{\beta-\dfrac{\alpha\zeta}{\varepsilon}}{\mu-\dfrac{\alpha^2}{\varepsilon}}\Phi^0-\dfrac{\lambda-\dfrac{\alpha\xi}{\varepsilon}}{\mu-\dfrac{\alpha^2}{\varepsilon}}\Psi^0 \\
\Phi^0=\vartheta-\dfrac{\xi\zeta}{\varepsilon}-\dfrac{\left(\beta-\dfrac{\alpha\zeta}{\varepsilon}\right)\left(\lambda-\dfrac{\alpha\xi}{\varepsilon}\right)}{\mu-\dfrac{\alpha^2}{\varepsilon}} \\
\Psi^0=-\gamma+\dfrac{\zeta^2}{\varepsilon}+\dfrac{\left(\beta-\dfrac{\alpha\zeta}{\varepsilon}\right)^2}{\mu-\dfrac{\alpha^2}{\varepsilon}}
\end{pmatrix}
\tag{A18}
$$

However, for eigen value (53) there is a more complicated eigenvector. For this case, the parameter A defined by expression (A2) does not depend on the propagation velocity. Therefore, the utilization of the corresponding parameter A (A2), the first equation in set (A17), and definitions (A1), (A14), (A16) leads to the following complicated eigenvector components:

$$
\begin{pmatrix} U^{0(9)} \\ \varphi^{0(9)} \\ \psi^{0(9)} \\ \Phi^{0(9)} \\ \Psi^{0(9)} \end{pmatrix}
=\begin{pmatrix}
U^0=\left(e\varphi^0+h\psi^0+g\Phi^0+f\Psi^0\right)\Big/CK_{emgc}^2 \\
\varphi^0=-\dfrac{\alpha K_A}{\varepsilon K_E}\psi^0-\dfrac{\zeta K_Z}{\varepsilon K_E}\Phi^0-\dfrac{\xi K_S}{\varepsilon K_E}\Psi^0 \\
\psi^0=-\dfrac{\beta K_B-\dfrac{\alpha\zeta K_A K_Z}{\varepsilon K_E}}{\mu K_M-\dfrac{\alpha^2 K_A{}^2}{\varepsilon K_E}}\Phi^0-\dfrac{\lambda K_L-\dfrac{\alpha\xi K_A K_S}{\varepsilon K_E}}{\mu K_M-\dfrac{\alpha^2 K_A{}^2}{\varepsilon K_E}}\Psi^0 \\
\Phi^0=\dfrac{\vartheta K_T}{K_{emgc}^2}-\dfrac{\xi\zeta K_S K_Z}{\varepsilon K_E K_{emgc}^2} \\
-\dfrac{\left(\dfrac{\beta K_B}{K_{emgc}^2}-\dfrac{\alpha\zeta K_A K_Z}{\varepsilon K_E K_{emgc}^2}\right)\left(\lambda K_L-\dfrac{\alpha\xi K_A K_S}{\varepsilon K_E}\right)}{\mu K_M-\dfrac{\alpha^2 K_A{}^2}{\varepsilon K_E}} \\
\Psi^0=-\dfrac{\gamma K_G}{K_{emgc}^2}+\dfrac{\zeta^2 K_Z{}^2}{\varepsilon K_E K_{emgc}^2}+\dfrac{\left(\dfrac{\beta K_B}{K_{emgc}^2}-\dfrac{\alpha\zeta K_A K_Z}{\varepsilon K_E K_{emgc}^2}\right)^2}{\dfrac{\mu K_M}{K_{emgc}^2}-\dfrac{\alpha^2 K_A{}^2}{\varepsilon K_E K_{emgc}^2}}
\end{pmatrix}
\tag{A19}
$$

where

$$K_E = K_{emgc}^2 - K_e^2 \tag{A20}$$

$$K_M = K_{emgc}^2 - K_m^2 \tag{A21}$$

$$K_G = K_{emgc}^2 - K_g^2 \tag{A22}$$

$$K_F = K_{emgc}^2 - K_f^2 \tag{A23}$$

$$K_A = K_{emgc}^2 - K_\alpha^2 \tag{A24}$$

$$K_T = K_{emgc}^2 - K_\vartheta^2 \tag{A25}$$

$$K_B = K_{emgc}^2 - K_\beta^2 \tag{A26}$$

$$K_Z = K_{emgc}^2 - K_\zeta^2 \tag{A27}$$

$$K_S = K_{emgc}^2 - K_\xi^2 \tag{A28}$$

$$K_L = K_{emgc}^2 - K_\lambda^2 \tag{A29}$$

(ii1) The second eigenvectors for case (A3)

To obtain the second eigenvectors, it is necessary to use the same equations that were used for the composition of the first eigenvectors, but the first equation in set (A17). Here, the second equation in set (A17) is used instead of the first equation. Therefore, two eigenvectors corresponding to eigenvalues (52) and (53) can be respectively inscribed as follows:

$$\begin{pmatrix} U^{0(1)} \\ \varphi^{0(1)} \\ \psi^{0(1)} \\ \Phi^{0(1)} \\ \Psi^{0(1)} \end{pmatrix} = \begin{pmatrix} U^{0(3)} \\ \varphi^{0(3)} \\ \psi^{0(3)} \\ \Phi^{0(3)} \\ \Psi^{0(3)} \end{pmatrix} = \begin{pmatrix} U^{0(5)} \\ \varphi^{0(5)} \\ \psi^{0(5)} \\ \Phi^{0(5)} \\ \Psi^{0(5)} \end{pmatrix} = \begin{pmatrix} U^{0(7)} \\ \varphi^{0(7)} \\ \psi^{0(7)} \\ \Phi^{0(7)} \\ \Psi^{0(7)} \end{pmatrix}$$

$$= \begin{pmatrix} U^0 = 0 \\ \varphi^0 = -\dfrac{\alpha}{\varepsilon}\psi^0 - \dfrac{\zeta}{\varepsilon}\Phi^0 - \dfrac{\xi}{\varepsilon}\Psi^0 \\ \psi^0 = -\dfrac{\beta - \dfrac{\alpha\zeta}{\varepsilon}}{\mu - \dfrac{\alpha^2}{\varepsilon}}\Phi^0 - \dfrac{\lambda - \dfrac{\alpha\xi}{\varepsilon}}{\mu - \dfrac{\alpha^2}{\varepsilon}}\Psi^0 \\ \Phi^0 = -\eta + \dfrac{\xi^2}{\varepsilon} + \dfrac{\left(\lambda - \dfrac{\alpha\xi}{\varepsilon}\right)^2}{\mu - \dfrac{\alpha^2}{\varepsilon}} \\ \Psi^0 = \vartheta - \dfrac{\xi\zeta}{\varepsilon} - \dfrac{\left(\beta - \dfrac{\alpha\zeta}{\varepsilon}\right)\left(\lambda - \dfrac{\alpha\xi}{\varepsilon}\right)}{\mu - \dfrac{\alpha^2}{\varepsilon}} \end{pmatrix} \tag{A30}$$

$$\begin{pmatrix} U^{0(9)} \\ \varphi^{0(9)} \\ \psi^{0(9)} \\ \Phi^{0(9)} \\ \Psi^{0(9)} \end{pmatrix} = \begin{pmatrix} U^0 = \left(e\varphi^0 + h\psi^0 + g\Phi^0 + f\Psi^0\right) \Big/ CK_{emgc}^2 \\ \varphi^0 = -\dfrac{\alpha K_A}{\varepsilon K_E}\psi^0 - \dfrac{\zeta K_Z}{\varepsilon K_E}\Phi^0 - \dfrac{\xi K_S}{\varepsilon K_E}\Psi^0 \\ \psi^0 = -\dfrac{\beta K_B - \dfrac{\alpha\zeta K_A K_Z}{\varepsilon K_E}}{\mu K_M - \dfrac{\alpha^2 K_A^{\,2}}{\varepsilon K_E}}\Phi^0 - \dfrac{\lambda K_L - \dfrac{\alpha\xi K_A K_S}{\varepsilon K_E}}{\mu K_M - \dfrac{\alpha^2 K_A^{\,2}}{\varepsilon K_E}}\Psi^0 \\ \Phi^0 = -\dfrac{\eta K_F}{K_{emgc}^2} + \dfrac{\xi^2 K_S^{\,2}}{\varepsilon K_E K_{emgc}^2} + \dfrac{\left(\dfrac{\lambda K_L}{K_{emgc}^2} - \dfrac{\alpha\xi K_A K_S}{\varepsilon K_E K_{emgc}^2}\right)^2}{\dfrac{\mu K_M}{K_{emgc}^2} - \dfrac{\alpha^2 K_A^{\,2}}{\varepsilon K_E K_{emgc}^2}} \\ \Psi^0 = \dfrac{\vartheta K_T}{K_{emgc}^2} - \dfrac{\xi\zeta K_S K_Z}{\varepsilon K_E K_{emgc}^2} \\ -\dfrac{\left(\dfrac{\beta K_B}{K_{emgc}^2} - \dfrac{\alpha\zeta K_A K_Z}{\varepsilon K_E K_{emgc}^2}\right)\left(\lambda K_L - \dfrac{\alpha\xi K_A K_S}{\varepsilon K_E}\right)}{\mu K_M - \dfrac{\alpha^2 K_A^{\,2}}{\varepsilon K_E}} \end{pmatrix} \tag{A31}$$

REFERENCES

Abbott, BP., Abbott, R., Abbott, TD., Abernathy, MR., Acernese, F., Ackley, K., Adams, C., Adams, T., Addesso, P., Adhikari, RX. *et al*., 2016. Observation of gravitational waves from a binary black hole merger. Physical Review Letters. 116(6):061102, pp16.

Al'shits, VI., Darinskii, AN. and Lothe, J. 1992. On the existence of surface waves in half-infinite anisotropic elastic media with piezoelectric and piezomagnetic properties. Wave Motion. 16(3):265-283.

Assis, AKT. 1994. Weber's electrodynamics. Kluwer Academic Publishers, Dordrecht. pp288.

Assis, AKT. 1999. Relational mechanics. Apeiron, Montreal, Canada. pp285.

Auld, BA. 1990. Acoustic Fields and Waves in Solids. Krieger Publishing Company (vol. I and II, 2nd edi.). pp878.

Bleustein, JL. 1968. A new surface wave in piezoelectric materials. Applied Physics Letters. 13(12):412-413.

Dieulesaint, E. and Royer, D. 1980. Elastic waves in solids: Applications to signal processing. J. Wiley, New York, USA. (Translated by Bastin, A. and Motz, M., Chichester). pp511.

Einstein, A. 1916. Die Grundlage der allgemeinen Relativitätstheorie. Annalen der Physik. 4(49):769-822.

Forsberg, M., Papadopoulos, DB. and Brodin, G. 2010. Influence of strong field vacuum polarization on gravitational-electromagnetic wave interaction. Physical Review D. 82(2):024001.

Füzfa, A. 2016. How current loops and solenoids curve space-time. Physical Review D. 93(2):024014. pp5.

Gulyaev, YuV. 1969. Electroacoustic surface waves in solids. Soviet Physics Journal of Experimental and Theoretical Physics Letters. 9(1):37-38.

Gulyaev, YuV. 1998. Review of shear surface acoustic waves in solids. IEEE Transactions on Ultrasonics, Ferroelectrics, and Frequency Control. 45(4):935-938.

Heaviside, O. 1893. A gravitational and electromagnetic analogy. The Electrician. 31(Part I):281-282 and 359.

Hegarty, JC. 1969. Gravitational effect of electromagnetic radiation. Nuovo Cimento B. 61(1):47-52.

Jefimenko, OD. 1992. Causality, electromagnetic induction, and gravitation: a different approach to the theory of electromagnetic and gravitational fields. Electret Scientific Publishing, USA. pp180.

Jefimenko, OD. 2000. Causality, electromagnetic induction and gravitation (2nd edi.). Electret Scientific Publishing, Star City, USA. 189-202.

Jefimenko, OD. 2006. Gravitation and cogravitation. Developing Newton's theory of gravitation to its physical and mathematical conclusion. Electret Scientific Publishing, Star City, USA. pp367.

Kleidis, K., Kouiroukidis, A., Nerantzi, P. and Papadopoulos, D. 2010. Charged cosmic strings interacting with gravitational and electromagnetic waves. General Relativity and Gravitation. 42(1):article 31.

Maxwell, JC. 1954. A treatise on electricity and magnetism. Dover Publications, New York (vol. I and II, 3rd edi.). pp560.

Melkumyan, A. 2007. Twelve shear surface waves guided by clamped/free boundaries in magneto-electro-elastic materials. International Journal of Solids and Structures. 44(10):3594-3599.

Möhle, K. 2013. Piezoelectrically tunable optical cavities for the gravitational wave detector LISA. Dissertation zur Erlangung des akademischen Grades doctor rerum naturalium (Dr. rer. nat.) Humboldt-Universität, Berlin, Germany. pp137.

Rivera, JP. 2009. A short review of the magnetoelectric effect and related experimental techniques on single phase (multi-) ferroics. The European Physical Journal B. 71(3):299-313.

Schmid, H. 2008. Some symmetry aspects of ferroics and single phase multiferroics. Journal of Physics: Condensed Matter. 20(43):434201, pp24.

Zakharenko, AA. 2010. Propagation of seven new SH-SAWs in piezoelectromagnetics of class 6 *mm*. LAP LAMBERT Academic Publishing GmbH & Co. KG, Saarbruecken-Krasnoyarsk. pp84.

Zakharenko, AA. 2013[a]. Piezoelectromagnetic SH-SAWs: A review. Canadian Journal of Pure and Applied Sciences. 7(1):2227-2240.

Zakharenko, AA. 2013[b]. New nondispersive SH-SAWs guided by the surface of piezoelectromagnetics. Canadian Journal of Pure and Applied Sciences. 7(3):2557-2570.

Zakharenko, AA. 2013[c]. Peculiarities study of acoustic waves' propagation in piezoelectromagnetic (composite) materials. Canadian Journal of Pure and Applied Sciences. 7(2):2459-2461.

Zakharenko, AA. 2015[a]. A study of new nondispersive SH-SAWs in magnetoelectroelastic medium of symmetry class 6 *mm*. Open Journal of Acoustics. 5(3):95-111.

Zakharenko, AA. 2015[b]. Dramatic influence of the magnetoelectric effect on the existence of the new SH-SAWs propagating in magnetoelectroelastic composites. Open Journal of Acoustics. 5(3):73-87.

Received: May 21, 2016; Revised: Sept 22, 2016;
Accepted: Sept 23, 2016

Canadian Journal of Pure and Applied Sciences
Vol. 10, No. 3, pp. 4029-4037, October 2016
Online ISSN: 1920-3853; Print ISSN: 1715-9997
Available online at www.cjpas.net

THRESHOLD VALUES OF ARSENIC, CADMIUM AND LEAD IN SOIL FOR RICE (*ORYZA SATIVA* L.) AND KALMI (*IPOMOEA AQUATICA*)

Swarnali Mahmood[1], M. Shahjahan Choudhury[2] and *S.M Imamul Huq[1]
[1]Department of Soil, Water and Environment, University of Dhaka, Dhaka 1000, Bangladesh
[2]Bangladesh-Australia Centre for Environmental Research (BACER-DU)
University of Dhaka, Dhaka 1000, Bangladesh

ABSTRACT

A pot experiment was conducted to assess the threshold values of arsenic (As), cadmium (Cd) and lead (Pb) in soil for rice (*Oryza sativa* L.) and kalmi (*Ipomoea aquatica*). Rice and kalmi were grown on a silt loam soil treated separately with different levels of As (0, 0.5, 1, 2 and 5 mg As/L of irrigation water), Cd (0, 5, 10, 15 and 20 mg Cd/kg soil) and Pb (0, 25, 50, 100 and 200 mg Pb/kg soil). The contents of As, Cd and Pb in soil for 10% reduction in dry matter yield of rice and kalmi were taken as the threshold values which were 14.10 mg, 4.34 mg and 46.17 mg per kg soil for As, Cd and Pb, respectively, while the same for kalmi were 4 mg, 6.57 mg and 34.84 mg per kg soil, respectively, for the three elements.

Keywords: Dry matter yield, threshold value, arsenic.

INTRODUCTION

Among the chemical contaminants, trace elements are considered to have specific ecological, biological, and health significance (Kabata-Pendias, 2011). All elements, even those that are metabolically essential (*e.g.*, Cu, Mn, etc.) are toxic when present in excess (Achard-Joris *et al*., 2007). Although metal contamination in the soils of Bangladesh has not reached a level of concern yet, the industrial wastes have been found to increase the metal loads in the surrounding agricultural soils (Joardar *et al*., 2005). The uptake of metals from contaminated soils by plants comprises a prominent path for such metals to enter the food chain where they may cause health hazards (Imamul Huq *et al*., 2000).

Arsenic (As), cadmium (Cd) and lead (Pb) are typical toxic trace elements in soils. Excess of these elements produces a harmful effect on biological systems. Irrigation with As contaminated groundwater leaves a risk of accumulation of this toxic trace element in soil and the eventual exposure of the food chain through plant uptake and animal consumption (Imamul Huq and Naidu, 2005). In plants, As interferes with the metabolic processes (Martin *et al*., 1992), and inhibits plant growth and biomass accumulation (Stepanok, 1998; Stoeva *et al*., 2003). Cd inhibits seed germination (Koeppe, 1977; Yu, 1991) and interferes with several physiological processes resulting in low productivity (Obata and Umebayashi, 1997). High doses of Pb exposure can restrict plant biomass (Gopal and Rizvi, 2008; Gichner *et al*., 2008; Islam *et al*., 2008; Piotrowska *et al*., 2009; Singh *et al*., 2010). Pb strongly inhibits seed germination, seedling development, root elongation, plant growth, transpiration, chlorophyll production, and water and protein content of plant (Pourrut *et al*., 2011), thereby, poses a serious problem for agriculture (Johnson and Eaton, 1980).

From plant growth, animal, and human health standpoint, soils are not considered polluted unless a threshold concentration exists that affects its biological processes (Kabata-Pendias, 2011). The threshold dose-response model is considered as the most dominant model in toxicology (Calabrese and Baldwin, 2003). Threshold values are not fixed physiological facts or physical constants but are statistical points representing the best estimate values from a group of responses (Mohapatra, 2006). Plant growth is commonly used as a general parameter to study the influence of excess trace elements, with growth rate inhibition often being the most obvious plant reaction (Fodor, 2002; Hagemeyer, 2004). Plant populations become stressed when a biotic or abiotic factor affects plant growth and development (Jackson, 1986). Once plant stress is detected, identified and quantified, thresholds for plants can be developed to indicate when control measures are needed (Nutter, 1990).

*Corresponding author e-mail: imamhuq@hotmail.com

For agricultural soils, the maximum acceptable concentrations of metals have been established by different countries (McLaughlin *et al*., 2000). The maximum acceptable concentration of As for agricultural soil recommended by the European Union is 20 mg/kg (Rahaman *et al*., 2013). The maximum acceptable concentrations of Pb and Cd in soils fall in the vast ranges of 50-300 and 1-20 mg/kg, respectively (Council Directive 86/278/EEC, 1986; McLaughlin *et al*., 2000). Although much debate is there on the contamination of our food crops by non-essential trace elements like As, Cd and Pb, there is, however, no information about the limit of these elements to cause yield reduction of crops. With these views in mind, the present work aimed to establish the threshold values of arsenic, cadmium and lead in soil for 10% yield reduction of two most commonly grown crops: rice and kalmi.

MATERIALS AND METHODS

Soil collection and preparation

The soil samples were collected from the experimental field of Bangladesh Jute Research Institute, Atigram Union, Manikganj Sadar upazilla, Manikganj district, Bangladesh, the geo-location being 23°52´60´´ N and 90°02´12´´ E. The sampling site was a medium high land and used as a vegetable land. The soil samples were collected from the surface to 15 cm of depth using a spade. After being transported into the laboratory, the whole sample was mixed thoroughly to make it a homogeneous sample.Then the collected soil samples were processed for pot experiment as well as for analysing the background properties following the procedures described in Imamul Huq and Alam (2005).

Plant culture

The seeds of rice (*Oryza sativa* L. var. BRRI dhan 41) and kalmi (*Ipomoea aquatica* var. BARI Gimakalmi-1) were collected from the local market. A total of 78 plastic pots of 2 L size each with sealed bottom were used in order to prevent draining of irrigation water. One kg processed soil was taken in each pot labelled with treatment symbols. Recommended fertilizers (BARC, 2012) were mixed with the soil to ensure optimum growth of the plants. Rice and kalmi were grown in semi-controlled net-house condition for 50 days and 42 days, respectively, and treated separately with different levels of As (0, 0.5, 1, 2 and 5 mg As/L of irrigation water), Cd (0, 5, 10, 15 and 20 mg Cd/kg soil) and Pb (0, 25, 50, 100 and 200 mg Pb/kg soil). The sources of As were 80% arsenite as sodium meta arsenite ($NaAsO_2$) and 20% arsenate as sodium arsenate (Na_2HAsO_4. H_2O) in solutions. The As treatments were applied to the selected pots with irrigation water and records were maintained about total amount supplied in each pot to keep track of the total As contents in soil for different treatments. A week before sowing the seeds, the soils of the selected pots were spiked with different Cd and Pb treatments separately as the solution of $CdCl_2.H_2O$ and $Pb(NO_3)_2$, respectively. All treatments were applied in triplicates. The pots were arranged in the net-house in a completely randomized design. The positions of the pots were changed every alternative day to allow equal exposure to sunlight.

For kalmi, 10 seeds were sown in each pot. For rice, soils were puddled and 10 seedlings at 7 days after germination were transplanted in each pot. The selected plants were supplied with arsenic mixed irrigation water every day as arsenic treatment. For other pots, irrigation was applied with tap water every day. Each pot received 50 ml of irrigation water every day, except rainy days. The records were kept for total water supplied in each pot as irrigation. The pH of the tap water used for irrigation was in the range of 6.3 to 6.7. The records of soil pH change were kept, but there was no significant change. The tap water was also analysed for trace element contents, but the concentrations of As, Cd and Pb were found to be below detection limit (2 µg/kg).The weeds were mainly grasses which were removed manually by uprooting just after germination not to allow adequate time for them to take up any metal or nutrients. The visual symptoms and growth parameters were noted during the plant growth.

Plant sample collection and preparation

The sampling of the plants was done by uprooting them carefully from the pots. The plants were put into the plastic bag with proper labelling and brought into the laboratory. After washing, the fresh weights of the collected plants were taken with an electric balance. Then the samples were first air-dried and then oven-dried at 70° ± 5°C for 48 hours. The oven dry weights of the plants were also taken. The oven-dried plant samples were then ground. The ground plant samples were mixed thoroughly to make it composite sample and kept in plastic containers with proper labelling and stored in dry place for chemical analyses.

Laboratory analyses

The soil sample was analysed in the laboratory for chemical and physicochemical properties before plant growth following the procedures described in Imamul Huq and Alam (2005). The concentrations of As, Cd and Pb were determined using atomic absorption spectrophotometer on aqua-regia digest of the soil samples and on nitric acid digest of the plant samples. The quality control/quality assurance (QC/QA) of the analyses was as described by Imamul Huq *et al*. (2008).

Estimation of threshold values

The threshold values of As, Cd and Pb were estimated through linear regressive dose-response curves in which the percent relative dry matter yields of plants were plotted against the total trace element contents present in

soil. The percent relative dry matter yield of plant was calculated as the percentage of dry matter production of a given treatment to that at control (zero treatment). The content of trace element (mg/kg) present in soil for 10% reduction in dry matter yield of the plants under study was taken as the threshold.

Data analyses

The experimental data of the experiment were statistically evaluated using Microsoft Excel and Minitab (version 17).

RESULTS AND DISCUSSION

Soil properties

The USDA textural class of the homogeneous experimental soil sample was silt loam(13.9% sand, 74.1% silt and 12% clay fractions) with slightly acidic pH (6.52), low organic matter (1.77%) content, total As and Pb contents of 1.37 and 1.13 mg/kg soil, respectively, and a total Cd content below detection limit (2 µg/kg).

% Relative yield as affected by arsenic

The effects of soil As on relative yields of rice (Fig. 1a) show that the % relative dry matter yield of rice initially increased at the lowest application rate of As and then significantly decreased with increasing As treatments ranging from 2% (at 6.37 mg As/kg soil) to 25% (at 26.37 mg As/kg soil). Increase in yield for small additions of As has also been observed for corn, potatoes, rye and wheat (Gulz *et al*., 2005). Similar observation that at low concentration of an antagonistic or otherwise non-essential element favours growth, were made by Imamul Huq and Larher (1983) with Na for a different crop. It could be due to the fact that at low concentration of As, the P availability or Fe availability was favoured which caused this yield increase. At low levels, however, As increases P uptake by plants, possibly resulting from As-induced physiological plant P deficiency (Carbonell *et al*., 1998; Burlo´ *et al*., 1999). On the other hand, Fe is the only micronutrient element which has been found to be synergistic with As in several plant culture experiments (Barrachina *et al*., 1994). The As concentration at which rice yield shows a decrease of 10% is judged to be the maximum allowable limit or critical content of arsenic in soil (Yan-Chu, 1994). For the present experiment, 10 % decline in rice yield was observed at 14.10 mg As/kg soil (Fig. 1a) which may be considered as the critical content or threshold value of As in soil for rice plants under the present study. Xiong *et al*. (1987) reported 10% rice yield decrease in sierozen soil at 25 ppm of As. Yan-Chu (1994) reported 10% yield loss of rice in purple soil for 10 ppm total As, in yellow-brown soil for 51 ppm total As.

The dry matter yield of kalmi plants also significantly decreased with increasing As treatments (Fig. 1b). Decline in relative yield of kalmi ranged from 4% (at 2.87 mg As/kg soil) to 44% (at 16.37 mg As/kg soil). In the present experiment, 10% yield reduction of kalmi plants was observed at 4 mg As/kg soil which may be considered as the critical level or threshold value of As in soil for kalmi plants.

% Relative yield as affected by cadmium

The relative dry matter yields of rice under elevated soil Cd treatments significantly decreased from 8% to 51% at 5 and 20 mg Cd/kg soil, respectively (Fig. 2a). In the present experiment, the threshold value for 10% decrease in rice yield was observed at 4.34 mg Cd/kg soil and moreover, 50% decline at 16.82 mg Cd/kg soil.

The relative dry matter yields of kalmi significantly declined from 5% (at 10 mg Cd/kg soil) to 54% (at 20 mg Cd/kg soil) as compared to the control (Fig. 2b). In the present experiment, the threshold value of Cd for 10% decline in the relative yield of kalmi was observed at 6.57 mg Cd/kg soil, and 50% yield decline at 20.12 mg Cd/kg soil.

% Relative yield as affected by lead

The relative dry matter yield decline of rice under elevated soil Pb concentrations (Fig. 3a) ranged from 5% (at 25 mg Pb/kg soil) to 34% (at 200 mg Pb/kg soil). In the present experiment, the threshold value of Pb for 10% yield reduction of Rice was observed at 46.17 mg Pb/kg soil.

The yield of kalmi significantly declined ranging from 10% (at 25 mg Pb/kg soil) to 52% (at 200 mg Pb/kg soil) as compared to the control (Fig. 3b). In the present experiment, the threshold value of Pb for 10% yield reduction of kalmi was observed at 34.84 mg Pb/kg soil, and for 50% yield reduction was observed at 194.26 mg Pb/kg soil.

Relationship between trace elements in soils and in plants

The As concentrations in rice plants ranged between 3.62 to 37.57 mg As/kg dry weight of plants (Fig. 4a) and that in kalmi plants ranged between 3.02 to 26.92 mg/kg dry weight of plants (Fig. 4b). The maximum concentrations of As in both rice and kalmi were observed at the highest application rate of As (5 mg As/L of irrigation water). The correlation analysis between the total As in soils and the corresponding As concentrations in plants for both rice and kalmi plants showed significant positive relationship ($r = 0.870864$, $p<0.1$ for rice; and $r = 0.963095$, $p<0.01$ for kalmi).

According to Kashem and Singh (1999), the normal and toxic Cd levels in plants vary from 0.2-2 mg/kg and 15-20 mg/kg, respectively. In the present experiment, the Cd contents in rice exceeded the toxic range at the treatments

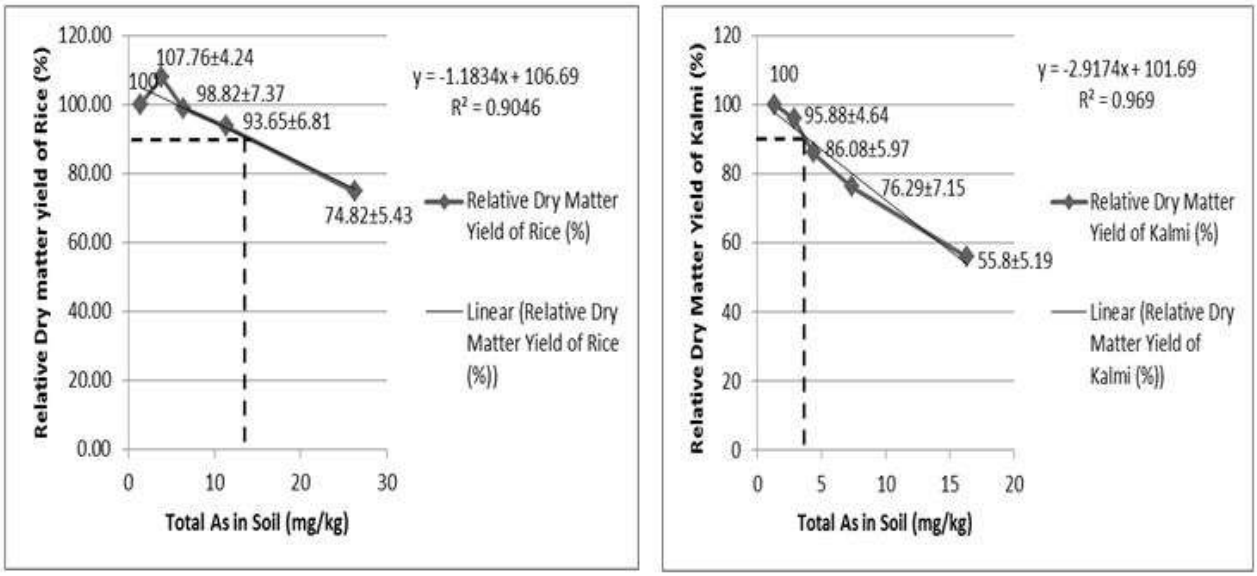

a b

Fig. 1. Relative yields of (a) rice and (b) kalmi vs. soil total As concentrations. The vertical dash-lines indicate the threshold values of As for 10% yield reduction.

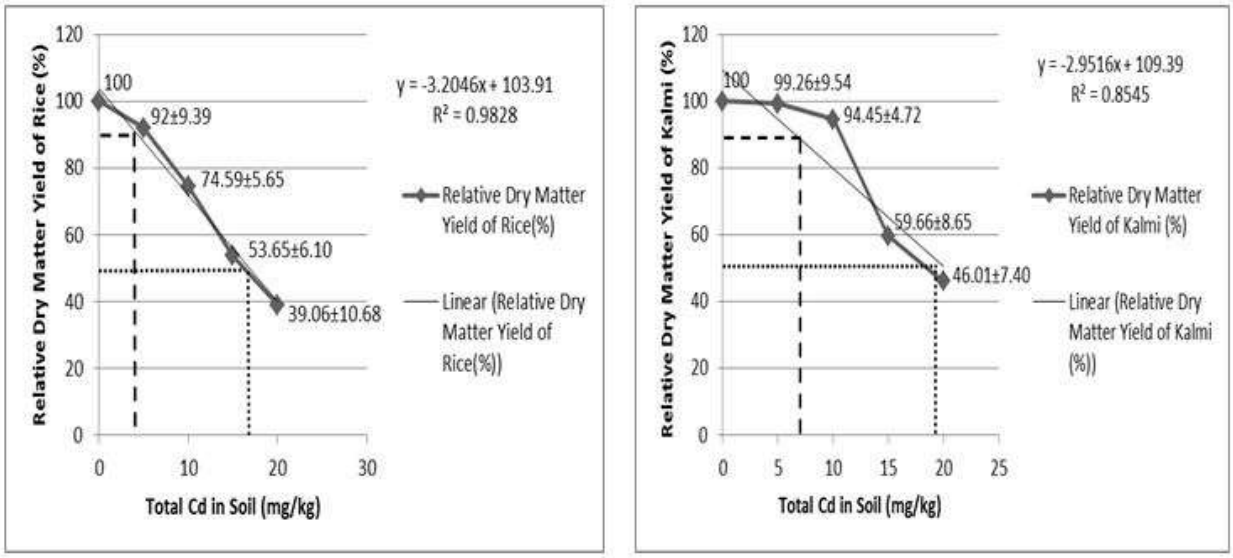

a b

Fig. 2. Relative yields of (a) rice and (b) kalmi *vs*. soil total Cd concentrations. The vertical dash-lines and dot-lines indicate the threshold values of Cd for 10% and 50% yield reduction, respectively.

of 10, 15 and 20 mg Pb/kg soil (Fig. 4c). For kalmi, the Cd contents exceeded the toxic range at 15 and 20 mg Cd/kg soil (Fig. 4d). The correlation analysis between the total Cd in soils and the corresponding Cd concentrations in plants for both rice and kalmi showed significant positive relationship ($r = 0.948534$, $p<0.02$ for rice; and $r = 0.984829$, $p<0.01$ for kalmi). Lund *et al*. (1981) also found significant positive correlations between Cd in the soil and Cd concentrations in the leaves of several crop species.

The normal and toxic Pb levels in plants vary from 0.1-2 mg/kg and 10-20 mg/kg, respectively (Kashem and Singh, 1999). In the present experiment, the Pb contents in rice

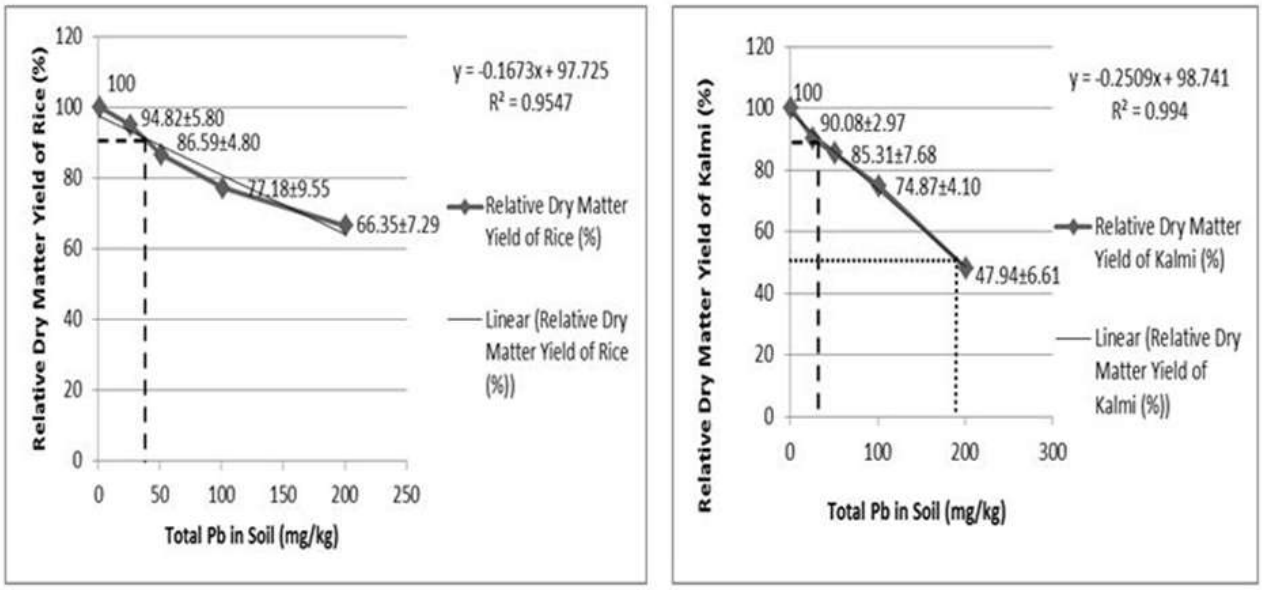

a **b**

Fig. 3. Relative yields of (a) rice and (b) kalmi *vs.* soil total Pb concentrations. The vertical dash-lines and dot-line indicate the threshold values of Pb for 10% and 50% yield reduction, respectively.

plants were observed to exceed the toxic range, except at control (Fig. 4e). Similarly, Pb contents in kalmi plants exceeded the toxic level at 100 and 200 mg Pb/kg soil (Fig. 4f). The correlation analysis between the total Pb in soils and the corresponding Pb concentrations in plants for both rice and kalmi showed significant positive relationship ($r = 0.972214$, $p<0.01$ for rice; and $r = 0.979699$, $p<0.01$ for kalmi). Korcak and Fanning (1985) also found a positive relationship between the concentration of Pb in the soil and that in the plant.

Accumulation of trace elements in plants

The accumulation of As, Cd and Pb in rice and kalmi plants was calculated by multiplying the concentration of trace elements in dry matter of plants (µg/g dry weight) with the corresponding total dry matter production (g/100 plants) and expressed as mg/100 plants. In most cases in this experiment, it was observed that the accumulation of trace elements in plants gradually increased and finally decreased at the highest application rate (Table 1). This might be due to the reduction of water movement from root to the shoots, lower germination of the seeds as well as reduction in fresh and dry weights of the plants under study. Another probable reason could be that some older leaves died at higher levels of treatments which were not taken to measure trace elements.

The total accumulation of As, Cd and Pb in both rice and kalmi was significantly affected by elevated treatments (Table 1). The highest As accumulation in rice (0.135 mg/100 plants) was observed at the rate of 2 mg As/L of irrigation water, and in kalmi (0.117 mg/100 plants) at the rate of 5 mg As/L of irrigation water. The maximum accumulation of Cd in rice (0.076 mg/100 plants) and in kalmi (0.091 mg/100 plants) was observed at the treatment of 15 mg Cd/kg soil. Pb accumulation in rice was observed to be the maximum (0.289 mg/100 plants) at the rate of 50 mg Pb/kg soil. The maximum Pb accumulation in kalmi (0.169 mg/100 plants) was observed at 100 mg Pb/kg soil.

Transfer of trace elements from soil to plants

To estimate the potential transfer of As, Cd and Pb to the food chain, the soil/plant transfer factor (Table 2) was calculated as the ratio of the total trace element in plant (mg/kg dry weight) to the corresponding total trace element in soil (mg/kg). In case of soil contamination with As, the maximum transfer to rice (3.06) was observed at 11.37 mg As/kg soil and that to kalmi (2.91) at 2.87 mg As/kg soil. In case of soil contamination with Cd, the maximum transfer to rice (2.23) was observed at 15 mg Cd/kg soil and that to kalmi (1.63) at 5 mg Cd/kg soil. In case of soil contamination with Pb, the maximum transfer to rice (3.22) was observed at 1.13 mg Pb/kg soil and that to kalmi (0.29) at 101.13 mg Pb/kg soil. Transfer factor values more than 0.1 indicate the affinity of the element towards the plant species (Farago and Mehra, 1992). It appears from the present observations that all the three elements showed their affinity at different concentrations in soil. Moreover, this affinity also differed with the growing conditions of the plant species as well as their genetic make-up.

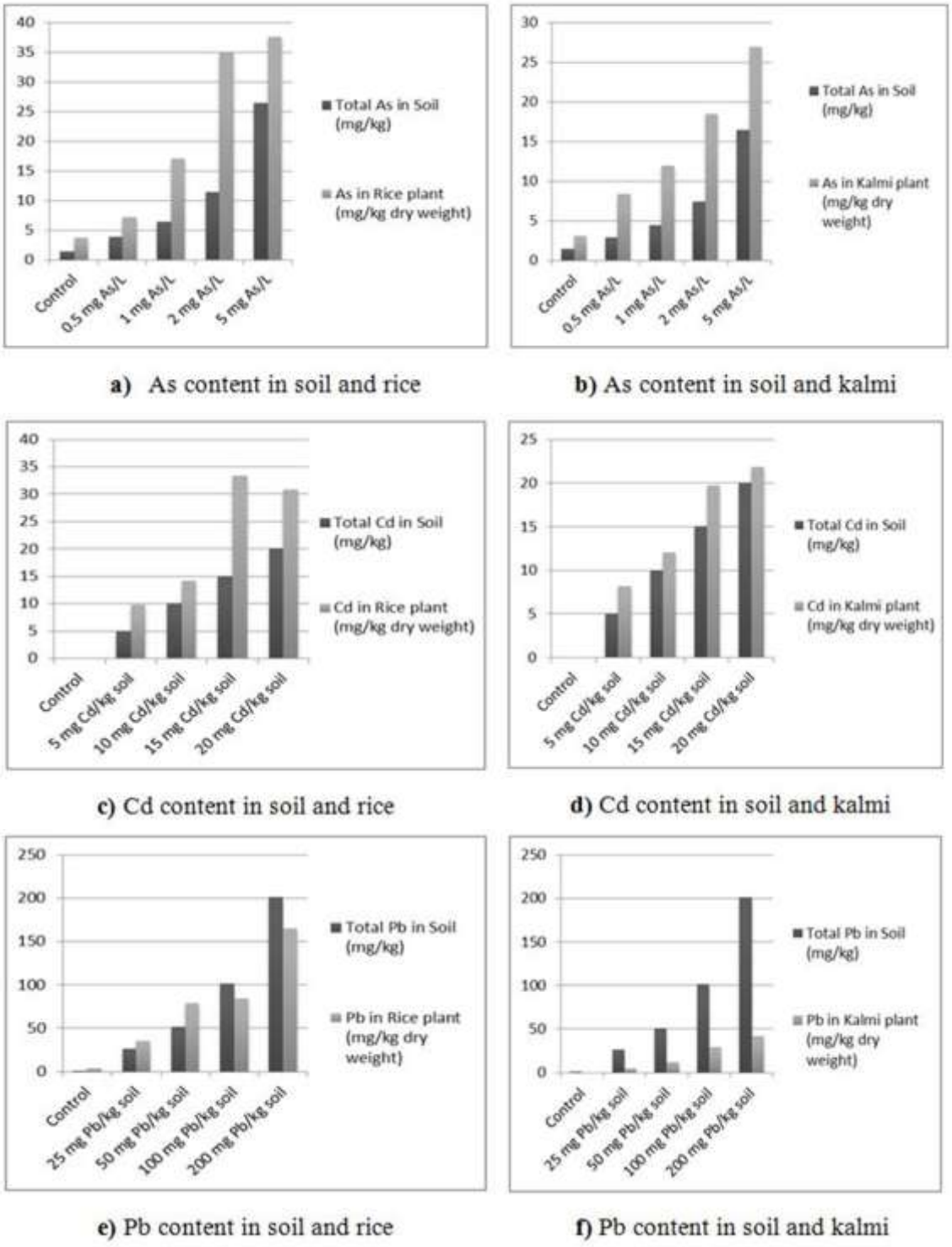

Fig. 4. As, Cd and Pb contents in soil and plants.

CONCLUSION

It is apparent from the present study that the threshold values for trace toxic elements vary with the nature of soil and the plant species. The threshold value for As in soil is higher than the average As contents in Bangladesh soil except some cases where As accumulation in soil has been reported due to irrigation with As contaminated ground water (Imamul Huq, 2008). Likewise, the threshold values for Cd and Pb are also above the average

Table 1. Accumulation of As, Cd and Pb in rice and kalmi plants at different levels of soil contamination

Mean accumulation of As (mg/100 plants)		
Treatments of As (mg/L of irrigation water)	Rice	Kalmi
0	0.015^{de}	0.023^{e}
0.5	0.033^{d}	0.062^{d}
1	0.071^{c}	0.079^{c}
2	0.135^{a}	0.109^{ab}
5	0.120^{ab}	0.117^{a}
Mean accumulation of Cd (mg/100 plants)		
Treatments of Cd (mg/kg soil)	Rice	Kalmi
0	-	-
5	0.038^{d}	0.063^{d}
10	0.045^{c}	0.089^{ab}
15	0.076^{a}	0.091^{a}
20	0.051^{b}	0.078^{c}
Mean accumulation of Pb (mg/100 plants)		
Treatments of Pb (mg/kg soil)	Rice	Kalmi
0	0.015^{d}	-
25	0.141^{c}	0.035^{d}
50	0.289^{a}	0.077^{c}
100	0.276^{ab}	0.169^{a}
200	0.265^{ab}	0.156^{ab}

Any two means having a common letter(s) in a column are not significantly different at 5% level of significance.

Table 2. Transfer factors of soil As, Cd and Pb for rice and kalmi plants at different levels of soil contamination

Treatments* / Crops	1	2	3	4	5
As					
Rice	2.64	1.86	2.66	3.06	1.42
Kalmi	2.20	2.91	2.71	2.50	1.65
Cd					
Rice	-	1.96	1.41	2.23	1.54
Kalmi	-	1.63	1.20	1.31	1.04
Pb					
Rice	3.22	1.34	1.53	0.83	0.82
Kalmi	-	0.19	0.23	0.29	0.21

*As: 1= zero, 2= 0.5 mgL^{-1}, 3= 1 mgL^{-1}, 4= 2 mgL^{-1}, 5= 5 mgL^{-1}
*Cd: 1= zero, 2= 5 $mgkg^{-1}$, 3= 10 $mgkg^{-1}$, 4= 15 $mgkg^{-1}$, 5= 20 $mgkg^{-1}$
*Pb: 1= zero, 2= 25 $mgkg^{-1}$, 3= 50 $mgkg^{-1}$, 4= 100 $mgkg^{-1}$, 5= 200 $mgkg^{-1}$

levels of these elements in Bangladesh soils. The present piece of information could be used to make risk analysis for soil contamination. However, further research with more plant species and different soils are emphasized.

ACKNOWLEDGEMENTS

The authors would like to acknowledge the Bangladesh Australia Centre for Environmental Research (BACER-DU), University of Dhaka for providing laboratory facilities. The first author greatly acknowledges the Ministry of Science and Technology, Government of the People's Republic of Bangladesh for awarding the National Science and Technology (NST) Fellowship for this research work.

REFERENCES

Achard-Joris, M., Moreau, JL., Lucas, M., Baudrimont, M., Mesmer-Dudons, N., Gonzalez, P., Boudou, A. and

Bourdineaud, JP. 2007. Role of metallothioneins in superoxide radical generation during copper redox cycling: Defining the fundamental function of metallothioneins. Biochimie. 89(12):1474-88.

BARC (Bangladesh Agricultural Research Council). 2012. Fertilizer Recommendation Guide. Bangladesh Agricultural Research Council (BARC), Farmgate, Dhaka, Bangladesh. 84-274.

Barrachina, AC., Carbonell, FB. and Beeneyto, JM. 1994. Effects of arsenic on the concentrations of micronutrients in tomato plants grown in hydroponic culture. J. Plant Nutr. 17(11):1887-1903.

Burló, F., Guijarro, I., Carbonell-Barrachina, AA., Valero, D. and Martínez-Sánchez, F. 1999. Arsenic species: Effects on and accumulation by tomato plants. J. Agric. Food Chem. 47:1247-1253.

Calabrese, EJ. and Baldwin, LA. 2003. The hormetic dose-response model is more common than the threshold model in toxicology. Toxicol. Sci. 71:246-250.

Carbonell, AA., Aarabi, MA., Delaune, RD., Gambrell, RP. and Patrick, WH. Jr. 1998. Arsenic in wetland vegetation: availability, phytotoxicity, uptake and effects on plant growth and nutrition. Sci. Total Environ. 217:189-199.

Council Directive 86/278/EEC. 1986. On the protection of the environment, and in particular of the soil, when sewage sludge is used in agriculture. O. J. L 181:6-12. http://eur-lex.europa.eu/legal-content/EN/TXT/PDF/?uri=CELEX:31986L0278&from=EN.

Farago, ME. and Mehra, A. 1992. Uptake of elements by the copper-tolerant plant *Armeria maritime*. In: Metal Compounds in Environment and Life 4 (Interrelation between Chemistry and Biology). Science and Technology Letters, Northwood. 163-169.

Fodor, F. 2002. Physiological responses of vascular plants to heavy metals. In: Physiology and Biochemistry of Metal Toxicity and Tolerance in Plants. Eds. Prasad, MNV. and Strzalka, K. Kluwer Academic Publisher, Dortrech. 149-177.

Gichner, T., Znidar, I. and Száková, J. 2008. Evaluation of DNA damage and mutagenicity induced by lead in tobacco plants. Mutat. Res. Genet. Toxicol. Environ. Mutagen. 652(2):186-190.

Gopal, R. and Rizvi, AH. 2008. Excess lead alters growth, metabolism and translocation of certain nutrients in radish. Chemosphere. 70(9):1539-1544.

Gulz, PA., Gupta, SK. and Schulin, R. 2005. Arsenic accumulation of common plants from contaminated soils. Plant Soil. 272:337-347.

Hagemeyer, J. 2004. Ecophysiology of plant growth under heavy metal stress. In: Heavy Metal Stress in Plants (3rd edi.). Ed. Prasad, MNV. Springer, Berlin. 201-222.

Imamul Huq, SM. 2008. Arsenic contamination in the food chain: Bangladesh Scenario. Paper presented at the UNESCO-UCI International Conference on Water Scarcity, Global Changes, and Groundwater Management Responses, held at the University of California, Irvine, USA.

Imamul Huq, SM. and Alam, MD. (Eds.). 2005. A Handbook on Analyses of Soil, Plant and Water. Bangladesh – Australia Center for Environmental Research, University of Dhaka, Dhaka, Bangladesh. 1-246.

Imamul Huq, SM. and Larher, F. 1983. Osmoregulation in higher plants: Effects of NaCl salinity on non-nodulated *Phaseolus aureus* L.I. growth and mineral contents. New Phytol. 93:203-208.

Imamul Huq, SM. and Naidu, R. 2005. Arsenic in ground water and contamination of the food chain: Bangladesh Scenario. In: Natural Arsenic in Groundwater: Occurrence, Remediation and Management. Eds. Bundschuh, J., Bhattacharya, P. and Chandrasekharam, D. Balkema, New York, USA. 95-101.

Imamul Huq, SM., Al-Mamun, S., Joardar, JC. and Hossain, SA.2008. Remediation of soil arsenic toxicity in *Ipomoea aquatica* using various sources of organic matter. Land Contam. Reclam. 16:333-341.

Imamul Huq, SM., Islam, NM. and Das, M. 2000. Effect of automobile exhausts on nutritional status of soil and plant. Bangladesh J. Soil Sci. 26:103-111.

Islam, E., Liu, D., Li, T., Yang, X., Jin, X., Mahmood, Q., Tian, S. and Li, J. 2008. Effect of Pb toxicity on leaf growth, physiology and ultra structure in the two ecotypes of Elsholtzia argyi. J. Hazard. Mater. 154(1-3):914-926.

Jackson, RD. 1986. Remote sensing of biotic and abiotic plant stress. Annu. Rev. Phytopathol. 24:265-287.

Joardar, JC., Rashid, MH. and Imamul Huq, SM. 2005. Adsorption of lead (Pb) by soils and their clay fraction. J. Asiat. Soc. Bangladesh Sci. 31:63-74.

Johnson, MS. and Eaton, JW. 1980. Environmental contamination through residual trace metal dispersal from a Derelict Lead – Zinc mine. J. Environ. Sci. 9(2):175-179.

Kabata-Pendias, A. 2011. Trace Elements in Soils and Plants, 4th ed. CRC Press, Taylor and Francis Group, LLC, Boca Raton, Florida, USA.

Kashem, MA. and Singh, BR. 1999. Heavy metal contamination of soil and vegetation in the vicinity of

industries in Bangladesh. Water Air Soil Pollut. 115:347-361.

Koeppe, DE. 1977. The uptake, distribution, and effect of cadmium and lead in plants. Sci. Total Environ. 7:197-206.

Korcak, RF. and Fanning, DS. 1985. Availability of applied metals as a function of type of soil material and metal source. Soil Sci. 140:23-34.

Lund, LJ., Betty, EE., Page, AL. and Elliot, RT. 1981. Occurrence of naturally high cadmium levels in soils and its accumulation by vegetation. J. Environ. Qual.10:551-556.

Martin, AR., Masscheleyn, PH. and Patrick, WH. Jr. 1992. The influence of chemical form and concentration of arsenic on rice growth and tissue arsenic concentration. Plant Soil. 139:175-183.

McLaughlin, MJ., Hamon, RE., McLaren, RG., Speir, TW. and Rogers, SL. 2000. Review: A bioavailability based rationale for controlling metal and metalloid contamination of agricultural land in Australia and New Zealand. Aust. J. Soil Res. 38:1037-1086.

Mohapatra, PK. 2006. Textbook of Environmental Biotechnology. I. K. International Pvt. Ltd. ISBN-10: 818823754X, ISBN-13: 9788188237548. pp. 476-509.

Nutter, FW. Jr. 1990. Remote sensing and image analysis in crop loss assessment. In: Crop Loss Assessment in Rice. International Rice Research Institute, PO. Box 933, Manila, Philippines. 93-105.

Obata, H. and Omebayashi, M. 1997. Effects of cadmium on mineral nutrient concentrations in plants differing in tolerance for cadmium. J. Plant Nutr. 20:97-105.

Piotrowska, A., Bajguz, A., Godlewska-Zylkiewicz, B., Czerpak, R. and Kaminska, M. 2009. Jasmonic acid as modulator of lead toxicity in aquatic plant *Wolffia arrhiza* (Lemnaceae). Environ. Exp. Bot. 66(3):507–513.

Pourrut, B., Shahid, M., Dumat, C., Winterton, P. and Pinelli, E. 2011. Lead uptake, toxicity and detoxification in plants. Rev. Environ. Contam. Toxicol. 213:113-136.

Rahaman, S., Sinha, AC., Patri, R. and Mukhopadhyay, D. 2013. Arsenic contamination: A potential hazard to the affected areas of West Bengal, India. Environ. Geochem. Health. 35(1):119-132. http://link.springer.com/article/10.1007%2Fs10653-012-9460-4.

Singh, R., Tripathi, RD., Dwivedi, S., Kumar, A., Trivedi, PK. and Chakrabarty, D. 2010. Lead bioaccumulation potential of an aquatic macrophyte *Najas indica* are related to antioxidant system. Bioresour. Technol. 101:3025-3032.

Stepanok, VV. 1998. The effect of arsenic on the yield and elemental composition of agricultural crops. Agrokhimiya. 12:57-63.

Stoeva, N., Berova, M. and Zlatev, Z. 2003. Physiological response of maize to arsenic contamination. Biol. Plantarum. 47:449-452.

Xiong, XZ., Zhang, XX., Li, PJ., Wang, YS., Ren, H., Wang, LP. and Song, SH. 1987. Environmental capacity of arsenic in soil and mathematical model. Huanjing Kexue. 8(1):8-14.

Yan-Chu, H. 1994. Arsenic distribution in soils. In: Arsenic in the environment, Part I: Cycling and Characterization. Ed. Nriagu, JO. Wiley, New York, USA. 17-49.

Yu, MH. 1991. Effects of lead, copper, zinc, and cadmium on growth and soluble sugars in germinating mung bean seeds. (Abstract) 12th Ann. Meet. Soc. Environ. Toxicol. Chem. pp. 169.

Received: April 19, 2016; Accepted: June 20, 2016

Canadian Journal of Pure and Applied Sciences
Vol. 10, No. 3, pp. 4039-4045, October 2016
Online ISSN: 1920-3853; Print ISSN: 1715-9997
Available online at www.cjpas.net

SEED OPTIONS FOR TOXICITY TESTS IN SOILS CONTAMINATED WITH OIL

Thiago Gonçalves Cavalcanti[1], Andrwey Augusto Galvão Viana[1], Thaffarel Pereira Guedes[1], Amanda de Souza Freire[1], Rafael de Almeida Travassos[2] and *Ulrich Vasconcelos[1]
[1]Laboratório de Microbiologia Ambiental, Departamento de Biotecnologia, Universidade Federal da Paraíba – UFPB, Campus I, CEP – 58.051-900, João Pessoa-PB
[2]Laboratório de Farmacobiotecnologia, Departamento de Biologia Celular e Molecular, Universidade Federal da Paraíba – UFPB, Campus I, CEP – 58.051-900, João Pessoa-PB

ABSTRACT

Determination of phytotoxicity is useful as a sequential test by which the microbiological removal of hydrocarbons present in soils is investigated. However, oil can stimulate the growth of some plants and the selection of appropriate seeds may require time. This study investigated the germination index of 11 edible plants seeds exposed to different concentrations of recalcitrant oils. All plants showed symptoms of toxicity and the indices in 9 of them were reduced proportionally to the contaminants concentration. Eudicots were more sensitive than monocots. Subsequently, a sandy soil was contaminated with lubricating oil and different bioremediation strategies were evaluated. Among the 9 selected seeds, 3 were randomly tested before and after 30 days of treatment. There was an increase in germination indices, especially when more than 30% of the contaminant was removed. The evaluated plants were considered good choices for ecotoxicity tests on soils contaminated by hydrocarbons, particularly *C. anguria*.

Keywords: Phytotoxicity, oil hydrocarbons, bioremediation, germination index.

INTRODUCTION

Oil is a generic term often used to denote a complex toxic mixture of aliphatic hydrocarbon, aromatic heterocyclic, salts and a small fraction of metals and organometallic compounds, formed naturally from the anaerobic conversion of organic material deposited in low permeability sediments under specified conditions of pressure and temperature. Petroleum hydrocarbons are a mixture of heterogeneous saturated compounds, aromatics and resins, inevitably introduced into the environment from various sources during all stages of the processing of crude oil and its derivatives, that is, from extraction to storage in retail outlets. Thus, petro derivatives represent one of the most important classes of xenobiotics responsible for negative impacts on the environment, in particular to animal and plant life, to bodies of water and the soil (Drozdova *et al.*, 2013; Sivaraman *et al.*, 2011).

Phytotoxicity is understood to mean intoxication in plants by substances in the environment, which can be absorbed and that accumulate in plant tissues (Araujo and Miller, 2005). The determination of phytotoxicity comprises one of the criteria used to evaluate the bioavailability of toxic compounds, such as petroleum hydrocarbons, needing simple, fast and reliable methods for this (Wang *et al.*, 2002).

In the literature, most studies related to phytotoxicity discuss the toxic effects of pesticides and certain metals, but the number of publications addressing the effect of oil derivative compounds has been growing (Meudec *et al.*, 2007; Hamdi *et al*., 2007; Sverdrup *et al.*, 2003). The phytotoxicity of polycyclic aromatic hydrocarbons (PAH) has been described as a significant negative effect on the metabolism of plants in concentrations that, in the majority of studies, can vary between 10 and 1000 mg / kg (Debiane *et al.*, 2008; Baek *et al.*, 2004). However, concentrations greater than 1000 mg / kg oil have been reported as stimulants of plant growth (Reynoso-Cuervas *et al.*, 2008).

Handbooks suggest that phytotoxicity assays be performed with at least three species, but this number can be reduced to one eudicot and one monocot. These studies seek to identify the most sensitive parameters, these being seed germination and elongation of the radical, being one of the most studied (OECD, 1984).

Most *in vitro* studies are usually carried out over 5 days in the absence of light. This guarantees a specific result for the phytotoxicity of the contaminant rather than the

*Corresponding author e-mail: u.vasconcelos@cbiotec.ufpb.br

product of the photo-oxidative reactions that may have occurred during the experiment (Wieczorek and Wieczorek, 2007). The main advantages of the method relate to the fact that plants grow regardless of seasonality and ease of handling. Furthermore, this can reveal potential candidates for phytoremediation (Reynoso-Cuervas *et al.*, 2008).

The objective of the present study was to identify plants potentially important in studies on the bioremediation of soils contaminated by oil, by determining the germination index, i.e. the ratio between the numbers of germinated seeds to the size of the emerging rootlets exposed to contaminated soil extract and distilled water.

MATERIALS AND METHODS

Soil

A sandy soil without a history of contamination by hydrocarbons was used, having a pH value of 7.9±0.1%, moisture content of 16.1±0.1% and water retention capacity established at 49.9±0.1%. These properties were identified employing the methodology described by EMBRAPA (1979) and Watwood *et al.* (1991).

Contaminants

The study used two types of oil: 1. a mixture of used lubricating oil, obtained from different gas stations in the city of João Pessoa, Paraíba, Brazil; and 2. marine fuel oil MF-380, kindly provided by Dr. Norma Gusmão from the Department of Antibiotics of the Universidade Federal de Pernambuco. The contaminants were characterized by USEPA methods and showed high levels of Total Petroleum Hydrocarbons (TPH), naphthalene, phenanthrene and pyrene (lubricating oil), as well as n-alkanes ranging from C12 to C34, besides fluorene, phenanthrene, pyrene and benzo[a]pyrene, with the polycyclic aromatic hydrocarbons being predominant (MF-380).

Selection of Plants for Ecotoxicity Testing

Eleven types of edible vegetable seeds were tested (Toca do Verde, Canoas, Brazil): 4 monocots and 7 eudicots, chosen randomly, whose characteristics are shown in Table 1.

All seeds were washed three times with distilled water to eliminate excess dye and preservatives. During the process, irregularly shaped seeds were removed. The seeds were dried on filter paper at room temperature for three hours.

The ecotoxicity tests were performed in triplicate according Tiquia *et al.* (1996) with samples from a system containing soil contaminated with lubricating oil mixture or MF-380 oil, in contaminant-ground ratios of 1:50, 1:10 and 1:5, and incubated for 5 days at room temperature. After the incubation period, soil extracts were prepared with 10 g of soil in 100 mL of distilled water. After vigorous agitation, the extract was filtered and approximately 5-10 ml was transferred to Petri dishes, carefully soaked in No. 1 filter paper (Whatman, 90 mm diameter) containing between seven to ten seeds, distributed over the surface of the paper. Control was carried out with distilled water replacing the soil extract. Incubation occurred at 22±1 °C in the absence of light for 5 days (New Ethics, 411D). After this period, the germinated seeds were counted and the size of the roots measured using a caliper. The Germination Index (GI) of the seeds was determined employing the equation (1):

$$I_G = [(S_1 x R_1) / (S_2 x R_2)] \times 100$$

Table 1. Plant characteristics for the ecotoxicity test.

Seeds	Size (mm)	Photoblastism
Monocots		
Allium cepa	2.0±0.1	Neutral
Allium porrum	2.9±0.2	Positive
Allium fistolosum	2.8±0.2	Negative
Zea mays	5.9±0.7	Neutral
Eudicots		
Artemisea dracunculus	1.1±0.2	Positive
Brassica nigra	1.0±.0.1	Positive
Brassica oleracea	1.0±0.1	Negative
Brassica rapa	3.0±0.1	Neutral
Cucumis anguria	5.6±0.8	Negative
Cucumis melo	12.2±1.0	Negative
Cuminum cyminum	4.6±0.5	Negative

Where: S_1- number of germinated seeds in soil extracts, R_1- average root length on soil extract, S_2- number of germinated seeds in control and R_2 mean root length in the control. The level of toxicity was rated as high when GI < 50%, moderate (GI = 50-80%) or null when GI > 80% (Anastasi *et al*., 2009).

For the test to be conducted in the absence of light, it was necessary to know the photoblastism of the seeds. Two Petri dishes for each plant were prepared as described above, soaking the filter paper with distilled water and incubating at 22°C for 5 days in the dark and under artificial light, as described by Cordazzo and Aracama (1998). After this period, the germinated seeds were counted, applying the equation 2:

$$PB= (S_d/ S_l)$$

Where: PB – photoblstism; S_d – the number of germinated seeds in the dark and S_l the number of germinated seeds in the light. The photoblastism was classified as positive if greater than 1, negative if less than 1 and neutral when the value was 1.

Application of Selected Seeds in Ecotoxicity Tests

The test was performed with three selected seeds in soil extracts before and after different bioremediation treatments. Bioremediation was conducted in laboratory-scale at room temperature for 30 days, using transparent polyethylene reactors filled with 200g of sandy soil contaminated with a mixture of lubricating oil at a ratio to soil of 1:40, thus establishing a condition of the total petroleum hydrocarbons contamination of approximately 16,000 mg/kg. Three test conditions were tried: 1- bioaugmentation with a strain of *Pseudomonas aeruginosa* TGC01, to which was added a corresponding suspension of approximately 10^7 CFU/mL; 2- biostimulation, by supplementation with 250 mg.kg of *Gossypium* sp. cake; and 3- association of bioaugmentation with biostimulation treatments. The abiotic loss was obtained in a sterile reactor with a solution of 10% (w/v) silver nitrate. Tests were conducted in duplicate.

RESULTS AND DISCUSSION

In the first part of this study, 17 different species of seeds were tested, of which 6 were excluded since their germination periods exceeded three days, that is, there was insufficient time necessary for their incubation as well as seed photoblastism may be implicated. According to Flores *et al.* (2011), some plants demand light energy for seed germination, particularly dark seeds. Otherwise light seeds usually germinate in absence of brightness. To know such a feature was interesting, given the conditions of absence of light in this test.

A total of six seeds, including grasses and *Solanaceae* did not germinate. This was attributed to the longer time required for these seeds, limiting their use under the conditions of this study, i.e. 5 days. Later it was found that germination would occur in around 10 to 15 days both in the presence and absence of light. In the eleven remaining species (Table 1), there was negative photoblastism in five seeds (*Brassica oleracea*, *Cucumis anguria*, *Cucumis melo*, *Cuminum cyminum* and *Allium fistolosum*), while in three others there was neutral photoblastism (*Brassica rapa*, *Allium Cepa* and *Zea mays*). Three species had positive photoblastism (*Artemisia dracunculus*, *Brassica nigra* and *Allium porrum*).

Seed germination is a complex mechanism that begins with a swelling of the seed and ends with the emergence of the primary root and cotyledon. This process can be influenced by several factors, such as moisture, pH and salinity of the medium. Additionally, the integument of the seed, besides serving as a light filter, participates in the early stages of germination by establishing a permeability barrier and interfering with the water diffusion processes and gas exchanges which exert a constricting effect or mechanical expansion in the embryo (Hamdi *et al.*, 2007).

In the studies on soils contaminated with petro derivates, ecotoxicity tests, such as those which use plants, are fundamental for two reasons: they disclose the need for intervention in these environments; and they indicate the effectiveness of a treatment after the reduction or removal of the contaminant. The results of the eleven tested seed germination rates are shown in Figure 1 and their numerical values in Table 2.

Phytotoxicity categories are assigned based on the germination index: high when the values are set between 0 and 50%, moderate between 50 and 80%. Any value above this is considered null. This may indicate that there are smaller concentrations of contaminants or that the metabolites produced during biodegradation are not toxic (Anastasi *et al*., 2009). As the test relates the number of germinated seeds to the root elongation events in the presence and absence of exposure to hydrocarbons, there is the possibility of obtaining indices greater than 100%, as observed in *C. cyminum* with a MF 380 marine sea oil ratio to soil of 1:50.

For the two types of contaminants tested, there were predominantly lower germination rates of 50%, followed by values classified as moderate phytotoxicity. The eudicots were more sensitive than the monocots. Some seeds, particularly those exposed to MF-380 marine oil, showed symptoms of toxicity relative to the concentration of the contaminant.

Table 2. Germination index of seeds exposed to different oil concentrations.

Plants	Lubricant oil			MF-380 marine oil		
	contaminant:soil ratio					
	1:50	1:10	1:5	1:50	1:10	1:5
C. cyminum	0.0±0.0	13.3±0.5	0.0±0.0	300.0±0.5	50.0±0.5	0,0±0.0
B.oleracea	30.2±0.1	48.3±0.1	49.5±0.1	53.8±0.1	28.6±0.1	40.6±0.1
A. dracunculus	56.8±0.2	44.7±0.2	27.3±0.2	82.9±0.2	52.2±0.2	58.4±0.2
C. anguria	42.2±0.8	0.0±0.0	80.2±0.8	12.9±0.8	0.0±0.0	42.6±0.8
C. melo	76.1±0.1	43.5±0.1	52.2±0.1	45.8±0.1	80.2±0.1	57.5±0.1
B. nigra	64.3±0.1	0.0±0.0	0.0±0.0	35.5±0.1	0.0±0.0	0.0±0.0
B. rapa	39.7±0.1	58.8±0.1	54.7±0.1	42.5±0.1	51.8±0.1	66.2±0.1
A. porrum	12.0±0.1	66.3±0.1	92.0±0.1	67.4±0.1	58.9±0.1	98.9±0.1
A. cepa	63.5±0.1	59.4±0.1	76.1±0.1	76.7±0.1	6.3±0.1	12.7±0.1
A. fistolatum	55.3±0.5	65.4±0.5	7.2±0.5	67.6±0.5	63.5±0.5	6.8±0.5
Z. mays	0.0±0.0	0.0±0.0	0.0±0.0	32.7±0.1	0.0±0.0	49.0±0.1

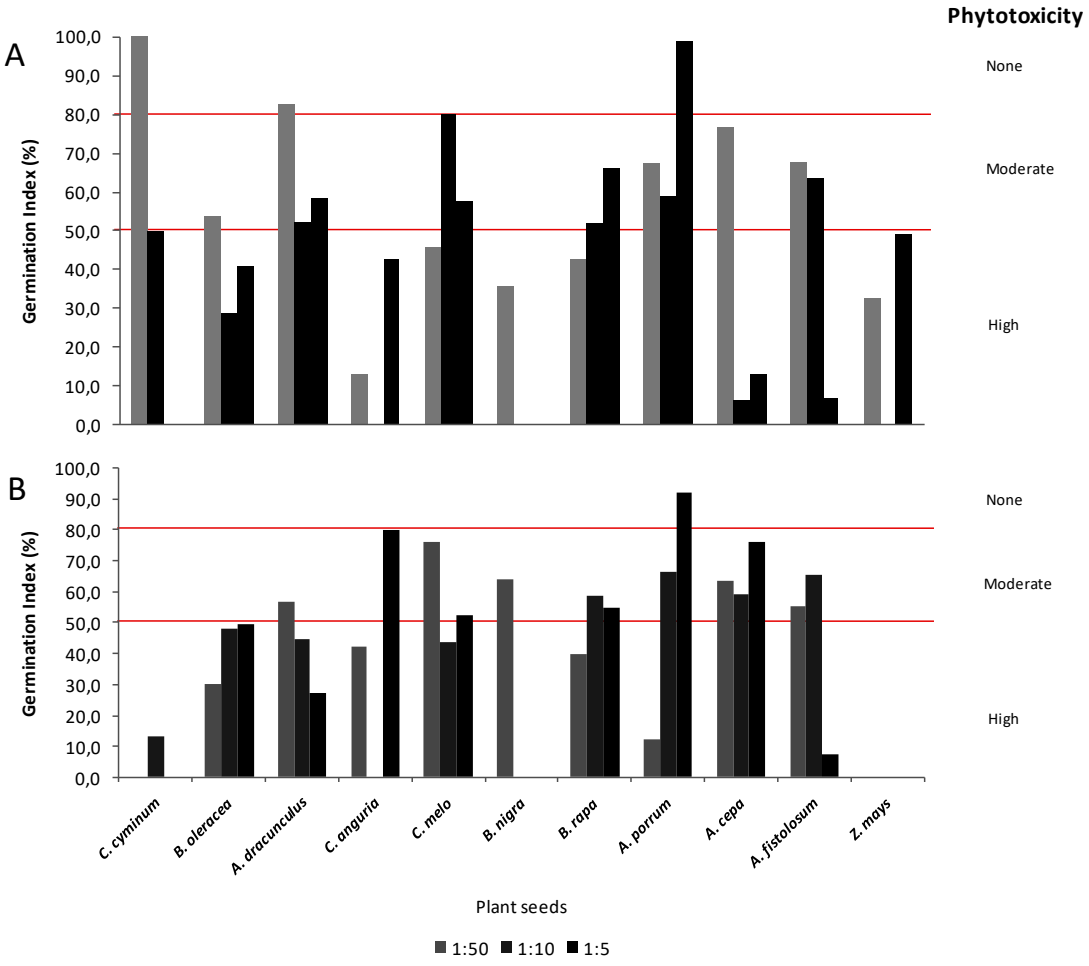

Fig. 1. Germination index of eleven seeds exposed to three different concentrations of MF-380 marine oil (A) and lubricant oil (B). Horizontal lines highlight grades of phytoxicity.

Besides the number of cotyledons, the size and color of the seeds are important characteristics that may influence the test response. Seeds with two small, dark cotyledons, e.g. *B. oleracea* and *B. nigra* are more sensitive than larger lighter seeds with one cotyledon (Tiquia *et al.*, 1996). However, in this study, *Z. mays* and *C. anguria* were also quite sensitive.

Among the eudicots that measured between 1.0 and 4.6 mm, *B. nigra*, *B. oleracea* and especially in *A. dracunculus* and *C. cyminum*, phytotoxicity was proportional to the amount of contaminant oil in the soil. *C. cyminum* provided the best evidence of negative photoblastism, subject to MF-380 marine oil. However, it is noteworthy that although *A. dracunculus* and *B. nigra* exhibited positive photoblastism, and measured about 45 times less than *C. cyminum*, there was a significant decrease in germination and root elongation in the plates containing the contaminated soil extract, suggesting that the plant can serve as a preferred choice among the eudicot plants with small seeds, especially *B. nigra* which reached GI=0% in the two largest concentrations of both contaminants evaluated. This finding may be due to seed size and color, since small, dark seeds are more sensitive to this test (Cordazzo and Aracama, 1998). A different pattern of intoxication symptoms, observed previously, occurred with *B. rapa*. While the mixture of used lubricating oil was highly phytotoxic, surprisingly higher concentrations of MF-380 marine oil reduced the phytotoxicity from high to moderate.

Despite the fact that hydrocarbon oil has been reported to be toxic and an important cause of adverse effects on the metabolism of plants in concentrations in the majority of studies varying from 10 to 1000 mg / kg (Debiane *et al.*, 2008; Baek *et al.*, 2004), concentrations greater than 1000 mg/Kg oil, have been reported as stimulants to plant growth (Reynoso-Cuervas *et al.*, 2008).

Among the larger seeds, measuring between 5.6 and 12.2 mm, germination rates were observed which were not proportionate to the concentration of the oil tested, as were the smaller seeds. This was probably due to the size of these seeds. In these cases, germination seems to be related more on the energy reserves than on environmental factors. Although large, light and containing many starch reserves, the seeds have low moisture content, depending much more on ground water for their development.

It should also be emphasized that the presence of oil may have formed a kind of film around the seeds, preventing water from the soil extract to penetrate their integument (Adam and Duncan, 2002; Storck *et al.*, 2013). Moreover, the presence of volatile compounds, more toxic in the root growth phase, may have contributed to the results. In comparison, the severity of the intoxication in *C. anguria* was more pronounced than in *C. melo.* This feature has already been recognized in a previous study (Vasconcelos *et al.*, 2010). *C. anguria* is a plant whose seeds have two cotyledons and germinate at temperatures in a range between 16.0 and 35.5°C. As the test was conducted at 22.0°C, this confirms the role of seed size in the results.

Among the monocots, except for *Z. mays*, the germination rates ranked phytotoxicity predominantly as moderate. Because it is a light and large seed, it was expected that the *Z. mays* germination rates would be high, but the tested oil concentrations proved very toxic, especially lubricating oil. Corn, when exposed to high concentrations of hydrocarbons, shows symptoms of water stress as well as a modification in calcium content. This is an important indication of environmental pressures having a direct effect on plant growth and development (Dupuy *et al.*, 2015).

Toxicity symptoms were stronger in the two seeds exposed to MF-380 marine oil compared to the mixture of lubricant oil: *A. fistolatum* and particularly *A. cepa*. In this plant, the toxic effect was proportional to the oil concentration, and the germination rate was up to 12 times lower than that obtained with the lowest concentration of oil.

The oil promoted a stimulating effect on *A. porrum*, resulting in an increase of the germination index as the oil concentration increased. This indicates that a low hydrocarbon concentration can cause metabolic stress due to the presence of volatile compounds. On the other hand, higher concentrations may promote conditions for the plant to grow at the expense of morphoanatomic and biochemical adaptations. Thus, plants whose growth is stimulated in the presence of high hydrocarbon concentrations are also good candidates for ecotoxicity tests.

Based on these results, the eleven plants can be used in ecotoxicity tests. It is important to clarify that this selection did not consider the presence of possible toxic metabolites arising from the bioprocess. The sensitivity of these plants to non-metabolized hydrocarbons provides means of choosing the proper species, as well as reduces search time for appropriate seeds.

In order to verify the use of the seeds as biomarkers of contamination by oil and its metabolites, three of the eleven evaluated seeds were randomly selected and exposed to soil extract contaminated by a mixture of lubricating oil before and after microbiological treatment for a period of 30 days (Table 3). Excluding the abiotic losses established at approximately 10% as reported in the literature (Vasconcelos *et al.*, 2011), removal of the TPH, respectively, to the conditions bioaugmentation, biostimulation and the combination of the two techniques was 29.6 ± 3.0%, 31.1±3.1% and 32.5±3.3%.

Table 3. Germination index of seeds before and after bioremediation.

Plants	Microcosms conditions and time (days)					
	BA + BS		BS		BA	
	0	30	0	30	0	30
Artemisia dracunculus	68.2	164.3	68.2	172.5	68.2	65.7
Brassica nigra	58.3	74.7	58.3	184.2	58.3	73.8
Cucumis anguria	21.6	37.6	21.6	51.4	21.6	34.8

BA+BS – association between bioaugmentation with *P. aeruginosa* and biostimulation with cottonseed cake; BS – bioestimulation; BA – biaugmentation. Standard deviation: *A. dracunculus* (±0.2%), *B. nigra* (±0.1%) e *C. anguria* (±0.8%)

In reactors whose contaminant removal was greater than 30%, the germination rates increased in all seeds exposed to the contaminant. *C. anguria* showed more symptoms of toxicity than *B. nigra* and *A. dracunculus*, respectively. In both after 30 days of treatment, the phytotoxicity was classified from moderate to null. This highlights the fact that the conditions that biostimulation was tested with cottonseed cake, as well as in association with bioaugmentation, may serve as an alternative for the removal of hydrocarbons. Additionally, in cases where these indices were higher than 80%, the residual oil concentration or metabolites formed during biodegradation were not considered toxic, suggesting that the longer continuity of the process leads to the mineralization of the contaminant. On the other hand, when only bioaugmentation was employed, oil removal was less than 8.9% under the best conditions, reflecting a moderate toxicity in *B. nigra* and *A. dracunculus* and high toxicity for *C. anguria*. Another study, Bouchez *et al.* (2000) suggests that under bioaugmentation conditions, the introduction of a highly concentrated microbial suspension requires adaptive time to compete first of all with the soil indigenous microbiota. In addition, until equilibrium in microbial density is reached, there may be a delay in the bioprocess of up to 15 days (Mille-Lindblom *et al.*, 2006), coinciding with what was observed in this study, that is, the establishment of the lowest percentage of TPH and removal of its fractions in 30 days.

C. anguria showed the greatest sensitivity among the tested seeds and this result was in agreement with previous research (Santos and Cardoso, 2001; Vasconcelos *et al.*, 2010). It is noteworthy that 30 days is a very short time to promote effective removal in the context of bioremediation of soil contaminated by oil. However, plants have provided indications that they may be used, given biological reduction of approximately 30% of the contaminant, suitable to raise the germination rates to accepted values considering the short period of process.

CONCLUSION

Determination of the phytotoxicity of oil hydrocarbons present in soils complements the test sequence, which investigated the characterization of a contaminant, its microbiological removal, as well as certification with respect to the degree of toxicity of the metabolism products. When a particular soil is affected by a complex mixture of hydrocarbons, the symptoms of physiological and biochemical stress on some plants, related to contaminant concentrations present, can provide important information about the health status of the area, from a biological point of view, and contribute to demonstrate the natural ability of soil recovery. This may signal the need for intervention or liberation, in terms of the processes surrounding bioremediation. Except for *B. rapa* and *A. porrum*, the germination rate in nine seeds was reduced. This provides information on the use of these plants as options for ecotoxicity testing, optimizing the time of selecting appropriate seeds for bioremediation of soils contaminated by hydrocarbons.

ACKNOWLEDGEMENT

The authors are greateful to Conselho Nacional de Desenvolvimento Científico e Tecnológico (CNPq) and Empresa Brasileira de Pesquisa Agropecuária (EMBRAPA Algodão) for providing, respectively, financial support and cottonseed cakes. The English text was revised by Sidney Pratt, Canadian, MAT (The Johns Hopkins University) RSAdip-TESL (Cambirdge University).

REFERENCES

Adam, G. and Duncan, H. 2002. Influence of diesel fuel on seed germination. Environmental Pollution. 120:2002.

Anastasi, A., Coppola, T., Prigione, V. and Varese, GC. 2009. Pyrene degradation and detoxification in soil by a consortium of basidiomycetes isolated from compost: role of laccases and peroxidases. Journal of Hazardous Materials. 165:1229-1233.

Araújo, ASF. and Monteiro, RTR. 2005. Plant bioassays to assess toxicity of textile sludge compost. Scientia Agricola. 62:286-290.

Baek, KH., Kim, HS., Oh, HM., Yoon, BD., Kim, J. and Lee, IS. 2004. Effect of crude oil, oil components, and

bioremediation on plant growth. Journal of Environmental Science and Health. 39:2465-2472.

Bouchez, T., Patureau, D., Dabert, P., Juretschko, S., Doré, J., Delgenès, P., Moletta, R. and Wagner, M. 2000. Ecological study of bioaugmentation failure. Environmental Microbiology. 2:179-190.

Cordazzo, CV. and Aracama, CV. 1998. Influência do dimorfismo de sementes de *Senecio crassiflorus* (poir.) DC (*Asteraceae*) na germinação e crescimento das plântulas. Atlântica. 20:121-130.

Debiane, D., Garçon, G., Verdin, A., Fontaine, J., Durand, R., Grandmougin-Ferjani, A., Shirali, P. and Lounès-Hadj Sahroui, A. 2008. *In vitro* evaluation of the oxidative stress and genotoxic potentials of anthracene on mycorrhizal chicory roots. Environmental and Experimental Botany. 64:120-127.

Drozdova, S., Ritter, W., Lendl, B. and Rosenberg, E. 2013. Challenges in determination of petroleum hydrocarbons in water by gas chromatography (hydrocarbon index). Fuel. 113:527-536.

Dupuy, J., Ouvrard, S., Leglize, P. and Sterckeman, T. 2015. Morphological and physiological responses of maize (*Zea mays*) exposed to sand contaminated by phenanthrene. Chemosphere. 124:110-115.

EMBRAPA. 1979. Manual de métodos de análise de solo. Ed. SNLCS. Rio de Janeiro, Brazil.

Flores, J., Jurado, E., Chapa-Vargas, L., Ceroni-Stuva, A., Dávila-Aranda, P., Galíndez, G., Gurvich, D., León-Lobos, P., Ordóñez, C., Ortega-Baes, P., Ramírez-Bullón, N., Sandoval, A., Seal, CE., Ullian, T. and Pritchard, HW. 2011. Seeds photoblastism and its relationship with some plant traits in 136 cacti taxa. Environmental and Experimental Botany. 71:79-88.

Hamdi, H., Benzarti, S., Manusadžianas, L., Aoyama, I. and Jedidi, N. 2007. Bioaugmentation and biostimulation effects on pah dissipation and soil ecotoxicity under controlled conditions. Soil Biology and Biochemistry. 39:1926-1935.

Meudec, A., Poupart, N., Dussauze, J. and Deslandes, E. 2007. Relationship between heavy fuel oil phytotoxicity and polycyclic aromatic hydrocarbon contamination in *Salicornia fragilis*. Science of the Total Environment. 381:146-156.

Mille-Lindblom, C., Fischer, H. and Tranvik, LT. 2006. Antagonism between bacteria and fungi: substrate competition and a possible tradeoff between fungal growth and tolerance towards bacteria. Oikos. 113:233-242.

OECD. 1984. Terrestrial plant, growth test OECD guidelines for testing of chemicals. OECD. Paris, France.

Reynoso-Cuervo, L., Gallegos-Martínez, ME., Cruz-Sosa, F. and Gutiérrez-Rojas, M. 2008. *In vitro* evaluation of germination and growth of five plant species on medium supplemented with hydrocarbons associated with contaminated soils. Bioresource Technology. 99:6379-6385.

Santos, DI. and Cardoso, VJM. 2001. Thermal-biological aspects on the seed germination of *Cucumis anguria* L.: Influence of the seed coat. Revista Brasileira de Botânica. 24:435-440.

Sivaraman, C., Ganguly, A., Nikolausz, M. and Mutnuri, S. 2011. Isolation of hydrocarbonoclastic bacteria from bilge oil contaminated water. International Journal of Environmental Science and Technology. 8:461-470.

Storck, CR., Nunes, GI., Oliveira, BB. and Basso, C. 2013. Folhas, talos, cascas e sementes de vegetais: composição nutricional, aproveitamento na alimentação e análise sensorial de preparações. Ciência Rural. 43:537-543.

Servdrup, LE., Krogh, PH., Nielsen, T. and Kjær, C. 2003. Toxicity of eight polycyclic aromatic compounds to red clover (*Trifolium pretense*), ryegrass (*Lolium perenne*), and mustard (*Sinapsis alba*). Chemosphere. 53:993-1003.

Tiquia, SM., Tam, NFY. and Hodgkiss, IJ. 1996. Effects of composting on phytotoxicity of spent pig-manure sawdust litter. Environmental Pollution. 93:249-256.

Vasconcelos, U., de França, FP. and Oliveira, FJS. 2011. Removal of high-molecular weight polycyclic aromatic hydrocarbons. Química Nova. 34:218-221.

Vasconcelos, U., Oliveira, FJS. and de França, FP. 2010. Evaluación de la eficacia del tratamiento por deserción térmica de un suelo contaminado con residuos aceitosos. Revista de Ingenería Sanitariay Ambiental. 4:59-63.

Watwood, ME., White, CS. and Dahn, CN. 1991. Methodological modifications for accurate and efficient determination of contaminant biodegradation in unsaturated calcareous soil. Applied and Environmental Microbiology. 57:717-720.

Wieczorek, JK. and Wieczorek, ZJ. 2007. Phytotoxicity and accumulation of anthracene applied to the foliage and sandy substrate in lettuce and radish plant. Ecotoxicology and Environmental Safety. 66:369-377.

Wang, X., Sun, C., Wang, Y. and Wang, L. 2002. Quantitative structure-activity relationships for the inhibition toxicity to root elongation of *Cucumis sativus* of selected phenols and interspecies correlation with *Tetrahymena pyiformis*. Chemosphere. 46:153-161.

Received: May 24, 2016; Accepted: July 9, 2016

Canadian Journal of Pure and Applied Sciences
Vol. 10, No. 3, pp. 4047-4051, October 2016
Online ISSN: 1920-3853; Print ISSN: 1715-9997
Available online at www.cjpas.net

AN EXACT METHOD TO CALCULATE THE NUCLEAR BINDING ENERGY

Bendaoud SAAD
National School of Applied Sciences (ENSA de Safi), Safi, Cadi Ayyad University
Sidi Bouzid's Road, B P 63, Safi-City, 46000, Morocco

ABSTRACT

The present study covers a part of the history of the nuclear binding energy. It is based on the formula of *Albert Einstein* mass-energy equivalence ($E = mc^2$). We present in this paper a brief history of Aston's whole number, mass-defect and nuclear binding energy, its exact definition, and especially its sign that raises fierce controversy between physicists and students.

Keywords: Aston's whole number rule, mass-defect, nuclear binding energy.

INTRODUCTION

Where does the sign minus (−) which exists in front of binding energy of nuclei come from? And what is its signification? Why certain authors consider it as being negative, and others, positive? Students ask worrying questions. When reading the various discussions of nuclear binding energy by different authors, it is easy to get confused. Binding energy is always negative. When they talk about its magnitude, they mean its absolute value, so they just state the positive number. Thus, the physicists have been very sloppy in definitions (Rideout, 2011). To clarify this basic concept, we must find answers to the following question: How does Aston's packing fraction become the binding energy?

Aston (1919) introduced three new concepts to determine masses of individual atoms and their isotopes: 1) *Whole Number Rule*, 2) *Mass-defect*, and 3) *Packing fraction*.

Firstly, the *Aston's Whole Number Rule* stated that the nuclei masses are integer multiples of a certain elementary particle of mass into the nucleus. This rule was a preliminary model for the atomic nucleus but its limitation was that the only particles known at this epoch were the proton and the electron. It was therefore proposed that the nucleus of an isotope of mass M and charge Z, both being integers, consisted of M protons and M-Z electrons. Thus, for example, the nucleus of $^{7}_{3}\mathrm{Li}$ consisted of 7 protons and 4 electrons, while that of $^{7}_{3}\mathrm{Li}$ consisted of 6 protons and 3 electrons (Squires, 1998). Although this model gave the correct mass and electric charge of the nucleus, and appeared to satisfy the whole number rule, it does not function fully well because it presents some defects. The conservation of electric and magnetic properties of the whole atom was not verified. For example, atom should be an electrically neutral particle i.e., sum of charges equal to zero; also the spins of some of the nuclei were anomalous.

The discovery of the neutron by Chadwick (Chadwick, 1932) in 1932 removed these problems. The actual model is that a nucleus of atomic number Z and mass number A contains Z protons and N neutrons. Someway, the mass number of an atom is the Aston's whole number rule (Aston, 1920). Moreover, isotopes are thus nuclei with the same number of protons and a different number of neutrons.

Secondly, the *mass-defect* is the deviation of the atomic mass M_A from its whole number A. Its mathematical expression was:

$$\Delta M = M_A - A \quad (1)$$

Where atomic mass M_A and whole number A are molar masses, i.e., in kg/mol. The mass of an individual atom is equals to the atomic mass (M_A) divided by Avogadro's constant (N_A). Mass defect may be defined as the amount of mass which would be converted into energy if a particular atom has to be assembled from its constituents (Fig. 1). The energy equivalent of mass defect is a measure of binding energy of the nucleus.

Thirdly, *Packing fraction*. Inside nuclei, the nucleons are very tightly packed together (Fig. 1). It can be shown that in the original process of the formation of these, energy must be released in very large amount before a stable packing state is reached. The loss of energy which is

*Corresponding author e-mail: b.saad@ica.ma

related to the binding forces between the nucleons means a corresponding loss of mass (mass-defect). The expression of Aston's *packing fraction* is

$$f = \frac{\Delta m}{A} = \frac{M_A - A}{A} \qquad (2)$$

Since M_A and A are expressed in molar atomic mass unit (kg/mol) i.e., the packing fraction is dimensionless.

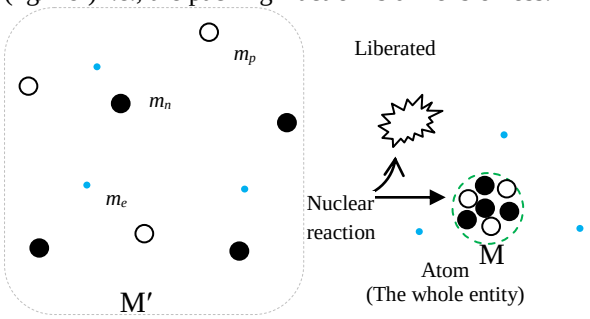

Fig. 1. Formation of the ^{6}Li atom.

Thus, the actual molar mass of one of more stable isotopes of chlorine $^{37}_{17}$Li is $M_{cl}=36,965\ 902\ 574\ g/mol$. According to equation (2) the packing fraction therefore is

$$f = \frac{36,965\ 902\ 574 - 37}{37} = -0,000921 \qquad (3)$$

Since packing fraction number are very small, It is generally multiplied by 1×10^4 to be significant; i.e., $f = -9,21$ (Sharma *et al*., 2001). In 1927, Aston reported a first curve of the packing fraction, as shown in Figure 2.

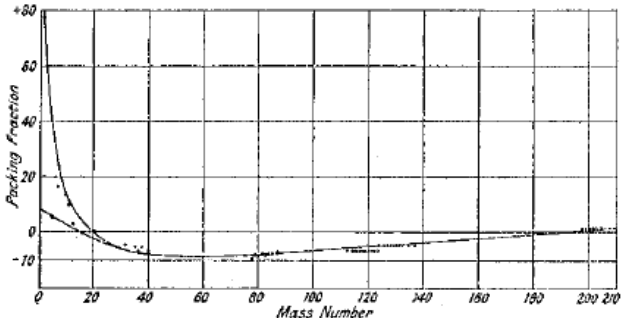

Fig. 2. The 1927 Aston's packing fraction curve (Audi, 2006; Raj, 2008).

RESULTS AND DISCUSSION

In 1919, F. W. Aston had invented the packing fraction to determine the atomic masses (Squires, 1998; Aston, 1942). Rapidly, packing fraction proved to be a very important physical quantity because it was not only used in the determination of the mass of atoms but it was considered as being a strong indicator of the stability of nuclei. Even in the relation (2), Aston's packing fraction is dimensionless and appears as if it means nothing. Aston's intuition with several other contemporary pioneer Chemists and Physicists was good: the packing fraction has been understood as being the nuclear binding energy or stability of the nuclei or the like. In order to show how Aston's packing fraction becomes a binding energy of nuclei, we need to use for the value of A into the numerator of (2) the sum of the masses of separate atom's constituents (protons, neutrons and electrons), rather than the mass number itself (Elsasser, 1933). Then, the amount A in the numerator of Aston's packing fraction will be quite different from the amount A in its denominator. Therefore, we shall use symbol *m(A,Z)* instead of symbol A into the numerator. Nevertheless, symbol A in the denominator is going to keep its original signification; it must represent the Aston's whole number rule. Then, we would expect that *m(A,Z)* would be given by the atomic number Z multiplied by the mass of the electron m_e plus the mass of the proton m_p (and this is the mass of hydrogen atom) plus the number of neutrons (N=A−Z) multiplied by the mass of the neutron m_n. Mathematically,

$$m(A,Z)=Z(m_e+m_p)+(A-Z)m_n \qquad (4)$$

For example, for the helium atom, $^{4}_{2}$He, with two electrons, two protons and two neutrons, we would then anticipate an atomic mass of $m(A,Z)=2m_e+2m_p+2m_n$ according to relation (4). Generally, the masses of the atom's constituents are $m_p=1,007\ 275\ 47\ u$, for the proton, $m_n=1,008\ 664\ 92\ u$, for the neutron, and $m_e=0,000\ 548\ 58\ u$, for the electron. Then, $m(4,2)=2(0,000\ 548\ 58 + 1,007\ 275\ 47 + 1,008\ 664\ 92)=4,034\ 077\ 06\ u$.

On the other hand, the mass of an atom is $m(^4\text{He})=4,002\ 603\ 25\ u$ according to the experimental measurements. The difference between the calculated and measured values which in the case of the helium equals $-0,031\ 473\ 81\ u$, is the current mass-defect, which is effectively a negative value. Therefore, the mass of an atom of helium is less than the mass of the six particles put together. In fact, the helium atom is lighter by about $0,031\ 473\ 81\ u$. Some of the mass has gone missing. Where should we find it?

Henceforth, the missing mass has been converted in energy. Therefore, the energy and mass are equivalent. The mass is just a "solid" form of energy. One can try to convert one to the other and back without breaking the law of conservation of matter. Taking into account adjustments introduced before into the relation (1), the

physical quantity that mass-defect ΔM represented is not mass-excess (M_A–A) but in reality, it represents molar mass-defect. Because $\Delta m=\Delta M/N_A$ and $m(^{A}X)=M_A/N_A$, the mass defect associated to an individual nucleus will be

$$\Delta m=m(^{A}_{Z}X)-m(A,Z) \quad (5)$$

and substituting $m(A,Z)$ by its mathematical expression (4) within relation (5), we obtain the following relation :

$$\Delta m=m(^{A}_{Z}X)-Z(m_e+m_p)-(A-Z)m_n \quad (6)$$

Now, replacing mass-defect Δm by the relation (6) into Aston's packing fraction (2), we found a new relation which is :

$$f=\frac{\Delta m}{A}=\frac{m(^{A}_{Z}X)-Z(m_e+m_p)-(A-Z)m_n}{A} \quad (7)$$

where $m(^{A}_{Z}X)$ is the mass of an atom. The new form of packing fraction is in *u* unit. Indeed, the relation (7) represents *the average mass-defect per nucleon* and probably this is exactly the relationship (in mass unit) that Aston wanted to use to achieve the 1927 Aston's curve (Fig. 2) instead of the (2) relationship.

With definition (6), all stable nuclei are found to have negative Δm values, this is where the sign minus (–) comes from, justifying the use of the term "mass defect". Figure 3 shows the mass Aston's curve for all stable elements on the periodic table. As we can see, mass packing fraction is negative for all existing nuclei except the hydrogen atom for which it is positive.

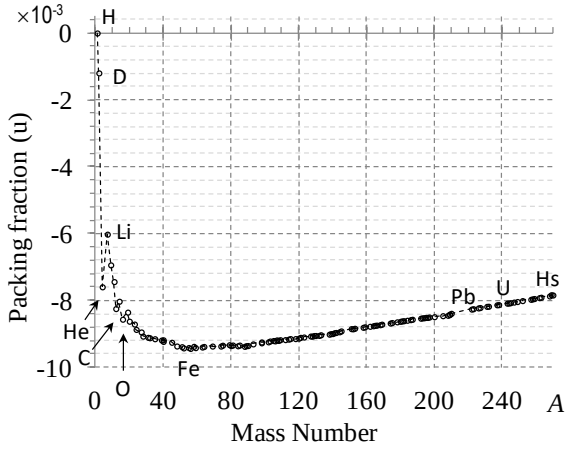

Fig. 3. Mass Aston's curve.

As a result, some mass gets transformed into energy in the formation of nucleus. Thus nuclei having negative value of mass packing fraction are more stable. The greater the negative value of the packing fraction, the greater the loss of mass of its nucleus and hence the greater will be the binding energy (Choppin *et al.*, 2001). Except the hydrogen element, positive packing fractions cannot exist because the nucleons into nuclei are bonded (Rideout, 2011). Indeed, when a nucleus receives certain definite quantity of energy (quantified amount of energy) it will be in an excited state and will become unstable (Hecht, 2007); in this case, the packing fraction will increase depending on the size of the amount of energy received, but always keeping the negative sign as long as the nucleus exists. Generally, the lower the packing fraction of an element, the greater the stability of its nucleus.

At this level of development, we need to introduce Einstein's famous law which is $E=\Delta mc^2$. This law allows us to find the relation which exists between average binding energy by nucleon which we denote it ξ_B, mass-defect Δm from relation (6) and the mass Aston's packing fraction f from relation (7) for a given nucleus which is

$$\xi_B=\frac{\Delta mc^2}{A}=fc^2 \quad (8)$$

where *c* is the speed of the light in the vacuum (c=2,997 924 58 $\times 10^8$ m/s). Because 1 $c^2 \cong$ 931,5 MeV/u, to obtained ξ_B in MeV (Megaelectron-volts), simply multiply *f or Δm/A wich is* in u by 931,5 value.

As shown on the graph in Figure 4, the average binding energy by nucleon, ξ_B, of nuclei in periodic table are negatives except the hydrogen atom, hence those elements are relatively stables. We note that the value of ξ_B varies in the rather narrow range [-9, 0] MeV.

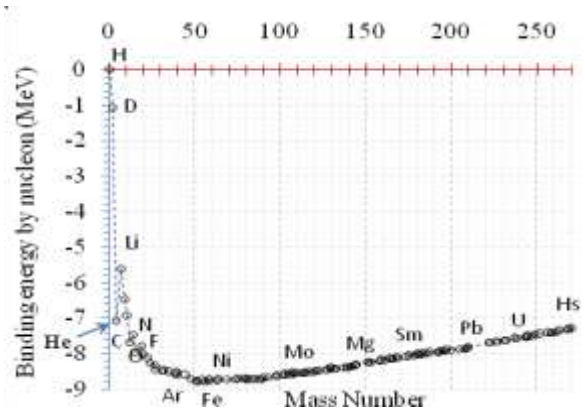

Fig. 4. Binding energy Aston's curve.

Then, to calculate the total energy liberated by the nucleus of an atom, we just need to mu ltiply ξ_B in relation (8) by its mass number A and we obtain

$$E_B=A\xi_\ell \quad (9)$$

Substituting relation (8) by its expression into relation (9) and Δm by its expression (6), and we obtain

$$E_B=\Delta mc^2=[m(^{A}_{Z}X)-Z(m_e+m_p)-(A-Z)m_n]c^2 \quad (10)$$

A useful practical relation to calculate the binding energy can be deducted from what precedes would be,

$$E_B=931{,}5\times\Delta m \quad (11)$$

Where the input Δm into this function is in u and the output E_B will be in MeV. This relationship between energy and mass would indicate that in the formation of deuterium by combination of a proton, a neutron and an electron together, the amount of material lost or the mass-defect $-0{,}002\ 371\ 47\ u$ would be observed as the liberation of an equivalent amount of energy during the formation of this nucleus which is

$$E_B=-0{,}002\ 371\ 47\times 931{,}5=-2{,}209\ MeV \quad (12)$$

This is quite a small amount of energy in the everyday world, but for a given big quantity of matter such in stars or nuclear reactors and atomic bombs, it will be colossal. But better indication on the stability of a nucleus is obtained when the binding energy is divided by the total number of nucleons into a nucleus to give the average binding energy by nucleon. We can write

$$\xi_\ell=\frac{E_B}{A} \quad (13)$$

It allows comparing the stability of an element with that of another one. For the deuterium, $^{2}_{1}H$, the value of E_B/A for the bond between any two nucleons (Schaeffer, 2012) is equal to $-2{,}209/2 = -1{,}11$ MeV, whereas for $^{4}_{2}He$ it is $-7{,}07$ MeV. Because $-7{,}07 < -1{,}11$; the $^{4}_{2}He$ nucleus is more stable than the $^{2}_{1}H$ nucleus. The lowest values of the average binding energy by nucleon (Fig. 4 or 5) are observed for transition metals (Fe, Co, Ni,...) which indicate maximum stability of their nuclei. Henceforth, on moving to the left or to the right, the values again raise showing increasing instability of nuclei. This is demonstrated by the phenomenon of radioactivity exhibited by high atomic weight elements. The nuclei in such case disintegrate emitting α, β^-, β^+ particles and/or γ radiations giving a lighter and more stable nucleus. From this curve, it is immediately apparent that fusion of light elements like $^{1}_{1}H$ and $^{4}_{2}He$ into heavy ones is highly exothermic, as fission of the heavy elements into lighter atoms, especially present in systems like the sun and stars. Indeed, a few minutes after the Big Bang, the universe contained no other elements than hydrogen and helium (Hinke *et al*., 2012; Haxel *et al*., 1949).

On the plot, we see that certain numbers of nucleons form especially stable nuclei. That effect is observed as small pseudo-periodic valleys which appear spaced out on the x-axis logarithmic scale (Fig. 5). The existence of nuclei with magic numbers (Steppenbeck *et al*., 2013) suggests closed shell configurations, as the orbits of atoms.

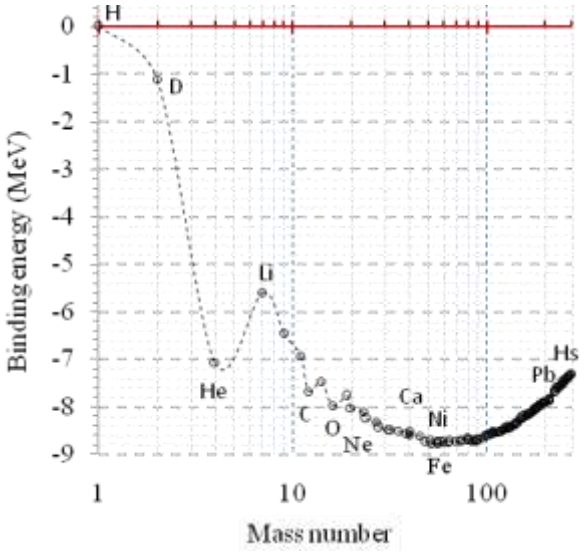

Fig. 5. Some magic elements on the binding energy log-curve.

Now, it is time to introduce a very interesting method to calculate the binding energy step by step, in only four steps as follows.

1st step : writing the nuclear reaction of the nucleus.

$$Z(^{0}_{-1}e+^{1}_{1}p)+(A-Z)\,^{1}_{0}n \rightarrow {}^{A}_{Z}X$$

2nd step: calculating mass-defect.

$$\Delta m=m(^{A}_{Z}X)-Z(m_e+m_p)-(A-Z)m_n$$

3rd step : calculating binding energy.

$$E_B=\Delta mc^2=Afc^2$$

4th step: calculating the average binding energy by nucleon.

$$\xi_B=\frac{E_B}{A}$$

The obtained value of E_B/A should fulfill Aston's condition which is $-9\ MeV < \xi_B < 0\ MeV$.

As example of application, the atomic mass of cobalt-60, ${}^{60}_{27}Co$, is M_A=59,933 817 17 g/mol.

What is the average binding energy by nucleon? The conversion factor of mass to energy is 1 u=931,494 028 23 MeV/c^2. By definition, 1 u = 1g/mol.

First step:

$$27({}^{0}_{-1}\mathrm{e} + {}^{1}_{1}\mathrm{p}) + 33\ {}^{1}_{0}\mathrm{n} \rightarrow {}^{60}_{27}\mathrm{Co}$$

Second step : $\Delta m = m({}^{A}_{Z}\mathrm{X}) - m(A,Z)$

$\Delta m = m({}^{A}_{Z}\mathrm{X}) - Z(m_e+m_p) - (A-Z)m_n$

$\Delta m = m({}^{60}_{27}\mathrm{Co}) - 27(m_e+m_p) - 33m_n$

$\Delta m = 59{,}933\ 817\ 17 - 27(0{,}000\ 548\ 58+1{,}007\ 275\ 47) - 33\times1{,}008\ 664\ 92$

Then,

$\Delta m = -0{,}563\ 348\ 61\ u$

Third step: $E_B=\Delta mc^2$.

$E_B = -0{,}593\ 347\ 61 \times 931{,}494\ 028\ 2$

$E_B = -524{,}754\ 935\ MeV$

Fourth step:

$$\xi_B = \frac{E_B}{A} = -\frac{524{,}754\ 935}{60} = -8{,}75 MeV$$

Finally, we find that

– 9 MeV < – 8,75 MeV < 0 MeV

CONCLUSION

The calculation of the nuclear binding energy has been exhaustively revised based on the original idea of Aston's whole number. A brief history is presented. The calculation of the nuclear binding energy is done through the famous formula of Albert Einstein on the mass-energy equivalence (E = mc^2). The concepts of Aston's whole number, mass defect and nuclear binding energy are very well defined and a new method for fast and easy calculation of the average nuclear binding energy (energy per nucleon) is proposed. Finally, this work has removed the ambiguity in the sign of the nuclear binding energy which should be therefore negative.

ACKNOWLEDGEMENT

Accurate data used in this paper are from the International Atomic Energy Agency (IAEA).

REFERENCES

Aston, FW. 1920. Isotopes and Atomic Weights. Nature 105:617-619.

Aston, FW. 1919. The mass-spectra of chemical elements Phil. Mag. 38:707-723.

Aston, FW. 1919. The Constitution of the Elements. Nature. 104:393-393.

Aston, FW. 1942. Mass Spectra and Isotopes. (2nd ed.). Edward Arnold & Co., London. pp. 167.

Audi, G. 2006. The history of nuclidic masses and of their evaluation. IJMS. 251:85-94.

Chadwick, J. 1932. The Existence of a Neutron. Proc. R. Soc. London. A 136(830):692-708.

Choppin, G., Liljenzin JO. and Rydberg, J. 2001 Radiochemistry and nuclear chemistry. (3rd edi.). Butterworth-Heinemann. 41-57.

Elsasser, WM. 1933. Sur le principe de Pauli dans les noyaux. J. Phys. Rad. 4:549-556.

Haxel, O., Jensen, JHD. and Suess, HE. 1949. Magic Numbers in Nuclear Structure. Phys. Rev. 75:1766.

Hecht, E. 2007. Physique: Ondes, optique et physique moderne. De Boeck. 365-367.

Hinke CB. *et al*., 2012. Superallowed Gamow–Teller decay of the doubly magic nucleus ^{100}Sn. Nature. 486 (7403):399-405.

Raj, G. 2008. Advanced Inorganic Chemistry. (31st edi.). Krishna Prakashan Media.

Rideout, K. 2011. Binding together bonds. Phys. Teach. 49(3):188-188.

Schaeffer, B. 2012. Ab initio calculation of ^{2}H and ^{4}He. Binding Energies. J. Modern Physics. 3:1709-1715.

Sharma, BK. 2001. Nuclear and Radiation Chemistry. Krishna Prakashan Media Ltd. 66-67.

Squires, G. 1998. Francis Aston and the mass spectrograph. J. Chem. Soc., Dalton Trans. 23:3893-389.

Steppenbeck, D. *et al*., 2013. Evidence for a new nuclear 'magic number' from the level structure of ^{54}Ca. Nature. 502:207-210.

Received: May 24, 2016; Accepted: July 9, 2016